^{7}LiF AND CaF_2:Mn EXPERIMENTAL DATA FOR EVALUATING TLD ENERGY RESPONSE THEORY

by

Robert Mark Ostmeyer
B.S., Kansas State University, 1979

A MASTER'S THESIS

submitted in partial fulfillment of the
requirements for the degree

MASTER OF SCIENCE

Department of Nuclear Engineering
KANSAS STATE UNIVERSITY
Manhattan, Kansas

1980

Approved by:

Major Professor

TABLE OF CONTENTS

Table of Contents - Continued

THIS BOOK
CONTAINS
NUMEROUS PAGES
WITH THE ORIGINAL
PRINTING BEING
SKEWED
DIFFERENTLY FROM
THE TOP OF THE
PAGE TO THE
BOTTOM.

THIS IS AS RECEIVED
FROM THE
CUSTOMER.

LIST OF TABLES

List of Tables - Continued

LIST OF FIGURES

List of Figures - Continued

List of Figures - Continued

List of Figures - Continued

List of Figures - Continued

1.0. INTRODUCTION

During the past decade, thermoluminescent dosimeters (TLDs) have received international attention for the measurement of gamma energy deposition, in various regions of low power critical assemblies. This interest was largely generated by the successful demonstration of the method by scientists within Argonne National Laboratory's Applied Physics Division[1,2,3]. Specific measurements for which this method has been employed include (1) characterizations of fast reactor assemblies[1,4-6], (2) energy deposition in shielding materials[7,8], (3) gamma heating measurements in fast breeder reactor blankets[9], and (4) energy deposition in reactor control rods[10,11].

1.1 History of Method Development and Evaluation

The particular advantage of using TLDs for gamma heating measurements, is the small size of the dosimeters. When placed within a gamma irradiated medium, the TLDs do not appreciably perturb the gamma field. This non-perturbation characteristic is desirable when a good estimate of the surrounding medium's radiation dose is required. Nevertheless, despite their small size, TLDs exhibit a linear response as a function of gamma dose over a wide range of radiation exposures[12]. However, it should be mentioned that this linear response characteristic holds only when the radiation makeup remains unchanged.

The theory used to relate absorption of gamma radiation in a medium, to that of the resulting ionization produced in a TLD, was forwarded by T.E. Burlin[13,14]. Based upon this theory, various com-

putational methods were developed to determine this relationship[15,16]. One such method is incorporated into the TERC/III computer code, which was developed by scientists at Argonne National Laboratory.

Once the computational methods were developed, raw TLD data were acquired for their evaluation[17,18]. This was accomplished by gamma irradiation of encased ^{7}LiF TLDs. The encasements included sleeves of B_4C, Teflon, iron, copper, lead, stainless steel, tantalum, and aluminum. The studied gamma energies ranged from 0.662 to 1.333 MeV. With comparison of the experimental results to the computational methods, good correlation was found to exist.

1.2 Scope of Experimentation

In order to further evaluate the various computational methods, a broader data base needed to be generated. As a result of this need, response data were obtained by irradiating encased ^{7}LiF and CaF_2:Mn TLDs. Encasements included sleeves made of lead, tantalum, tin, zirconium, copper, stainless steel, iron, aluminum and natural LiF. Gamma energies ranged from 0.122 to 1.333 MeV. The experimentally determined energy response results, and comparisons between these results and TERC/III calculations, are presented.

To compliment the energy response study, the results of a sleeve thickness investigation are also reported. For this study, ^{7}LiF and CaF_2:Mn response data were obtained using a variety of sleeve thicknesses. The investigated gamma energies and sleeve materials were the same as those used for the TLD energy response study.

2.0 EXPERIMENTAL EQUIPMENT AND MATERIALS

Equipment and materials, which were available for the performance of the experimental phase of these investigations, are described in this chapter. Except for the TLD encasing materials, which were on loan from Argonne National Laboratory, all items were purchased with available research funds.

2.1 TLD Response Measurement Equipment

During execution of the TLD energy response study, individual dosimeter responses were measured using a Harshaw 2000 TLD Reader. A photograph of the equipment is shown in Fig. 2.1. This particular analyzer consisted of two major components, a 2000-A Thermoluminescence (TL) Detector and a 2000-B Automatic Integrating Picoammeter. A CO_2 gas metering system was connected to the 2000-A unit for the purpose of purging the TLD heating chamber of residual air. In the course of normal operation, the TL detector utilized a photomultiplier tube (PMT) to measure the individual TL emissions released during prescribed TLD heating cycles. During measurement of these heat induced emissions, the PMT currents were simultaneously integrated by the 2000-B unit. These integrations produced LED readings of total charge, which were relative measures of total TLD response. This was the desired quantity used to relate the instrument output to the gamma-ray induced excitation within the dosimeters.

To complete the sleeve-thickness study, individual TLD responses were measured with two analyzers, namely the Harshaw 2000, and a photon

THIS BOOK CONTAINS NUMEROUS PAGES WITH PICTURES THAT ARE CROOKED COMPARED TO THE REST OF THE INFORMATION ON THE PAGE.

THIS IS AS RECEIVED FROM CUSTOMER.

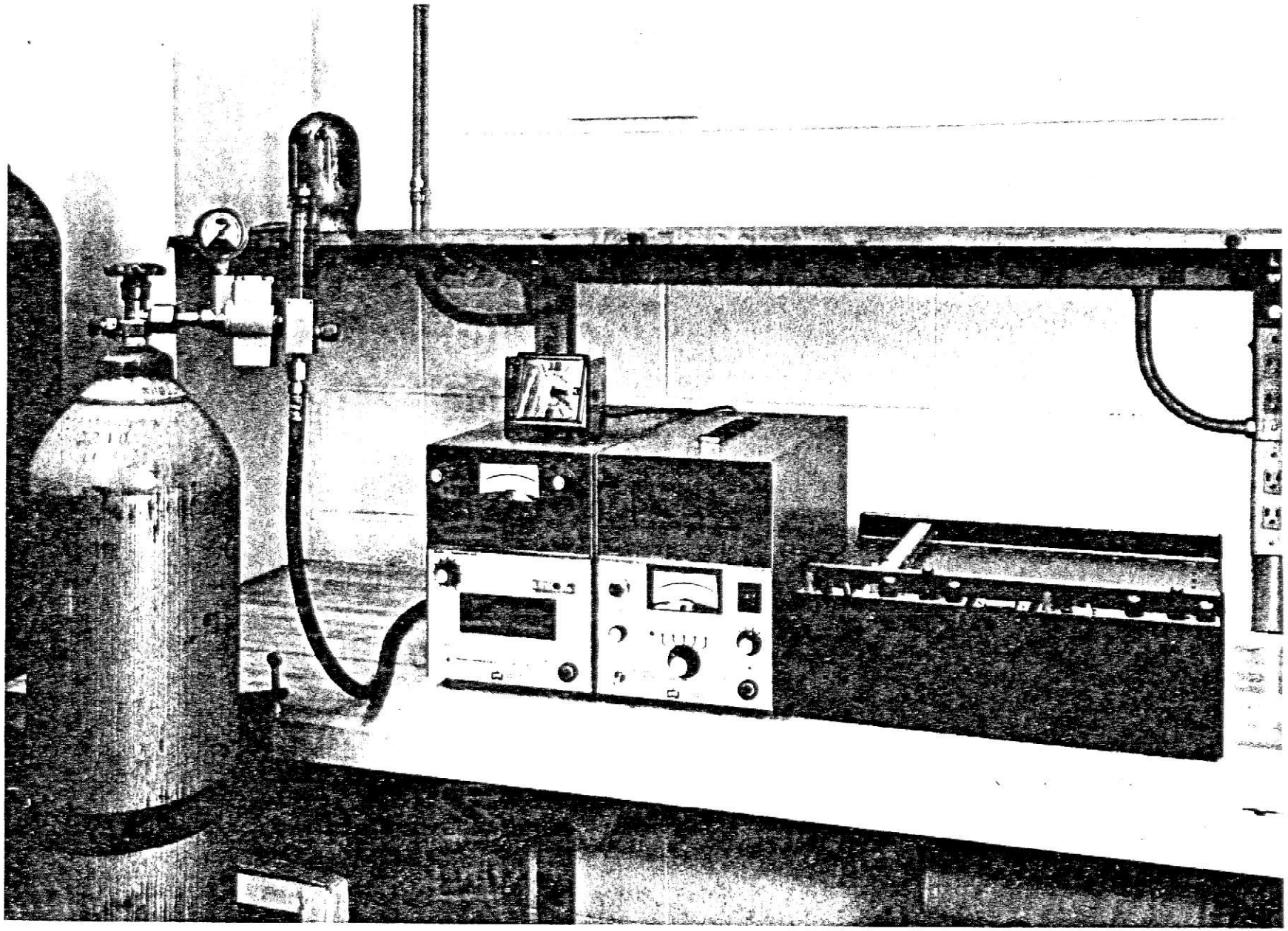

Fig. 2.1. Photograph of the Harshaw Model 2000 TLD analyzer and CO_2 gas purge system.

detection system which was developed within the Nuclear Engineering Department at Kansas State University. A detailed discussion of the photon analyzer's operating characteristics is presented in Ref. 19. Basically, the photon detecting system differs from the Harshaw analyzer in only two respects. First, the total number of photons detected by the PMT (rather than the PMT current) is integrated and second, N_2 (rather than CO_2) gas is used for purging of the TLD heating chamber. In a manner similar to the integrated charge result for the Harshaw 2000, the integrated number of photon counts is the quantity used to relate instrument output to the radiation induced excitation within the TLDs.

An X-Y recorder was employed in concurrence with both analyzers during data acquisition. It was used to generate glow curves (PMT response rate versus time) and temperature profiles whenever permanent records were required. Normally, only the integrated responses were recorded.

2.2 Annealing Equipment

Two ovens (see Fig. 2.2) and a draft-free drawer were available for annealing of TLDs prior to radiation exposures. The first oven, a Thermolyne Type 10500 furnace with solid state temperature control, and an operating range of 30-1200°C, was used for TLD annealing at 400°C. A Thelco Model 16 Precision Oven, with an operating range of 0-200°C, was employed for TLD annealing at 100°C.

Pyrex petri dishes were used as TLD receptacles during the pre-annealing procedure. Pyrex glass was chosen because its surface is

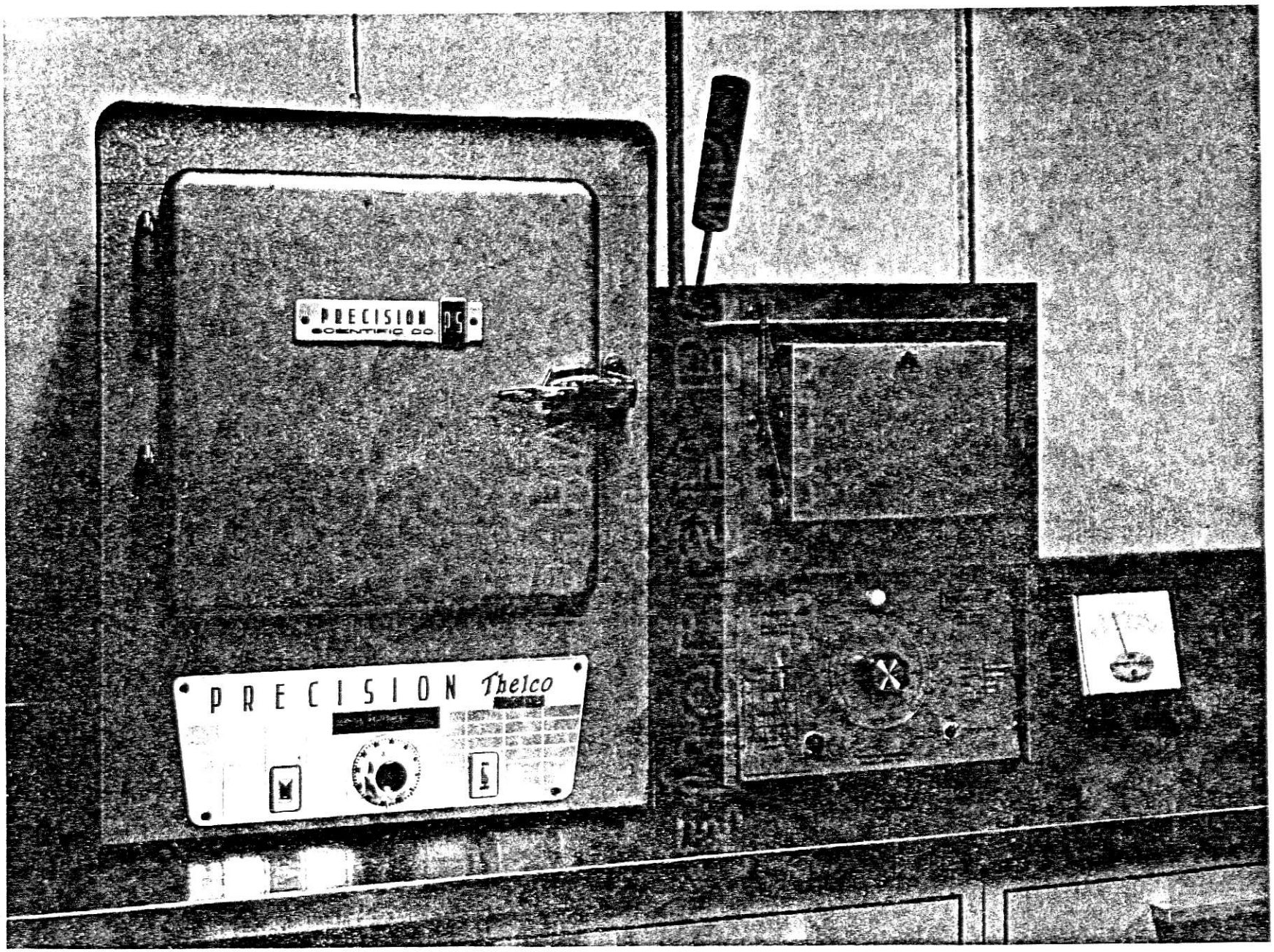

Fig. 2.2. Photograph of the TLD annealing ovens.

resistant to oxidation at high temperatures. If a material not resistant to this formation was chosen, the surfaces of the TLDs could have been contaminated. This occurrence would have had a detrimental affect on the precision of the dosimeters.

A draft free drawer, located directly below the ovens, was used for cooling the TLD ladened petri dishes. Situated at the bottom of the drawer was a sheet of asbestos upon which the receptacles were placed. The asbestos pad was used to avoid any appreciable drawer-bottom conduction cooling of the dishes. Prevention of this phenomenon allowed for slower and more reproducible TLD cooling rates. Rapid cooling tends to increase the size of the undesirable low temperature TLD response peaks[12].

2.3 Handling Equipment

TLDs were handled using a special plastic tipped tweezers. The tweezers was used to avoid abrasion or crushing of the delicate dosimeters. If incurred, both of these phenomena could have affected a TLD's response characteristics.

In order to maintain the individuality of each TLD, the dosimeters were stored in numbered coin envelopes. The envelopes were chosen because of their amenability to storage and cataloging.

2.4 Thermoluminescent Dosimeters

One thousand new TLDs of two varieties were purchased for the energy response study. The first type consisted of Harshaw TL-700 (^{7}LiF) 1x1x6 mm rods enriched to 99.993 percent ^{7}Li. The second consisted of

Harshaw TL-400 (CaF_2:Mn) rods of the same size. A closeup photograph of the two varieties is shown in Fig. 2.3.

2.5 Encasement Materials

The set of encasement materials (sleeves) employed for the TLD energy response study consisted of ten encasements each of the materials lead, tantalum, tin, zirconium, copper, iron, stainless steel, aluminum, and natural LiF. All sleeves were cylindrical in shape and approximately one-half inch in length. For each encasement, the radial wall mass thickness was nominally 0.7 g/cm^2. The number of sleeves available and their associated physical parameters are presented in Table 2.1.

For the sleeve thickness investigation, the encasements consisted of the same variety of materials discussed above (see Table 2.2). As may be observed, there were a number of different radial wall thicknesses for each encasement material. Also, indicated for each wall thickness is a wall-curvature correction ratio with the associated corrected wall thickness. These corrected thicknesses were calculated to compensate for wall curvature since the encased dosimeters were irradiated using essentially a monodirectional gamma flux. This correction is discussed in much greater detail in Section 5.3. All the sleeves employed during both investigations are shown in Fig. 2.4.

2.6 Gamma Ray Sources

Six sources, purchased from Isotope Products Laboratory, were used for the energy response and sleeve thickness investigations. A com-

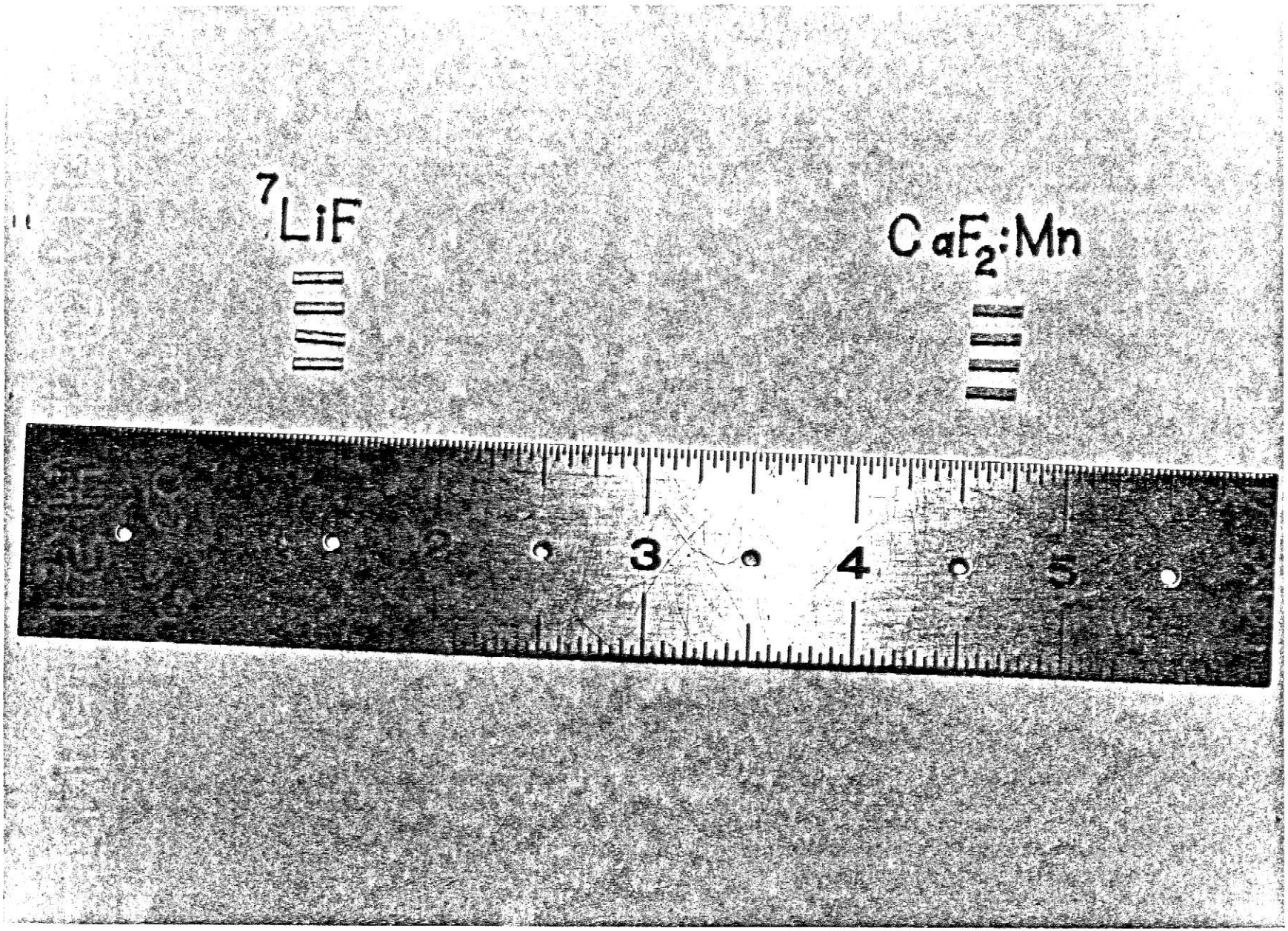

Fig. 2.3. Photograph depicting the types of thermoluminescent dosimeters used for data acquisition.

Table 2.1. Encasement materials used during measurement of the energy response of encased ^{7}LiF and CaF_2:Mn TLDs.

Material	Quantity	Atomic Number	Density (g/cm^3)	Hole Diameter (cm)	Wall Thickness (g/cm^2)
Lead	10	82	11.34	0.151	0.734
Tantalum	10	73	16.60	0.151	0.696
Tin	10	50	7.30	0.151	0.608
Zirconium	10	40	6.50	0.151	0.541
Copper	10	29	8.94	0.163	0.694
Iron	10	26	7.87	0.151	0.656
Stainless Steel	10	--	7.80	0.151	0.693
Aluminum	10	13	2.70	0.151	0.514
LiF	10	--	2.63	0.151	0.483

Table 2.2. Encasement materials used during measurement of the wall thickness effect on the energy response of encased ^{7}LiF and CaF_2 TLDs.

Wall Thickness (g/cm^2)	Hole Diameter (cm)	Wall Curvature Correction Ratio	Corrected Wall Thickness (g/cm^2)
Lead sleeves, Z = 82, Density = 11.34 g/cm^3			
0.734	0.151	1.263	0.927
0.864	0.151	1.236	1.068
1.109	0.151	1.197	1.328
1.440	0.151	1.164	1.676
1.728	0.151	1.144	1.976
2.160	0.151	1.120	2.419
2.592	0.151	1.105	2.863
3.456	0.151	1.082	3.741
4.321	0.151	1.069	4.618
8.641	0.151	1.039	8.975
Tantalum sleeves, Z = 73, Density = 16.60 g/cm^3			
0.338	0.151	1.500	0.507
0.632	0.151	1.361	0.860
0.696	0.151	1.345	0.936
0.845	0.151	1.305	1.103
1.265	0.151	1.236	1.564
1.623	0.151	1.197	1.943
2.108	0.151	1.164	2.454
3.162	0.151	1.120	3.541
Tin sleeves, Z = 50, Density = 7.30 g/cm^3			
0.210	0.151	1.425	0.299
0.302	0.151	1.344	0.406
0.395	0.151	1.296	0.512
0.488	0.151	1.259	0.614
0.580	0.151	1.230	0.713
0.608	0.151	1.223	0.744
0.766	0.151	1.189	0.911
1.322	0.151	1.125	1.487
1.739	0.151	1.101	1.915
2.712	0.151	1.070	2.902

Table 2.2 - continued

Wall Thickness (g/cm^2)	Hole Diameter (cm)	Wall Curvature Correction Ratio	Corrected Wall Thickness (g/cm^2)
Zirconium Sleeves, Z = 40, Density = 6.50 g/cm^3			
0.197	0.151	1.425	0.226
0.269	0.151	1.344	0.362
0.352	0.151	1.296	0.456
0.434	0.151	1.259	0.547
0.517	0.151	1.230	0.632
0.541	0.151	1.223	0.662
0.682	0.151	1.189	0.811
1.177	0.151	1.125	1.324
1.549	0.151	1.101	1.705
2.415	0.151	1.070	2.584
Copper sleeves, Z = 29, Density = 8.94 g/cm^3			
0.257	0.151	1.425	0.366
0.371	0.151	1.344	0.499
0.485	0.151	1.296	0.629
0.599	0.151	1.259	0.754
0.694	0.163	1.243	0.863
0.712	0.151	1.230	0.876
0.747	0.151	1.223	0.914
0.940	0.151	1.189	1.118
1.623	0.151	1.125	1.826
2.135	0.151	1.101	2.382
Stainless steel sleeves, Density = 7.80 g/cm^3			
0.244	0.151	1.425	0.319
0.323	0.151	1.344	0.434
0.422	0.151	1.296	0.547
0.521	0.151	1.259	0.656
0.620	0.151	1.230	0.763
0.693	0.142	1.203	0.834
0.818	0.151	1.189	0.972
1.413	0.151	1.125	1.589
1.858	0.151	1.101	2.046
2.899	0.151	1.070	3.103

Table 2.2 - continued

Wall Thickness (g/cm^2)	Hole Diameter (cm)	Wall Curvature Correction Ratio	Corrected Wall Thickness (g/cm^2)
	Iron sleeves, Z = 26, Density = 7.87 g/cm^3		
0.226	0.151	1.425	0.332
0.362	0.151	1.344	0.438
0.426	0.151	1.296	0.552
0.526	0.151	1.259	0.662
0.626	0.151	1.230	0.770
0.656	0.151	1.223	0.802
0.824	0.151	1.189	0.982
1.425	0.151	1.125	1.603
1.875	0.151	1.101	2.065
2.925	0.151	1.070	3.131
	Aluminum sleeves, Z = 13, Density = 2.70 g/cm^3		
0.069	0.151	1.450	0.100
0.103	0.151	1.360	0.140
0.137	0.151	1.305	0.179
0.171	0.151	1.264	0.216
0.206	0.151	1.237	0.255
0.274	0.151	1.193	0.327
0.343	0.151	1.164	0.399
0.514	0.151	1.120	0.576
0.686	0.151	1.096	0.752
1.028	0.151	1.069	1.099
1.371	0.151	1.054	1.445
	LiF Sleeves[a], Density = 2.63 g/cm^3		
0.483	0.151	1.335	0.645
0.870	0.151	1.075	0.935

[a]Three sleeves of each size.

THIS BOOK CONTAINS NUMEROUS PAGES WITH DIAGRAMS THAT ARE CROOKED COMPARED TO THE REST OF THE INFORMATION ON THE PAGE.

THIS IS AS RECEIVED FROM CUSTOMER.

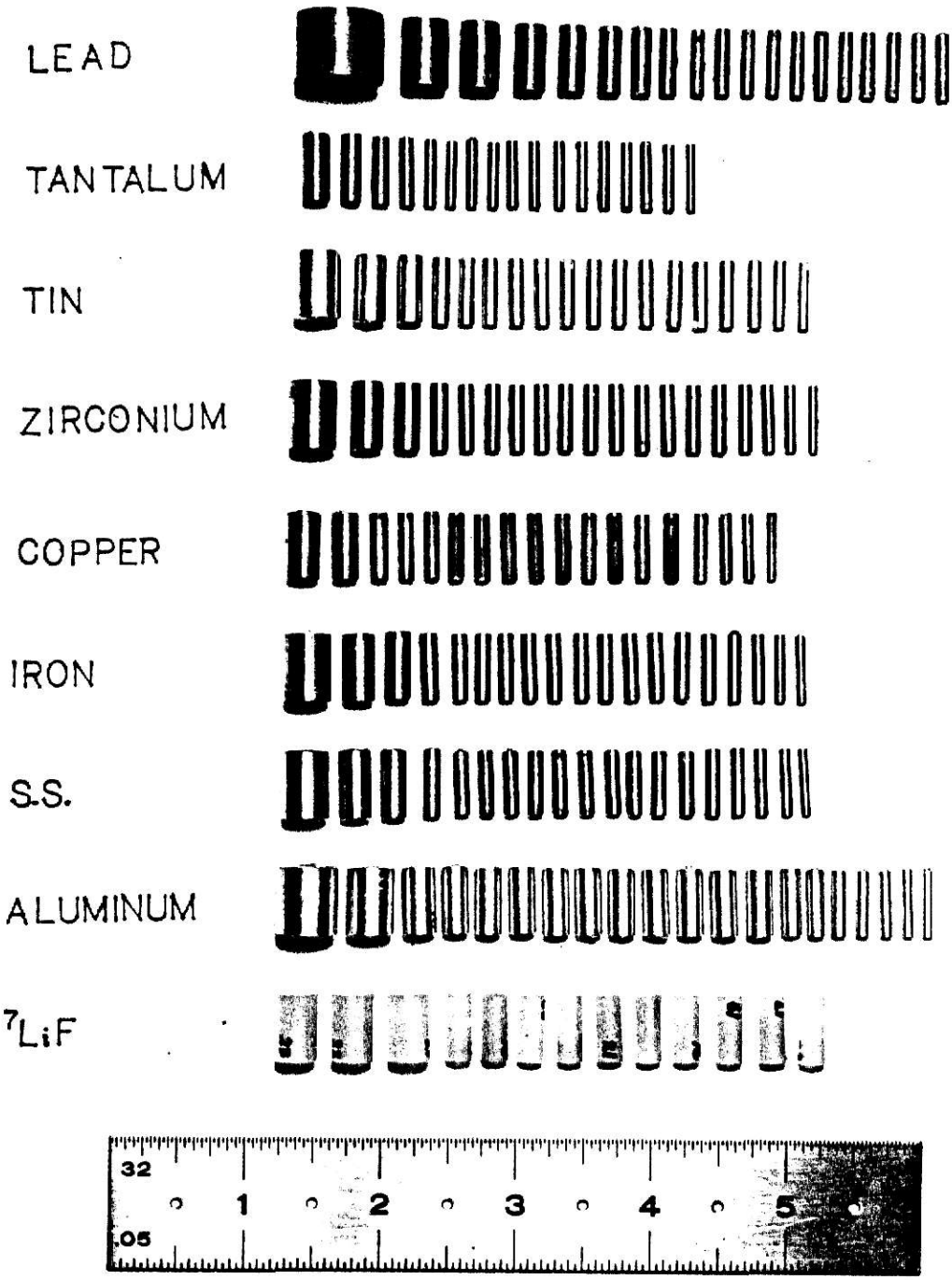

Fig. 2.4. Photograph of TLD sleeves used during data acquisition.

prehensive listing of the sources, along with their half-lives, gamma energies, and activities is presented in Table 2.3. As may be noted, at the time of calibration, each source had an activity of nominally 5 mCi.

Each source was sealed in a capsule of the type illustrated in Fig. 2.5. This style of capsule was selected since the effective gamma emitter volume was small. It was, therefore, possible to characterize the sources using the point source approximation. It may also be noted that the radial thickness of the wall surrounding the source materials was only 6 mils. A thin cladding wall was desirable to minimize radial attenuation of the primary gammas.

2.7 Irradiation Device

A special device was designed and constructed for irradiating the encased TLDs. As shown in Fig. 2.6, it consisted of a 4 ft x 4 ft x 1 in styrofoam platform suspended from the floor by nylon support cords. Styrofoam was selected to minimize direct gamma-ray backscatter from the irradiation device. The platform could be suspended at elevations of three to seven feet. Hence, when elevated for irradiations, the platform was removed from all solid surfaces by a minimum distance of 7 feet. A styrofoam receptacle was located at the center of the platform to support the gamma sources. Circular indentations were placed on the styrofoam surface with radii ranging from 5 to 30 cm in 5 cm increments. Therefore, individual dosimeters could be placed at various known positions from the sources during the irradiations.

Table 2.3. Gamma-ray sources purchased for use in the TLD energy response and sleeve thickness studies.

Nuclide	Half-life	Gamma-ray Energy (MeV)	Activity (mCi)	Calibration Date
Co-57	270 day	0.122, 0.136	5.26 ± 0.53	7/18/79
Ce-141	32.5 day	0.145	6.40 ± 0.64	7/18/79
Hg-203	47 day	0.279	5.15 ± 0.52	7/18/79
Sn-113	115 day	0.393	5.86 ± 0.59	8/01/79
Cs-137	30 yr	0.662	5.27 ± 0.21	8/01/79
CO-60	5.3 yr	1.173, 1.333	5.06 ± 0.23	8/01/79

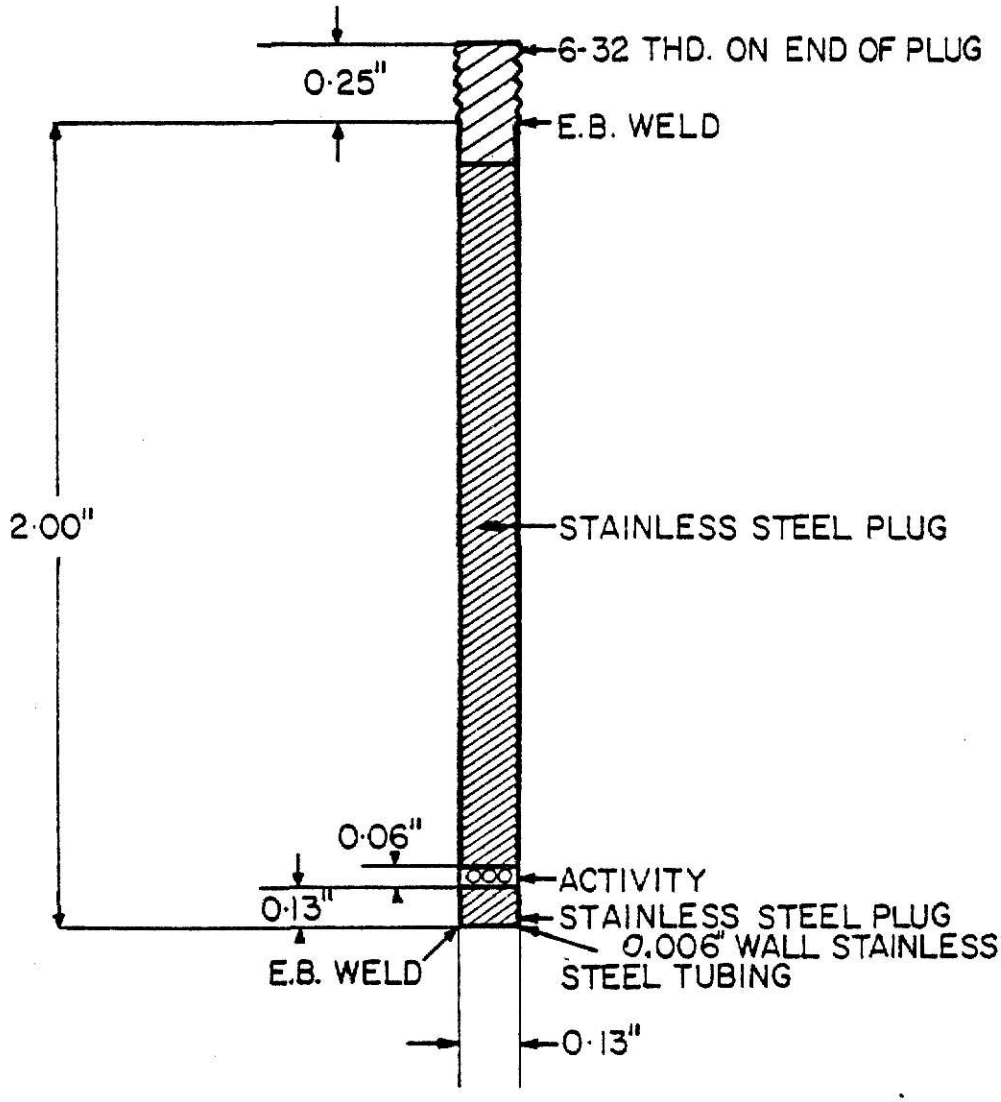

Fig. 2.5. Gamma-ray source capsule for the TLD energy response and sleeve thickness studies.

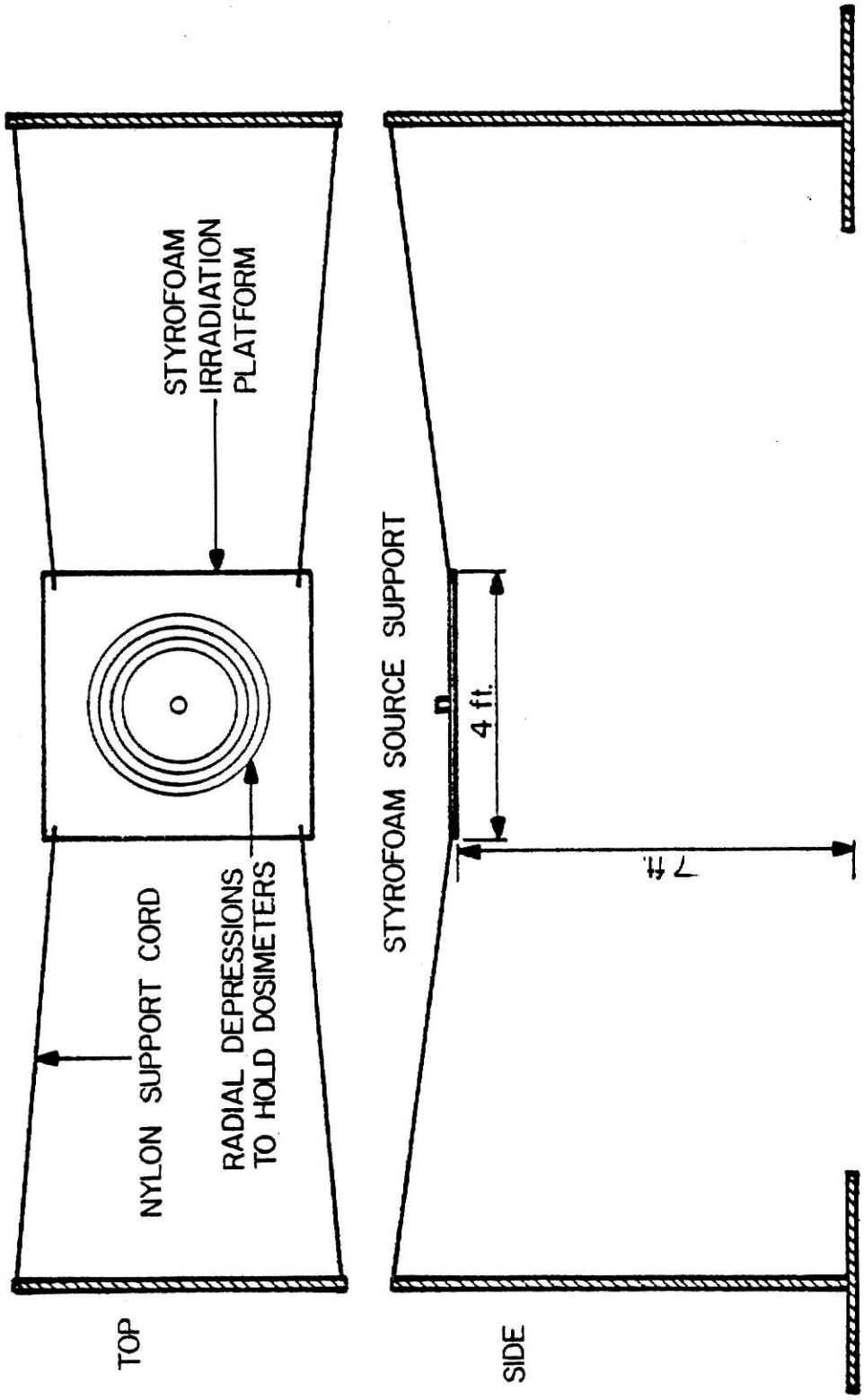

Fig. 2.6. Device designed for irradiating thermoluminescent dosimeters (TLDs).

3.0 EXPERIMENTAL PROCEDURES

Establishment and adherence to a good experimental procedure was necessary for acquisition of high precision data. Incorporated into this procedure were methods that had previously proven successful[17,20]. These methods included systematic processes for TLD handling, preannealing, encapsulation, calibration, exposure/wait/readout schedule, sensitivity selection, and response measurement.

3.1 TLD Handling

During handling of the TLDs, care was taken to never touch the dosimeters with the hands or fingers. Doing so would have contaminated the TLD surfaces and hence, could have affected the corresponding response characteristics. As a result of this precaution, the dosimeters were always maneuvered using the plastic tipped tweezers discussed in Section 2.3.

In order to maintain its identity, when not in use, each TLD was stored in its own numbered coin envelope. To remove the TLDs from the envelopes, the dosimeters were gently dropped onto clean sheets of tissue. This procedure protected the brittle TLDs from fracture or chipping upon striking a hard surface.

3.2 TLD Preannealing

Pre-irradiation annealing of the TLDs was performed with the use of the following sequence: (1) the dosimeters were placed in the pyrex petri dishes in such a manner to maintain individual identity,

(2) heated at 400°C for one hour, (3) cooled in the draft free drawer for ten minutes, (4) heated for two hours at 100°C, and (5) again placed in the draft free drawer to cool to room temperature.

3.3 TLD Calibration

A limited exposure-response calibration was performed for both the ^{7}LiF and CaF_2:Mn TLDs. The calibrations included the range of dosimeter radiation doses that were expected to be employed during the energy response and sleeve-thickness investigations. Results for the two dosimeter types, covering a TLD dose range of 0.2 to 3.0 rads, are illustrated in Figs. 3.1 and 3.2. As is observed, each set of data was fit with a least squares line which in both cases, indicate approximately zero response for zero radiation exposure. The correlation coefficients corresponding to these lines were nominally unity, indicating that for the dose regions studied, both dosimeter types responded linearly as a function of gamma dose.

3.4 TLD Encapsulation

For both the energy response and the sleeve-thickness effects studies, an exacting encapsulation method was followed. This method included loading the dosimeters into the encapsulations (sleeves) using the handling procedure discussed in Section 3.1. Plugs, fabricated from the same material as the sleeves, were then fitted into the openings at the ends of the encasements. Therefore, the TLDs were completely surrounded by the desired sleeve materials. The identity of each

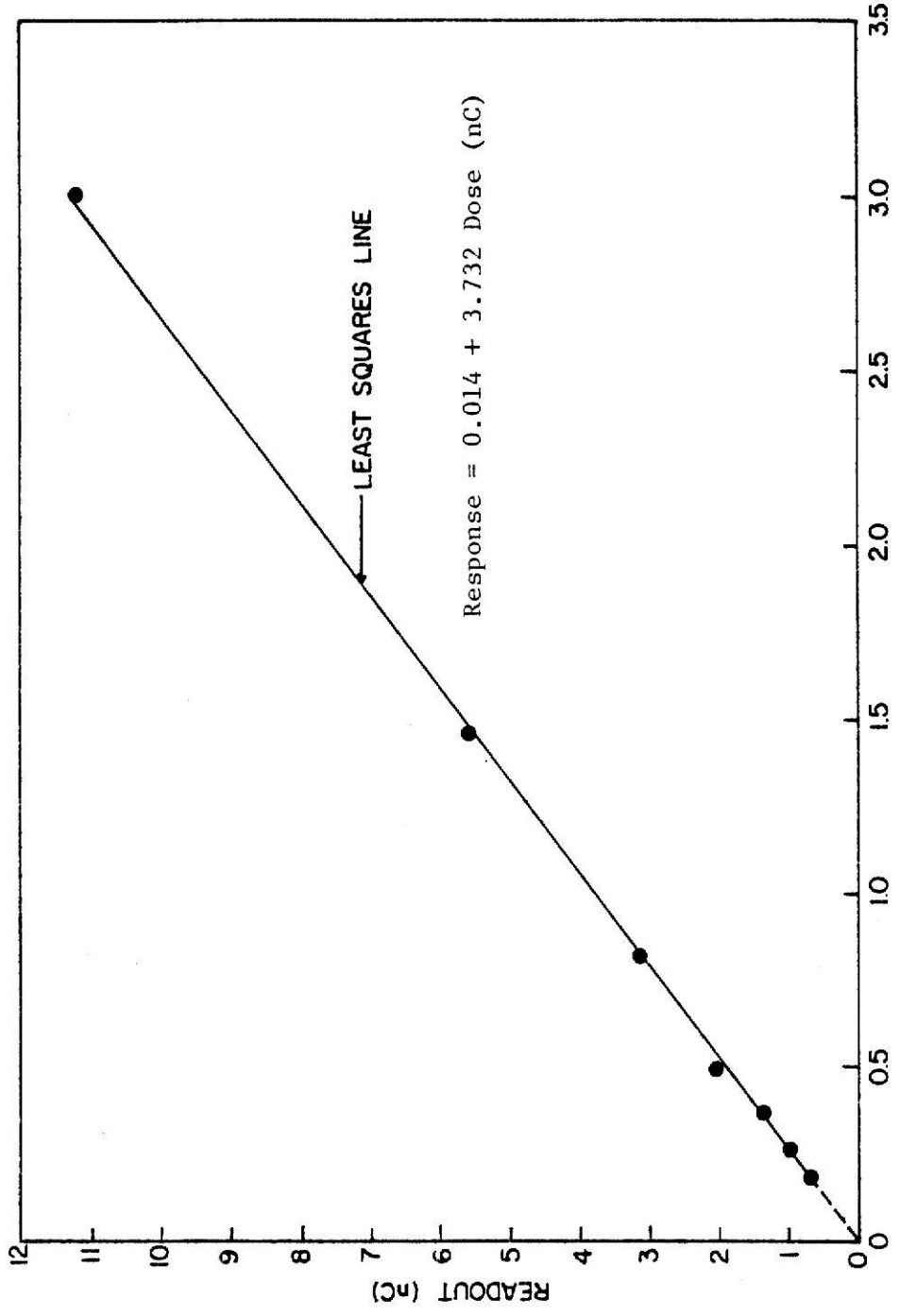

Fig. 3.1. Calibration curve for 1x1x6 mm ^{7}LiF thermoluminescent dosimeters irradiated by a nominal 3.2 mCi Cs-137 source.

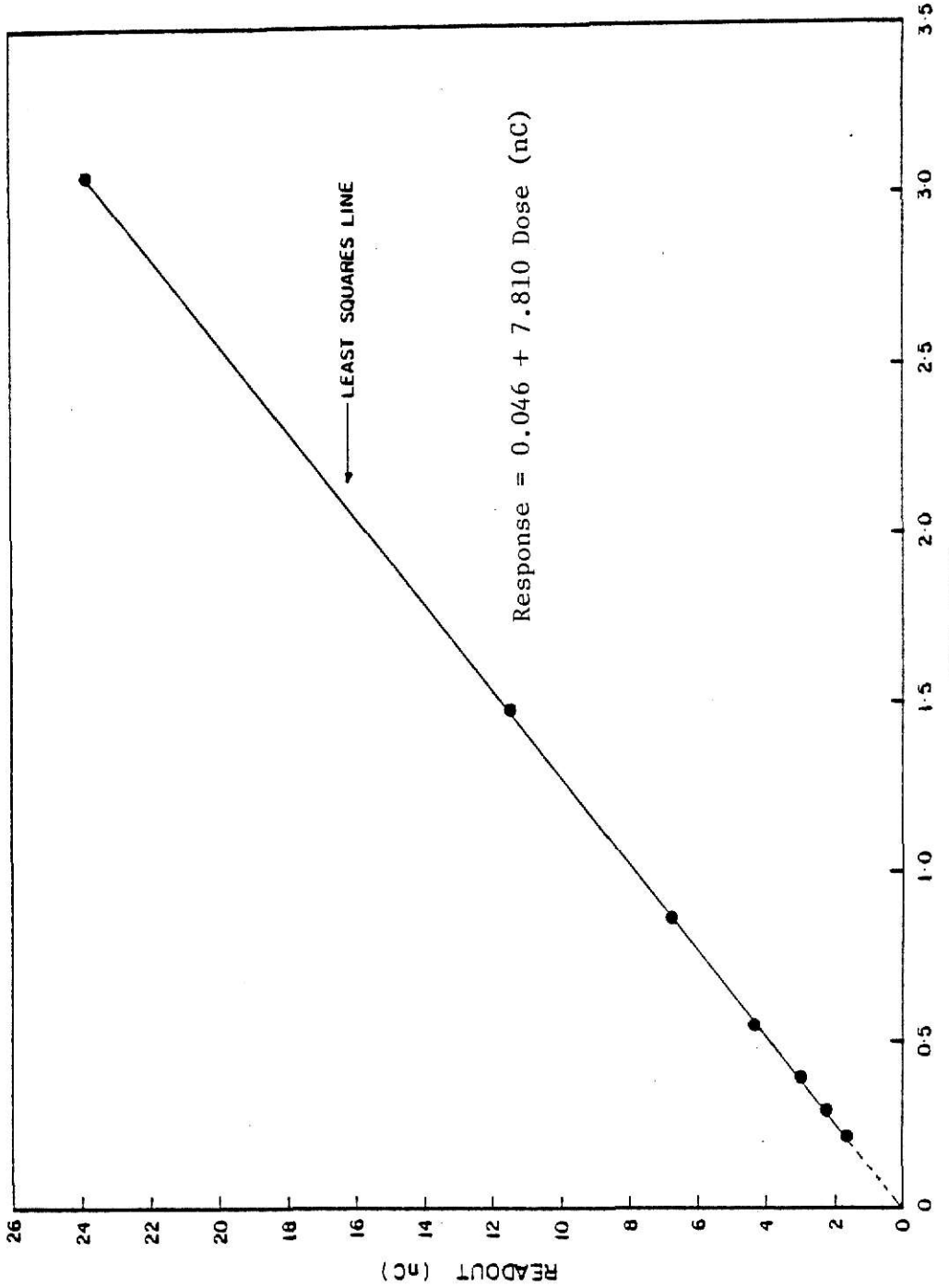

Fig. 3.2. Calibration curve for 1x1x6 mm CaF_2:Mn thermoluminescent dosimeters irradiated by a nominal 3.2 mCi Cs^{137} source.

dosimeter was always maintained throughout the encasing process.

To prevent contaminating the surface of the TLDs, the entire collection of sleeves was rinsed with acetone. This removed any residual oils or foreign particles that may have been present within the encasements.

3.5 Exposure/Wait/Response Measurement Schedule

To prepare for each radiation exposure, the individual sets of encased TLDs were placed at known concentric positions on the irradiation device discussed in Section 2.7. Each dosimeter was arranged with its axis perpendicular to the gamma source receptacle. Once the dosimeters were in place, the desired gamma source was positioned in this receptacle which was located at the center of the irradiation device. The device was then suspended at an elevation of seven feet for the duration of each exposure. For the individual irradiations, the sets of dosimeters were exposed in a dark room for periods of time ranging from several hours to several weeks. Doses obtained ranged from nominally 0.5 to 5.0 rads. The background radiation dose received by the TLDs during the gamma exposures, was assumed to be negligible. This dose was normally less than one percent of the total.

Upon completion of each irradiation, the TLDs were placed in envelopes and stored for nominally twenty-four hours before individual TLD responses were measured. The purpose of this delay was to allow for the disintegration of the low energy traps that were present in the exposed TLDs. At room temperatures, these traps decay and emit their associated photons. If the dosimeters were processed immediately

after exposure, these decaying traps would have introduced a time dependent systematic error.

Also, the dosimeters were always kept in a dark environment, between exposure and readout, by storing the TLDs in a dark drawer. This measure was a precaution to guard against the troublesome light induced fading associated with the dosimeters. Incandescent lighting was used during the time lapse between the removal of the TLDs from the dark environment and TLD readout.

3.6 TLD Response Measurement Procedure

A systematic procedure was strictly adhered to for the measurement of each TLD response. This procedure consisted of a four minute readout cycle with the following steps: (1) at time t=0 the total TLD response was measured, then (2) at t=1.5 min the TLD background response was measured, (3) at t=3.0 min the dosimeter was replaced with a new TLD, followed by (4) a new readout cycle beginning at t=4.0 min. Net dosimeter responses were obtained by subtracting the second measurement (background TL response) from the first for each respective TLD. Nominally, the background response ranged from 0.1 to 10% of the first reading.

As mentioned in Section 2.1, the Harshaw Model 2000 analyzer was employed throughout the energy response study. The equipment settings used for the TLD readout process are listed in Table 3.1. Also, the temperature profiles, utilized for the response measurement of the ^{7}LiF and CaF_2:Mn dosimeters, are depicted in Figs. 3.3 and 3.4, respectively. A 30 sec response integration period was utilized for both types of

Table 3.1. Analyzer settings used for the response measurement of the ^{7}LiF and CaF_2:Mn TLDs.

Analyzer Control	Harshaw 2000 Analyzer		Photon Counting Analyzer
	^{7}LiF	CaF_2:Mn	CaF_2:Mn
High Voltage	500 V	600 V	2200 V
Ammeter Range	Automatic	Automatic	--
X0.1/X1 Range	X1	X1	--
Meter Selection	Current	Current	--
[a]Period	30 sec	30 sec	--
[b]Period	40 sec	40 sec	--
Current Suppression	3 pA	3 pA	--
N_2 Gas Flow Rate	--	--	20% Maximum
CO_2 Gas Flow Rate	10 ft^3/h	10 ft^3/h	--

[a]Heating cycle period used for the TLD energy response study.

[b]Heating cycle period used for the sleeve thickness effects study.

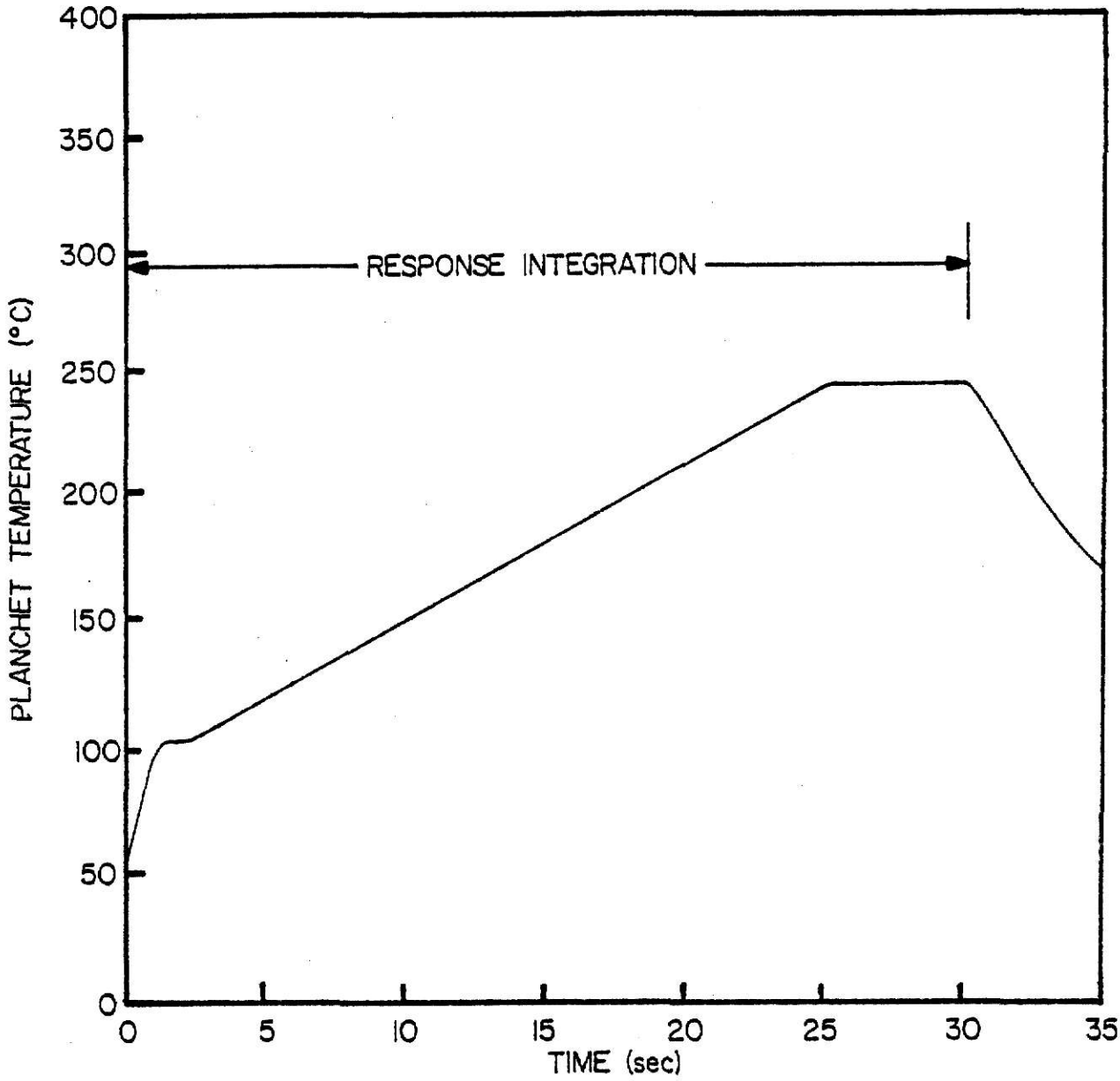

Fig. 3.3. Heating cycle used for the response measurement of the ^{7}LiF TLDs during the TLD energy response study.

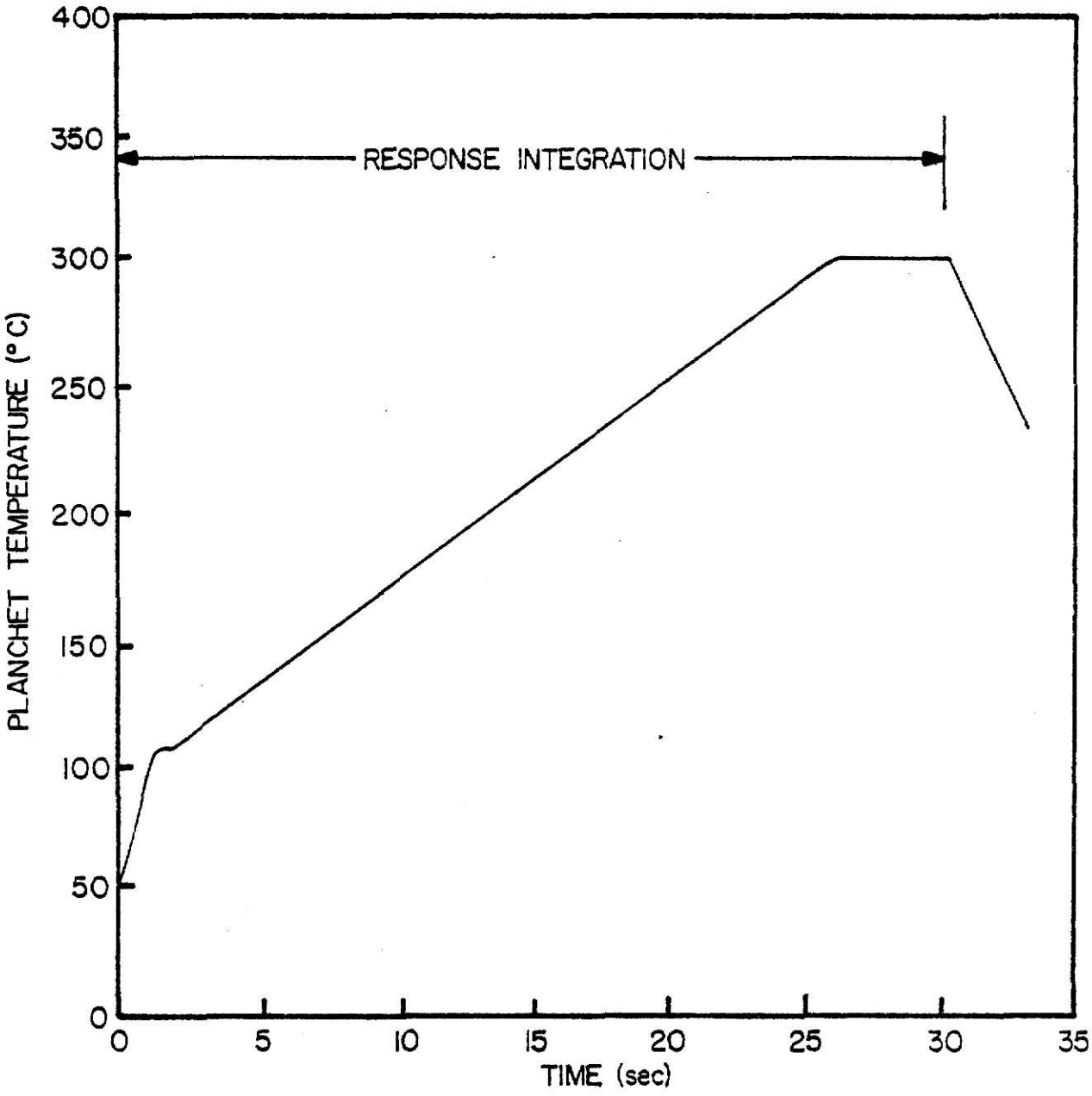

Fig. 3.4. Heating cycle used for the response measurement of the CaF_2:Mn TLDs during the TLD energy response study.

TLDs. In both cases, the start of this period was in sequence with the dosimeter heating cycle.

For the sleeve-thickness effects study, both the Harshaw 2000 and the photon detection systems were utilized. The employed analyzer settings are also listed in Table 3.1. Further information concerning the operation of the photon system is contained in Ref. 19. Additionally, the temperature profiles utilized for the sleeve thickness response measurements are depicted in Figs. 3.5 and 3.6. As may be noted in these figures, the response integration ranges for the two dosimeter types differed somewhat. For the response measurement of the ^{7}LiF TLDs, the integration period was initiated in sequence with the TLD heating cycle reaching 100°C. The cycle was terminated upon reaching 300°C. In a corresponding manner, the CaF_2:Mn period was initiated at 150°C and terminated at 350°C.

Typical glow curves for the ^{7}LiF and CaF_2:Mn TLDs are shown in Figs. 3.7 and 3.8, respectively. For the ^{7}LiF material, the response rate peaks out at a temperature of approximately 185°C. Correspondingly, for CaF_2:Mn the maximum occurs at approximately 250°C.

3.7 Sensitivity Selection

Intra-batch sensitivity selections were performed to improve the precision of all acquired data. For both types of TLDs, this procedure involved the irradiation of sets of nominally 200 dosimeters at one time. The response was measured for each dosimeter following a 24 hr wait period. A typical result for ^{7}LiF is depicted by Fig. 3.9.

After the individual responses were obtained, each dosimeter set was randomly divided into subgroups of 100 TLDs. For these subgroups, individual dosimeter identification numbers and response readings were input into the Sort and Dose computer code (written by Dr. G. G. Simons). This code numerically sorted the TLDs as to their relative sensitivity. Each dosimeter was also assigned a sensitivity ratio. This quantity was, in effect, the ratio of an individual TLD's reading to its respective group mean response. For a given group, it was not uncommon for these ratios to deviate from unity by as much as 20%.

Precision subsets were then obtained from the subgroups, in terms of TLD identification number and relative sensitivity. For these subsets, each TLD's relative sensitivity was nominally within $\pm$ 6% of the sort group mean. Dosimeters with readings outside of this range were not used for data acquisition. The selection of the 6% figure was not based on any rigorous statistical considerations but rather, was chosen because it guaranteed large enough precision subsets for the individual encased dosimeter irradiations. The sort data, utilized for both the energy response and the sleeve thickness studies, are tabulated in Appendix C.

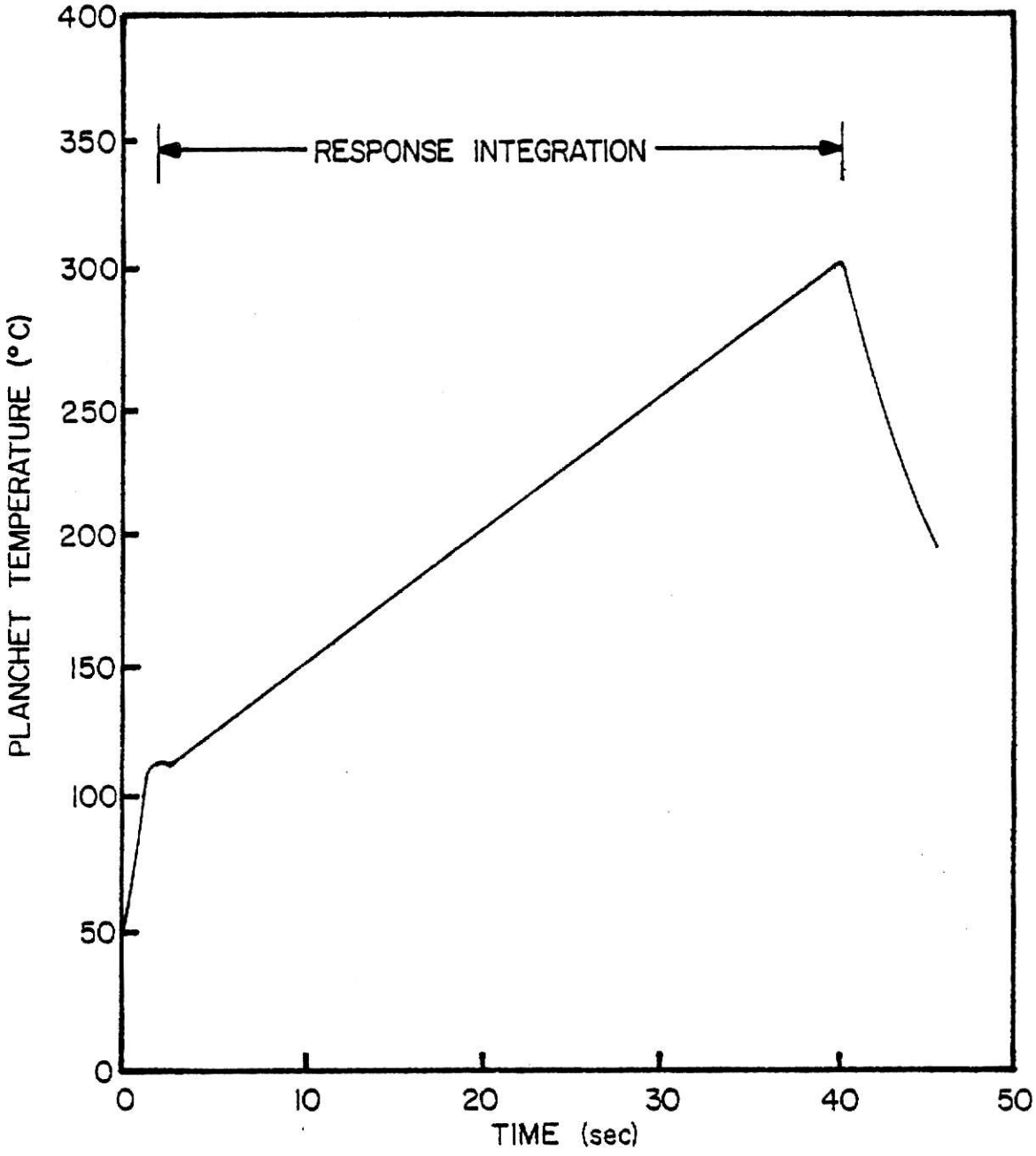

Fig. 3.5. Heating cycle used for the response measurement of the ^{7}LiF TLDs during the sleeve thickness effects study.

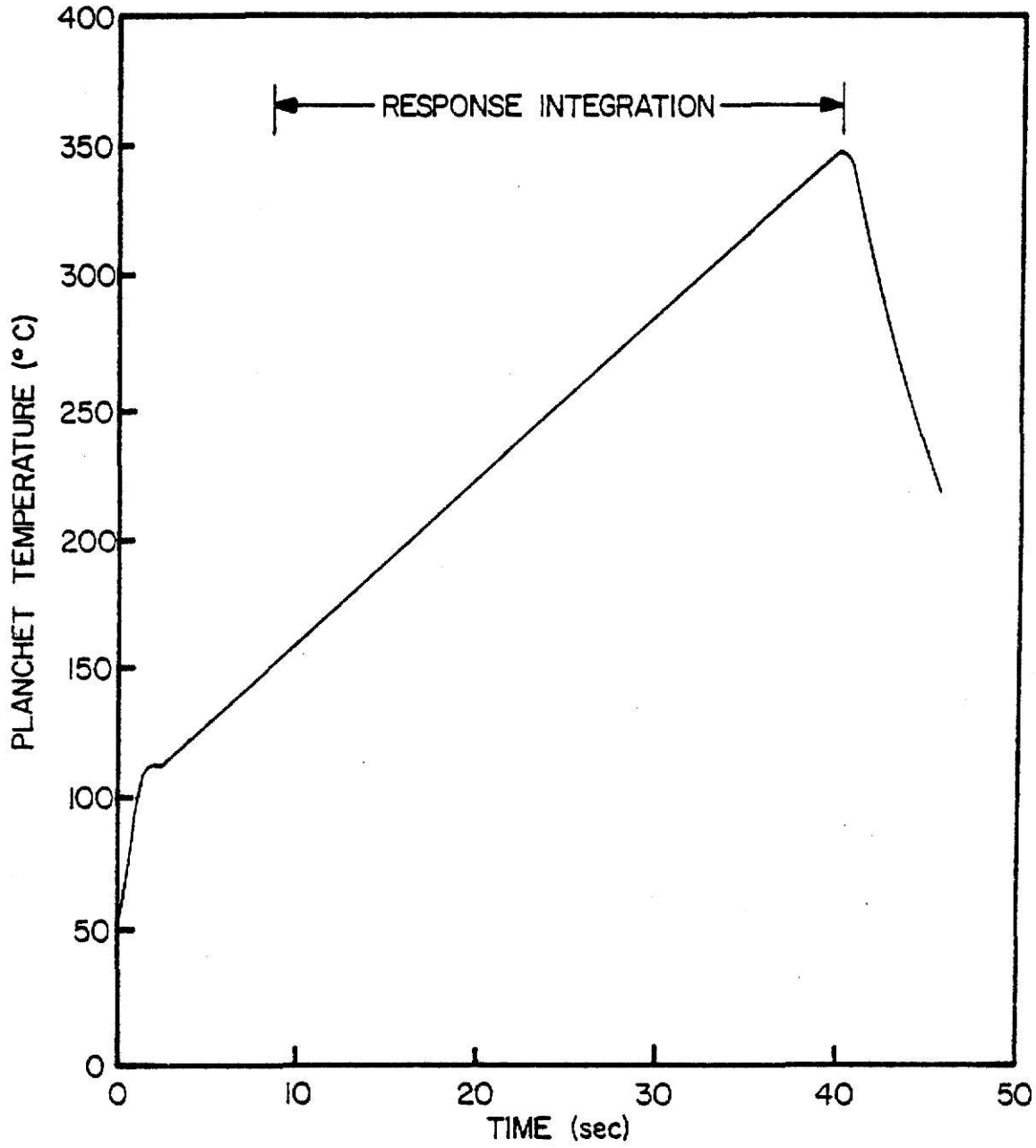

Fig. 3.6. Heating cycle used for the response measurement of the CaF_2:Mn TLDs during the sleeve thickness effects study.

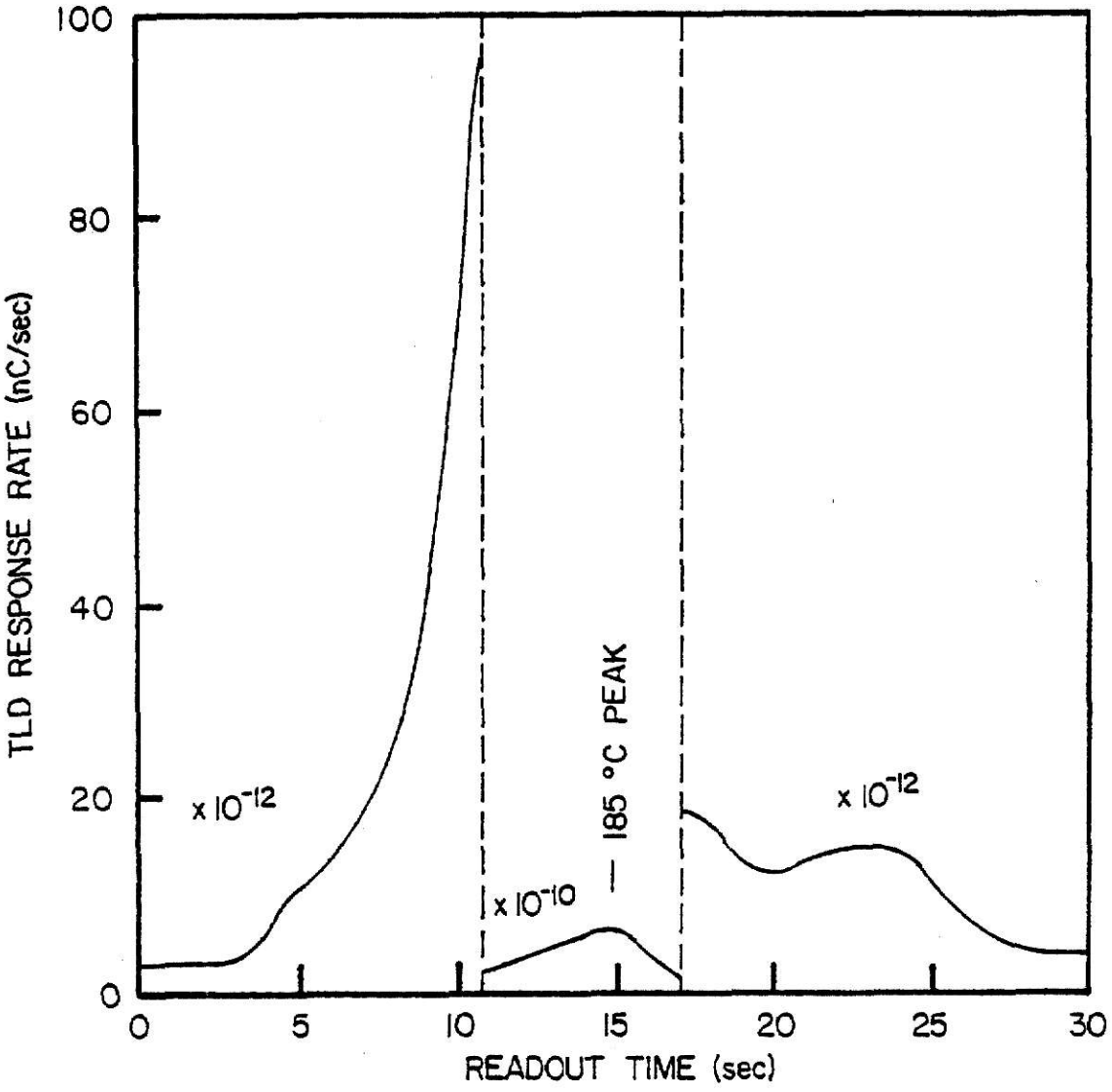

Fig. 3.7. Typical glow curve for ^{7}LiF TLDs with the TLD temperature corresponding to the maximum response rate indicated.

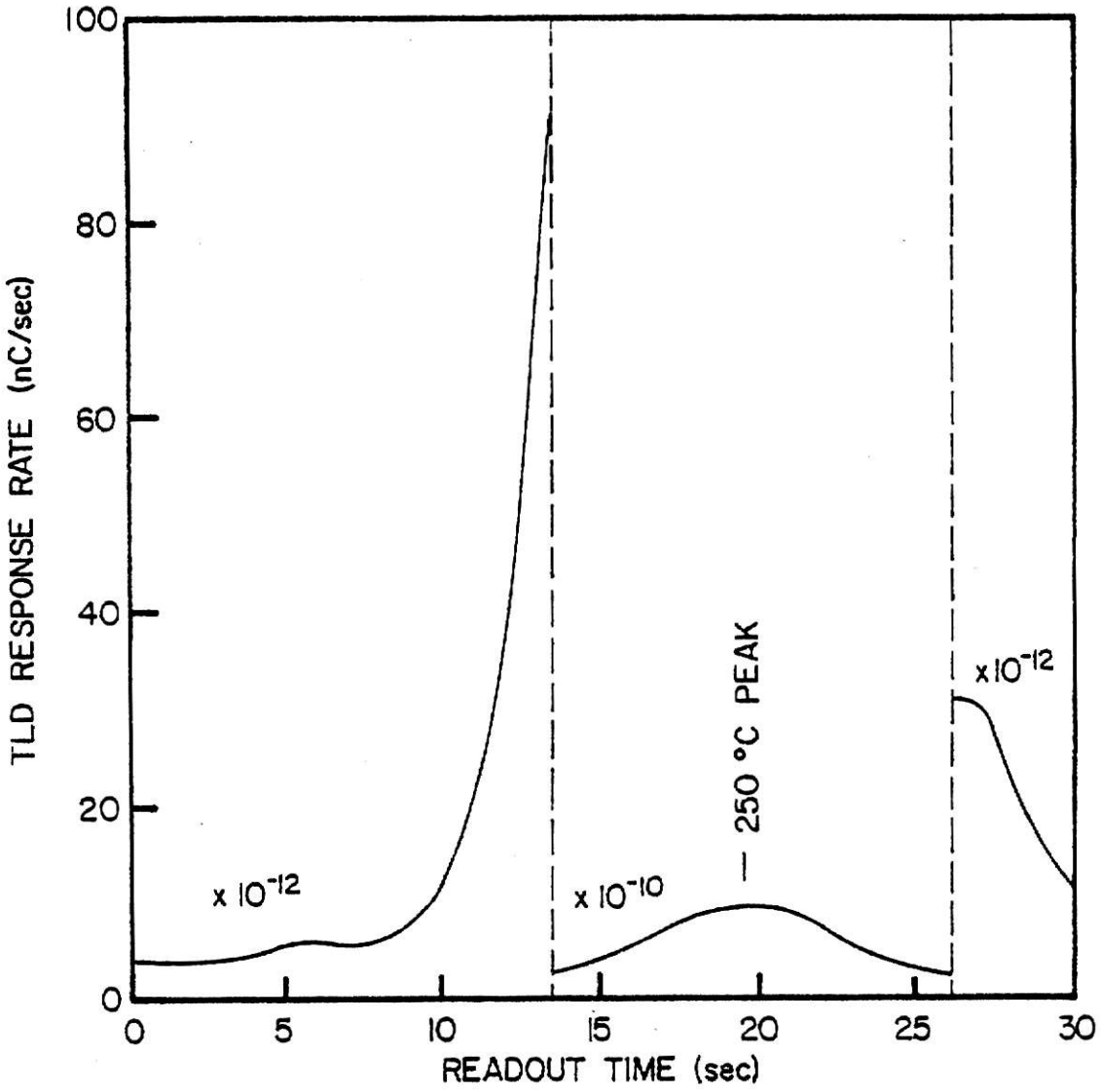

Fig. 3.8. Typical glow curve for the CaF_2:Mn TLDs with the TLD temperature corresponding to the maximum response rate indicated.

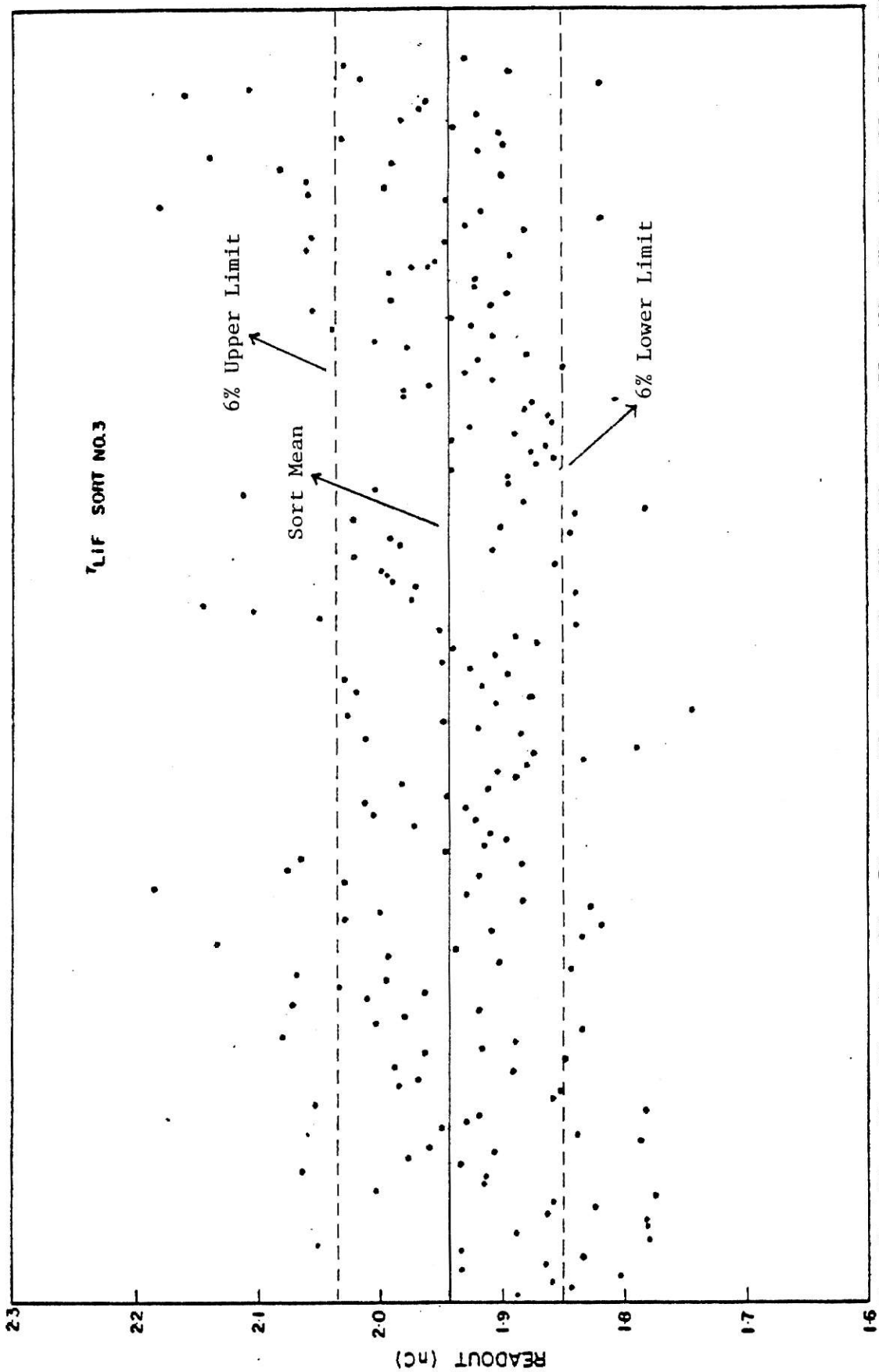

Fig. 3.9. Typical sensitivity data measured for ^{7}LiF TLDs exposed to a 3.2 mCi Cs-137 gamma-ray source.

4.0 EXPERIMENTAL RESULTS

4.1 TLD Energy Response Results

For the energy response study, CaF_2:Mn and ^{7}LiF TLDs were encased in lead, tantalum, tin, zirconium, copper, stainless steel, iron, aluminum, and natural LiF. These encapsulated TLDs were exposed to gamma-rays with energies ranging from 0.122 to 1.333 MeV. TLD, sleeve, and source characteristics were discussed in Sections 2.4, 2.5, and 2.6 respectively.

For each irradiation, ninty TLDs of one type were encapsulated within the nine types of sleeve materials listed in Table 2.1. This created nine groups of ten identically encased dosimeters. The TLDs employed for each irradiation were chosen from one of the precision subsets. To minimize systematic errors, they were selected in such a manner that every ninth dosimeter, based upon its relative sensitivity, was encapsulated in one type of encasement.

Upon the completion of each irradiation, the individual TLD responses were measured and recorded. The raw TL data were then processed to obtain the average TLD response for each sleeve material (see Appendix C). Since this study was based upon the relative response of encapsulated TLDs, each averaged reading was normalized to the appropriate average value obtained for the iron encased dosimeters. Normalized data for both the ^{7}LiF and CaF_2:Mn TLDs, are presented in Tables 4.1 and 4.2, respectively.

It is observed that in general, the ^{7}LiF results show marked trends. The ratios tend to increase with increasing Z number and decreasing

Table 4.1. TLD analyzer output normalized to iron encased ^{7}LiF TLDs from a precision subset.

Sleeve Material	Z	Normalized TLD readout ± $\sigma_{\bar{x}}$					
		Gamma-ray Energy (MeV)					
		0.136 (11%) 0.122 (87%)	0.145	0.279	0.393	0.662	1.173 (100%) 1.333 (100%)
Lead	82	0.486±0.010	0.508±0.008	1.559±0.018	1.657±0.025	1.613±0.029	1.354±0.020
Tantalum	73	0.520±0.016	0.612±0.021	1.485±0.024	1.487±0.025	1.396±0.023	1.245±0.023
Tin	50	1.041±0.013	1.156±0.020	1.259±0.016	1.185±0.012	1.077±0.015	1.086±0.020
Zirconium	40	1.168±0.014	1.182±0.014	1.128±0.017	1.091±0.017	1.058±0.013	1.051±0.012
Copper	29	0.955±0.020	1.001±0.014	1.037±0.015	0.985±0.012	0.976±0.010	0.997±0.012
Iron	26	1.000±0.010	1.000±0.015	1.000±0.014	1.000±0.009	1.000±0.013	1.000±0.013
S.S.	--	0.992±0.014	0.971±0.016	1.007±0.012	1.002±0.012	1.005±0.015	0.994±0.014
Aluminum	13	0.922±0.012	0.987±0.014	0.970±0.019	0.997±0.012	0.981±0.013	0.974±0.015
LiF	--	0.918±0.015	1.022±0.014	0.982±0.016	1.019±0.009	0.987±0.016	0.959±0.016

Table 4.2. TLD analyzer output normalized to iron encased CaF_2:Mn TLDs from a precision subset.

Sleeve Material	Z	Normalized TLD Readout ± $\sigma_{\bar{x}}$					
		Gamma-ray Energy (MeV)					
		0.136 (11%) 0.122 (87%)	0.145	0.279	0.393	0.662	1.173 (100%) 1.333 (100%)
Lead	82	0.401±0.008	0.523±0.008	1.262±0.018	1.526±0.024	1.464±0.021	1.380±0.019
Tantalum	73	0.492±0.019	0.660±0.012	1.204±0.021	1.412±0.016	1.319±0.015	1.306±0.025
Tin	50	0.999±0.015	1.088±0.013	1.103±0.014	1.149±0.021	1.074±0.016	1.133±0.012
Zirconium	40	1.002±0.019	0.989±0.022	1.016±0.016	1.082±0.019	1.062±0.014	1.048±0.017
Copper	29	0.977±0.016	0.952±0.007	0.987±0.015	1.002±0.015	0.986±0.010	1.072±0.017
Iron	26	1.000±0.018	1.000±0.010	1.000±0.015	1.000±0.017	1.000±0.013	1.000±0.016
S.S.	--	1.002±0.015	0.995±0.012	0.982±0.014	1.006±0.015	1.009±0.012	1.002±0.014
Aluminum	13	1.022±0.015	--	0.987±0.012	--	1.001±0.011	1.003±0.016
LiF	--	1.005±0.015	--	1.017±0.016	--	1.005±0.015	1.004±0.015

gamma energy. However, for the case of the high Z encasements and low energy gammas, the ratios tend to decrease. This presents an effective span of ratios ranging from 0.486 to 1.657. It is likewise noted that for the normalized results, the standard deviation of the means have a range of 1.0 to 3.5%.

The normalized CaF_2:Mn responses exhibit trends similar to those for ^7LiF. Except in this case, the effective span of ratios ranges from 0.401 to 1.526. It is also observed that the range of the standard deviation of the means, 1.0 to 2.5%, is somewhat smaller than the ^7LiF equivalent.

A second data reduction technique, based upon the relative sensitivity of the individual TLDs, was also utilized for data processing. It consisted of dividing the individual TLD responses by the associated dosimeter sensitivity ratios. After application of the ratios, the data were processed in the same manner as indicated for the non-sensitivity corrected results. The purpose for using the ratios, was to effectively force the relative sensitivity of each TLD to that of the precision subsets. For both types of TLDs, the corrected results are illustrated in Tables 4.3 and 4.4.

The trends and magnitudes of the normalized results remained nearly unchanged, with the application of the sensitivity ratios. But, the standard deviation of the means were reduced. For the ^7LiF results, the nominal upper limit was lowered from 3.5 to 2.5%. This then created a new span of deviations ranging from 1.0 to 2.5%. Both nominal limits were reduced for the CaF_2:Mn data. These changes were from 1.0 to 0.50,

Table 4.3. TLD analyzer output normalized to iron encased ^{7}LiF TLDs corrected for individual sensitivity.

Sleeve Material	Z	Normalized Sensitivity Corrected TLD Readout ± $\sigma_{\bar{x}}$					
		Gamma-ray Energy (MeV)					
		0.136 (11%) 0.122 (87%)	0.145	0.279	0.393	0.662	1.173 (100%) 1.333 (100%)
Lead	82	0.484±0.009	0.504±0.008	1.543±0.027	1.634±0.020	1.604±0.020	1.337±0.018
Tantalum	73	0.521±0.008	0.606±0.016	1.472±0.026	1.474±0.022	1.391±0.016	1.231±0.015
Tin	50	1.042±0.016	1.155±0.014	1.251±0.022	1.178±0.012	1.076±0.014	1.078±0.016
Zirconium	40	1.171±0.014	1.186±0.013	1.122±0.023	1.093±0.013	1.063±0.012	1.047±0.015
Copper	29	0.978±0.013	0.999±0.012	1.032±0.018	0.993±0.010	0.976±0.013	0.991±0.013
Iron	26	1.000±0.014	1.000±0.010	1.000±0.022	1.000±0.012	1.000±0.012	1.000±0.013
S.S.	--	0.990±0.014	0.967±0.011	1.001±0.018	1.001±0.017	1.008±0.011	0.992±0.013
Aluminum	13	0.924±0.012	0.985±0.010	0.966±0.018	0.993±0.012	0.982±0.011	0.970±0.013
LiF	--	0.919±0.012	1.021±0.010	0.982±0.017	1.020±0.012	0.995±0.012	0.959±0.011

Table 4.4. TLD analyzer output normalized to iron encased CaF_2:Mn TLDs corrected for individual sensitivity.

Sleeve Material	Z	Normalized Sensitivity Corrected TLD Readout ± $\sigma_{\bar{x}}$					
		Gamma-ray Energy (MeV)					
		0.136 (11%) 0.122 (87%)	0.145	0.279	0.373	0.662	1.173 (100%) 1.333 (100%)
Lead	82	0.408±0.005	0.521±0.008	1.255±0.010	1.508±0.011	1.450±0.011	1.376±0.014
Tantalum	73	0.488±0.006	0.658±0.010	1.193±0.011	1.399±0.014	1.309±0.012	1.297±0.016
Tin	50	0.995±0.009	1.086±0.018	1.095±0.007	1.142±0.016	1.065±0.012	1.127±0.013
Zirconium	40	1.000±0.007	1.029±0.007	1.015±0.008	1.084±0.009	1.065±0.011	1.051±0.010
Copper	29	0.974±0.006	0.949±0.007	0.981±0.008	0.998±0.009	0.983±0.014	1.068±0.011
Iron	26	1.000±0.008	1.000±0.005	1.000±0.006	1.000±0.007	1.000±0.009	1.000±0.012
S.S.	--	1.001±0.010	0.994±0.004	0.978±0.007	1.006±0.009	1.008±0.010	1.002±0.011
Aluminum	13	1.020±0.008	--	1.009±0.013	--	0.999±0.013	1.001±0.010
LiF	--	1.007±0.009	--	1.008±0.013	--	1.009±0.010	1.005±0.011

and from 2.5 to 2.0% for a new nominal deviation range of 0.5 to 2.0%.

4.2 Sleeve Thickness Effects Results

For the sleeve thickness study, CaF_2:Mn and ^7LiF TLDs were encased in the same nine materials investigated during the energy response study. These encapsulated TLDs were irradiated using gamma rays with energies ranging from 0.122 to 1.333 MeV. The sleeve and source characteristics were discussed in Sections 2.4 and 2.6 respectively.

For each individual irradiation, eighty-six dosimeters of one type were encased using the sleeves listed in Table 2.2. For each of the material types, data were obtained for a variety of sleeve wall thicknesses. The TLDs used for this investigation were those employed during the energy response study. Prior to their use, these dosimeters were preannealed. The TLDs used during each irradiation were selected from the precision subsets. Also, the corresponding sensitivity ratios were applied to each TLD's post-irradiation measured response. These responses are plotted versus the curvature corrected wall thicknesses in Figs. 4.1-4.12.

To facilitate the generation of the effective attenuation coefficients, which are discussed in Section 5.3, the sleeve thickness data were least squares fit to a straight line. These fits were to the natural log of the TLD responses as a function of curvature corrected wall thicknesses. The correlation coefficients corresponding to the least squares fits, nominally ranged from 0.7 to unity.

For both the ^7LiF and CaF_2:Mn data, the slopes of the lines tend to increase as a function of increasing Z number and decreasing gamma

energy. This phenomenon is due to the sleeve attenuation of the primary gammas. For the lower Z number materials, these slopes are nominally zero for all gamma energies. The slopes are also small for the higher energy gammas, and all the various Z number materials. This would effectively indicate that the attenuation for the last two sited cases is small.

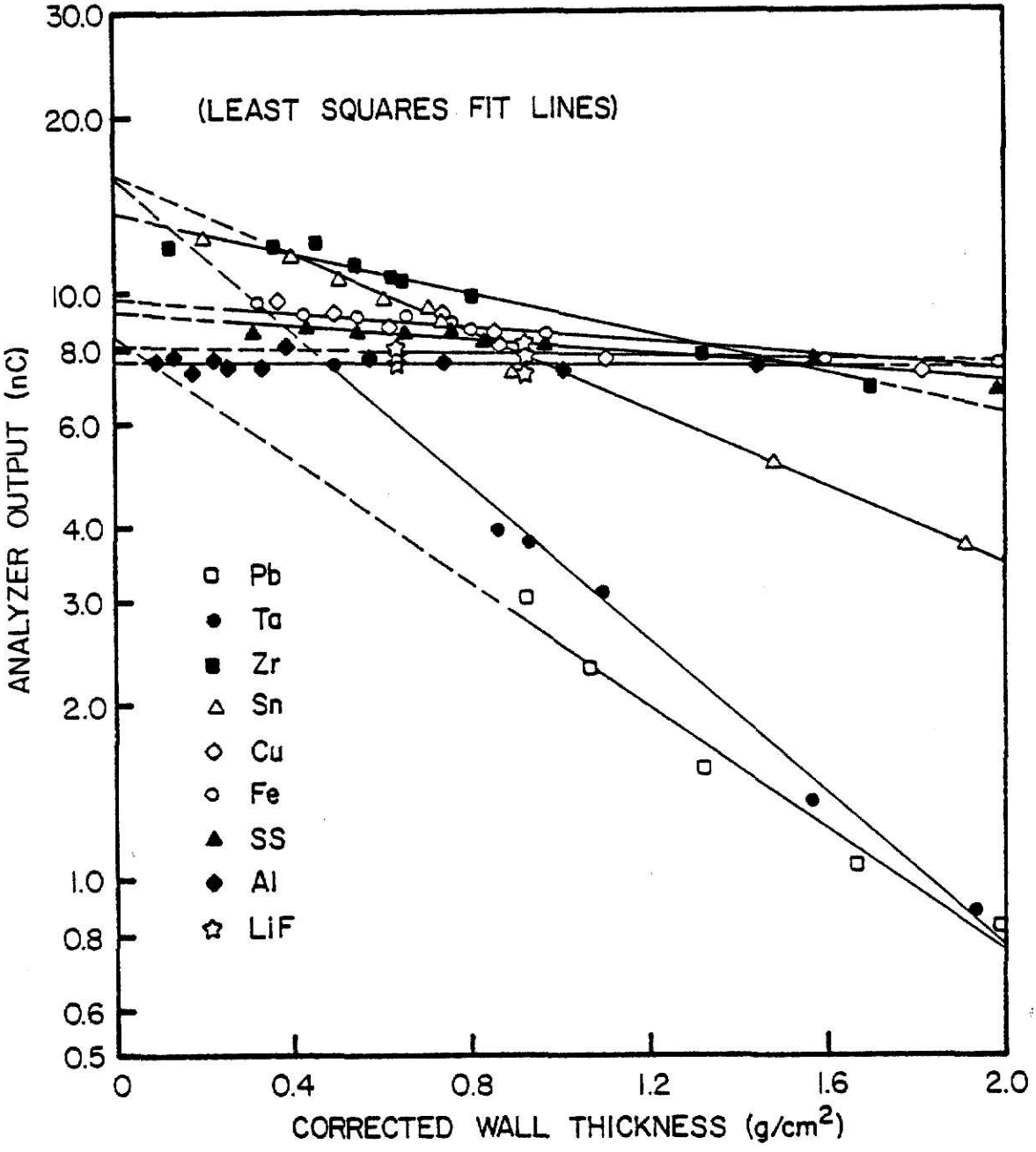

Fig. 4.1. Sleeve thickness data obtained by exposing encased ^{7}LiF TLDs to the Co-57 source (with results for each encasement material included).

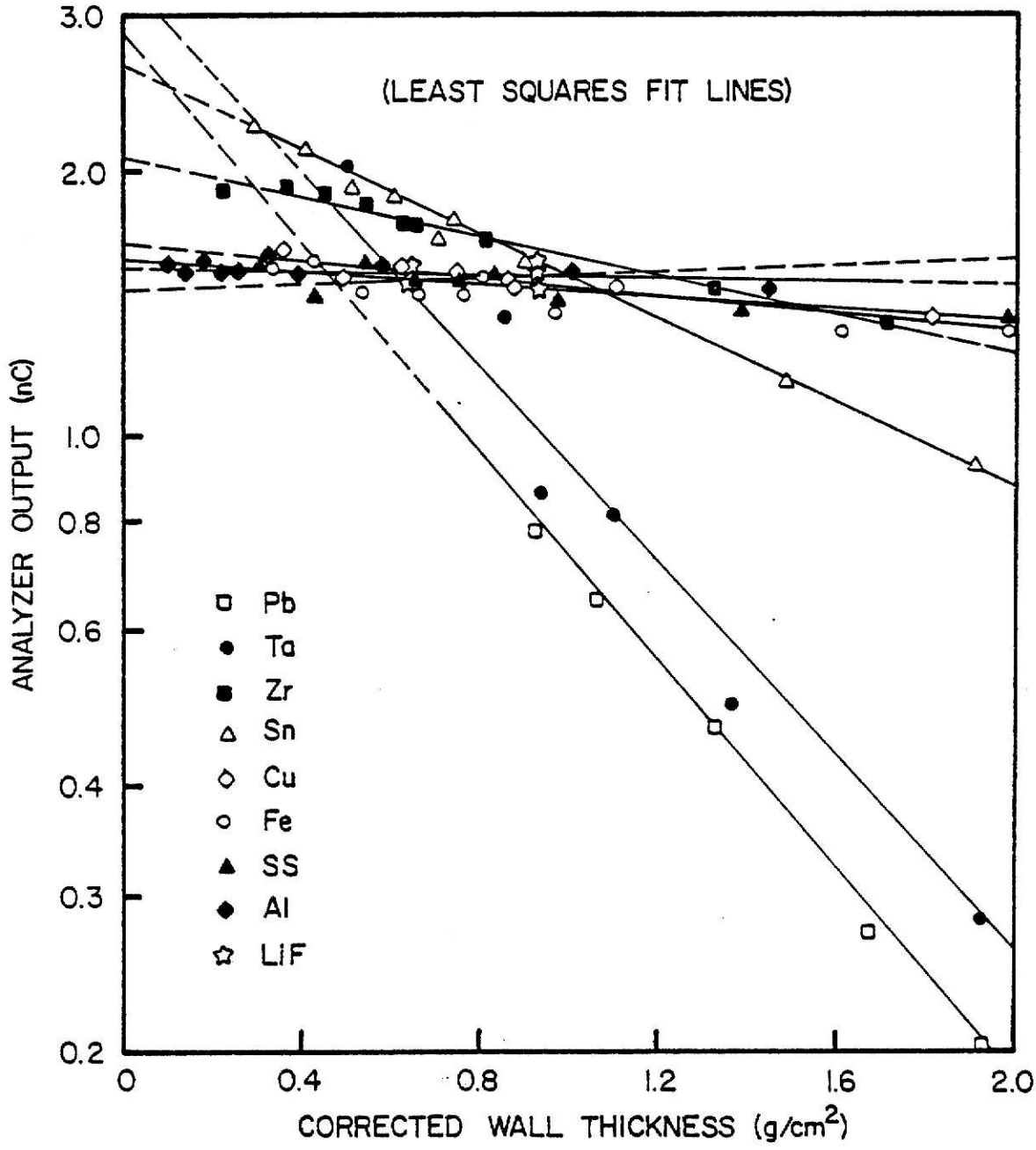

Fig. 4.2. Sleeve thickness data obtained by exposing encased ^{7}LiF TLDs to the Ce-141 source (with results for each encasement material included).

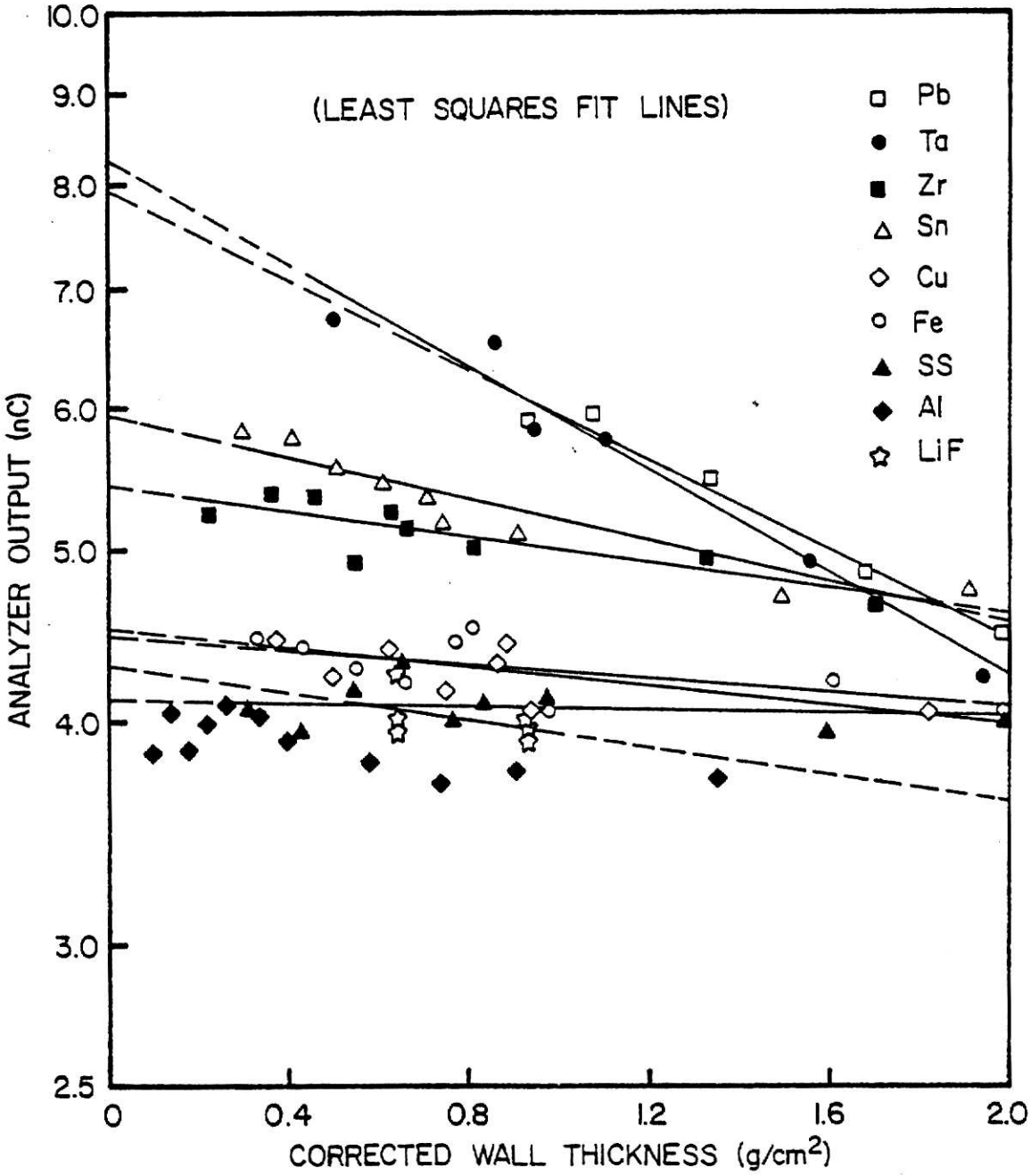

Fig. 4.3. Sleeve thickness data obtained by exposing encased ^{7}LiF TLDs to the Hg-203 source (with results for each encasement material included).

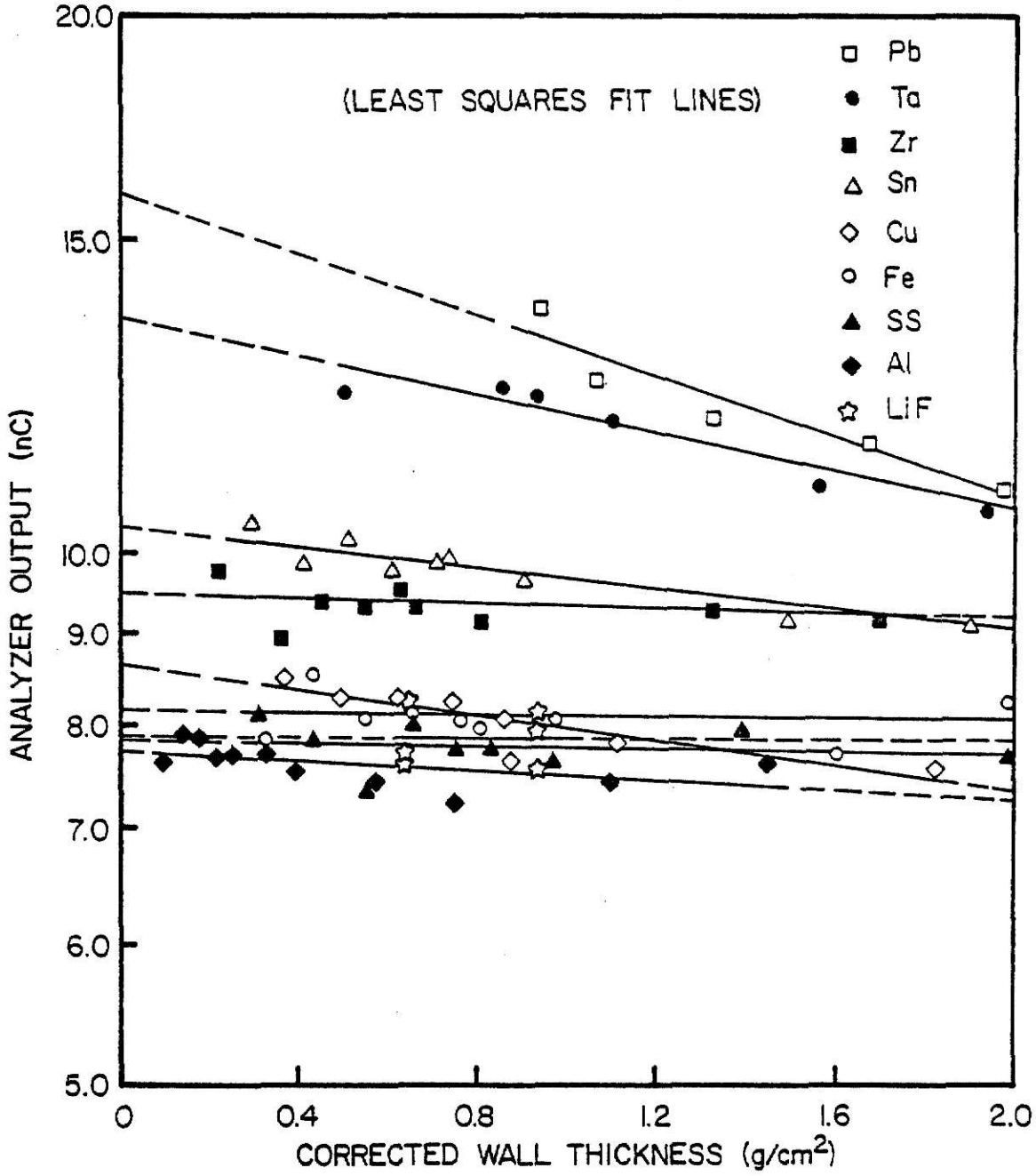

Table 4.4. Sleeve thickness data obtained by exposing encased ^{7}LiF TLDs to the Sn-113 source (with results for each encasement material included).

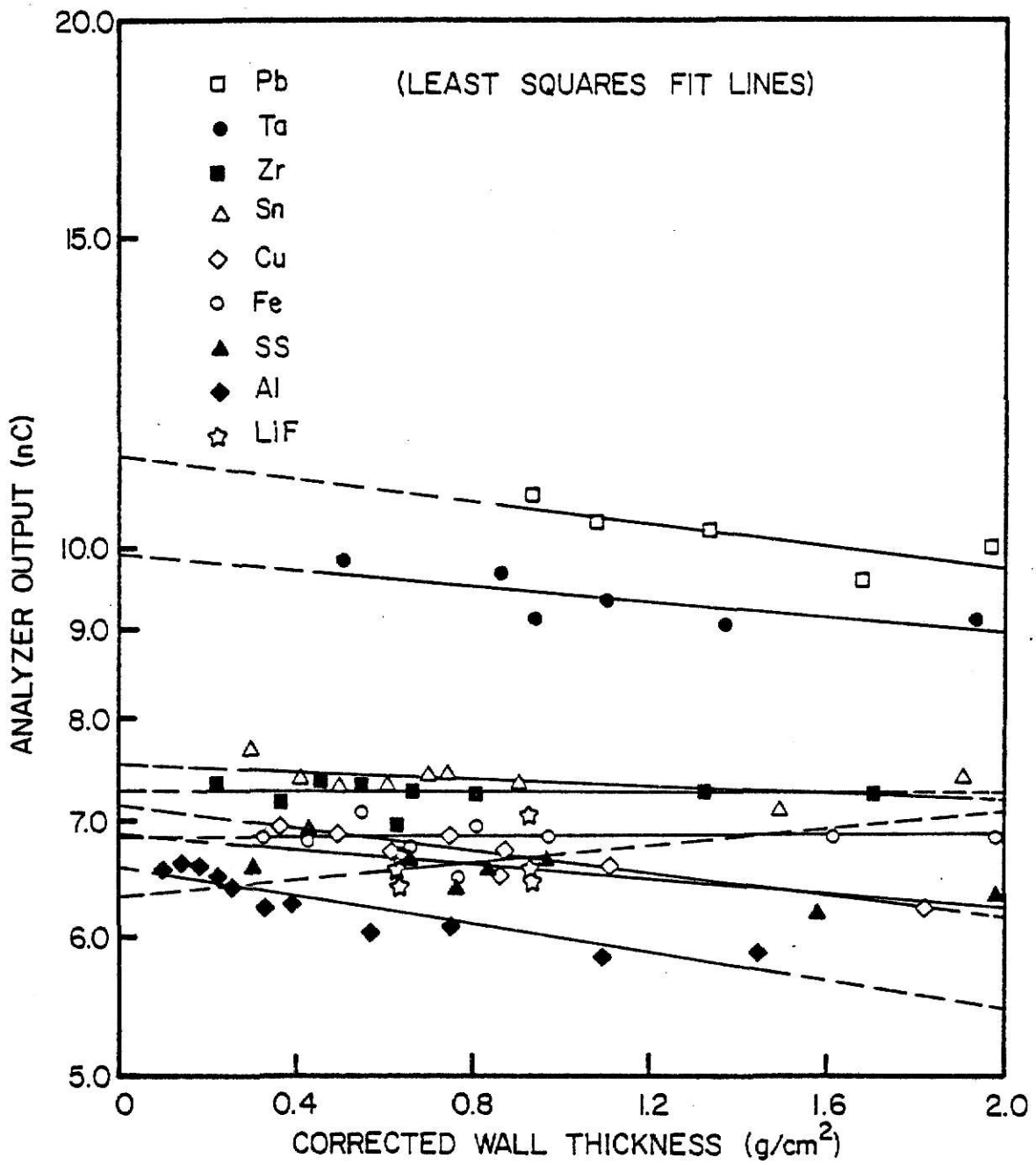

Fig. 4.5. Sleeve thickness data obtained by exposing encased ^{7}LiF TLDs to the Cs-137 source (with results for each encasement material included).

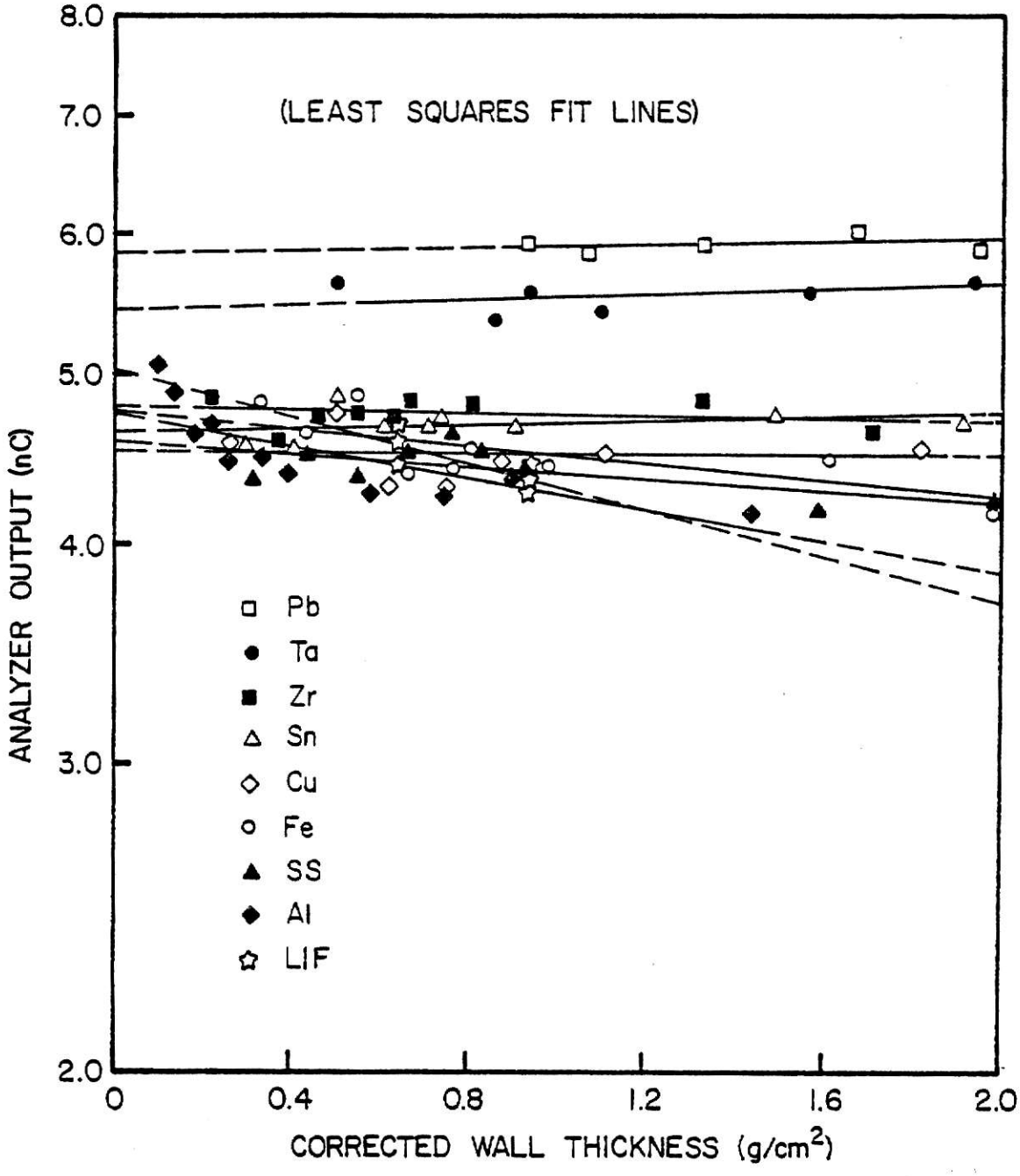

Fig. 4.6. Sleeve thickness data obtained by exposing encased ^{7}LiF TLDs to the Co-60 source (with results for each encasement material included).

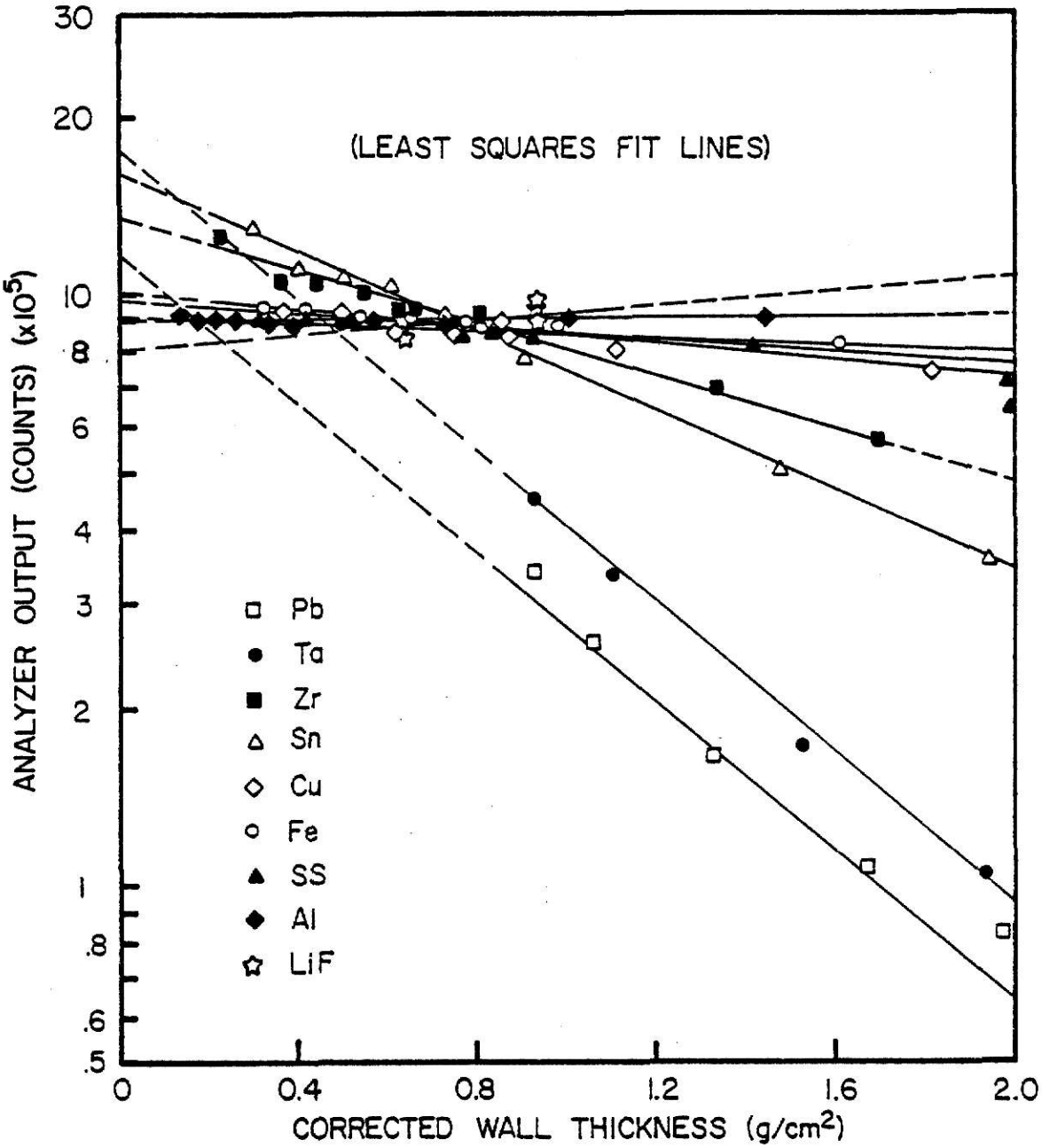

Fig. 4.7. Sleeve thickness data obtained by exposing encased CaF_2:Mn TLDs to the Co-57 source (with results for each encasement material included).

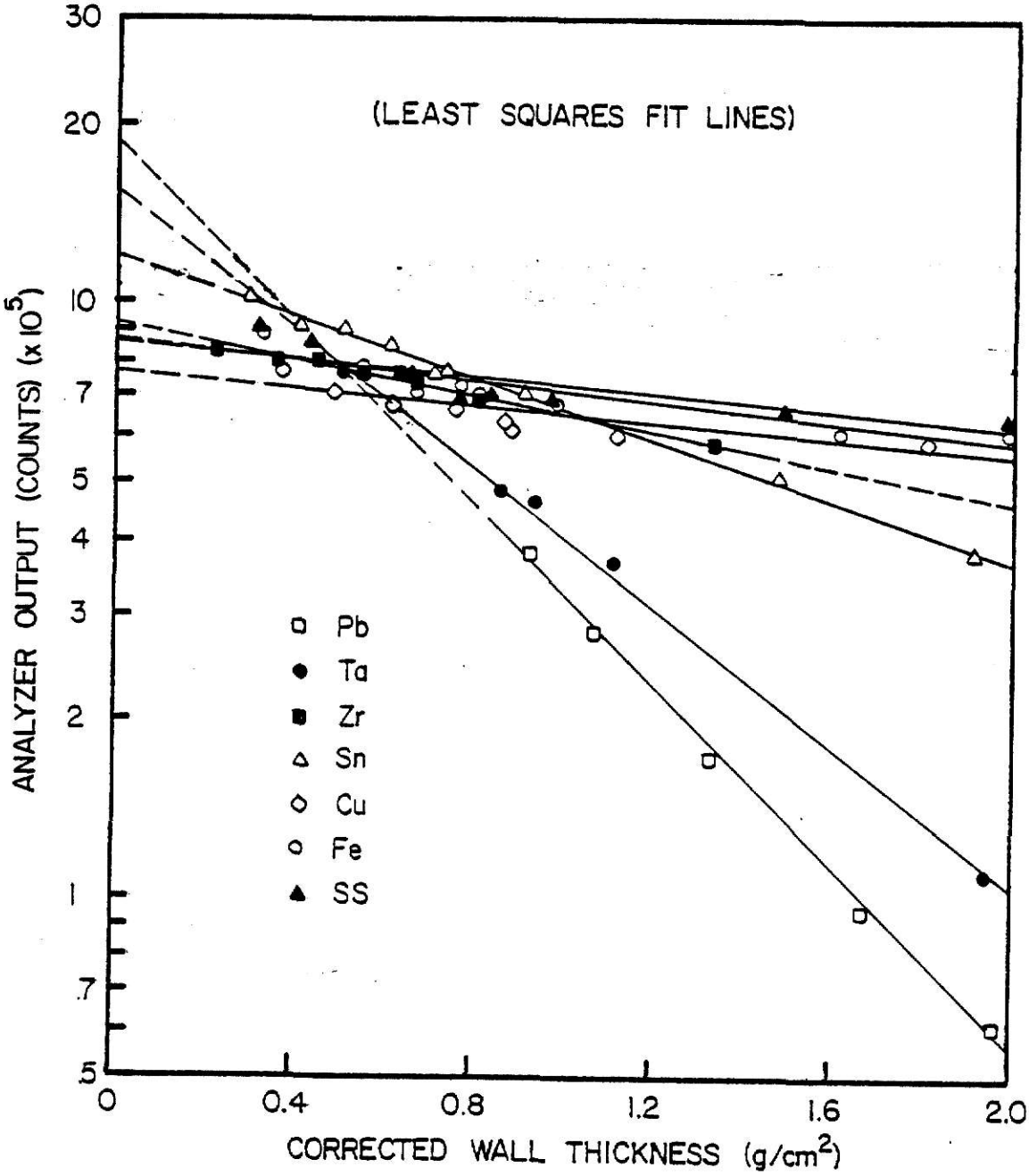

Fig. 4.8. Sleeve thickness data obtained by exposing encased CaF_2:Mn TLDs to the Ce-141 source (with results for each encasement material included).

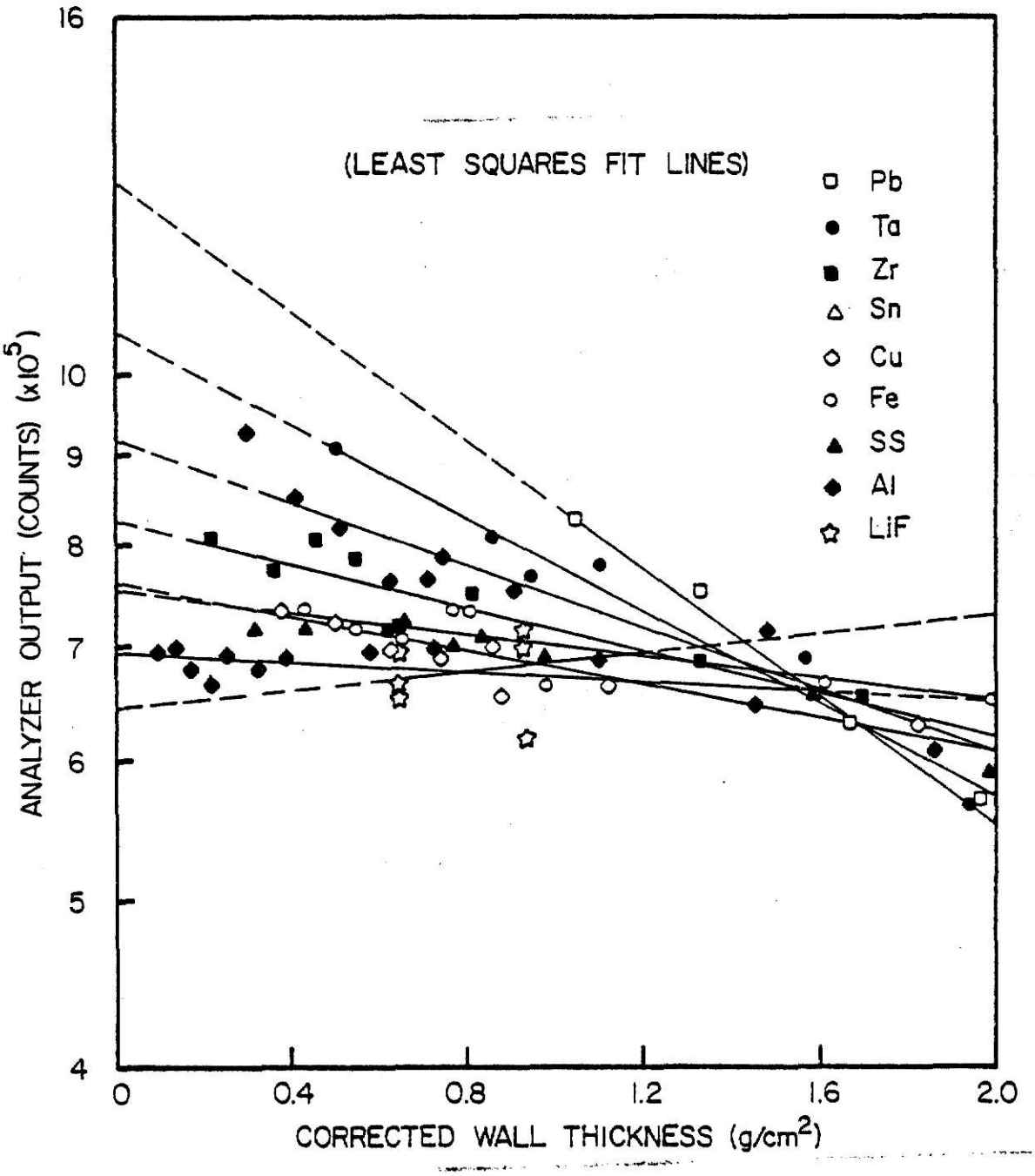

Fig. 4.9. Sleeve thickness data obtained by exposing encased CaF_2:Mn TLDs to the Hg-203 source (with results for each encasement material included).

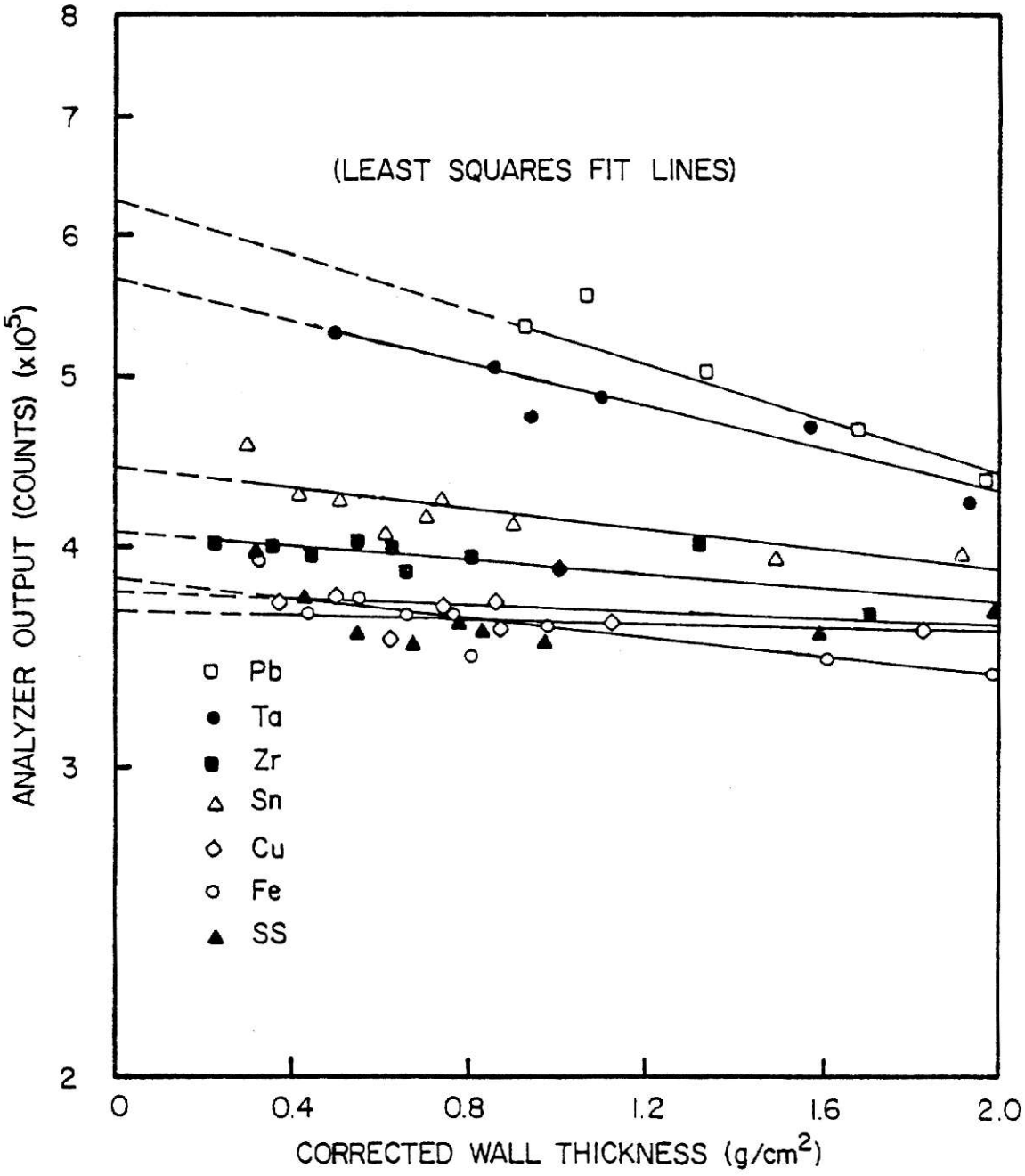

Fig. 4.10. Sleeve thickness data obtained by exposing encased CaF_2:Mn TLDs to the Sn-113 source (with results for each encasement material included).

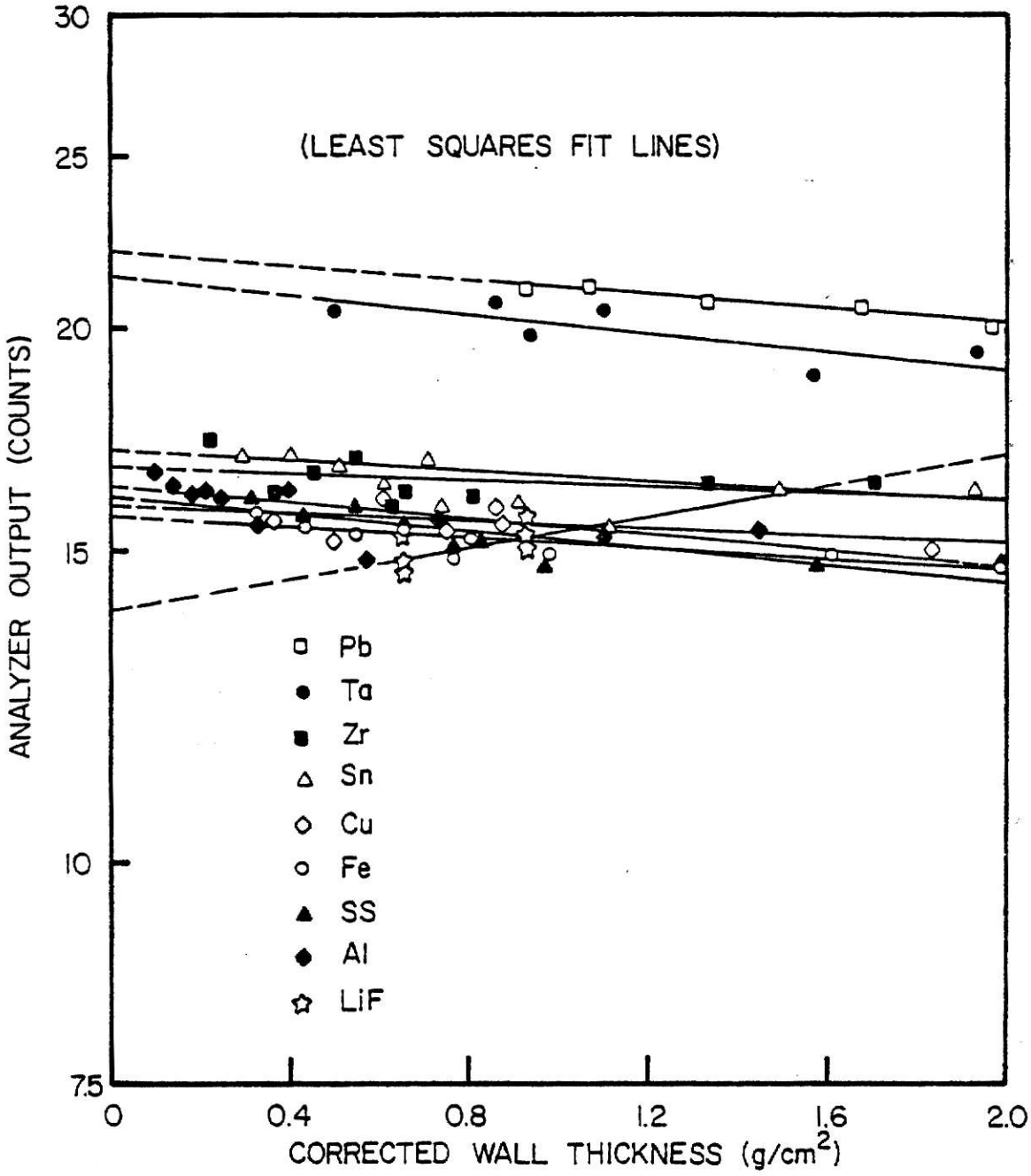

Fig. 4.11. Sleeve thickness data obtained by exposing encased CaF_2:Mn TLDs to the Cs-137 source (with results for each encasement material included).

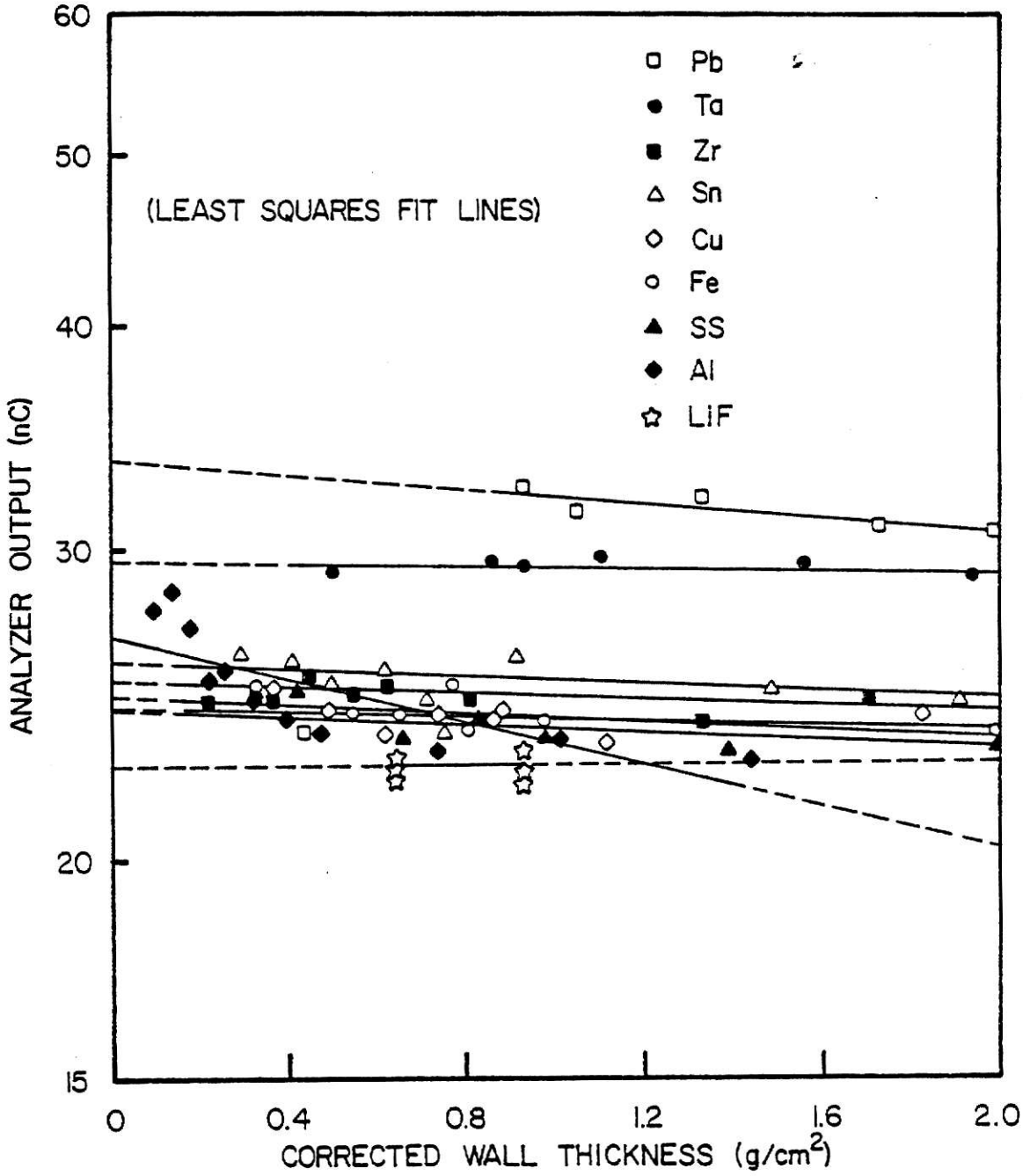

Fig. 4.12. Sleeve thickness data obtained by exposing encased CaF_2:Mn TLDs to the Co-60 source (with results for each encasement material included).

5.0 THEORETICAL CONSIDERATIONS

5.1 The Dose Ratio Factor

The dose ratio factor calculated by the TERC/III computer code, for a gamma of type k and energy T_k, is defined as (see Appendix D)

$$f_i(T_k) = [E_{Di}^{calc}/E_{Mi}^{calc}]_k \qquad (5.1)$$

where E_{Di}^{calc} is the predicted dose to the dosimeter and E_{Mi}^{calc} is the predicted absorbed dose in the medium of type i surrounding the dosimeter. A discussion of the solid-state ionization theory employed by the code to perform the calculations may be found in Ref. 17. Plots of this ratio as a function of gamma energy, for both encased ^{7}LiF and CaF_2:Mn TLDs, are depicted in Figs. 5.1 and 5.2. As is observed, the calculations were performed for the encasement materials lead, tantalum, tin, zirconium, copper, stainless steel, iron, aluminum and natural LiF. Tables of the code input parameters, and the corresponding output, are included in Appendix B for all sleeve materials considered in this research.

5.2 The Calculated Dose

The absorbed dose in a material of type i, exposed to a point gamma emitter with photons of type k, is calculated using the equation

$$[E_{Mi}^{calc}]_k = \frac{tS}{4\pi r^2} [T_k w_k (\frac{\mu_{en}(T_k)}{\rho})_{Mi}] \frac{MeV}{g} \qquad (5.2)$$

where t is the exposure time (sec), S is the source activity of the gamma emitter (sec^{-1}), r is the emitter-to-material distance (cm), w_k is the probability of emission of a gamma of type k per disinte-

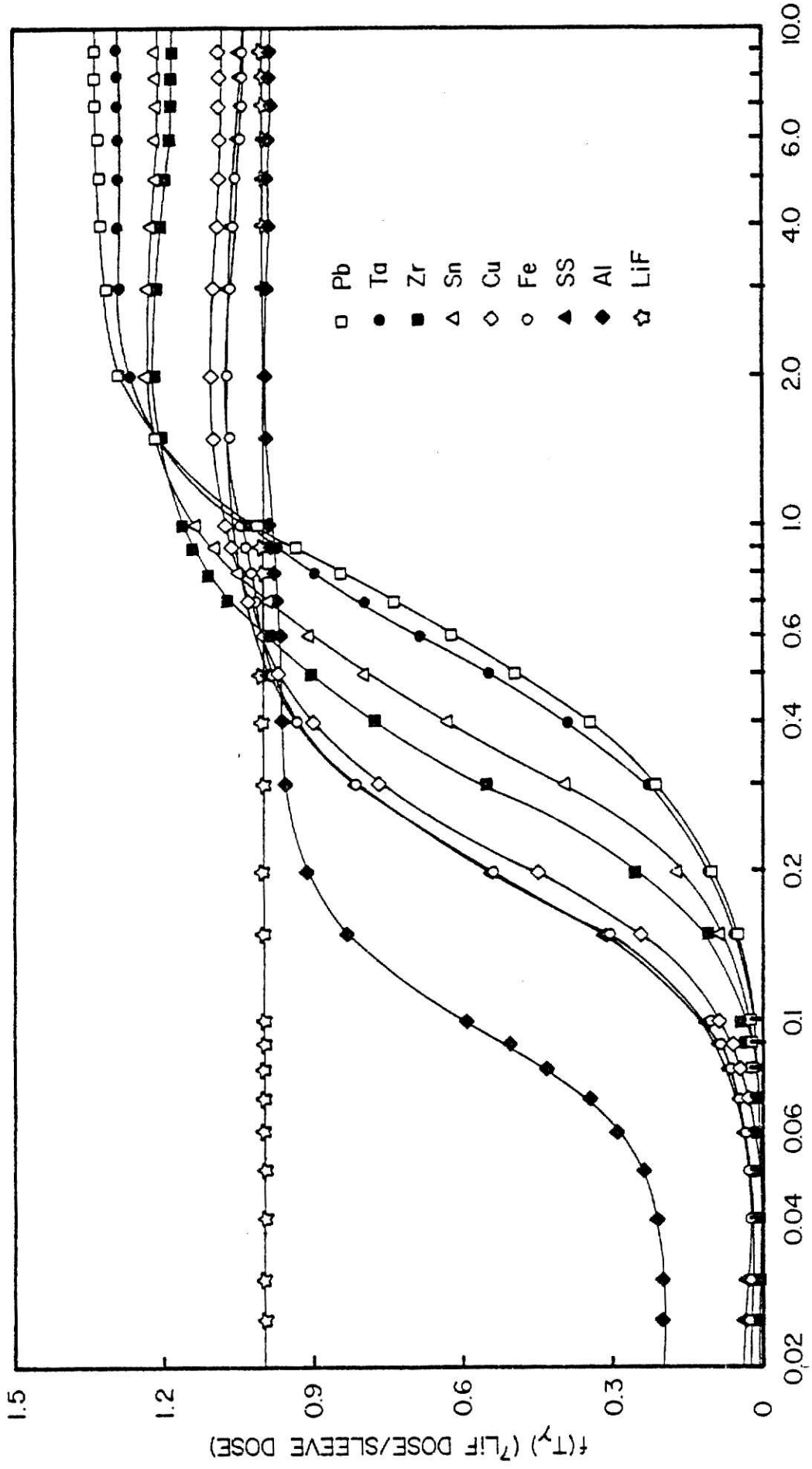

Fig. 5.1. Variation of $f(T_k)$ as a function of gamma-ray energy and encasement material for ^7LiF.

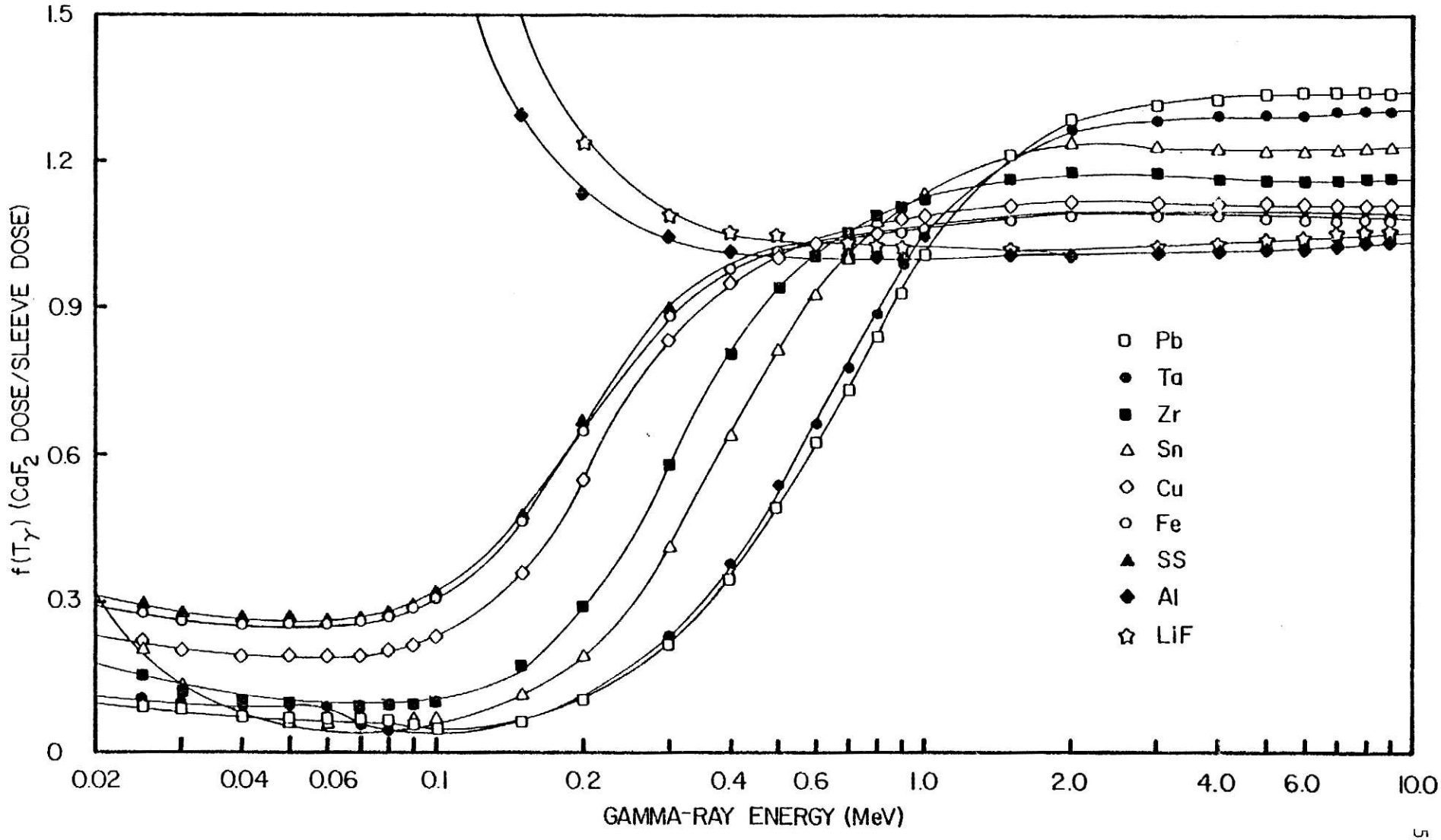

Fig. 5.2. Variation of $f(T_k)$ as a function of gamma-ray energy and encasement material for CaF_2:Mn.

gration, and $(\frac{\mu_{en}(T_k)}{\rho})_{Mi}$ is the mass energy absorption coefficient for the absorbing material (cm^2/g) at the gamma energy T_k (MeV). Substituting Eq. 5.1 into Eq. 5.2 yields the following relationship for the calculated TLD dose

$$[E_{Di}^{calc}]_k = \frac{tS}{4\pi r^2} [f_i(T_k)\ T_k w_k\ (\frac{\mu_{en}(T_k)}{\rho})_{Mi}]\ \frac{MeV}{g} . \qquad (5.3)$$

To obtain the dose for a nonmonoenergetic gamma flux, Eq. 5.3 can be rewritten as

$$E_{Di}^{calc} = \sum_k [E_{Di}^{calc}]_k = B \sum_k [f_i(T_k)\ T_k w_k\ (\frac{\mu_{en}(T_k)}{\rho})_{Mi}]\ \frac{MeV}{g} \qquad (5.4)$$

where B represents the energy independent quantity $tS/4\pi r^2$.

By choosing a reference material of type j, an equation independent of B

$$C = \frac{E_{Di}^{calc}}{E_{Dj}^{calc}} = \frac{\sum_k [T_k w_k f_i(T_k)\ (\frac{\mu_{en}(T_k)}{\rho})_{Mi}]}{\sum_k [T_k w_k f_j(T_k)\ (\frac{\mu_{en}(T_k)}{\rho})_{Mj}]} \qquad (5.5)$$

results by assuming that the irradiation conditions were the same for the materials i and j. Tabulations of this C ratio for encased ^7LiF and CaF_2:Mn dosimeters are presented in Tables 5.1 and 5.2. Mass energy absorption coefficients, obtained from the Storm and Israel Nuclear Data Tables[24], and the TERC/III generated dose ratios are listed in Appendix B.

In order to compare the experimental results and calculations, a ratio corresponding to Eq. 5.5 was also written for the experimentally determined doses E_{Di}^{exp} and E_{Dj}^{exp}

Table 5.1. Calculated TLD dose ratios for encased ^{7}LiF TLDs derived from TERC/III results with iron encased TLDs as the normalizing values.

Sleeve Material	Z	Normalized TERC/III Calculations					
		Gamma-ray Energy (MeV)					
		0.136 (11%) 0.122 (87%)	0.145	0.279	0.393	0.662	1.173 (100%) 1.333 (100%)
Lead	82	2.551	2.749	2.287	1.839	1.573	1.382
Tantalum	73	2.401	2.425	1.951	1.584	1.393	1.269
Tin	50	1.625	1.541	1.332	1.170	1.117	1.090
Zirconium	40	1.308	1.251	1.158	1.073	1.053	1.047
Copper	29	1.061	1.044	1.027	1.013	1.012	1.014
Iron	26	1.000	1.000	1.000	1.000	1.000	1.000
S.S.	--	0.998	0.999	1.000	1.002	1.004	1.008
Aluminum	13	0.737	0.855	0.946	0.975	0.973	0.966
LiF	--	0.713	0.841	0.937	0.963	0.953	0.932

Table 5.2. Calculated TLD dose ratios for encased CaF_2:Mn TLDs derived from TERC/III results with iron encased TLDs as the normalizing values.

Sleeve Material	Z	Normalized TERC/III Calculations					
		Gamma-ray Energy (MeV)					
		0.136 (11%) 0.122 (87%)	0.145	0.279	0.393	0.662	1.173 (100%) 1.333 (100%)
Lead	82	1.656	1.913	1.982	1.667	1.475	1.335
Tantalum	73	1.599	1.746	1.732	1.466	1.326	1.237
Tin	50	1.281	1.290	1.265	1.137	1.097	1.080
Zirconium	40	1.145	1.138	1.129	1.059	1.044	1.051
Copper	29	1.032	1.026	1.022	1.010	1.010	1.012
Iron	26	1.000	1.000	1.000	1.000	1.000	1.000
S.S.	--	0.999	0.999	1.000	1.001	1.003	1.006
Aluminum	13	0.861	0.911	0.956	0.980	0.978	0.971
LiF	--	0.883	0.920	0.948	0.971	0.961	0.941

$$E = E_{Di}^{exp} / E_{Dj}^{exp} \quad . \qquad (5.6)$$

Comparison of the C over E ratios, for a given encasement material and gamma emitter, was employed as a method for determining the agreement between theory and experiment.

5.3 Relative Source Counts

A second technique utilized, for comparing the energy response data to the TERC/III calculations, was the relative source counts method. It was based upon redefining Eq. 5.4 as follows

$$S_{rel} = \frac{Q\ E_{Di}^{exp}}{\sum_{k} [T_k w_k f_i(T_k)\ (\frac{\mu_{en}(T_k)}{\rho})_{Mi}]} \qquad (5.7)$$

where E_{Di}^{exp} replaced E_{Mi}^{calc}, and Q was a constant. If the irradiation conditions are the same, S_{rel} would ideally be constant for all encased TLDs exposed to a given gamma source. The degree of constancy, of S as a function of sleeve material atomic number, formed the basis for intercomparing the measured and calculated doses to the encapsulated dosimeters.

5.4 Sleeve Wall Attenuation Considerations

It is readily conceded that with cavity ionization considerations it is difficult to determine precisely, (1) the minimum surrounding wall thickness required for electronic equilibrium in the cavity, and (2) the apparent gamma-ray attenuation in that minimum thickness. As a result of these considerations, the selection of the best wall

thickness to utilize for TLD encapsulation becomes arduous. Too thin of a wall would not maintain electronic equilibrium and as a result, would induce an improperly low cavity or dosimeter response to a particular gamma radiation. Conversely, too large of a wall thickness would exhibit the same effect but in this case, the result would be due to the attenuation of the primary gammas.

What is generally meant by electronic equilibrium is that as much energy enters as leaves an encased cavity, or as in this case, the encased TLD. This energy is carried by energetic electrons, produced via compton, photoelectric, and pair production gamma interactions in the sleeve wall and dosimeter materials. In general, there is no universally accepted procedure for selecting an appropriate dimension of wall thickness large enough to fully attain electronic equilibrium. As a result, during experimentation it was assumed that equilibrium would be maintained, if the sleeve wall thickness was at least as great as the extrapolated range of the most energetic electrons.

The extrapolated ranges for electrons with energies ranging from 0.1 to 3.0 MeV, may be represented by the empirical formula forwarded by Katz and Penfold[21],

$$\text{Range } (mg/cm^2) = 412\ E^n \qquad (5.8)$$

$$n = 1.265 - 0.0954\ \ln E$$

where E is the electron energy (MeV). This relation is illustrated in Fig. 5.3 as a function of electron energy. For the purpose of selecting a single proper sleeve wall thickness, it was assumed that

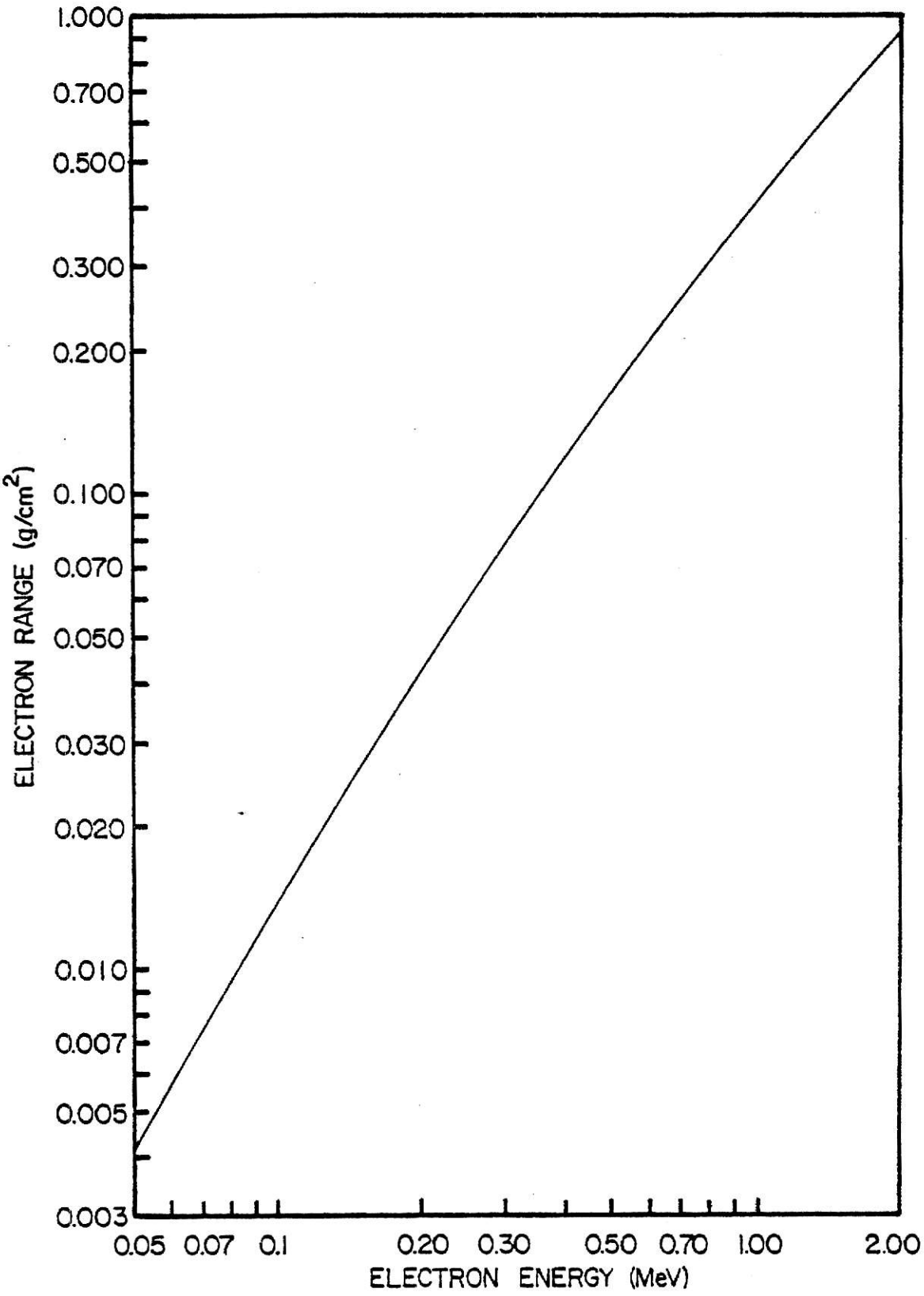

Fig. 5.3. Katz and Penfold empirical range-energy relationship for electrons absorbed in a medium.

the most energetic electrons could not have a greater energy than the gamma rays under consideration. The most energetic of these gammas were the 1.17 and 1.33 MeV photons emitted by the Co-60 source. Hence based upon the above assumption, it was determined that a nominally 0.6 g/cm^2 thick wall, would assure that equilibrium was maintained for all energies investigated in this study. However, this thickness is too large for the low energy gammas. As a result, the encasement materials severely attenuated the low energy photon beams. It was, therefore, necessary to evaluate the effect of the material surrounding the TLD as a function of sleeve thickness.

For a narrow beam experiment where an absorbing shield is involved, the detector response resulting from an attenuated gamma beam is given by the equation[22]

$$R_a = R_o \exp[-\frac{\mu_t}{\rho}(T_k)\ x_e] \qquad (5.9)$$

where R_o is the unattenuated-beam detector response, x_e is the effective mass thickness of the shield (g/cm^2), and $\frac{\mu_t}{\rho}(T_k)$ is the shields total mass attenuation coefficient (cm^2/g) for gamma energy T_k (MeV). With the use of this equation, it is assumed that any photon interaction which occurs within the shield medium, be it scatter or absorption, removes the interacting gammas from the photon beam and hence effectively reduces the associated detector response. But, the case considered during this investigation was that of broad beam attenuation and as a result, the response R_a has in addition a component due to gammas that are scattered into the detector.

Hence, under normal circumstances the broad beam detector response will be larger than that predicted by Eq. 5.9. The exact extent depends on a number of factors: (1) the geometrical configuration of the source or the original photon beam, (2) the configuration of the attenuating medium, (3) the geometric relationship of the source and detector to one another and to the attenuating medium, (4) the directional source strength, (5) the energy spectrum of the source photons, (6) the composition of the attenuating medium, and (7) the type and efficiency of the detector or dosimeter response.

For broad beam attenuation, it is noted by A. B. Chilton that for the case of thin shields, the total response curve on a semi-logarithmic plot is usually close to a straight line[22]. Hence, he suggests that effective mass attenuation coefficients $(\frac{\mu_{eff}}{\rho}(T_k))$ can be determined as the slope of the lines fitted through these limited segments. These coefficients will in effect compensate for the gamma buildup that is inherent with broad beam attenuation. Thus, Eq. 5.9 becomes

$$R_a = R_o \exp[-\frac{\mu_{eff}}{\rho}(T_k)\ x_e]. \qquad (5.10)$$

This concept was applied to the data acquired during the sleeve thickness study. The effective attenuation coefficients were assigned the slopes of the least squares line fits through each set of encased TLD responses. These coefficients were determined for all combinations of TLD type, sleeve material, and gamma energies considered.

For this investigation, the gamma beams were assumed to be of the broad beam monodirectional form and perpendicular to the axis of the encasing sleeves. This physical arrangement is presented in Fig. 5.4. Due to the curvature of the sleeve wall, the photons have distances

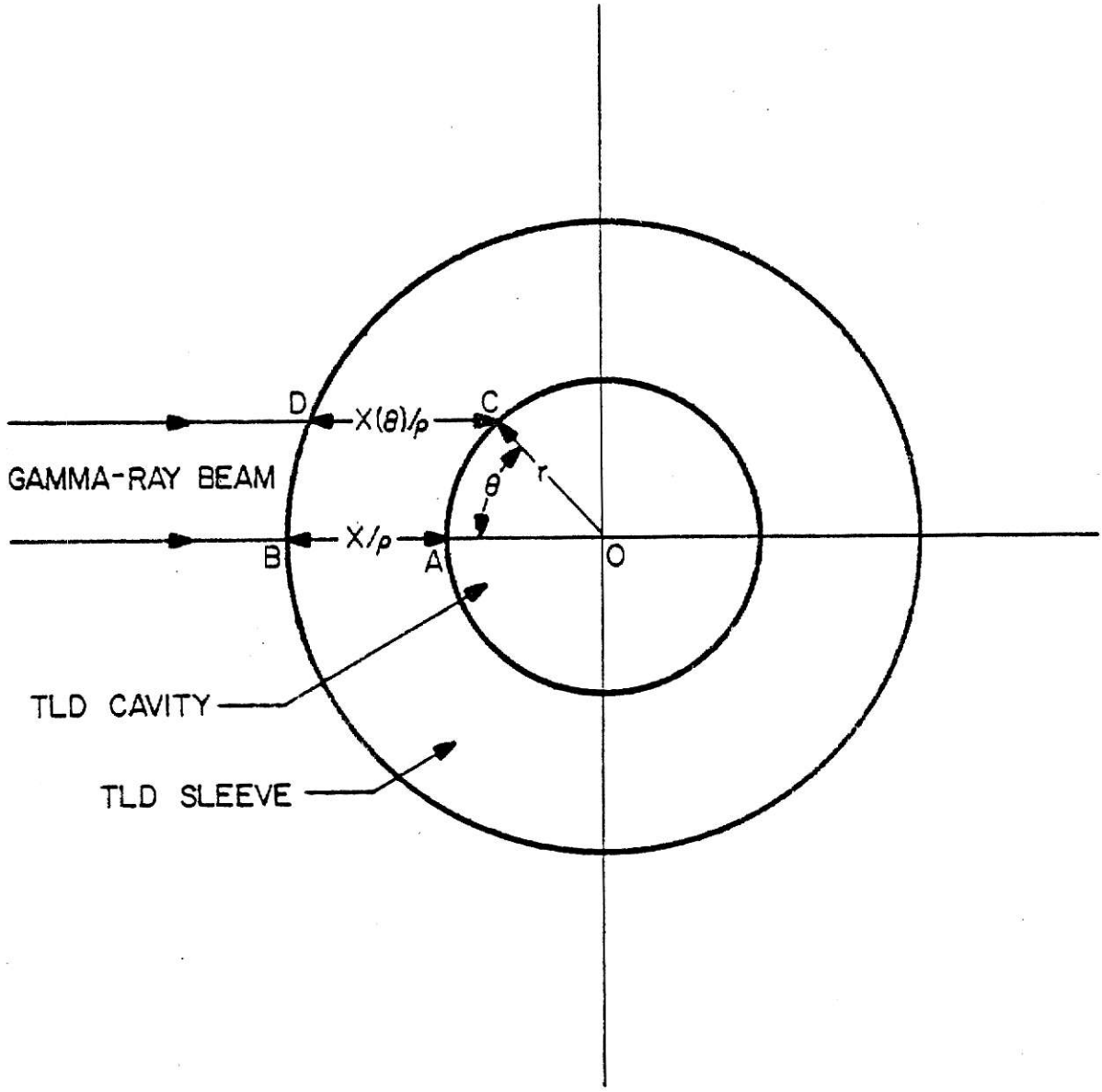

Fig. 5.4. Illustration of the TLD sleeve in relation to the gamma-ray beam.

to travel through ranging from that of the radial wall thickness, to that depicted by ray DC when θ equals 90°. Hence, it was apparent that an average, or effective wall thickness $(\frac{x_e}{\rho})$, needed to be obtained for each size TLD encasement. A method for deriving these averages was outlined in Ref. 23. According to this method, the photon pathlength traversed as a function of θ can be represented by the equation

$$\frac{x_\theta}{\rho} = \frac{r + \frac{x}{\rho}}{\sin\theta} \sin[\theta - \sin^{-1} (\frac{r}{r+x/\rho}) \sin\theta)] \text{ cm} \qquad (5.11)$$

where r is the sleeve cavity radius (cm), and x/ρ is the radial sleeve wall thickness (cm). The effective wall thickness was defined as the following average

$$\frac{x_e}{\rho} = \frac{\int_0^{\pi/2} \left\{ \frac{r + x/\rho}{\sin\theta} \sin[\theta - \sin^{-1} (\frac{r}{r + x/\rho} \sin\theta)] \right\} d\theta}{\int_0^{\pi/2} d\theta} \text{ cm.} \qquad (5.12)$$

A plot of the percent correction to x/ρ, as a function of radial wall thickness and cavity radius, is presented in Fig. 5.5. For a given radius this correction decreases as a function of increasing radial wall dimension.

With the application of the attenuation concept to the TLD dose ratio, it is possible to derive an expression for the dose ratio factor corrected for sleeve wall attenuation $f_i(T_k)^{corr}$. Given a gamma of type k and an encasement material of type i

$$f_i(T_k)^{corr} = f_i(T_k) \exp[- \frac{\mu_{eff}}{\rho} (T_k) x_e]_{Mi}. \qquad (5.13)$$

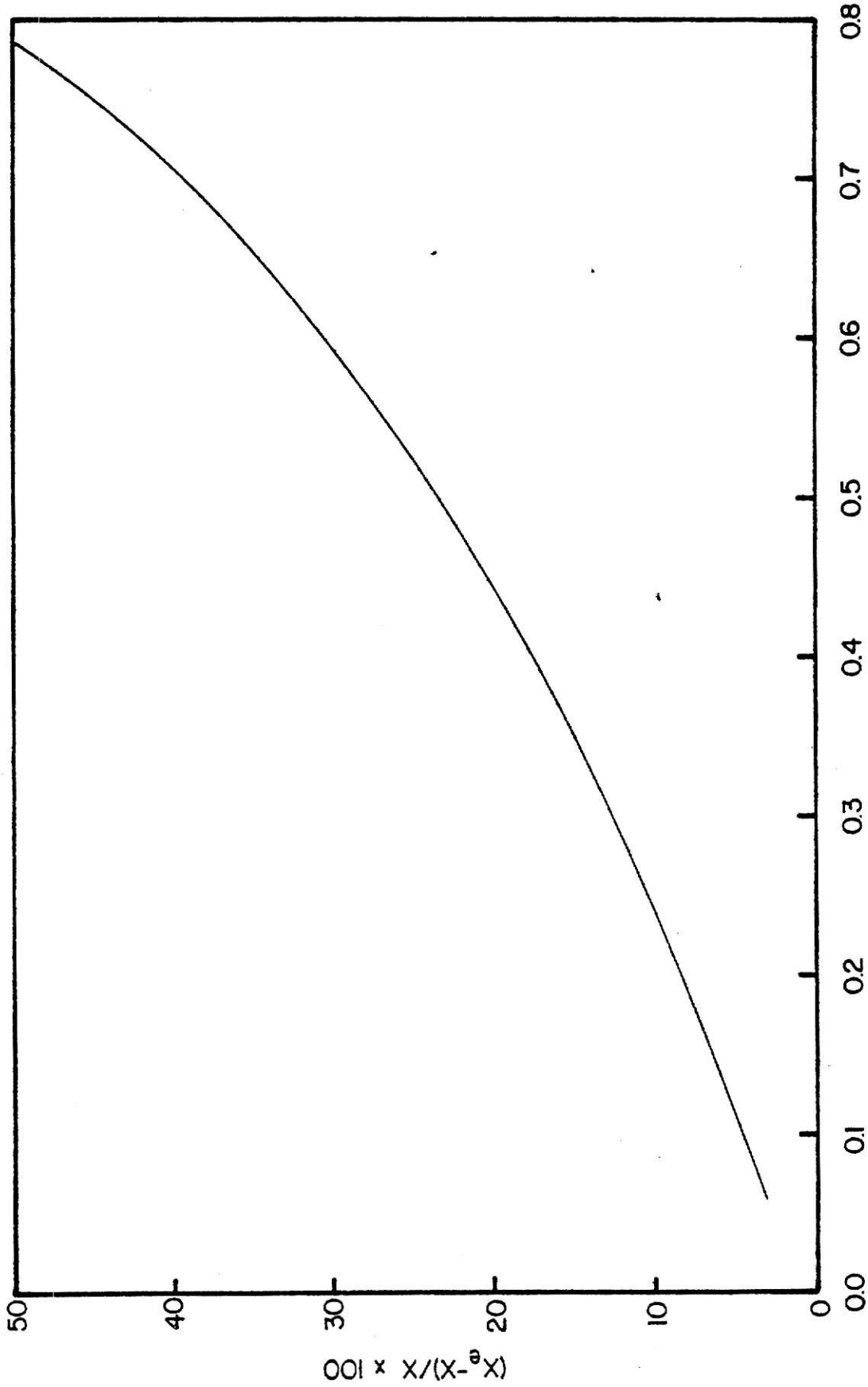

Fig. 5.5. Percent curvature correction to the encasing sleeve walls (as a function of cavity radius (r), and radial wall thickness (x/ρ)).

This concept can also be applied to Eq. 5.3, to obtain an attenuation corrected calculated TLD dose, $[E_{Di}]_k^{ac}$. For a material of type i and a gamma of type k

$$[E_{Di}]_k^{ac} = B[f_i(T_k)T_k w_k \left(\frac{\mu_{en}}{\rho}(T_k)\right)_{Mi}] \exp[-\frac{\mu_{eff}}{\rho}(T_k)x_e]_{Mi} \frac{MeV}{g} \qquad (5.14)$$

where B represents the quantity $tS/4\pi r^2$.

By choosing a reference material of type j, an attenuation corrected expression independent of B can be obtained

$$C_k^{ac} = \frac{[f_i(T_k)\left(\frac{\mu_{en}}{\rho}(T_k)\right)_{Mi}] \exp[-\frac{\mu_{eff}}{\rho}(T_k)x_e]_{Mi}}{[f_j(T_k)\left(\frac{\mu_{en}}{\rho}(T_k)\right)_{Mj}] \exp[-\frac{\mu_{eff}}{\rho}(T_k)x_e]_{Mj}} \quad . \qquad (5.15)$$

It is also possible to obtain an attenuation corrected expression similar to Eq. 5.7. The corrected relative source counts for a material of type i and a gamma of type k is given by

$$[S_{rel}]_k^{ac} = \frac{QE_{Di} \exp[\frac{\mu_{eff}}{\rho}(T_k)x_e]_{Mi}}{[T_k w_k f_i(T_k)\left(\frac{\mu_{en}}{\rho}(T_k)\right)_{Mi}]} \quad . \qquad (5.16)$$

6.0 SLEEVE WALL ATTENUATION OF PRIMARY GAMMAS

6.1 The Effective Attenuation Coefficient

Effective attenuation coefficients $(\frac{\mu_{eff}}{\rho})$, discussed in Section 5.4, were calculated for each TLD type, sleeve material, and gamma source. These coefficients are in effect the slopes of the least squares line fits to the data represented in Figs. 4.1-4.12. The results for both the encased ^{7}LiF and CaF_2:Mn dosimeters are listed in Tables 6.1 and 6.2 respectively.

As expected, the coefficients increase as a function of increasing encasement material Z number and decreasing gamma energy. However, for cases involving minimal sleeve attenuation, the effective attenuation coefficients are the same order of magnitude as their corresponding standard deviations. Therefore, for these cases it was impossible to determine meaningful coefficients. Conversely, for the cases involving significant sleeve attenuation, i.e., lower energy gammas and higher Z materials, the effective attenuation coefficients are nominally much greater than their corresponding standard deviations.

The consistency of the effective attenuation coefficients were evaluated with respect to the dose buildup concept. If scattered gamma rays add a signifcant component to the TLD dose, these measured coefficients would satisfy two requirements. First, they should be nominally less than the corresponding total attenuation coefficients. Secondly, they should also be greater than the associated mass energy absorption coefficients. Comparisons were made between the experimentally determined effective attenuation coefficients, and the mass energy

Table 6.1. Effective attenuation coefficients for encased ^{7}LiF TLDs calculated with sleeve curvature corrections to the sleeves and with TLD readouts corrected for individual sensitivity.

Sleeve Material	Z	Sleeve Attenuation Correction Coefficient (cm^2/g) ± σ					
		Gamma-ray Energy (MeV)					
		0.136 (11%) 0.122 (87%)	0.145	0.279	0.393	0.662	1.173 (100%) 1.333 (100%)
Lead	82	1.218±0.102	1.385±0.033	0.288±0.029	0.193±0.036	0.073±0.036	-0.008±0.016
Tantalum	73	1.510±0.065	1.274±0.108	0.332±0.032	0.127±0.022	0.054±0.022	-0.014±0.019
Tin	50	0.773±0.022	0.547±0.014	0.135±0.019	0.073±0.012	0.020±0.014	-0.013±0.015
Zirconium	40	0.409±0.020	0.253±0.014	0.082±0.021	0.015±0.019	0.002±0.014	0.005±0.015
Copper	29	0.178±0.035	0.103±0.018	0.060±0.023	0.084±0.020	0.072±0.013	0.003±0.032
Iron	26	0.137±0.010	0.099±0.020	0.046±0.019	0.007±0.020	-0.005±0.016	0.062±0.022
S.S.	--	0.139±0.016	0.084±0.021	0.016±0.018	0.006±0.020	0.044±0.014	0.043±0.017
Aluminum	13	0.018±0.022	0.031±0.013	0.060±0.020	0.034±0.018	0.095±0.013	0.103±0.029
LiF	--	0.072±0.101	-0.033±0.087	0.087±0.083	0.001±0.112	-0.055±0.102	0.151±0.065

Table 6.2. Effective attenuation coefficients for encased CaF_2:Mn TLDs calculated with sleeve curvature corrections to the sleeves and with TLD readouts corrected for individual sensitivity.

Sleeve Material	Z	Sleeve Attenuation Correction Coefficient (cm^2/g) ± σ					
		Gamma-ray Energy (MeV)					
		0.136 (11%) 0.122 (87%)	0.145	0.279	0.393	0.662	1.173 (100%) 1.333 (100%)
Lead	82	1.385±0.013	1.735±0.051	0.418±0.022	0.178±0.027	0.096±0.010	0.043±0.019
Tantalum	73	1.471±0.047	1.340±0.063	0.304±0.034	0.141±0.026	0.058±0.022	0.005±0.010
Tin	50	0.789±0.025	0.589±0.015	0.207±0.030	0.067±0.019	0.026±0.018	0.026±0.014
Zirconium	40	0.493±0.026	0.341±0.022	0.143±0.027	0.045±0.007	0.019±0.021	0.022±0.012
Copper	29	0.169±0.030	0.172±0.041	0.104±0.020	0.015±0.016	0.031±0.017	0.014±0.018
Iron	26	0.096±0.007	0.202±0.038	0.073±0.018	0.063±0.017	0.033±0.007	0.024±0.017
S.S.	--	0.132±0.015	0.177±0.051	0.111±0.013	0.016±0.022	0.053±0.014	0.040±0.014
Aluminum	13	-0.007±0.007	--	0.030±0.016	--	0.053±0.019	0.137±0.036
LiF	--	-0.145±0.090	--	-0.063±0.138	--	-0.098±0.057	0.004±0.051

absorption and total attenuation equivalents. The TLD energy response mass energy absorption coefficients were used for this intercomparison. The total attenuation coefficients were abstracted from the Storm and Israel tabulations of photon cross-sections[24]. As shown in Figs. 6.1-6.9, the experimentally determined coefficients tend to be bounded by their corresponding absorption and total attenuation coefficients. It appears, therefore, that the TLDs do receive a buildup dose due to gamma scatter.

6.2 Attenuation Corrected TERC/III Calculations

Attenuation corrections were applied to the TLD dose ratios ($f(T_k)$) using Eq. 5.13. An effective sleeve wall thickness of 0.7 g/cm^2 was selected, since it was representative of the encasement thicknesses used to measure the energy response of the TLDs.

As illustrated in Figs. 6.10-6.15, application of the attenuation correction tends to reduce the magnitude of the dose ratio factor. Above nominally 0.4 MeV, the attenuation corrections are less than 5%. These corrections are considered to be unimportant, since their magnitude is less than the statistical error normally associated with absorbed dose measurements made with TLDs. However, the attenuation corrections are large for two specific cases, and therefore are considered very important. These cases are (1) TLDs encased in lead, tantalum, tin, and zirconium, exposed to gamma energies below 0.4 MeV, and (2) copper, iron, and stainless steel encased TLDs exposed to gamma energies nominally below 0.2 MeV.

Attenuation corrections were also applied, using Eq. 5.15, to the C ratios listed in Tables 5.1 and 5.2. The curvature corrected wall thicknesses (x_e) were those used during the TLD energy response study. Comparison of the attenuation corrected C ratios (see Tables 6.3 and 6.4) to the uncorrected results show the effect of accounting for sleeve wall attenuation. The C ratio result for tantalum encased TLDs, decreased by 73% for the lowest energy gamma emitter, namely the Co-57 source which emits 0.122 and 0.136 MeV gammas. Likewise, the result for lead encased CaF_2:Mn TLDs, was decreased by 77% for the Ce-141 0.145 MeV gamma.

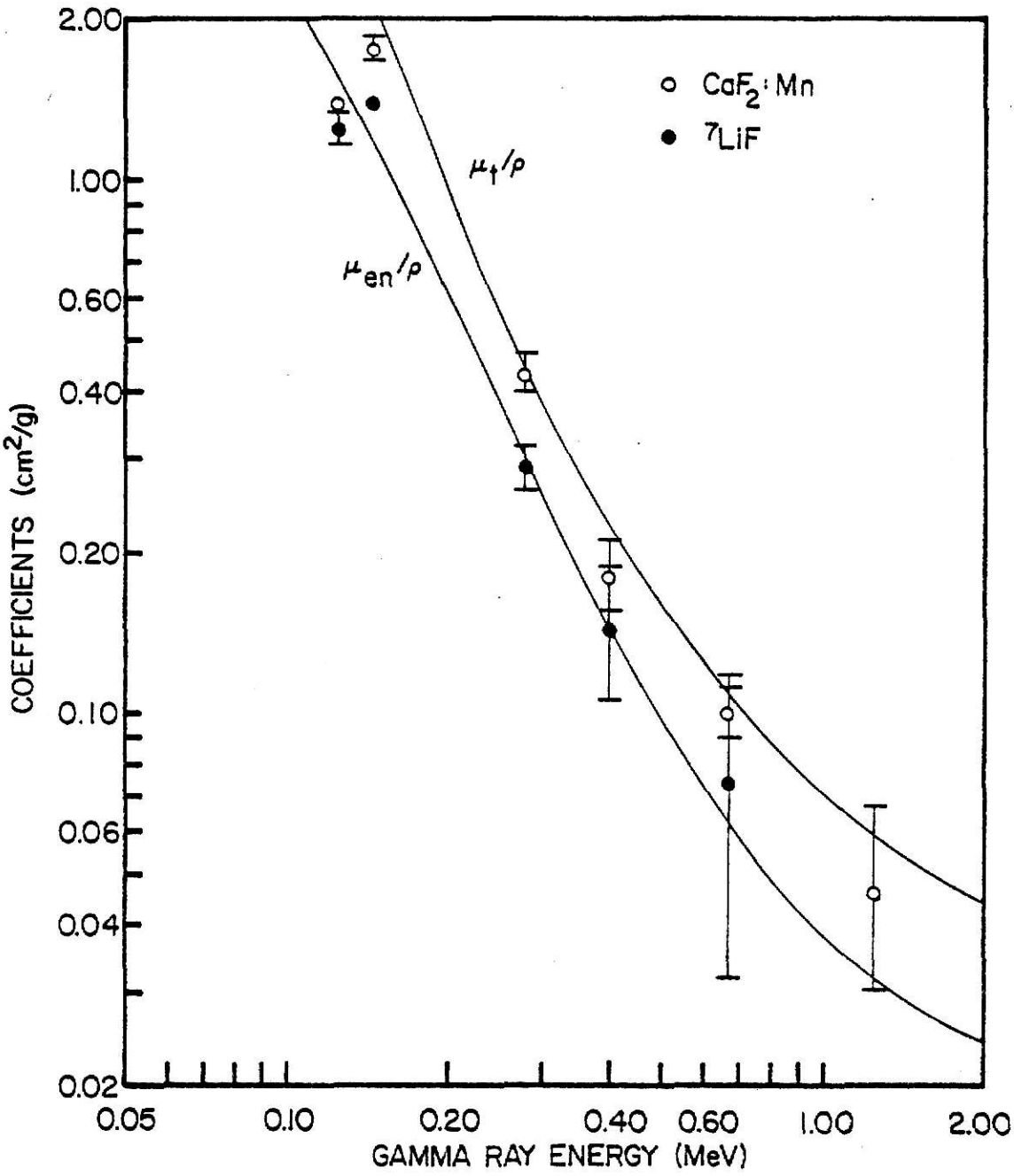

Fig. 6.1. Comparison of the experimentally determined effective attenuation coefficients for lead encased ^{7}LiF and CaF_2:Mn TLDs to the total attenuation and mass energy absorption coefficients for lead.

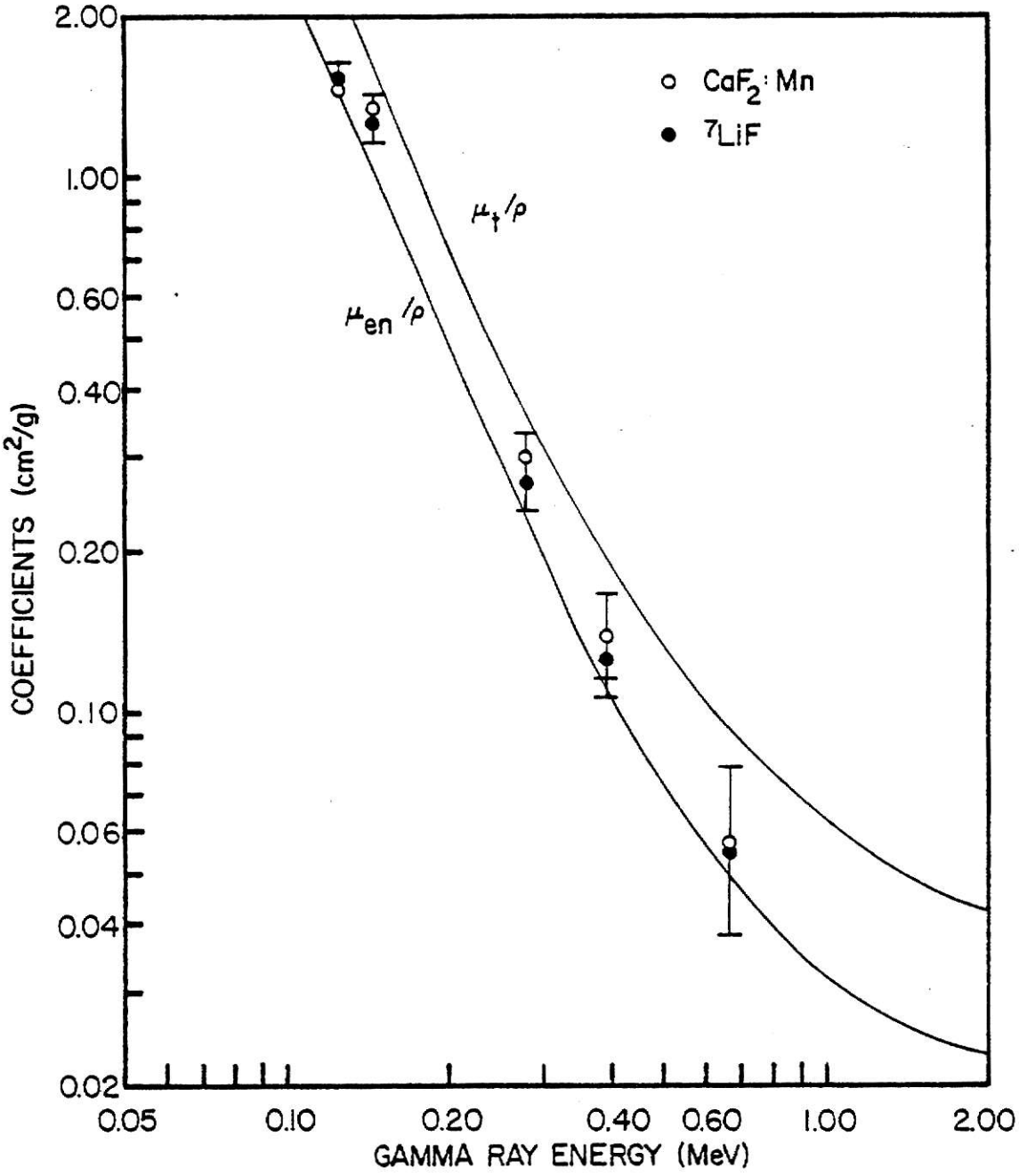

Fig. 6.2. Comparison of the experimentally determined effective attenuation coefficients for tantalum encased ^{7}LiF and CaF_2:Mn TLDs to the total attenuation and mass energy absorption coefficients for tantalum.

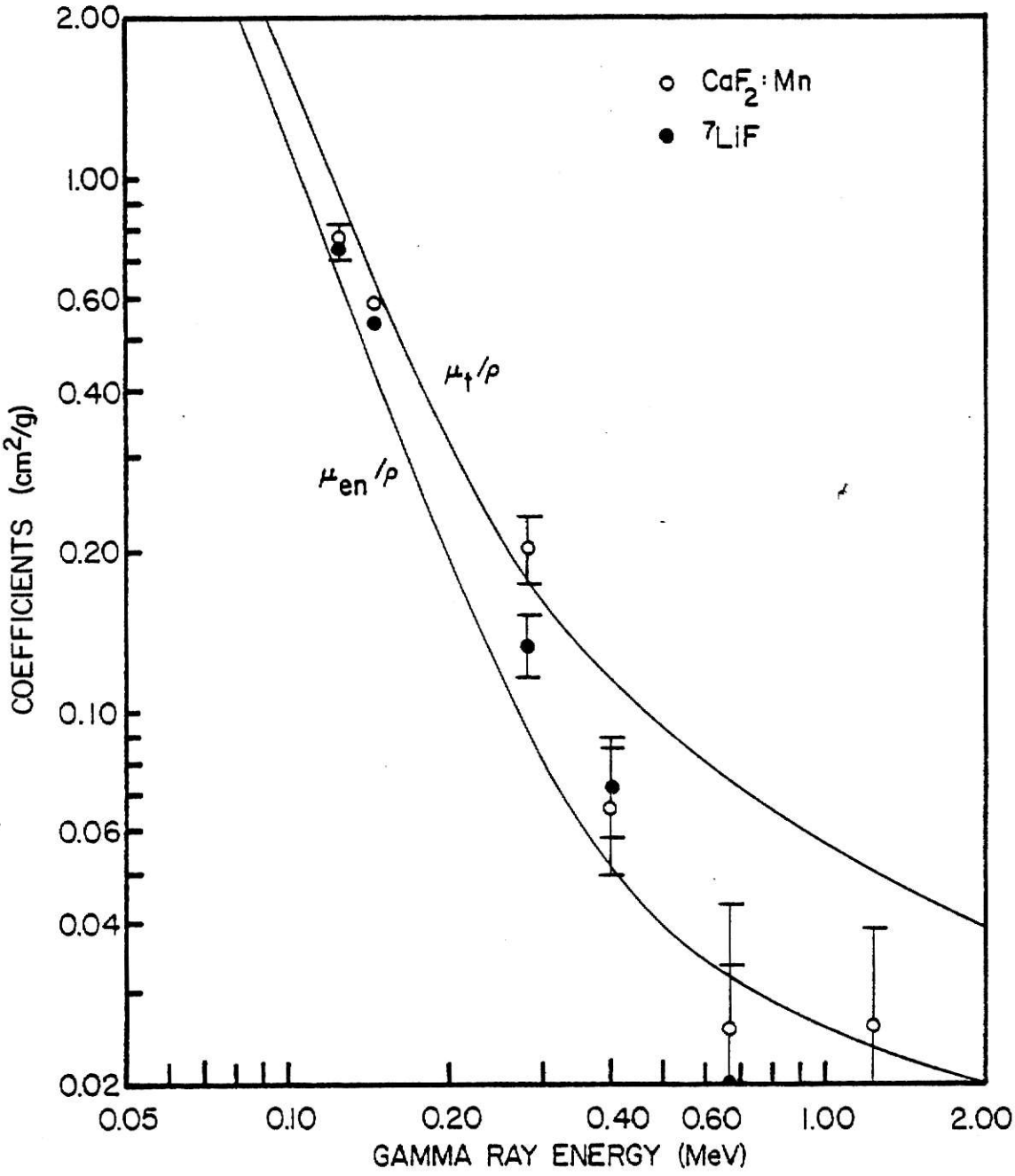

Fig. 6.3. Comparison of the experimentally determined effective attenuation coefficients for tin encased ^{7}LiF and CaF_2:Mn TLDs to the total attenuation and mass energy absorption coefficients for tin.

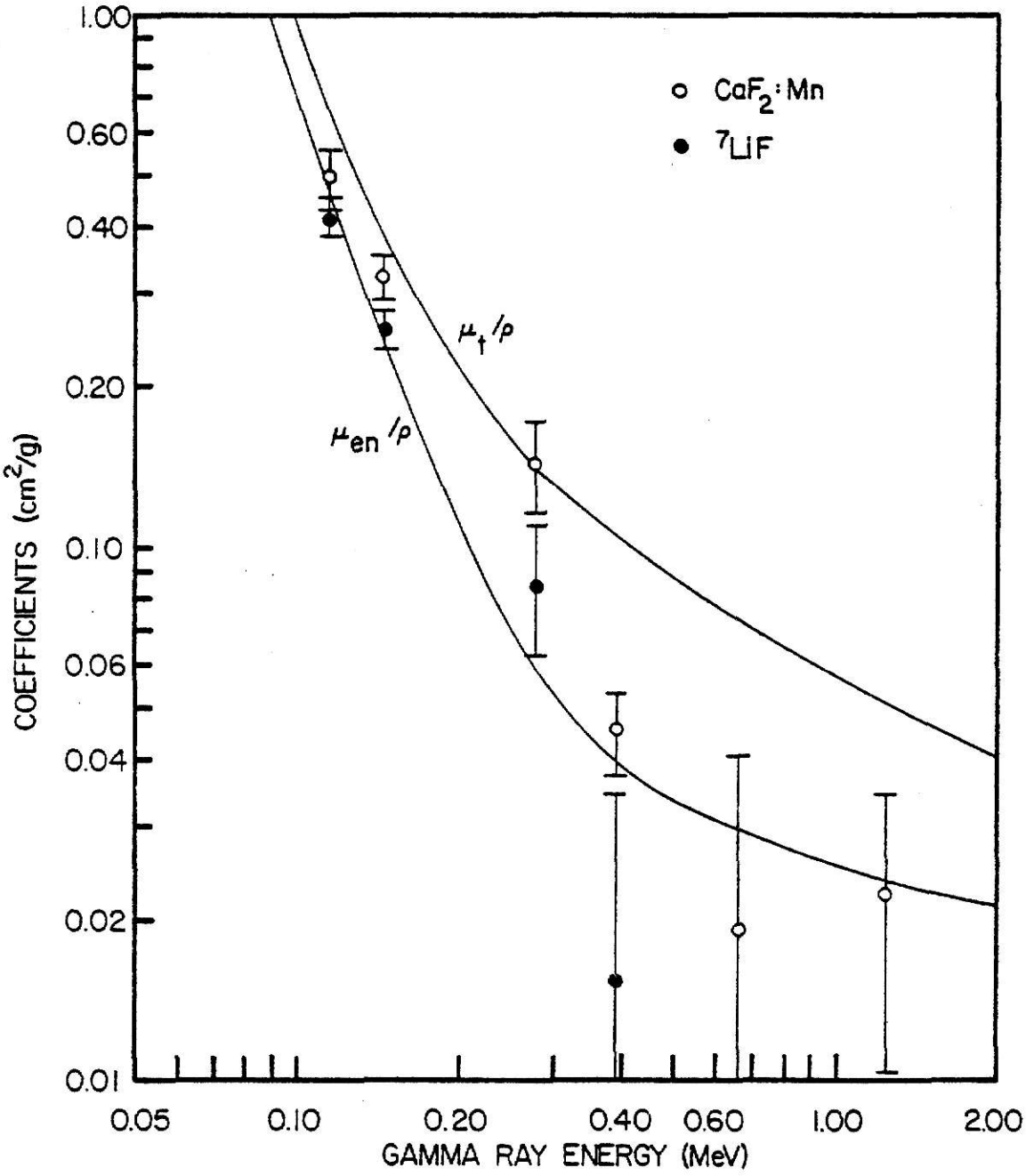

Fig. 6.4. Comparison of the experimentally determined effective attenuation coefficients for zirconium encased ^{7}LiF and CaF_2:Mn TLDs to the total attenuation and mass energy absorption coefficients for zirconium.

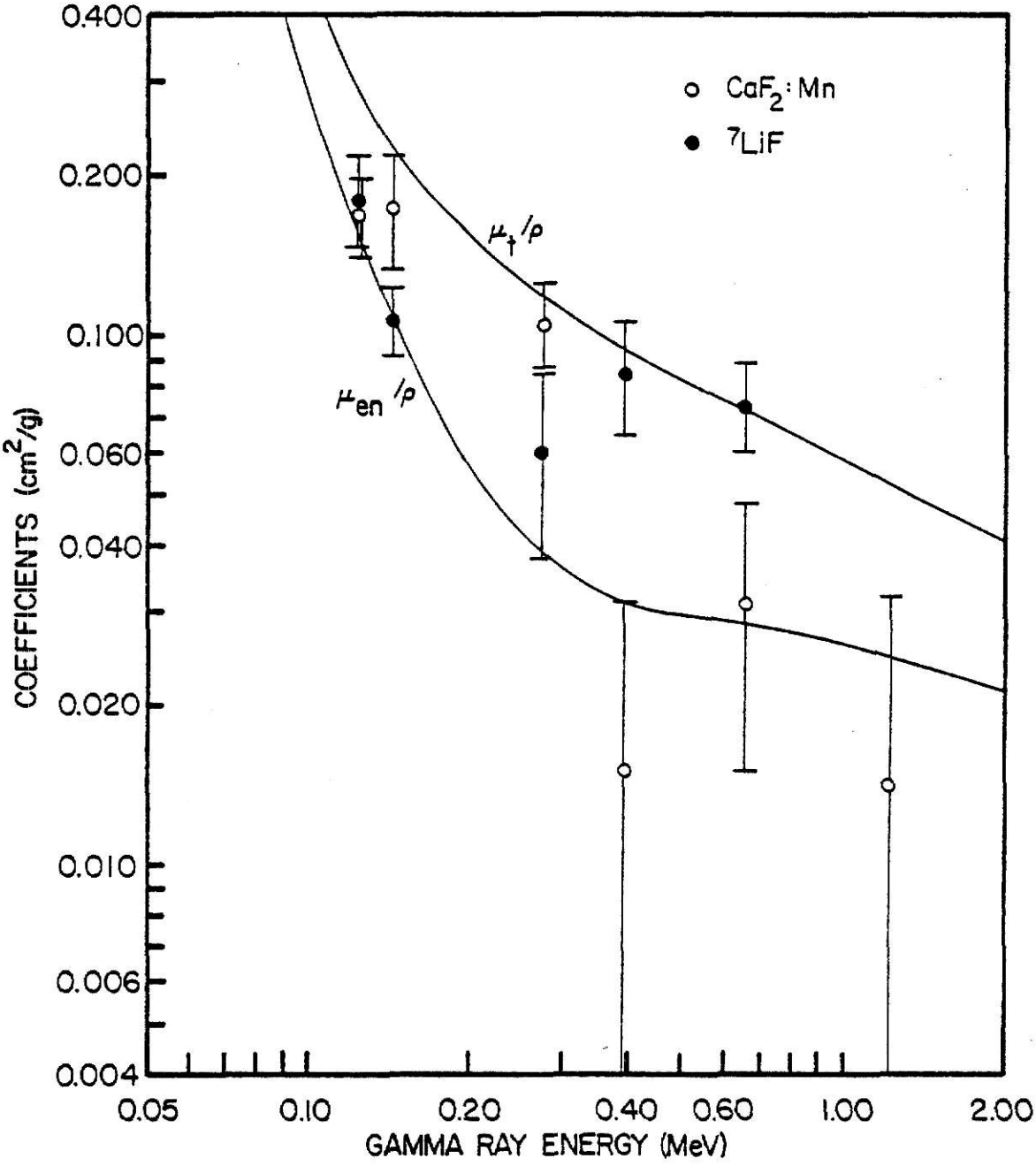

Fig. 6.5. Comparison of the experimentally determined effective attenuation coefficients for copper encased ^{7}LiF and CaF_2:Mn TLDs to the total attenuation and mass energy absorption coefficients for copper.

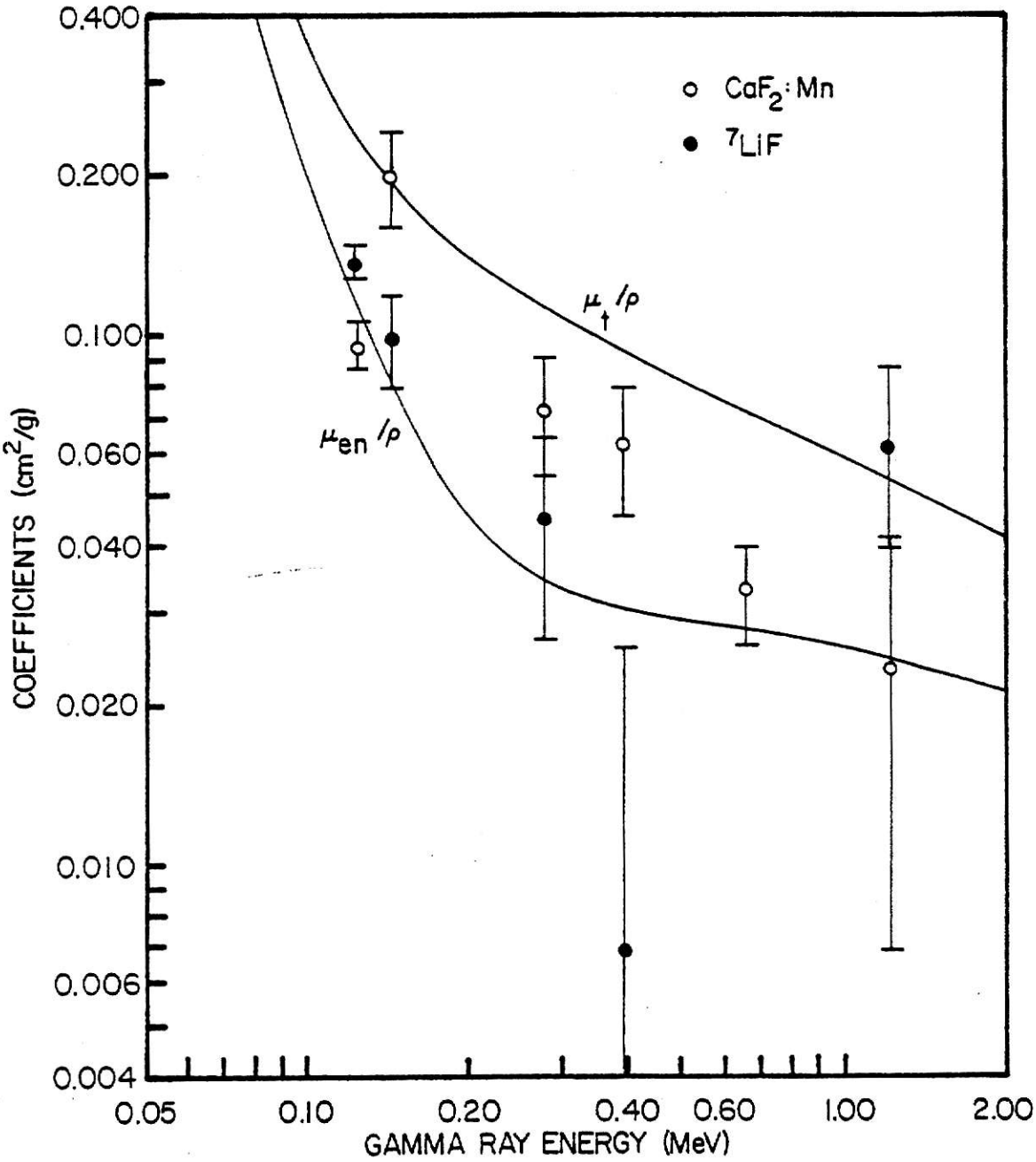

Fig. 6.6. Comparison of the experimentally determined effective attenuation coefficients for iron encased ^{7}LiF and CaF_2:Mn TLDs to the total attenuation and mass energy absorption coefficients for iron.

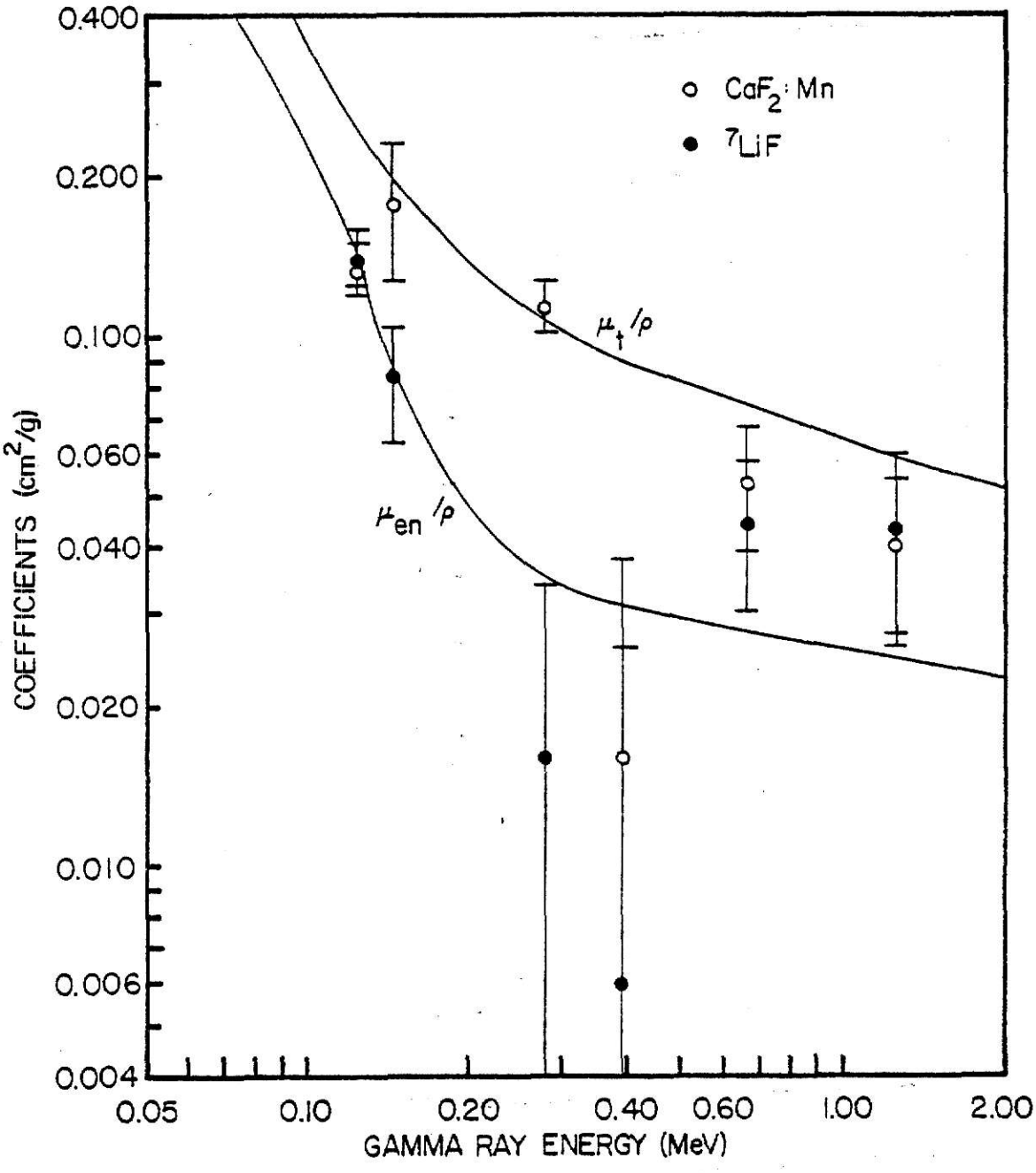

Fig. 6.7. Comparison of the experimentally determined effective attenuation coefficients for stainless steel encased ^{7}LiF and CaF_2:Mn TLDs to the total attenuation and mass energy absorption coefficients for stainless steel.

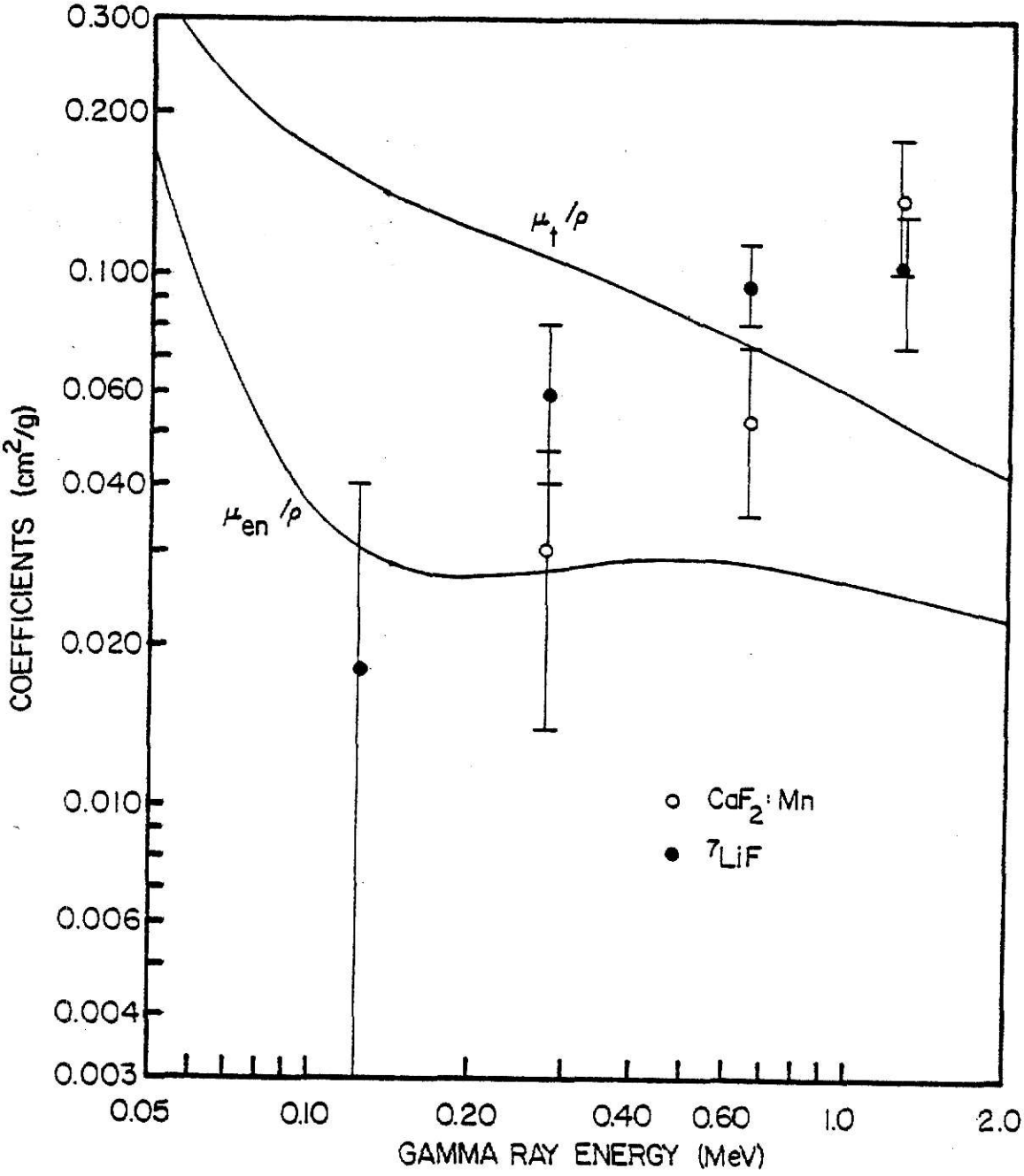

Fig. 6.8. Comparison of the experimentally determined effective attenuation coefficients for aluminum encased ^{7}LiF and CaF_2:Mn TLDs to the total attenuation and mass energy absorption coefficients for aluminum.

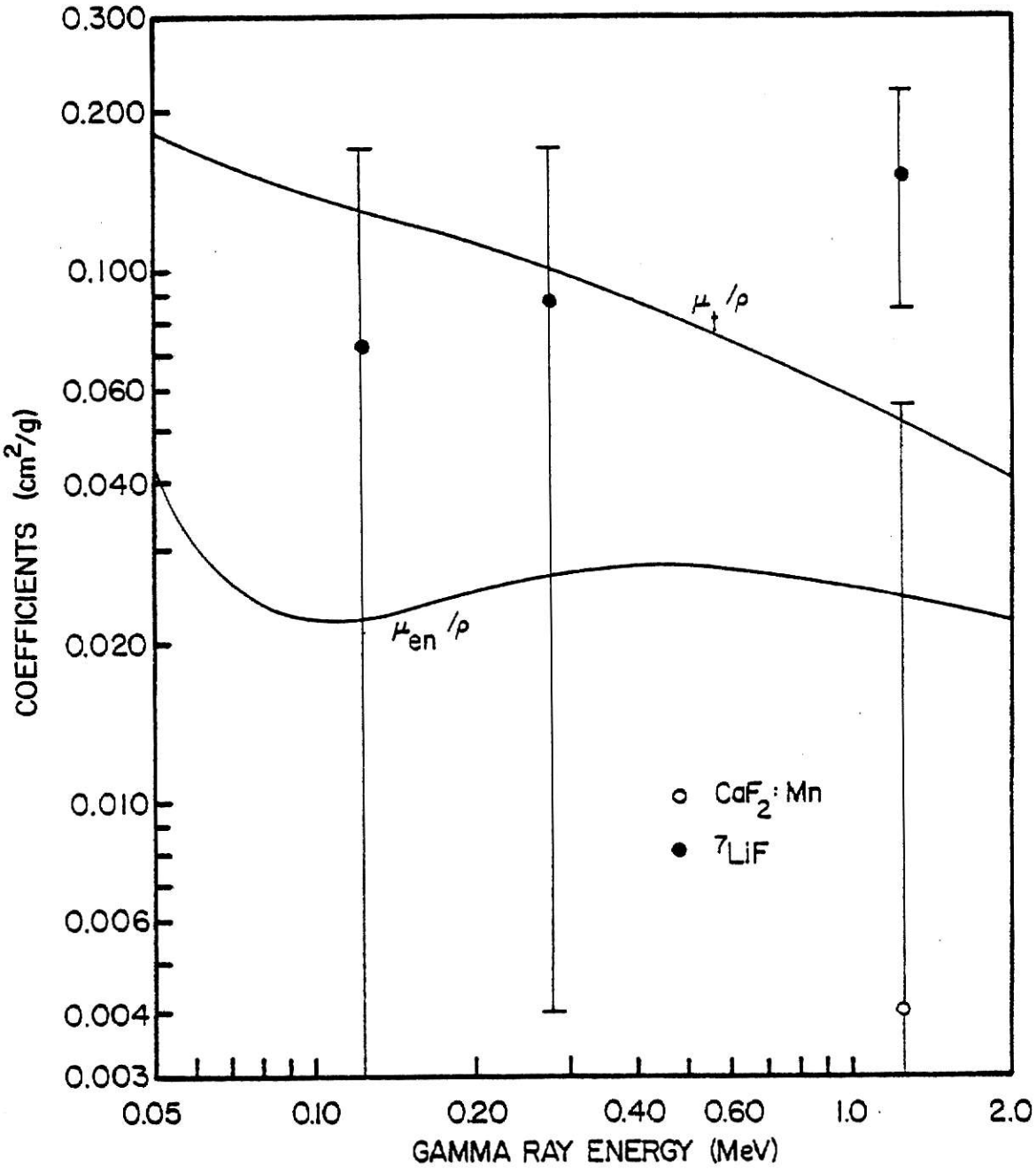

Fig. 6.9. Comparison of the experimentally determined effective attenuation coefficients for LiF encased ^{7}LiF and CaF_2:Mn TLDs to the total attenuation and mass energy absorption coefficients for LiF.

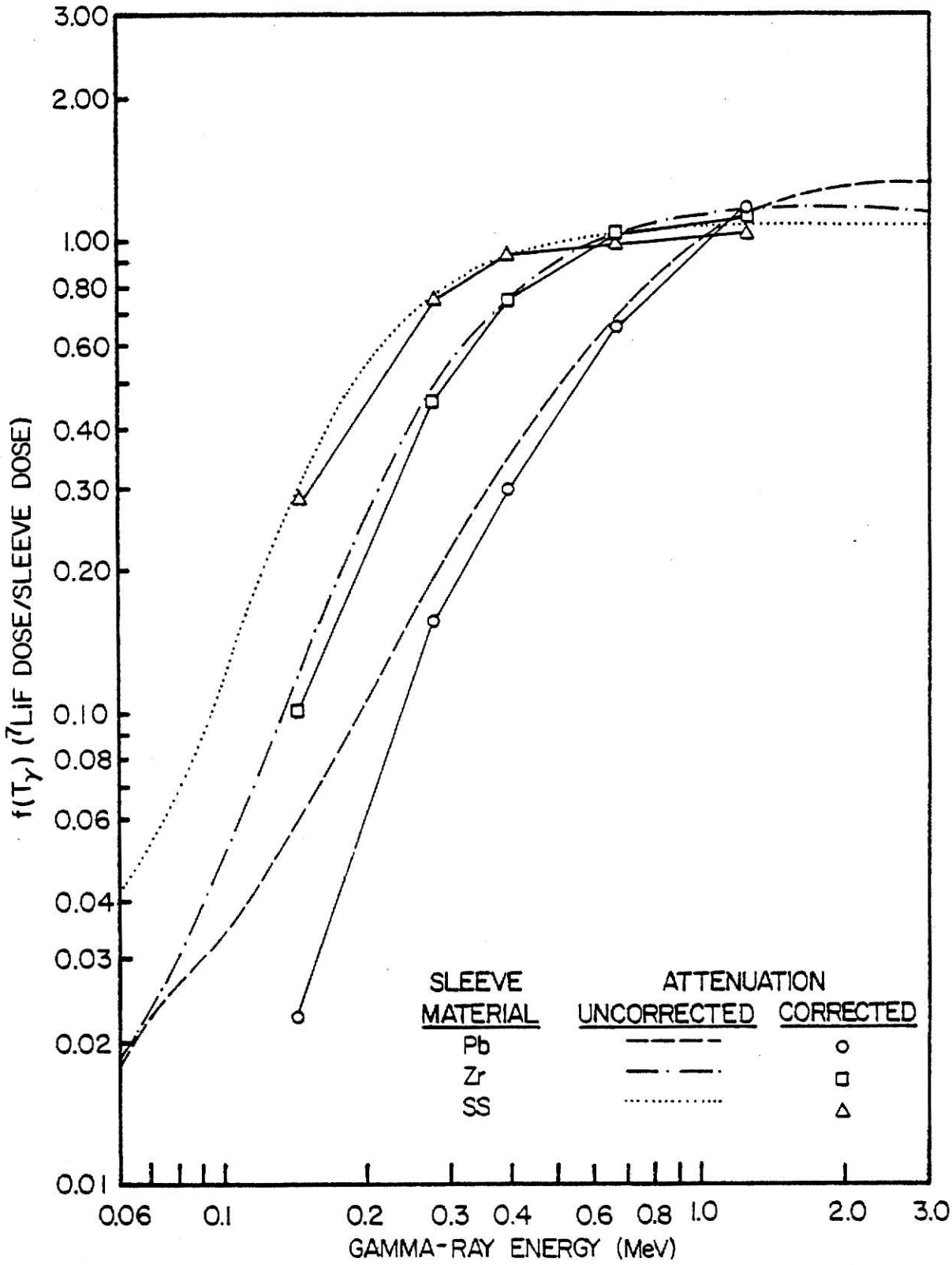

Fig. 6.10. Illustration of the attenuation correction to the dose ratio for ^{7}LiF TLDs encased in 0.7 g/cm^{2} Pb, Zr and stainless steel sleeves.

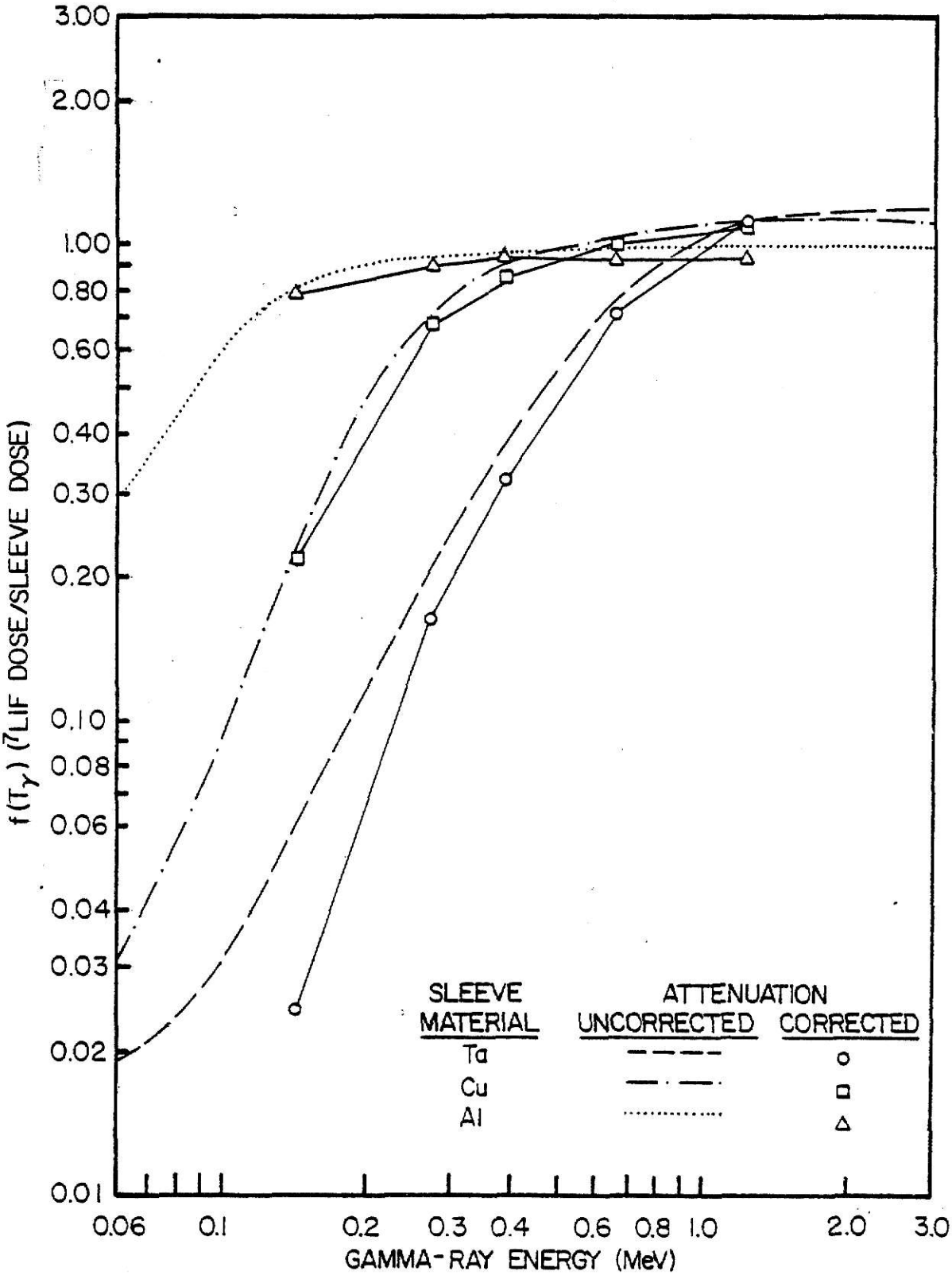

Fig. 6.11. Illustration of the attenuation correction to the dose ratio for ^{7}LiF TLDs encased in 0.7 g/cm^2 Ta, Cu, and Al sleeves.

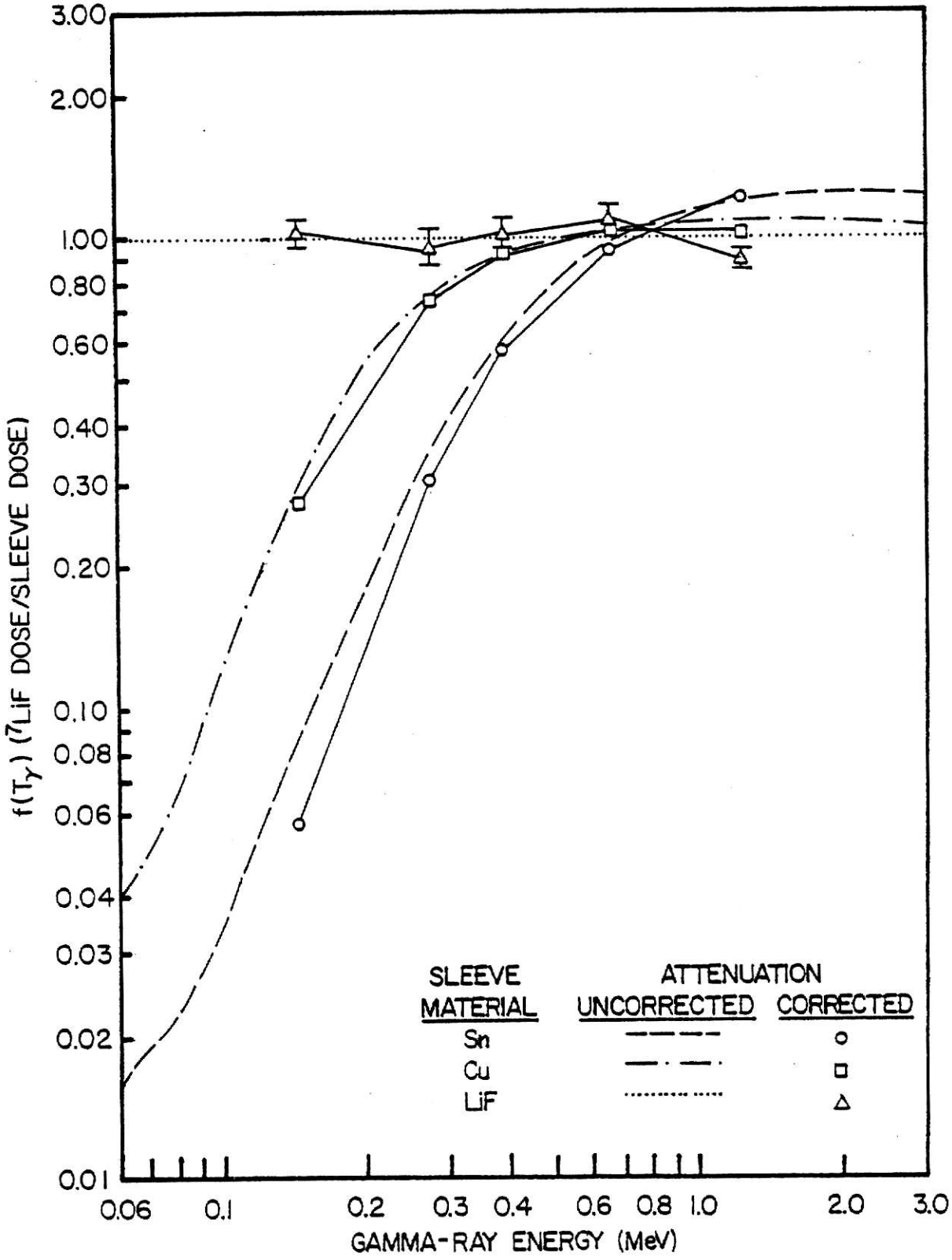

Fig. 6.12. Illustration of the attenuation correction to the dose ratio for ^{7}LiF TLDs encased in 0.7 g/cm^{2} Sn, Cu, and LiF sleeves.

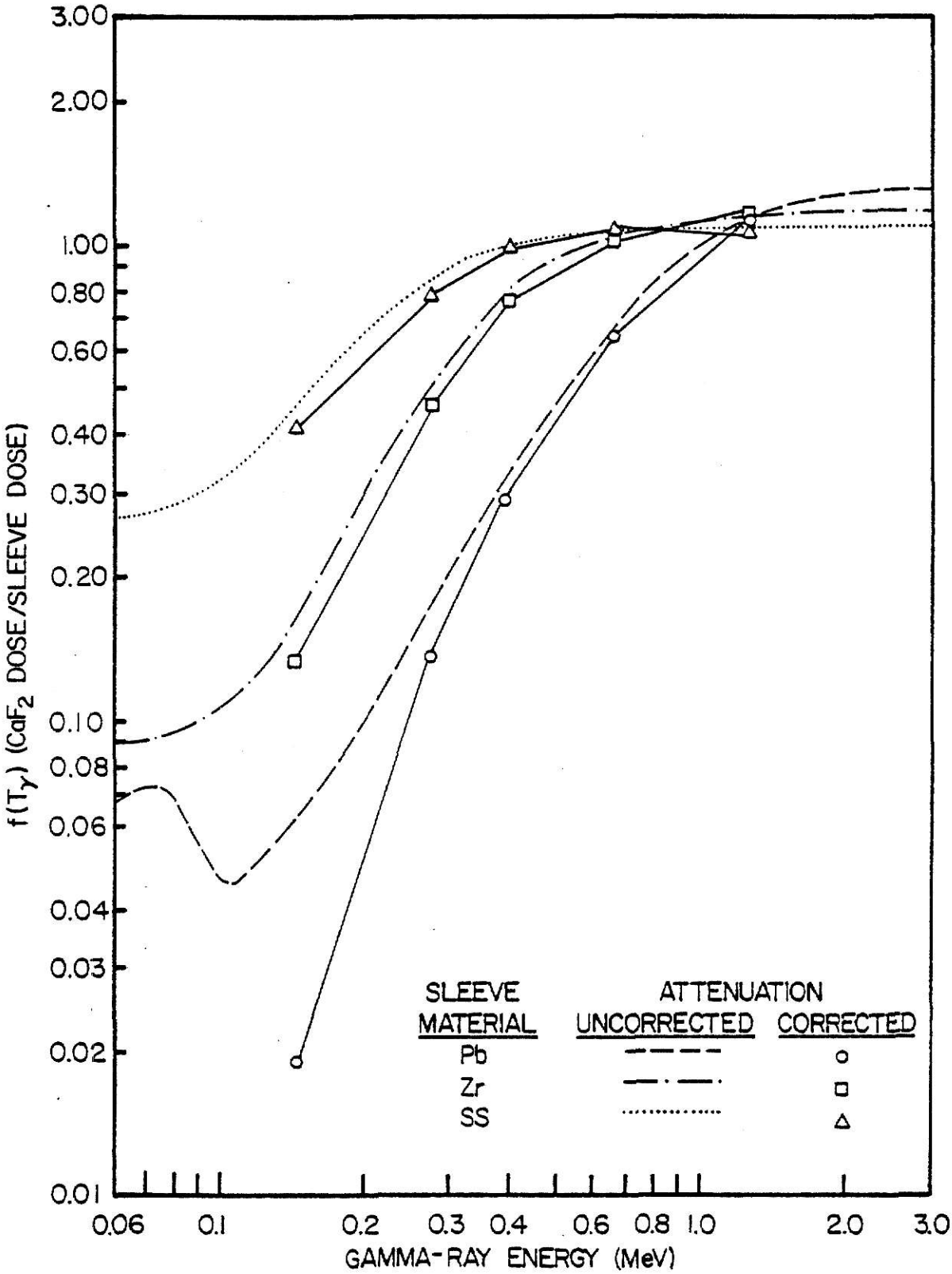

Fig. 6.13. Illustration of the attenuation correction to the dose ratio for CaF_2:Mn TLDs encased in 0.7 g/cm^2 Pb, Zr, and stainless steel sleeves.

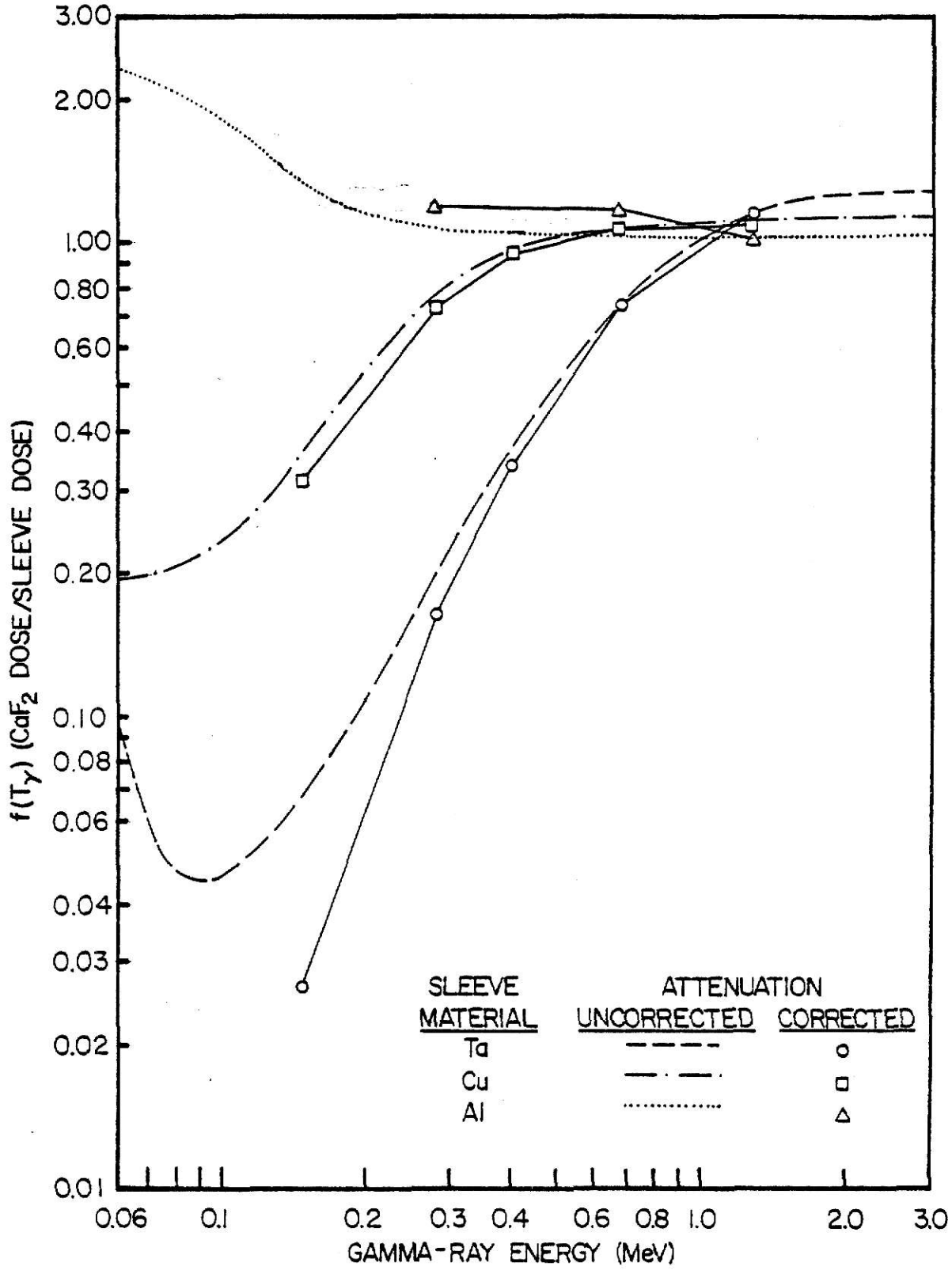

Fig. 6.14. Illustration of the attenuation correction to the dose ratio for CaF_2:Mn TLDs encased in 0.7 g/cm^2 Ta, Cu, and Al sleeves.

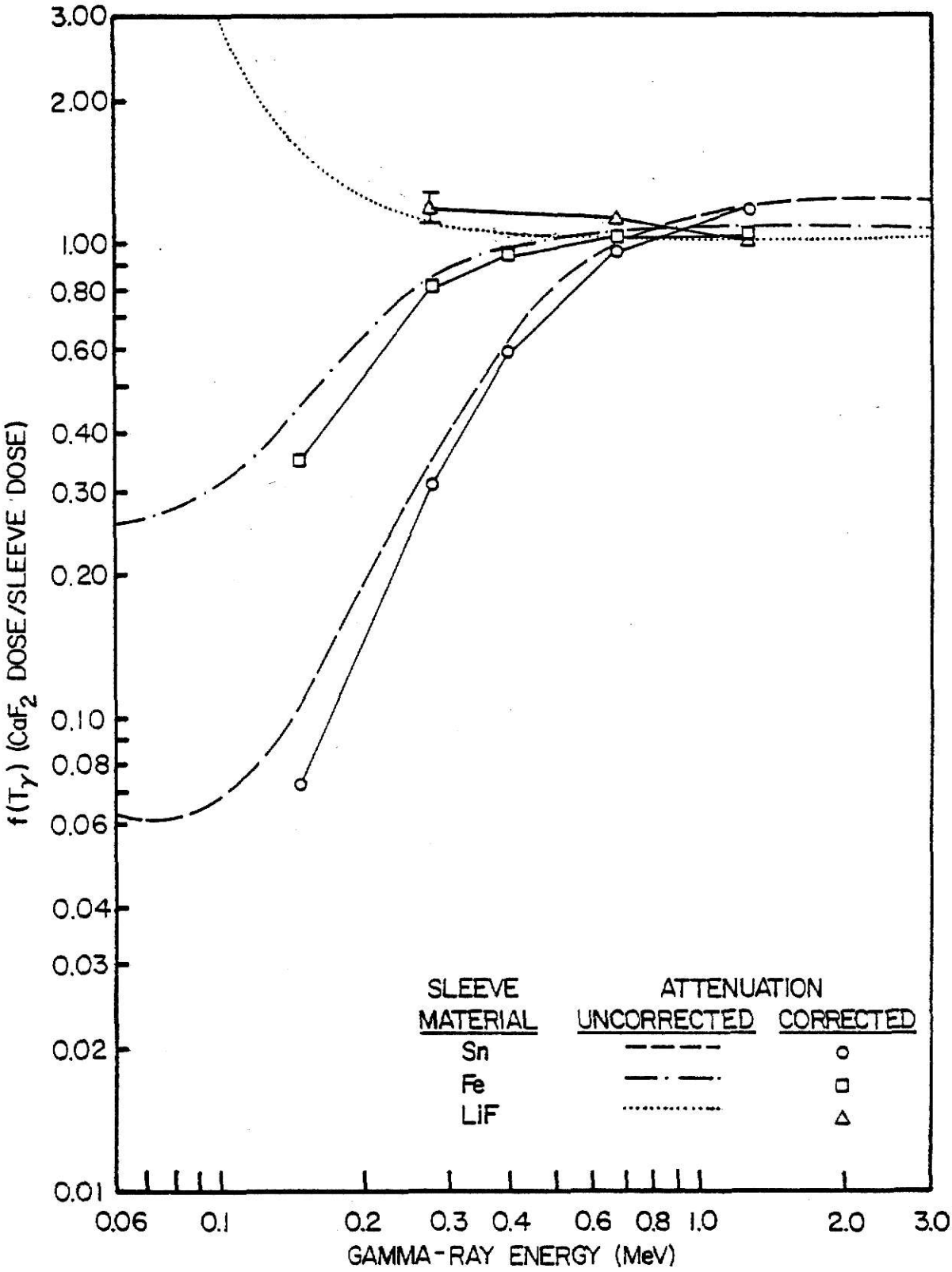

Fig. 6.15. Illustration of the attenuation correction to the dose ratio for CaF_2:Mn TLDs encased in 0.7 g/cm^2 Sn, Fe, and LiF sleeves.

Table 6.3. Calculated TLD dose ratios for encased ^{7}LiF TLDs derived from attenuation corrected TERC/III results with iron encased TLDs as the normalizing values.

Sleeve Material	Z	Sleeve Attenuation Corrected Normalized TERC/III Calculations ± σ					
		Gamma-ray Energy (MeV)					
		0.136 (11%) 0.122 (87%)	0.145	0.279	0.393	0.662	1.173 (100%) 1.333 (100%)
Lead	82	0.921±0.087	0.824±0.028	1.817±0.056	1.546±0.057	1.464±0.052	1.463±0.034
Tantalum	73	0.652±0.040	0.797±0.082	1.484±0.050	1.414±0.037	1.319±0.032	1.351±0.034
Tin	50	1.020±0.019	1.111±0.021	1.250±0.026	1.114±0.020	1.096±0.018	1.157±0.024
Zirconium	40	1.114±0.017	1.146±0.021	1.149±0.022	1.070±0.020	1.048±0.016	1.097±0.021
Copper	29	1.016±0.032	1.034±0.023	1.012±0.025	0.947±0.022	0.947±0.016	1.063±0.035
Iron	26	1.000±0.011	1.000±0.023	1.000±0.022	1.000±0.023	1.000±0.018	1.000±0.025
S.S.	--	0.992±0.015	1.008±0.024	1.024±0.022	1.003±0.023	0.964±0.017	1.022±0.023
Aluminum	13	0.814±0.012	0.909±0.016	0.948±0.018	0.961±0.018	0.918±0.014	0.957±0.023
LiF	--	0.760±0.050	0.930±0.054	0.919±0.051	0.968±0.072	0.983±0.066	0.889±0.040

Table 6.4. Calculated TLD dose ratios for encased CaF_2:Mn TLDs derived from attenuation corrected TERC/III results with iron encased TLDs as the normalizing values.

Sleeve Material	Z	Sleeve Attenuation Corrected Normalized TERC/III Calculations ± σ					
		Gamma-ray Energy (MeV)					
		0.136 (11%) 0.122 (87%)	0.145	0.279	0.393	0.662	1.173 (100%) 1.333 (100%)
Lead	82	0.496±0.006	0.450±0.025	1.426±0.036	1.487±0.042	1.386±0.015	1.308±0.029
Tantalum	73	0.436±0.019	0.586±0.039	1.382±0.048	1.351±0.038	1.290±0.028	1.255±0.021
Tin	50	0.769±0.015	0.979±0.032	1.150±0.031	1.138±0.022	1.105±0.016	1.080±0.019
Zirconium	40	0.892±0.016	1.068±0.036	1.089±0.025	1.081±0.015	1.059±0.016	1.056±0.017
Copper	29	0.963±0.026	1.040±0.049	0.991±0.022	1.049±0.016	1.010±0.016	1.019±0.021
Iron	26	1.000±0.008	1.000±0.043	1.000±0.020	1.000±0.015	1.000±0.008	1.000±0.019
S.S.	--	0.966±0.013	1.013±0.053	0.967±0.017	1.039±0.020	0.985±0.013	0.988±0.019
Aluminum	13	0.934±0.006	--	0.996±0.017	--	0.974±0.012	0.915±0.023
LiF	--	1.047±0.061	--	0.975±0.088	--	0.966±0.036	0.898±0.032

7.0 COMPARISON OF EXPERIMENT AND THEORY

7.1 Calculated and Experimental TLD Doses

Comparisons were made between the calculated doses for encapsulated TLDs, and their corresponding experimentally determined counterparts. These comparisons were performed by dividing the C ratios, calculated using Eq. 5.5, by the corresponding E ratios defined by Eq. 5.6. The employed C ratios were those tabulated in Tables 5.1 and 5.2. Tabulations of the experimental results are listed in Tables 4.1-4.4. For both types of TLDs, the C/E results are listed in Tables 7.1-7.4. These results include ratios determined with and without using sensitivity corrected experimental data.

As illustrated, the C/E results are nominally unity, except for the case of the higher Z materials and lower energy gammas. For this general exception, the ratios exceed unity by factors as great as 5.4 for lead encased ^{7}LiF TLDs, and 4.1 for lead encased CaF_2:Mn TLDs.

This greater than unity phenomenon may be attributed to one or both of two possible explanations. The first of these, which has already proven significant, is low energy gamma attenuation by the high atomic number encasing materials. The second, and less probable of the two has to do with the input data used to perform the calculations. As reported by Storm and Israel[24], the mass energy absorption coefficients may be inaccurate by as much as 10% for low energy gammas. These inaccuracies would then be exhibited, to various degrees, in the C terms of the C/E ratios.

Table 7.1. Comparison of dose ratios using encapsulated ^{7}LiF TLDs from a precision subset.

Sleeve Material	Z	(C/E) ± $\sigma_{\bar{x}}$ Gamma-ray Energy (MeV) 0.136 (11%) 0.122 (87%)	0.145	0.279	0.393	0.662	1.173 (100%) 1.333 (100%)
Lead	82	5.245±0.102	5.408±0.085	1.467±0.017	1.110±0.017	0.975±0.018	1.020±0.015
Tantalum	73	4.618±0.137	3.963±0.138	1.314±0.021	1.066±0.015	0.998±0.017	1.019±0.019
Tin	50	1.561±0.019	1.333±0.023	1.058±0.013	0.987±0.010	1.037±0.014	1.004±0.018
Zirconium	40	1.120±0.014	1.059±0.013	1.027±0.016	0.984±0.015	0.995±0.012	0.996±0.011
Copper	29	1.111±0.023	1.042±0.015	0.990±0.014	1.028±0.013	1.037±0.010	1.017±0.012
Iron	26	1.000±0.010	1.000±0.015	1.000±0.014	1.000±0.009	1.000±0.013	1.000±0.013
S.S.	--	1.006±0.014	1.029±0.017	0.994±0.012	0.999±0.012	0.999±0.015	1.014±0.015
Aluminum	13	0.800±0.011	0.866±0.013	0.976±0.019	0.978±0.012	0.992±0.014	0.991±0.015
LiF	--	0.777±0.013	0.823±0.011	0.954±0.016	0.946±0.009	0.965±0.016	0.972±0.017

Table 7.2. Comparison of dose ratios using encapsulated CaF_2:Mn TLDs from a precision subset.

Sleeve Material	Z	(C/E) ± $\sigma_{\bar{x}}$					
		Gamma-ray Energy (MeV)					
		0.136 (11%) 0.122 (87%)	0.145	0.279	0.393	0.662	1.173 (100%) 1.333 (100%)
Lead	82	4.128±0.080	3.661±0.059	1.571±0.023	1.093±0.017	1.007±0.014	0.968±0.013
Tantalum	73	3.251±0.124	2.648±0.048	1.438±0.025	1.038±0.022	1.005±0.011	0.947±0.018
Tin	50	1.282±0.020	1.186±0.015	1.146±0.014	0.989±0.018	1.022±0.015	0.953±0.014
Zirconium	40	1.143±0.021	1.150±0.025	1.111±0.017	0.979±0.017	0.983±0.013	0.993±0.017
Copper	29	1.056±0.018	1.077±0.010	1.036±0.015	1.009±0.015	1.024±0.011	0.944±0.015
Iron	26	1.000±0.018	1.000±0.009	1.000±0.015	1.000±0.017	1.000±0.013	1.000±0.016
S.S.	--	0.997±0.015	1.005±0.012	1.018±0.014	0.995±0.014	0.994±0.012	1.004±0.014
Aluminum	13	0.842±0.012	--	0.969±0.012	--	0.976±0.011	0.968±0.015
LiF	--	0.878±0.013	--	0.933±0.015	--	0.956±0.014	0.938±0.014

Table 7.3. Comparison of dose ratios using encased ^{7}LiF TLDs where the experimental values were corrected for the sensitivity of individual TLDs.

Sleeve Material	Z	(C/E) ± $\sigma_{\bar{x}}$					
		Gamma-ray Energy (MeV)					
		0.136 (11%) 0.122 (87%)	0.145	0.279	0.393	0.662	1.173 (100%) 1.333 (100%)
Lead	82	5.273±0.093	5.453±0.090	1.483±0.026	1.126±0.014	0.981±0.012	1.033±0.014
Tantalum	73	4.606±0.067	4.000±0.105	1.326±0.024	1.075±0.016	1.001±0.014	1.030±0.012
Tin	50	1.561±0.024	1.334±0.017	1.065±0.018	0.994±0.010	1.039±0.014	1.012±0.015
Zirconium	40	1.117±0.013	1.055±0.012	1.032±0.021	0.982±0.012	0.991±0.011	1.000±0.014
Copper	29	1.085±0.015	1.045±0.012	0.995±0.017	1.020±0.010	1.037±0.014	1.023±0.014
Iron	26	1.000±0.014	1.000±0.010	1.000±0.022	1.000±0.012	1.000±0.012	1.000±0.013
S.S.	--	1.008±0.015	1.033±0.012	0.999±0.018	1.001±0.017	0.996±0.011	1.016±0.014
Aluminum	13	0.798±0.010	0.868±0.009	0.980±0.018	0.982±0.012	0.991±0.011	0.996±0.014
LiF	--	0.776±0.010	0.824±0.008	0.954±0.016	0.944±0.011	0.958±0.012	0.972±0.011

Table 7.4. Comparison of dose ratios using encased CaF_2:Mn TLDs where the experimental values were corrected for the sensitivity of individual TLDs.

Sleeve Material	Z	(C/E) ± σ_x					
		Gamma-ray Energy (MeV)					
		0.136 (11%) 0.122 (87%)	0.145	0.279	0.393	0.662	1.173 (100%) 1.333 (100%)
Lead	82	4.054±0.048	3.671±0.056	1.579±0.013	1.105±0.008	1.017±0.008	0.970±0.010
Tantalum	73	3.281±0.039	2.655±0.042	1.452±0.013	1.047±0.010	1.013±0.009	0.954±0.012
Tin	50	1.287±0.011	1.188±0.020	1.155±0.007	0.995±0.014	1.030±0.011	0.958±0.011
Zirconium	40	1.138±0.008	1.105±0.007	1.113±0.009	0.977±0.008	0.980±0.010	0.990±0.010
Copper	29	1.059±0.007	1.081±0.008	1.043±0.008	1.012±0.010	1.027±0.016	0.948±0.010
Iron	26	1.000±0.008	1.000±0.005	1.000±0.006	1.000±0.007	1.000±0.009	1.000±0.012
S.S.	--	0.998±0.010	1.005±0.004	1.023±0.007	0.996±0.009	0.995±0.010	1.005±0.010
Aluminum	13	0.844±0.007	--	0.947±0.012	--	0.979±0.013	0.970±0.010
LiF	--	0.877±0.008	--	0.941±0.012	--	0.953±0.010	0.937±0.010

7.2 Comparison of Attenuation Corrected Doses

Comparisons were also made between the sensitivity corrected experimentally determined doses (tabulated in Tables 4.3 and 4.4), and the attenuation corrected calculated doses (tabulated in Tables 6.3 and 6.4). The results are shown in Tables 7.5 and 7.6. As is observed, the attenuation corrected C/E results are all nominally closer to the desired value of unity, than their uncorrected counterparts. This indicates that the attenuation corrected calculated doses, predict the experimentally determined quantities better than the uncorrected calculations. However, the attenuation corrected calculations are not acceptable for cases where the TLDs were encapsulated in lead and tantalum and exposed to the Co-57, Ce-141, and Hg-203 sources. These particular results tend to deviate from unity by as much as 90% for the ^{7}LiF, and 20% for the CaF_2:Mn dosimeters.

7.3 The Effective Source Counts Comparison

The relative number of source decays (S_{rel}) were calculated using both the attenuation corrected expression given by Eq. 5.16, and the non-attenuation corrected expression given by Eq. 5.7. Calculations were performed for each combination of TLD, sleeve material, and gamma-ray energy. The employed TLD responses (E_D^{exp}) were selected from the sensitivity corrected TLD energy response data. Both the attenuation corrected, and non-attenuation corrected results are shown in Figs. 7.1-7.12. These results are plotted as a function of the effective atomic number[25] for the TLD encasing materials.

For both the encased ^{7}LiF and CaF_2:Mn TLDs, the relative number of source decays is nominally constant over the range of effective atomic numbers investigated using the Co-60, Cs-137, and Sn-113 sources.

Since there is little attenuation of the primary gammas associated with these sources, application of the attenuation correction does not significantly change the source decay results. However, these source results are quite different when data taken with the Hg-203, Ce-141, and Co-57 sources are used.

For these lower energy sources, non-attenuation corrected source decays tend to decrease as a function of increasing effective atomic number. Furthermore, this trend becomes more pronounced as the gamma energy decreases. For the Co-57 results, the relative source decays vary by factors as great as seven for the encased ^{7}LiF, and six for the encased CaF_2:Mn TLDs. This phenomenon is indicative of the attenuation of the primary gammas by the TLD encasement walls.

With the application of the attenuation corrections, the results for the lower energy sources are nominally improved. However, these corrections do not force the relative source decays to be constant as a function of effective atomic number. For the Co-57 results, the source decays still vary by factors as great as 2.0 for the encased ^{7}LiF, and 1.4 for the encased CaF_2:Mn dosimeters.

Table 7.5. Comparison of ^{7}LiF dose ratios where the experimental values were corrected for sensitivity and the calculations were corrected for sleeve wall attenuation.

Sleeve Material	Z	(C/E) ± $\sigma_{\bar{x}}$ Gamma-ray Energy (MeV)					
		0.136 (11%) 0.122 (87%)	0.145	0.279	0.393	0.662	1.173 (100%) 1.333 (100%)
Lead	82	1.903±0.184	1.635±0.063	1.178±0.042	0.947±0.037	0.913±0.035	1.094±0.029
Tantalum	73	1.251±0.079	1.314±0.139	1.008±0.038	0.960±0.029	0.948±0.025	1.097±0.031
Tin	50	0.980±0.023	0.962±0.022	0.999±0.027	0.946±0.020	1.019±0.021	1.074±0.028
Zirconium	40	0.951±0.019	0.966±0.021	1.014±0.030	0.978±0.023	0.985±0.019	1.047±0.026
Copper	29	1.038±0.035	1.035±0.026	0.981±0.030	0.963±0.023	0.971±0.021	1.072±0.038
Iron	26	1.000±0.018	1.000±0.025	1.000±0.031	1.000±0.024	1.000±0.022	1.000±0.028
S.S.	--	1.002±0.021	1.043±0.027	1.023±0.028	1.001±0.029	0.956±0.020	1.030±0.027
Aluminum	13	0.881±0.017	0.923±0.019	0.982±0.026	0.968±0.022	0.935±0.017	0.986±0.027
LiF	--	0.827±0.054	0.911±0.054	0.936±0.055	0.949±0.071	0.988±0.067	0.927±0.043

Table 7.6. Comparison of CaF_2:Mn dose ratios where the experimental values were corrected for sensitivity and the calculations were corrected for sleeve wall attenuation.

Sleeve Material	Z	(C/E) ± σ_x Gamma-ray Energy (MeV)					
		0.136 (11%) 0.122 (87%)	0.145	0.279	0.393	0.662	1.173 (100%) 1.333 (100%)
Lead	82	1.213±0.021	0.864±0.050	1.137±0.030	0.986±0.029	0.955±0.012	0.950±0.023
Tantalum	73	0.894±0.041	0.890±0.061	1.158±0.062	0.966±0.029	0.985±0.023	0.968±0.016
Tin	50	0.773±0.017	0.901±0.033	1.049±0.028	0.996±0.024	1.038±0.019	0.958±0.020
Zirconium	40	0.887±0.017	1.036±0.035	1.073±0.026	0.998±0.016	0.994±0.018	0.995±0.018
Copper	29	0.989±0.027	1.095±0.051	1.010±0.024	1.051±0.022	1.027±0.022	0.954±0.022
Iron	26	1.000±0.011	1.000±0.044	1.000±0.022	1.000±0.025	1.000±0.012	1.000±0.023
S.S.	--	0.965±0.016	1.019±0.053	0.988±0.019	1.033±0.025	0.977±0.016	0.991±0.020
Aluminum	13	0.915±0.009	--	0.987±0.021	--	0.974±0.018	0.913±0.024
LiF	--	1.040±0.061	--	1.039±0.095	--	1.042±0.040	0.952±0.035

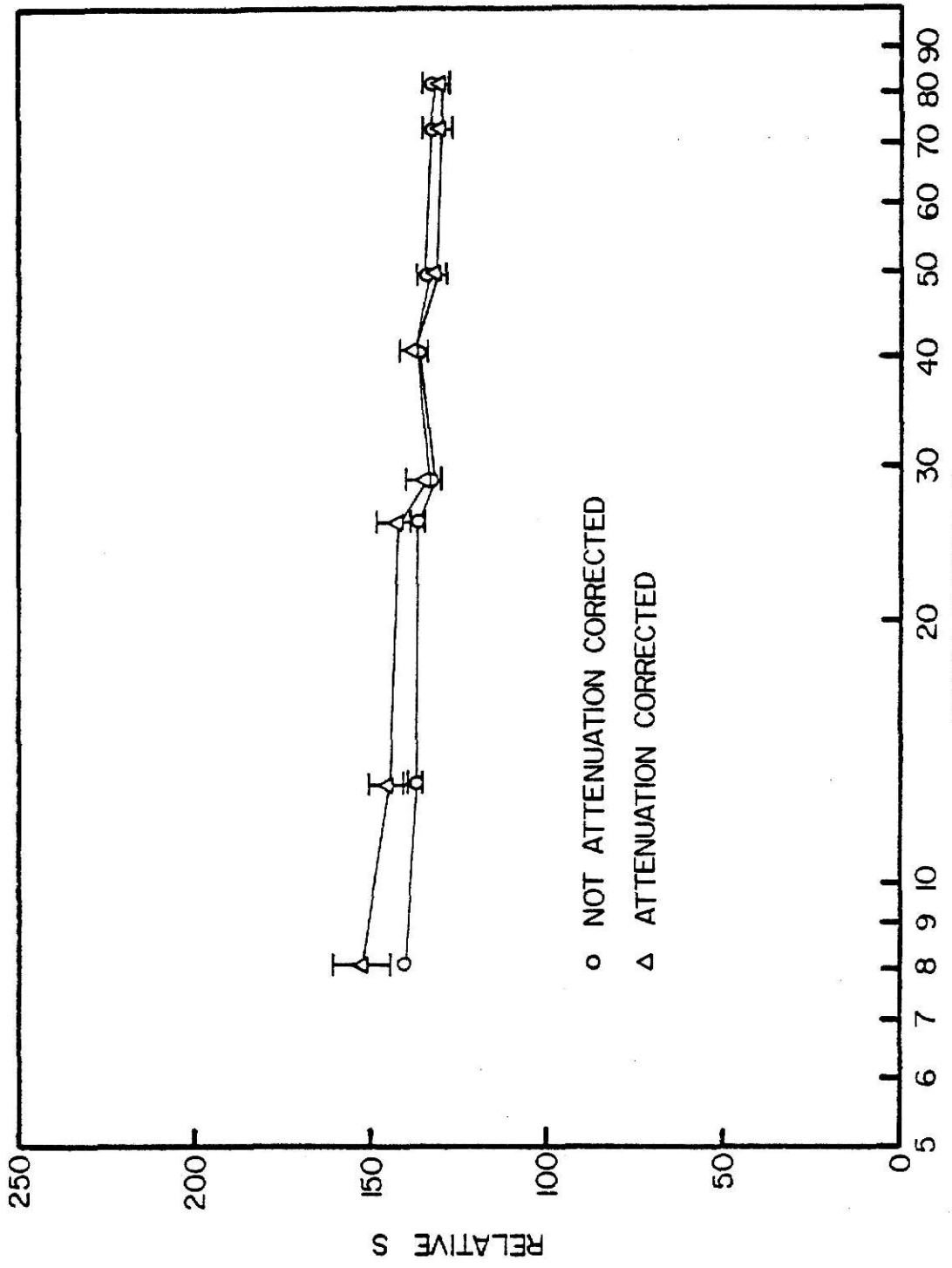

Fig. 7.1. Relative number of source decays from Co-60 irradiated encased ^{7}LiF TLDs as a function of encasement material atomic number.

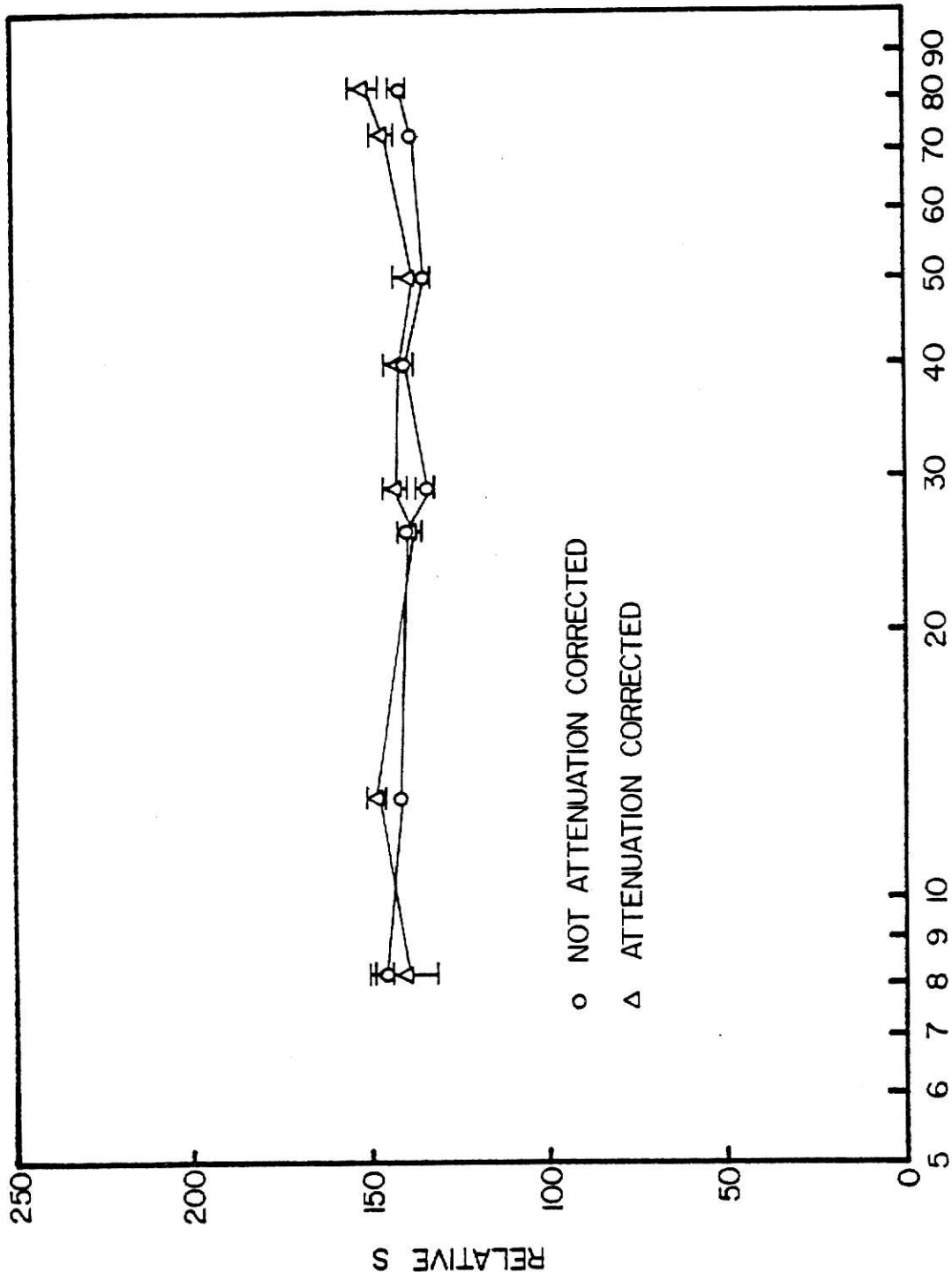

Fig. 7.2. Relative number of source decays from Cs-137 irradiated encased ^{7}LiF TLDs as a function of encasement material atomic number.

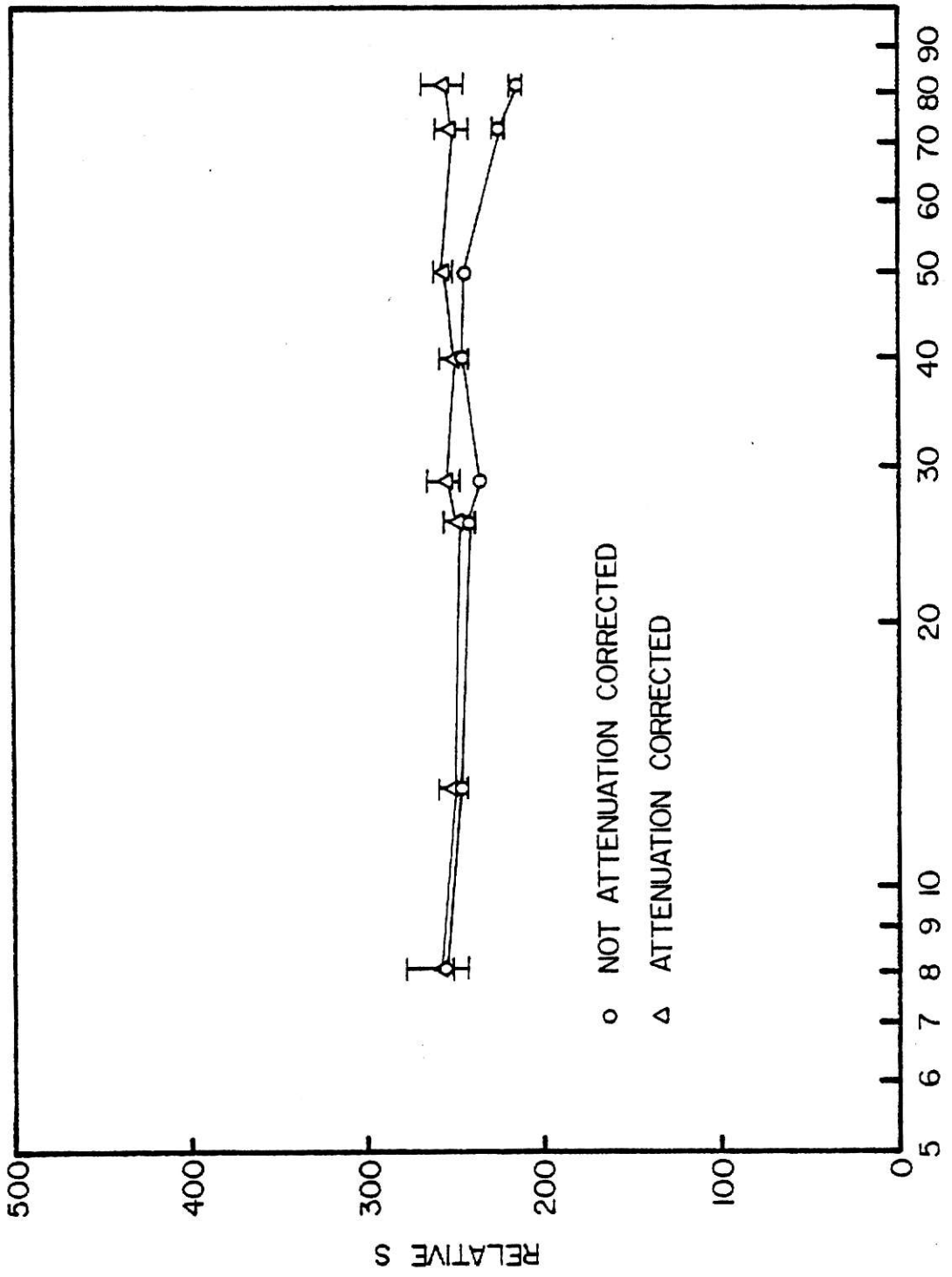

Fig. 7.3. Relative number of source decays from Sn-113 irradiated encased ^{7}LiF TLDs as a function of encasement material atomic number.

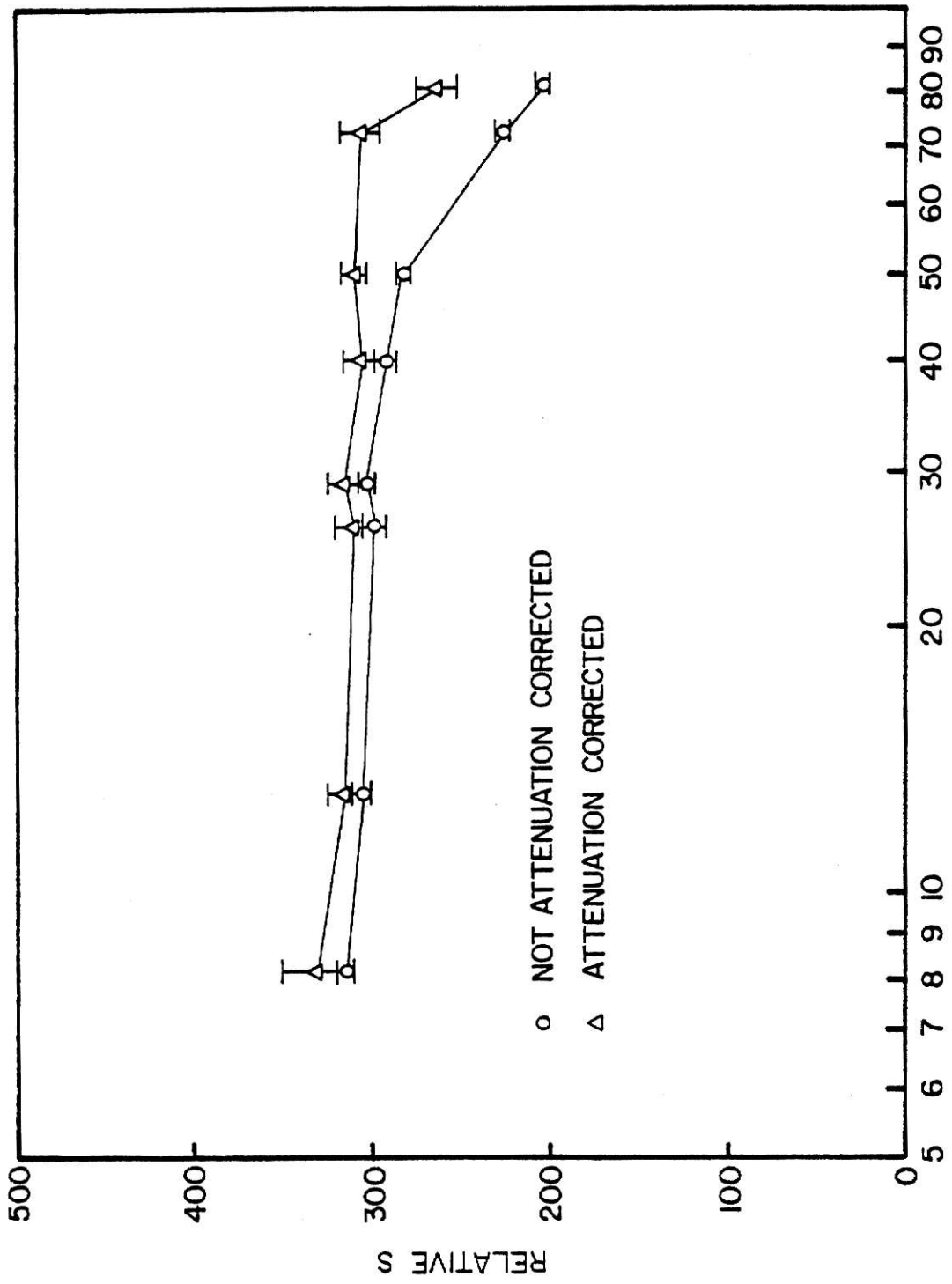

Fig. 7.4. Relative number of source decays from Hg-203 irradiated encased ^{7}LiF TLDs as a function of encasement material atomic number.

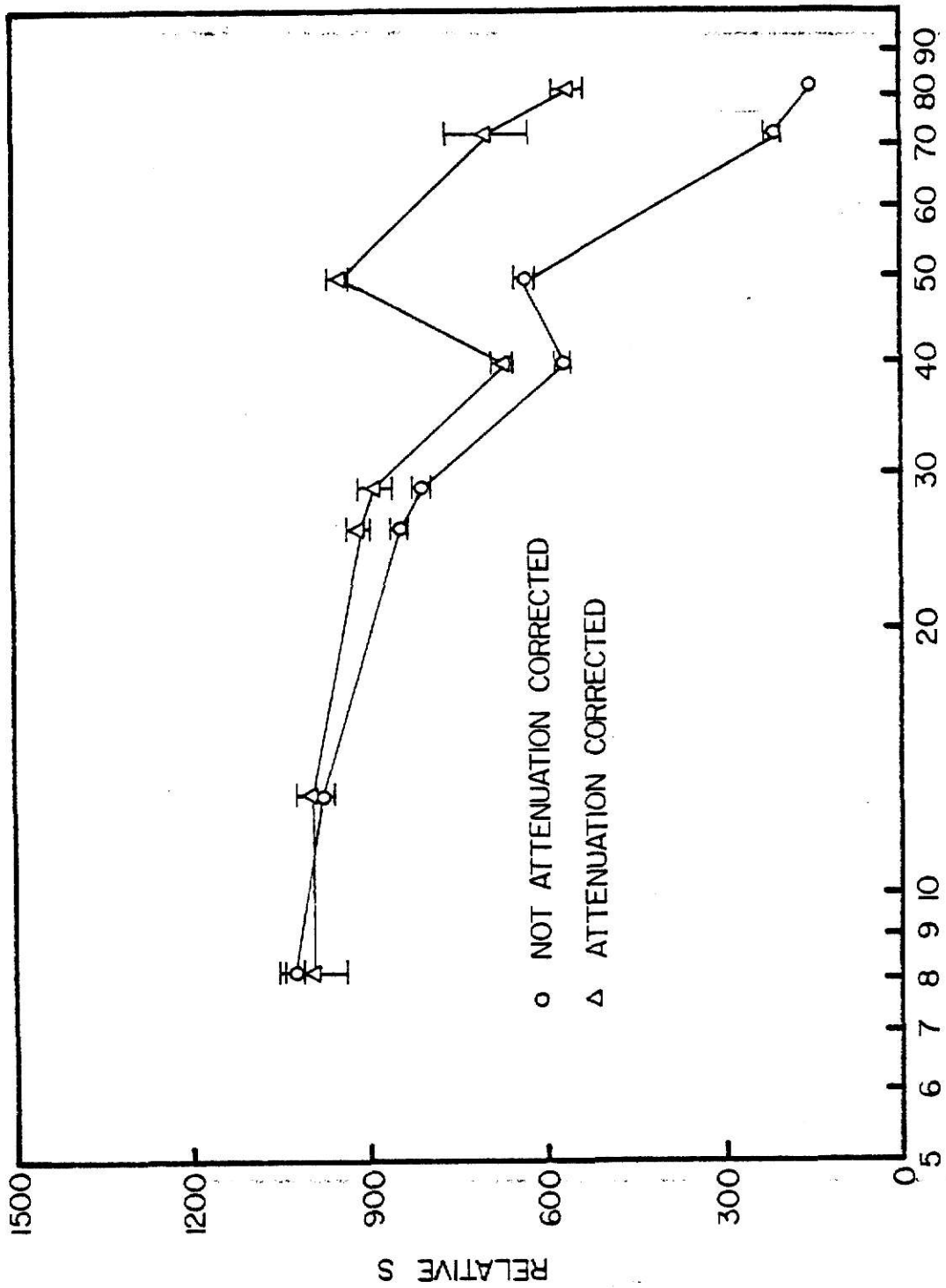

Fig. 7.5. Relative number of source decays from Ce-141 irradiated encased ^{7}LiF TLDs as a function of encasement material atomic number.

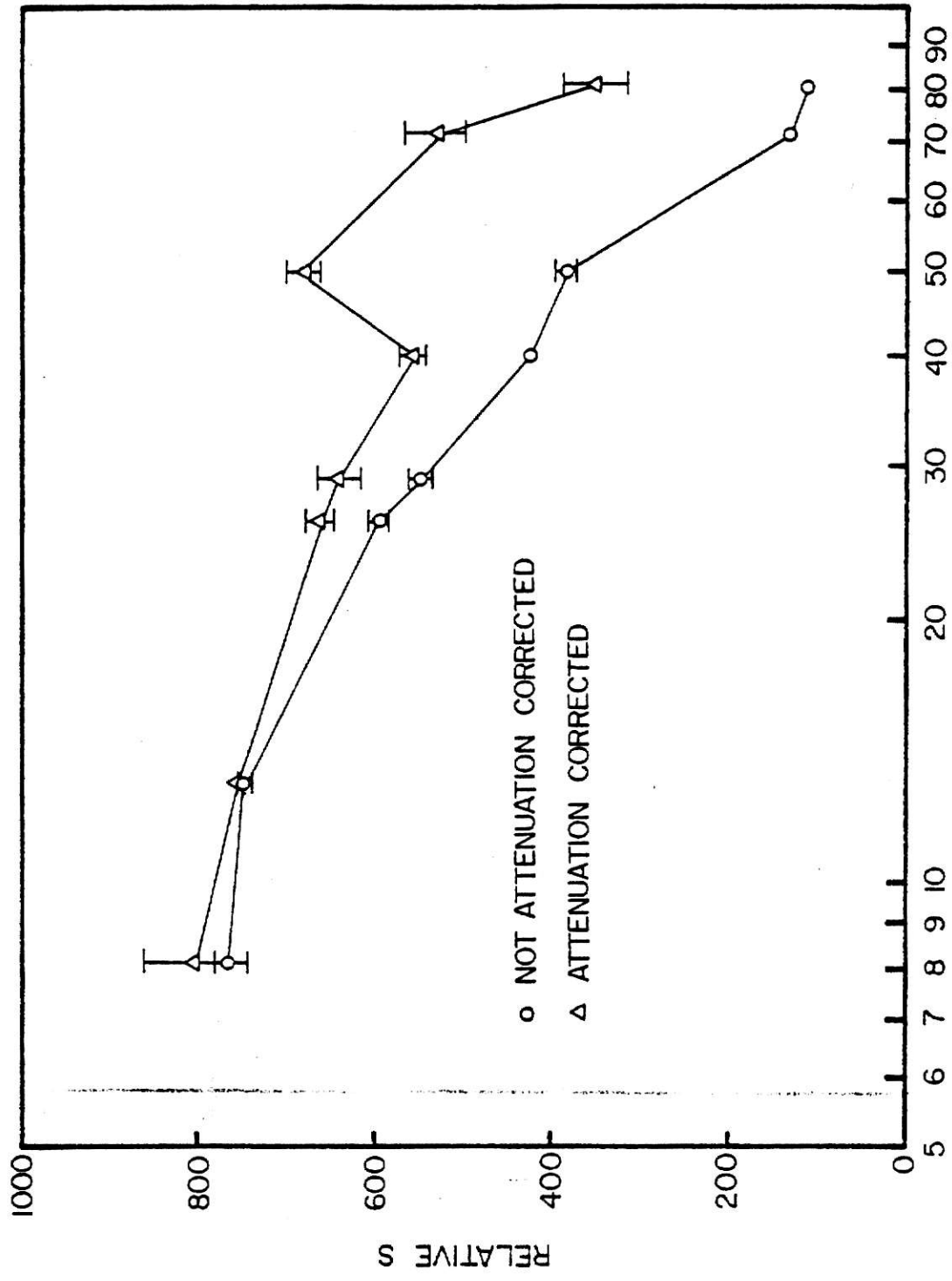

Fig. 7.6. Relative number of source decays from Co-57 irradiated encased ^{7}LiF TLDs as a function of encasement material atomic number.

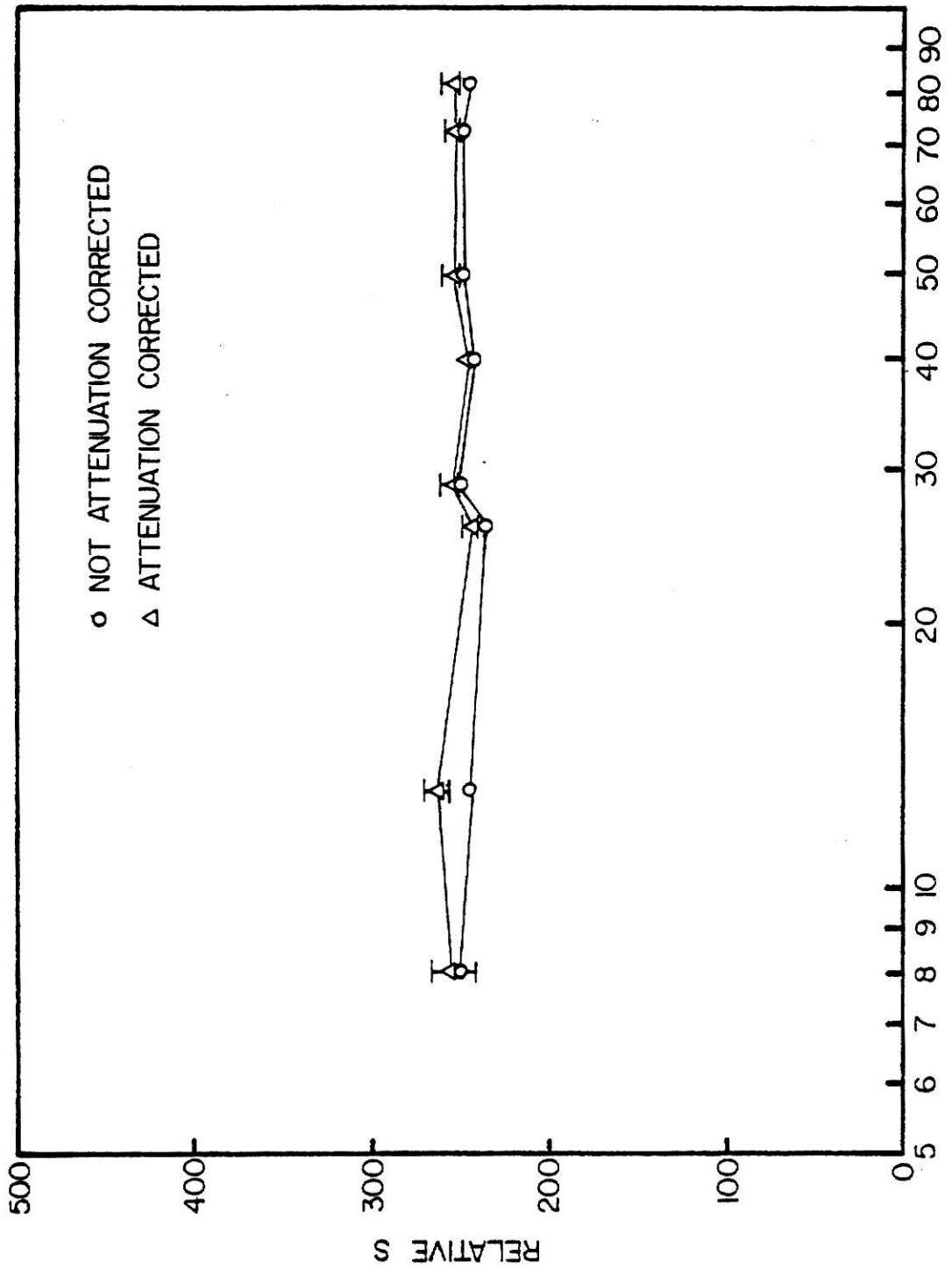

Fig. 7.7. Relative number of source decays from Co-60 irradiated encased CaF_2:Mn TLDs as a function of encasement material atomic number.

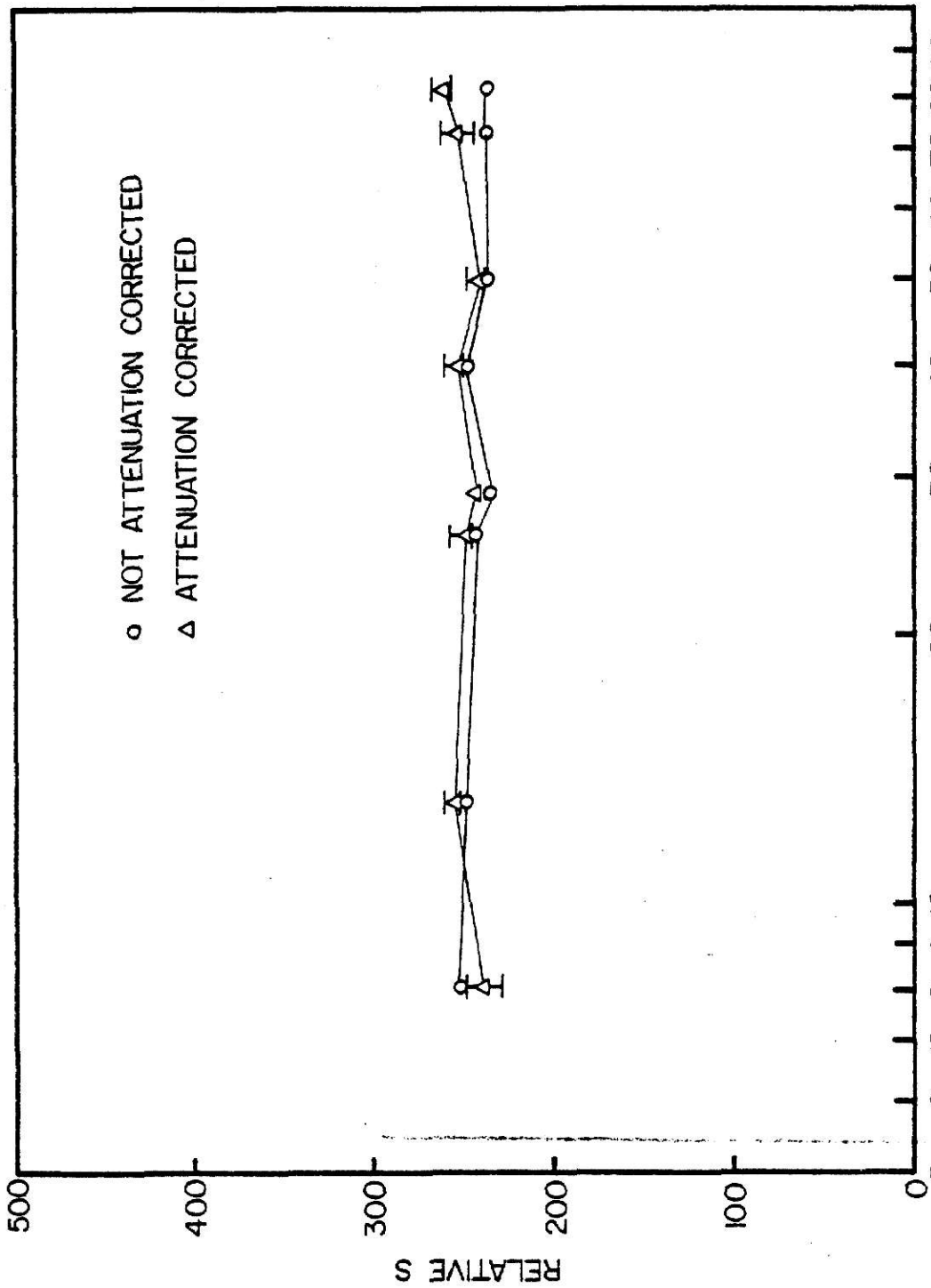

Fig. 7.8. Relative number of source decays from Cs-137 irradiated encased CaF_2:Mn TLDs as a function of encasement material atomic number.

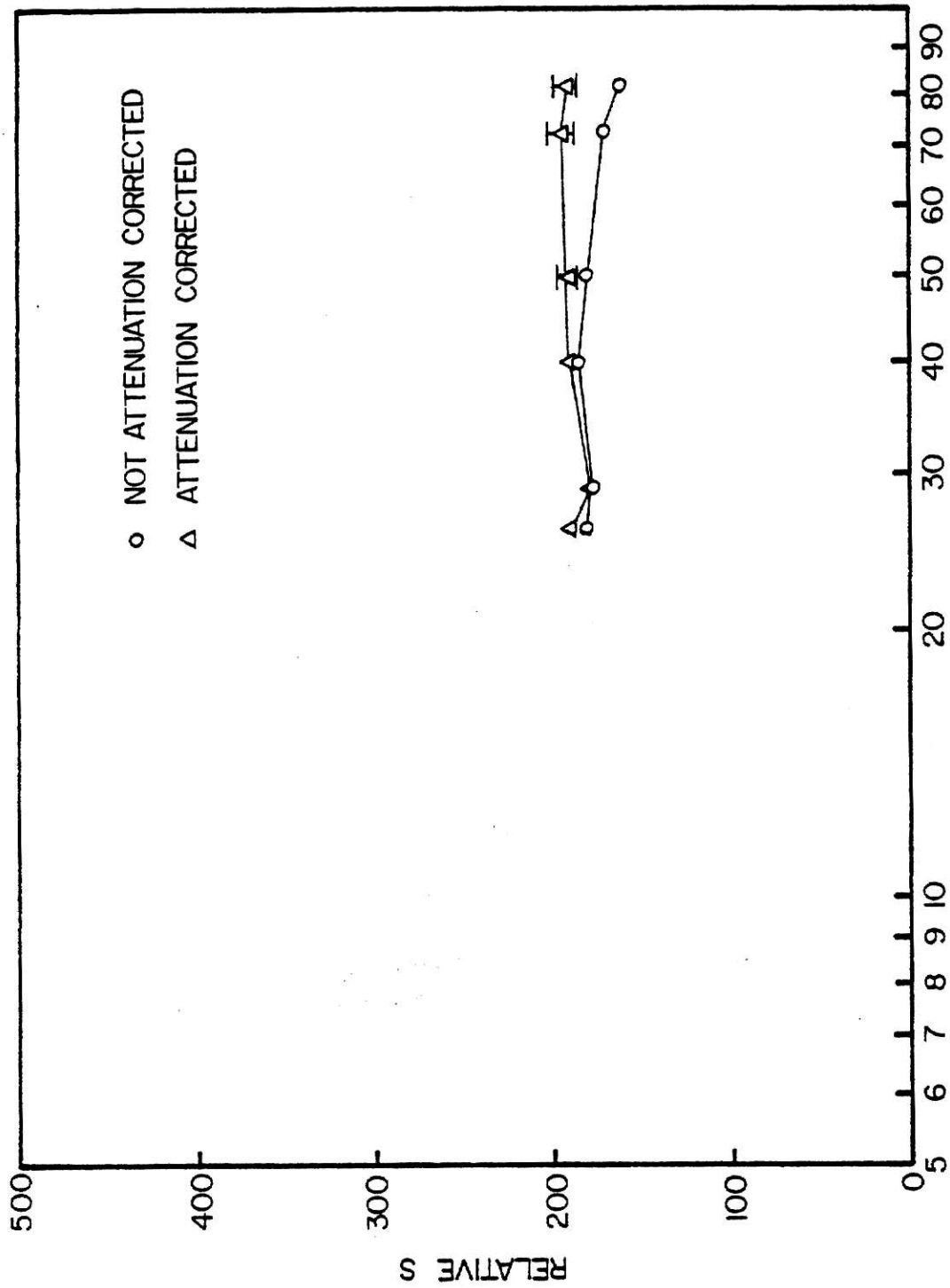

Fig. 7.9. Relative number of source decays from Sn-113 irradiated encased CaF_2:Mn TLDs as a function of encasement material atomic number.

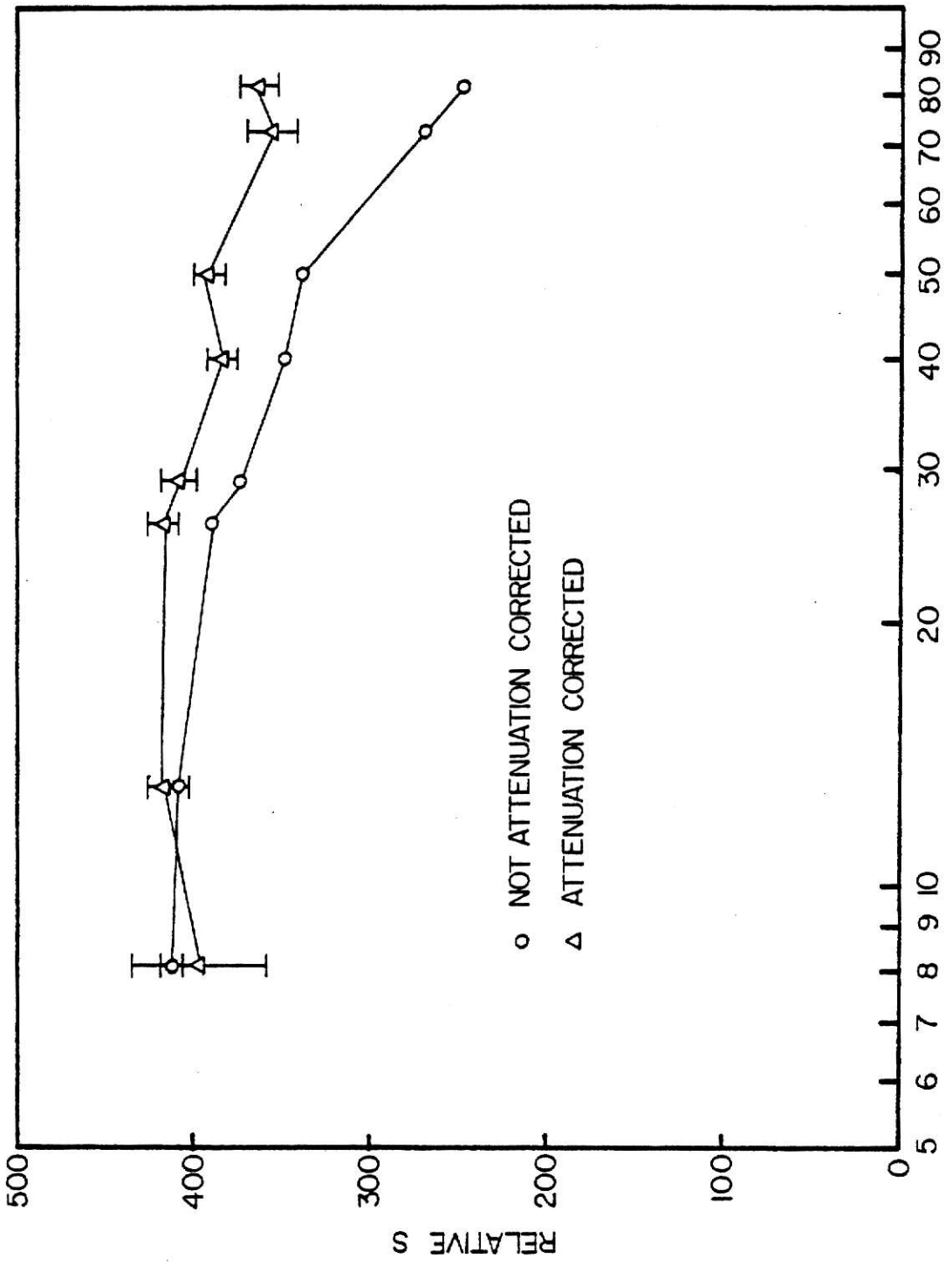

Fig. 7.10. Relative number of source decays from Hg-203 irradiated encased CaF_2:Mn TLDs as a function of encasement material atomic number.

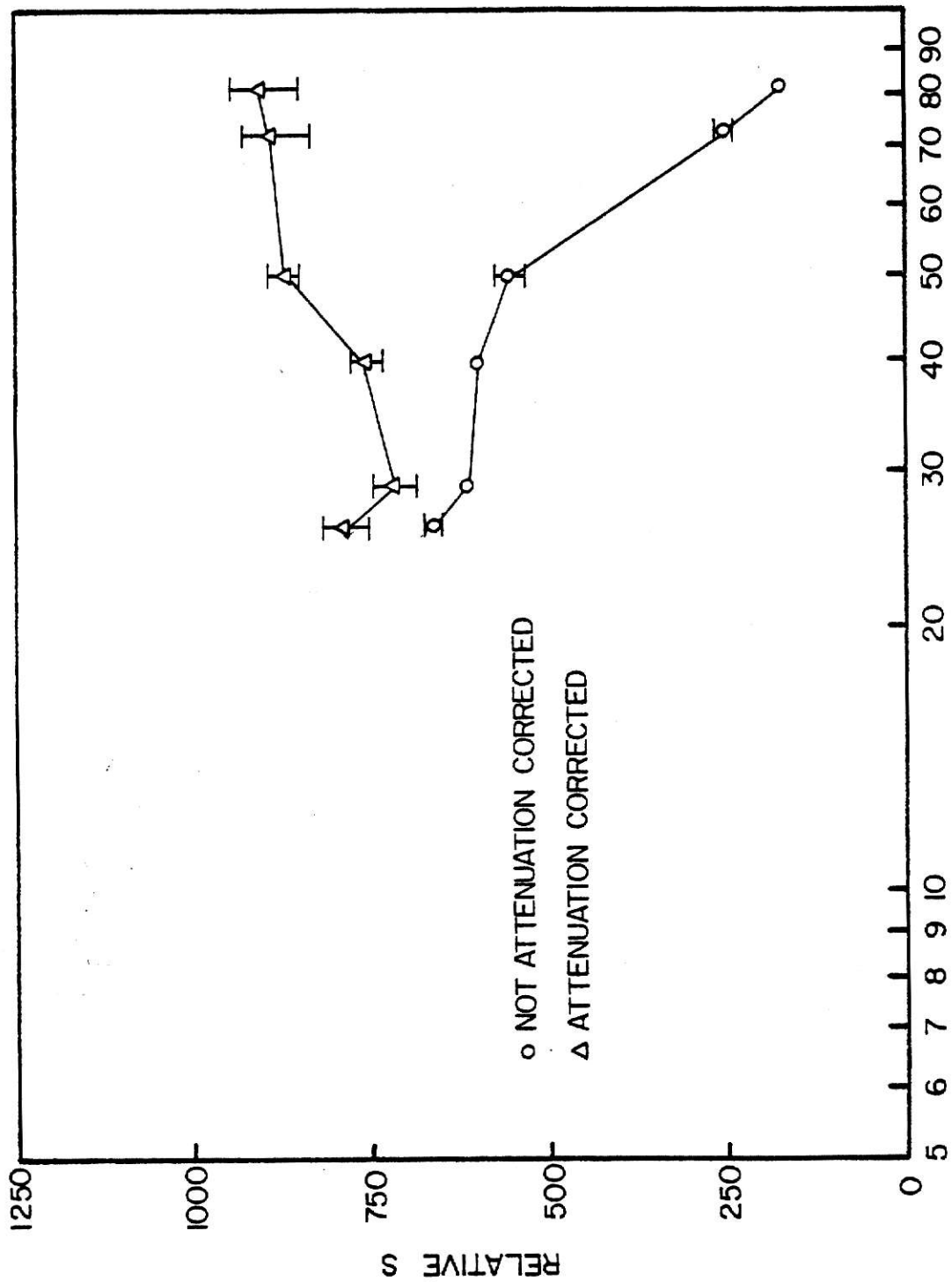

Fig. 7.11. Relative number of source decays from Ce-141 irradiated encased CaF_2:Mn TLDs as a function of encasement material atomic number.

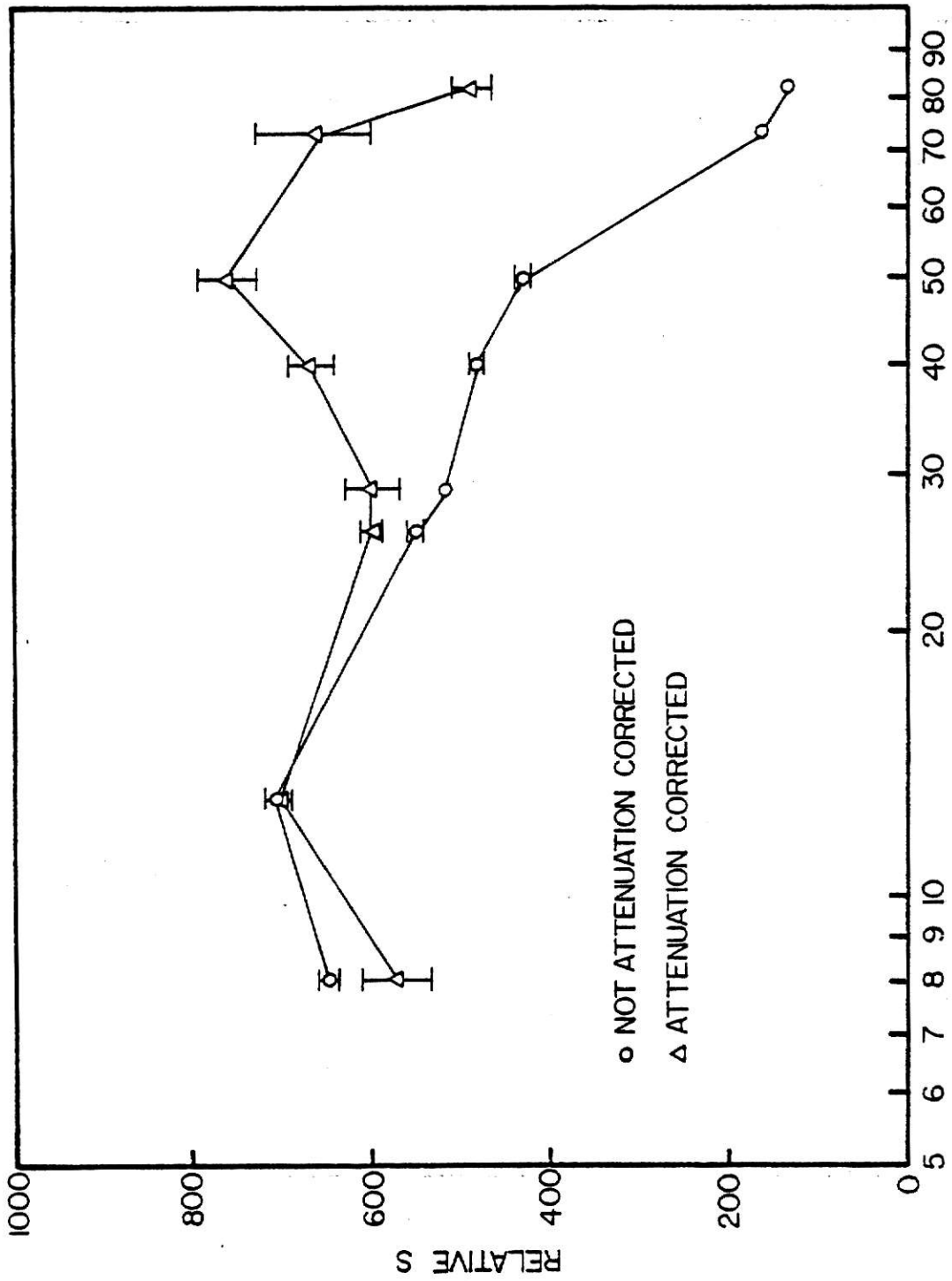

Fig. 7.12. Relative number of source decays from Co-57 irradiated encased CaF_2:Mn TLDs as a function of encasement material atomic number.

8.0 CONCLUSIONS

Presented within this thesis are benchmark data which can, in particular, be used directly to characterize the energy response of encapsulated ^{7}LiF and CaF_2:Mn TLDs. In general, these data are suitable for evaluating ionization theory models.

Normally, the reproducibility of TLD response data, is as dependent on the techniques used to acquire these data, as it is on the TLDs themselves. The standard deviations associated with the normalized TLD responses (E), showed that consistent results were obtainable, using the experimental procedures outlined in Chapter 3.0. Adherence to these prescribed procedures and sensitivity selection are cited as the primary reasons for the small random errors. By using intra-batch sensitivity selection, measurement of gamma doses to within nominally 2% for the CaF_2:Mn and 3% for the ^{7}LiF TLDs was possible (using 10 TLDs per configuration). These random errors were reduced to 1% for the CaF_2:Mn and 2% for the ^{7}LiF TLDs, when the sensitivity correction ratios were applied to the individual TLD responses. Therefore, it would appear that if properly determined, these ratios can be quite effective in compensating for the wide range of sensitivities exhibited by new TLDs.

Generally, C/E comparisons of calculation and experiment offer a powerful means for deciding the range over which the results of a particular ionization theory model are applicable. Even the most complex models are restricted in accuracy by the values of the input data used. As a result, gamma energy and atomic number limits must be

established for each model before it can be used with confidence.

Based upon the C/E results depicted in Tables 7.1-7.4, a fundamental deficiency is observed to exist for the TERC/III calculations. In predicting the dose to encapsulated TLDs, the TERC code does not take sleeve wall attenuation of primary gamma rays into account. As a result, the application of the TERC/III calculations should be limited to cases involving minimal gamma attenuation, i.e., less than 5% attenuation.

However, if a prescription which can be used to account for the effect of sleeve wall thickness is developed, the applicability of the TERC/III calculations can be broadened. Such a prescription was outlined in Section 5.3, under the guise of an effective attenuation correction. For this correction, effective attenuation coefficients were determined using the data acquired during the sleeve thickness study. With the use of these coefficients, corrections were applied to the TERC/III calculations. Via the comparison of these corrected calculations to the experimental results (C/E ratios tabulated in Tables 7.5 and 7.6), it was shown that the attenuation correction allowed for better prediction of the TLD dose. Nevertheless, based upon the relative source decays results (illustrated in Figs. 7.1-7.12), this correction appears to still be insufficient for cases involving extreme gamma attenuation. However, it is assumed that these deficiencies can be accounted for by the determination of better effective attenuation coefficients.

9.0 SUGGESTIONS FOR FURTHER STUDY

Normally, following the completion of any research project, proposals for additional study become apparent. There are basically two areas in which suggestions for further study have evolved from this work. The first of these suggestions involves research into TLD characteristics.

Sensitivity variations among TLDs appear to limit the precision with which dose measurements can be made. Although portions of these variations are attributable to ordinary statistical fluctuation, the primary cause appears to be the physical parameters associated with individual TLDs. Such parameters are differences in TLD mass, elemental concentration, and surface condition. However, if these physical differences can be accounted for, individual TLD results can be corrected. The end result being improved dose measurement precision. Such a correction was illustrated when the relative sensitivity ratios were applied to the TLD energy response data. With the correction, the precision associated with both the ^{7}LiF and CaF_2:Mn results showed marked improvement. Therefore, as a result of this observation, an experiment designed specifically to study TLD sensitivity would be considered most useful.

The second suggestion for further study is concerned with the acquisition of additional sleeve thickness data. This would augment the results reported within this thesis. These data should be acquired using new TLDs encased in sleeves with radial-wall mass thicknesses

ranging from nominally 0.05 to 1.0 g/cm^2. Basically, the use for such data would be twofold. First, the results could be used to determine more accurate effective attenuation coefficients. The need for such coefficients was illustrated throughout this thesis. Secondly, the results could also be used to determine the minimum sleeve wall thickness needed to maintain electronic equilibrium. Such a determination would be very valuable, since minimizing the sleeve wall thicknesses would also minimize sleeve wall attenuation of primary gammas. In effect, this procedure could take some of the emphasis off of the attenuation correction.

REFERENCES

1. G. G. Simons and A. P. Olsen, "Analysis and Measurements of Gamma-Ray Heating in the Demonstration Benchmark Plutonium-Fueled Critical Assembly," Nucl. Sci. Eng. Vol. 53, 176 (1974).

2. G. G. Simons and T. J. Yule, "Gamma-Ray Heating Measurements in Zero-Power Fast Reactors with Thermoluminescent Dosimeters," Nucl. Sci. Eng., Vol. 53, 162 (1974).

3. G. S. Stanford and R. W. Johnson, "Determination of Gamma-Ray Heating in a Critical Facility by Thermoluminescent Dosimetry," ANL-7373, Argonne National Laboratory (1968).

4. M. S. Karlo and M. J. Driscoll, "Gamma Heating in LMFBR Media," COO-2250-18, MITNE-179, Massachusetts Institute of Technology (1976).

5. Raymond Gold, "Status of Gamma-Ray Heating Characterization in LMFBR," HEDL-TME 75-126, Hanford Engineering Development Laboratory (1975).

6. A. D. Kripe, "Gamma-Ray Energy Deposition in Fast Nuclear Reactors," Ph.D. Thesis, University of London (1976).

7. Jan Adams Van Prooyen, "High Energy Gamma-Ray Energy Deposition Within Shielding Materials," Ph.D. Thesis, University of Virginia (1974).

8. C. E. Clifford, et al., "Experimental Studies of Radiation Heating in Iron and Stainless Steel Shields for the CRBR Project," ORNL-5161, Oak Ridge National Laboratory (1977).

9. P. A. Scheinert and M. J. Driscoll, "Gamma Heating Measurement in Fast Breeder Reactor Blankets," COO-2250-10, MITNE-164, Massachusettes Institute of Technology (1974).

10. J. T. Ward, "Gamma Heating Rates in FTR Europia Control Assemblies," HEDL-TME 75-35, Hanford Engineering Development Laboratory (1975).

11. R. J. Tuttle, "Measurements of Gamma-Ray Heating by Thermoluminescent Dosimeters," TI-707-140-022, Atomics International (1972).

12. J. R. Cameron, N. Suntharalingam, and G. N. Kenny, Thermoluminescent Dosimetry, The University of Wisconsin Press, Madison (1968).

13. T. E. Burlin, "Further Examination of Theories Relating the Absorption of Gamma-Ray Energy in a Medium to the Ionization Produced in a Cavity," Phys. Med. Biol., Vol. 11, No. 2, 255-266 (1966).

References - continued

14. T. E. Burlin, "A General Theory of Cavity Ionization," Brit. J. Radiol., Vol. 39, 727-734 (1966).

15. G. G. Simons, "Energy Response Calculations for Encapsulated ^{7}LiF TLDs," Applied Physics Division Annual Report, July 1, 1970 - June 30, 1971, Argonne National Laboratory Report, ANL-7910, 398-400 (Jan. 1972).

16. G. Bertilsson, "Application of the Cavity Theory to LiF-Teflon Dosimeters," Fourth International Conference on Luminescence Dosimetry, Poland (Aug. 1974).

17. G. G. Simons and L. L. Emmons, "Evaluation of Gamma Gamma-Ray Response Calculations for ^{7}LiF TLDs," NIM, Vol. 160, 79-85 (1979).

18. G. G. Simons and L. L. Emmons, "Experimental Evaluation of a Model for Calculating the Gamma-Ray Response of Encapsulated Solid-State Dosimeters," ZPR-TM-238, Argonne National Laboratory (1976).

19. D. W. Hanna, "Development and Optimization of a Thermoluminescent Dosimeter (TLD) Analyzer System for Low-Dose Measurements Utilizing Photon Counting Techniques, Masters Thesis, Kansas State University (1979).

20. G. G. Simons and T. S. Huntsmann, "Evaluation of Thermoluminescent Dosimeters for Gamma Ray Dose Measurements in ZPPR," unpublished report (1971).

21. R. D. Evans, The Atomic Nucleus, The McGraw Hill Book Company, Inc. (1955).

22. A. B. Chilton, "Broad Beam Attenuation," Engineering Compendium on Radiation Shielding, R. G. Jaeger, et al., Eds., Springer-Verlag New York, Inc., New York, 202-233 (1968).

23. G. P. Barnard, E. J. Axton, and A. R. S. Marsh, "A Study of Cavity Ion Chambers for use with 2 MV X-rays: Equilibrium Wall Thickness: Wall-Absorption Correction," Phys. in Med. Biol. Vol. 3, 366-394, (1959).

24. Ellery Storm and H. T. Israel, Photon Cross Sections from 1 keV to 100 MeV for Elements Z=1 to Z=100, Nucl. Data Tables, A-7, 565 (1970).

25. C. J. Jayachardrau, "Calculated Effective Atomic Number and Kerma Values for Tissue - Equivalent and Dosimetry Materials," Phys. Med. Biol., Vol. 16, No. 4, 617 (1971).

ACKNOWLEDGEMENTS

The author wishes to express his most sincere gratitude to Dr. G. G. Simons for his guidance throughout the performance of this research, and for his diligence in reviewing this manuscript. Special thanks are also extended to the Department of Energy, without whose funding this work would not have been possible. The financial support provided by the KSU Department of Nuclear Engineering is likewise gratefully acknowledged. Furthermore, the author wishes to extend his appreciation to Shelly Kemnitz, for her typing of this manuscript, and to Chuck O'Brien, for his drafting of the figures.

Finally, the author wishes to thank his fiancee, Annette, for her patience and understanding, and to express his appreciation for the encouragement and support of his parents.

APPENDIX A: Statistics Equations for Data Reduction

This appendix contains a discussion of the statistics used to reduce the TLD data (see Ref. A.1).

A.1 The Mean Experimental Response

For N similarly exposed TLDs, the mean response ($\overline{R}$) was calculated using the relation

$$\overline{R} = \left(\sum_{h=1}^{N} R_h\right)/N \qquad (A.1)$$

where R_h was defined as the net analyzer response (nC) for each dosimeter h. Corresponding to Eq. A.1 was the following relation for the experimentally determined standard deviation of the mean ($\sigma_{\overline{R}}$)

$$\sigma_{\overline{R}} = \left[\left(\sum_{h=1}^{N} R_h^2 - \left(\sum_{h=1}^{N} R_h\right)^2/N\right)/(N-1)\right]^{1/2}/N^{1/2} \quad . \qquad (A.2)$$

A.2 Normalized Experimental Result

The normalized experimental dose (E), for dosimeters encased in a material of type i and those encased in a material of type j, was defined as

$$E = \overline{R}_i/\overline{R}_j \qquad (A.3)$$

where the mean responses ($\overline{R}$) were considered to be directly proportional to the TLD doses (E_D^{exp}). Associated with Eq. A.3 was the equation for the standard deviation of the mean ($\sigma_{\overline{x}}$) for the normalized result

$$\sigma_{\overline{x}} = E\left[(\sigma_{\overline{R}}/\overline{R})_i^2 + (\sigma_{\overline{R}}/\overline{R})_j^2\right]^{1/2} \quad . \qquad (A.4)$$

A.3 The Effective Attenuation Coefficient

During the sleeve thickness study, the TLD data were least squares fit to the straight lines

$$\ln R = a + b\, x_e \qquad (A.5)$$

$$a = \frac{[\sum_{h=1}^{N} (x_e)_h \sum_{h=1}^{N} \ln R_h - \sum_{h=1}^{N} (x_e)_h \sum_{h=1}^{N} (x_e)_h \ln R_h]}{[N \sum_{h=1}^{N} (x_e)_h^2 - (\sum_{h=1}^{N} (x_e)_h)^2]}$$

$$b = \frac{[N \sum_{h=1}^{N} (x_e)_h \ln R_h - \sum_{h=1}^{N} (x_e)_h \sum_{h=1}^{N} \ln R_h]}{[N \sum_{h=1}^{N} (x_e)_h^2 - (\sum_{h=1}^{N} (x_e)_h)^2]}$$

where N = number of net TLD responses,

R_h = net response for TLD h, and

$(x_e)_h$ = curvature corrected wall thickness of the encasement for TLD h.

The effective attenuation coefficients (μ_{eff}), defined in Section 5.3, were the slopes of the least squares lines. Hence

$$\mu_{eff} = -b \; . \qquad (A.6)$$

Determination of the standard deviation (σ_μ) associated with μ_{eff}, was accomplished using the following equation.

$$\sigma_\mu = [Ns^2/(N \sum_{h=1}^{N} (x_e)_h^2 - (\sum_{h=1}^{N} (x_e)_h)^2]^{1/2} \qquad (A.7)$$

$$s^2 = [\sum_{h=1}^{N} (\ln R_h - a - b(x_e)_h)^2]/(N-2).$$

A.4 The Attenuation Corrected Calculations

The standard deviation (μ_{fc}) associated with the attenuation corrected TLD dose ratio (f_i^{corr}), defined by Eq. 5.13, was determined using the relation

$$\sigma_{fc} = f_i^{corr} \, (x_e \sigma_{\mu eff})_i \, . \qquad (A.8)$$

The following relation was used to calculate the standard deviation (σ_{Ca}) for the attenuation corrected normalized calculation (C^{ac}), given in Eq. 5.15

$$\sigma_{Ca} = C^{ac} \, [(x_e \, \sigma_u)_i^2 + (x_e \, \sigma_u)_j^2]^{1/2} \, . \qquad (A.9)$$

A.5 The Comparison of Experiment and Theory

To indicate the degree of correlation between experiment and theory, the normalized calculations (C), defined by Eqs. 5.5 and 5.15, were ratioed to the normalized experimental results (E), defined by Eq. 5.6,

$$\text{Correlation} = C/E \, . \qquad (A.10)$$

For cases involving non-attenuation corrected calculations, the standard deviation for Eq. A.10 ($\sigma_{C/E}$) was calculated using

$$\sigma_{C/E} = C \, \sigma_{\bar{x}}/E^2 \, . \qquad (A.11)$$

For cases involving attenuation corrected calculations,

$$\sigma_{Ca/E} = (C^{ac}/E)[(\sigma_{\bar{x}}/E)^2 + (\sigma_{ca}/C^{ac})^2]^{1/2} \, . \qquad (A.12)$$

A.6 The Relative Source Counts Comparison

To perform the relative source counts comparison, the experimental doses (E_D^{exp}), in Eqs. 5.7 and 5.16, were replaced with the corresponding experimental responses ($\bar{R}$). As a result, the standard deviation (σ_S) associated with the non-attenuation corrected source counts (S_{rel}), defined by Eq. 5.7, was calculated using the equation

$$\sigma_S = S_{rel}\ \sigma_{\bar{R}}/\bar{R} \ . \tag{A.13}$$

To determine the standard deviation (σ_{Sa}) associated with the attenuation corrected relative source counts (S_{rel}^{ac}), defined by Eq. 5.16, the following relation was used

$$\sigma_{Sa} = S_{rel}^{ac}\ [(\sigma_{\bar{R}}/\bar{R})^2 + (\sigma_\mu\ x_e)^2]^{1/2} \ . \tag{A.14}$$

References

A.1 P. R. Bevington, Data Reduction and Error Analysis for the Physical Sciences, McGraw Hill Book Company, New York (1969).

Table B.1. Partial compilation of input parameters used to calculate the dose ratio $[f(T_\gamma)]$ using TERC/III for 1x1x6 mm ^7LiF and CaF_2 TLDs.

Material	<Z/A>[a']	Density ρ (g/cm^3)	Mean Chord Length[b'], g (g/cm^2)	Ionization Potential[c'], I (eV)	Density effect Parameters				
					c	a	m	x_0	x_1
^7LiF	0.4616	2.63	0.2430	86.5	-3.07	0.456	2.76	-0.07	2.0
CaF_2	0.4867	3.04	0.2806	158	-4.50	0.100	3.40	0.08	3.0

[a'] Calcuated using the equation: $\langle Z/A \rangle = \sum_j \epsilon_j (Z_j/A_j)$.

For ^7LiF: $\epsilon_1 = 0.269$, $Z_1 = 3$, $A_1 = 7$, $\epsilon_2 = 0.731$, $Z_2 = 9$, and $A_2 = 18.9984$

For CaF_2: $\epsilon_1 = 0.513$, $Z_1 = 20$, $A_1 = 40.08$, $\epsilon_2 = 0.487$, $Z_2 = 9$, and $A_2 = 18.9984$

[b'] $g = 4V\rho/s$ (g/cm^2)

[c'] $\ln I = (Z/A)^{-1} \sum_j \epsilon_j (Z_j/A_j) \ln I_j$

APPENDIX B: TERC/III Input and Output

Contained within this appendix are tabulations of the information employed by the TERC/III computer code, to calculate the TLD dose ratios (f_i). Also included are tabulations of these calculated dose ratios, with the corresponding mass energy absorption coefficients.

Table B.1. Partial compilation of input parameters used to calculate the dose ratio [f(T)] using TERC/III for 1x1x6 mm ^{7}LiF and CaF_2 TLDs.

Material	<Z/A>[a']	Density ρ (g/cm^3)	Mean Chord Length[b'], g (g/cm^2)	Ionization Potential[c'], I (eV)	Density effect Parameters				
					c	a	m	x_0	x_1
^{7}LiF	0.4616	2.63	0.2430	86.5	-3.07	0.456	2.76	-0.07	2.0
CaF_2	0.4867	3.04	0.2806	158	-4.50	0.100	3.40	0.08	3.0

[a'] Calcuated using the equation: $\langle Z/A \rangle = \sum_j \epsilon_j (Z_j/A_j)$.

For ^{7}LiF: $\epsilon_1 = 0.269$, $Z_1 = 3$, $A_1 = 7$, $\epsilon_2 = 0.731$, $Z_2 = 9$, and $A_2 = 18.9984$

For CaF_2: $\epsilon_1 = 0.513$, $Z_1 = 20$, $A_1 = 40.08$, $\epsilon_2 = 0.487$, $Z_2 = 9$, and $A_2 = 18.9984$

[b'] $g = 4V\rho/s$ (g/cm^2)

[c'] $\ln I = (Z/A)^{-1} \sum_j \epsilon_j (Z_j/A_j) \ln I_j$

Table B.2. Partial compilation of input parameters used to calculate the dose ratio [$f(T_\gamma)$] using TERC/III for each encasement material.

Material	Atomic Number Z	Atomic Weight A	Ionization Potential I (eV)	Density Effect Parameters				
				c	a	m	X_0	X_1
Lead	82	207.2	826.	-6.21	0.355	2.64	0.4	3.0
Tantalum	73	180.9	701	-6.03	0.028	3.91	0.30	4.0
Tin	50	118.7	517	-6.28	0.404	2.52	0.20	3.0
Zirconium	40	91.22	420	-5.39	0.250	2.80	0.20	3.0
Copper	29	63.57	323	-4.43	0.109	3.39	0.20	3.0
Iron	26	55.84	273	-4.62	0.127	3.29	0.10	3.0
Stainless Steel	$25.23^{a'}$	$54.98^{b'}$	$273^{c'}$	-4.62	0.127	3.29	0.10	3.0
Aluminum	13	27	164	-4.21	0.091	3.51	0.05	3.0

$$a'_Z = \sum_j E_j Z_j \quad \text{where } E_j \equiv \text{fraction by weight of the jth element}$$

$$b'_A = \sum_j E_j A_j$$

$$c'_{\ln I} = (Z/A)^{-1} \sum_j E_j \, (Z_j/A_j) \, \ln I_j$$

Table B.3. ^{7}LiF and CaF_2:Mn TLD total mass energy absorption coefficients used for TERC/III calculations.

Electron Energy (MeV)	Total Mass Energy Absorption Coefficients (cm^2/g) ^{7}LiF	CaF_2:Mn
0.010	5.73	48.2
0.015	1.56	15.2
0.020	0.629	6.59
0.030	0.177	1.95
0.040	0.0767	0.822
0.050	0.0439	0.425
0.060	0.0317	0.247
0.080	0.0234	0.111
0.10	0.0219	0.0658
0.15	0.0231	0.0362
0.20	0.0248	0.0309
0.30	0.0266	0.0294
0.40	0.0273	0.0293
0.50	0.0276	0.0294
0.60	0.0273	0.0289
0.80	0.0266	0.0280
1.0	0.0257	0.0271
1.5	0.0235	0.0248
2.0	0.0217	0.0230
3.0	0.0191	0.0206
4.0	0.0174	0.0193
5.0	0.0161	0.0185
6.0	0.0154	0.0181
8.0	0.0142	0.0181
10.0	0.0136	0.0177

Table B.4. LiF mass energy absorption coefficients used for TERC/III calculations.

Electron Energy (MeV)	Mass Energy Absorption Coefficients (cm^2/g)		
	Photoelectric	Compton	Pair Production
0.010	5.73	0.00228	0.0
0.015	1.55	0.00380	0.0
0.020	0.625	0.00552	0.0
0.030	0.169	0.00784	0.0
0.040	0.0666	0.0101	0.0
0.050	0.0319	0.012	0.0
0.060	0.0179	0.0138	0.0
0.080	0.00691	0.0165	0.0
0.10	0.00329	0.0186	0.0
0.15	0.000863	0.0222	0.0
0.20	0.000348	0.0244	0.0
0.30	0.000102	0.0265	0.0
0.40	0.0000428	0.0273	0.0
0.50	0.0	0.0276	0.0
0.60	0.0	0.0273	0.0
0.80	0.0	0.0266	0.0
1.0	0.0	0.0257	0.0
1.5	0.0	0.0235	0.0
2.0	0.0	0.0216	0.000181
3.0	0.0	0.0184	0.000713
4.0	0.0	0.0161	0.00132
5.0	0.0	0.0142	0.00192
6.0	0.0	0.0129	0.00247
8.0	0.0	0.0108	0.00344
10.0	0.0	0.0094	0.00424

Table B.5. Aluminum mass energy absorption coefficients used for TERC/III calculations.

Electron Energy (MeV)	Mass Energy Absorption Coefficients (cm^2/g)		
	Photoelectric	Compton	Pair Production
0.010	25.4	0.00199	0.0
0.015	7.32	0.00350	0.0
0.020	3.06	0.00496	0.0
0.030	0.850	0.00763	0.0
0.040	0.344	0.00998	0.0
0.050	0.169	0.0121	0.0
0.060	0.0944	0.0139	0.0
0.080	0.0375	0.0169	0.0
0.10	0.0180	0.0192	0.0
0.15	0.00480	0.0230	0.0
0.20	0.00197	0.0252	0.0
0.30	0.000567	0.0275	0.0
0.40	0.000241	0.0283	0.0
0.50	0.000131	0.0288	0.0
0.60	0.0000815	0.0283	0.0
0.80	0.0000422	0.0277	0.0
1.0	0.0000261	0.0268	0.0
1.5	0.0	0.0243	0.0000545
2.0	0.0	0.0223	0.000330
3.0	0.0	0.0190	0.00128
4.0	0.0	0.0165	0.00234
5.0	0.0	0.0146	0.00337
6.0	0.0	0.0132	0.00433
8.0	0.0	0.0110	0.00596
10.0	0.0	0.00730	0.00730

Table B.6. Iron mass energy absorption coefficients used for TERC/III calculations.

Electron Energy (MeV)	Mass Energy Absorption Coefficients (cm^2/g)		
	Photoelectric	Compton	Pair Production
0.010	138.0	0.00161	0.0
0.015	49.2	0.00290	0.0
0.020	22.6	0.00420	0.0
0.030	7.20	0.00673	0.0
0.040	3.13	0.00892	0.0
0.050	1.61	0.0110	0.0
0.060	0.939	0.0127	0.0
0.080	0.393	0.0156	0.0
0.10	0.198	0.0179	0.0
0.15	0.0570	0.0217	0.0
0.20	0.0238	0.0240	0.0
0.30	0.00713	0.0264	0.0
0.40	0.00316	0.0272	0.0
0.50	0.00172	0.0275	0.0
0.60	0.00110	0.0274	0.0
0.80	0.000559	0.0266	0.0
1.0	0.000346	0.0257	0.0
1.5	0.000161	0.0235	0.000111
2.0	0.0000985	0.0213	0.000641
3.0	0.0000549	0.0180	0.00240
4.0	0.0000373	0.0155	0.00433
5.0	0.0000284	0.0137	0.00613
6.0	0.0000224	0.0123	0.00776
8.0	0.0000158	0.0102	0.0105
10.0	0.0000123	0.00860	0.0127

Table B.7. Stainless steel mass energy absorption coefficients used for TERC/III calculations.

Electron Energy (MeV)	Mass Energy Absorption Coefficients (cm^2/g)		
	Photoelectric	Compton	Pair Production
0.010	135.0	0.00161	0.0
0.015	48.1	0.00291	0.0
0.020	22.1	0.00418	0.0
0.030	7.04	0.00675	0.0
0.040	3.06	0.00894	0.0
0.050	1.57	0.0110	0.0
0.060	0.917	0.0128	0.0
0.080	0.384	0.0157	0.0
0.10	0.194	0.0180	0.0
0.15	0.0556	0.0217	0.0
0.20	0.0232	0.0241	0.0
0.30	0.00696	0.0264	0.0
0.40	0.00308	0.0273	0.0
0.50	0.00169	0.0275	0.0
0.60	0.00107	0.0274	0.0
0.80	0.000545	0.0266	0.0
1.0	0.000337	0.0257	0.0
1.5	0.000157	0.0235	0.000111
2.0	0.0000963	0.0214	0.000637
3.0	0.0000533	0.0180	0.00239
4.0	0.0000364	0.0155	0.00431
5.0	0.0000276	0.0137	0.00610
6.0	0.0000219	0.0123	0.00773
8.0	0.0000163	0.0102	0.0105
10.0	0.0000125	0.00863	0.0126

Table B.8. Copper mass energy absorption coefficients used for TERC/III calculations.

Electron Energy (MeV)	Mass Energy Absorption Coefficients (cm^2/g)		
	Photoelectric	Compton	Pair Production
0.010	153.0	0.00146	0.0
0.015	59.0	0.00270	0.0
0.020	28.2	0.00397	0.0
0.030	9.34	0.00642	0.0
0.040	4.16	0.00860	0.0
0.050	2.18	0.0106	0.0
0.060	1.28	0.0123	0.0
0.080	0.541	0.0152	0.0
0.10	0.276	0.0174	0.0
0.15	0.0810	0.0213	0.0
0.20	0.0340	0.0236	0.0
0.30	0.0103	0.0258	0.0
0.40	0.00462	0.0266	0.0
0.50	0.00254	0.0270	0.0
0.60	0.00160	0.0268	0.0
0.80	0.000817	0.0261	0.0
1.0	0.000510	0.0251	0.0
1.5	0.000237	0.0229	0.000124
2.0	0.000147	0.0209	0.000707
3.0	0.0000799	0.0175	0.00263
4.0	0.0000543	0.0152	0.00472
5.0	0.0000409	0.0134	0.00666
6.0	0.0000323	0.0119	0.00846
8.0	0.0000229	0.00986	0.0114
10.0	0.0000177	0.00827	0.0137

Table B.9. Zirconium mass energy absorption coefficients used for TERC/III calculations.

Electron Energy (MeV)	Mass Energy Absorption Coefficients (cm^2/g)		
	Photoelectric	Compton	Pair Production
0.010	70.0	0.00129	0.0
0.015	22.9	0.00236	0.0
0.020	36.0	0.00351	0.0
0.030	16.1	0.00574	0.0
0.040	8.19	0.00786	0.0
0.050	4.62	0.00977	0.0
0.060	2.86	0.0115	0.0
0.080	1.29	0.0141	0.0
0.10	0.687	0.0164	0.0
0.15	0.218	0.0203	0.0
0.20	0.0944	0.0224	0.0
0.30	0.0298	0.0248	0.0
0.40	0.0135	0.0255	0.0
0.50	0.00759	0.0258	0.0
0.60	0.00490	0.0256	0.0
0.80	0.00249	0.0249	0.0
1.0	0.00158	0.0239	0.0
1.5	0.000726	0.0219	0.000182
2.0	0.000447	0.0198	0.000990
3.0	0.000240	0.0166	0.00353
4.0	0.000162	0.0143	0.00616
5.0	0.000123	0.0125	0.00865
6.0	0.0000957	0.0111	0.0109
8.0	0.0000673	0.00911	0.0143
10.0	0.0000523	0.00759	0.0172

Table B.10. Tin mass energy absorption coefficients used for TERC/III calculations.

Electron Energy (MeV)	Mass Energy Absorption Coefficients (cm^2/g)		
	Photoelectric	Compton	Pair Production
0.010	131.0	0.00114	0.0
0.015	43.4	0.00215	0.0
0.020	19.6	0.00319	0.0
0.030	15.0	0.00528	0.0
0.040	10.0	0.00721	0.0
0.050	6.39	0.00903	0.0
0.060	4.26	0.0107	0.0
0.080	2.11	0.0133	0.0
0.10	1.18	0.0155	0.0
0.15	0.398	0.0192	0.0
0.20	0.180	0.0214	0.0
0.30	0.0593	0.0236	0.0
0.40	0.0276	0.0244	0.0
0.50	0.0157	0.0246	0.0
0.60	0.0101	0.0246	0.0
0.80	0.00528	0.0238	0.0
1.0	0.00330	0.0227	0.0
1.5	0.00153	0.0209	0.000237
2.0	0.000939	0.0188	0.00123
3.0	0.000503	0.0157	0.00423
4.0	0.000336	0.0135	0.00731
5.0	0.000252	0.0118	0.0101
6.0	0.000197	0.0105	0.0125
8.0	0.000138	0.00842	0.0163
10.0	0.000107	0.00695	0.0194

Table B.11. Tantalum mass energy absorption coefficients used for TERC/III calculations.

Electron Energy (MeV)	Mass Energy Absorption Coefficients (cm^2/g)		
	Photoelectric	Compton	Pair Production
0.010	206.0	0.000912	0.0
0.015	115.0	0.00174	0.0
0.020	55.6	0.00266	0.0
0.030	19.2	0.00456	0.0
0.040	8.92	0.00636	0.0
0.050	4.83	0.00805	0.0
0.060	2.93	0.00958	0.0
0.080	3.18	0.0121	0.0
0.10	2.21	0.0142	0.0
0.15	0.945	0.0180	0.0
0.20	0.479	0.0202	0.0
0.30	0.178	0.0224	0.0
0.40	0.0882	0.0231	0.0
0.50	0.0519	0.0233	0.0
0.60	0.0346	0.0232	0.0
0.80	0.0185	0.0225	0.0
1.0	0.0117	0.0213	0.0
1.5	0.00546	0.0196	0.000416
2.0	0.00332	0.0178	0.00196
3.0	0.00174	0.0145	0.00622
4.0	0.00115	0.0124	0.0102
5.0	0.000859	0.0107	0.0136
6.0	0.000669	0.00939	0.0163
8.0	0.000463	0.00752	0.0207
10.0	0.000359	0.00622	0.0241

Table B.12. Lead mass energy absorption coefficients used for TERC/III calculations.

Electron Energy (MeV)	Mass Energy Absorption Coefficients (cm^2/g)		
	Photoelectric	Compton	Pair Production
0.010	123.0	0.000855	0.0
0.015	88.4	0.00165	0.0
0.020	68.3	0.00251	0.0
0.030	25.1	0.00430	0.0
0.040	12.0	0.00608	0.0
0.050	6.66	0.00770	0.0
0.060	4.10	0.00922	0.0
0.080	1.89	0.0117	0.0
0.10	2.21	0.0138	0.0
0.15	1.12	0.0175	0.0
0.20	0.605	0.0197	0.0
0.30	0.237	0.0219	0.0
0.40	0.121	0.0225	0.0
0.50	0.0730	0.0228	0.0
0.60	0.0488	0.0227	
0.80	0.0266	0.0220	0.0
1.0	0.0162	0.0208	0.0
1.5	0.00797	0.0191	0.000497
2.0	0.00483	0.0173	0.00226
3.0	0.00253	0.0141	0.00692
4.0	0.00169	0.0119	0.0112
5.0	0.00125	0.0103	0.0148
6.0	0.000968	0.0901	0.0177
8.0	0.000669	0.00718	0.0219
10.0	0.000517	0.00593	0.0252

Table B.13. Mass energy absorption coefficients and resulting dose ratios calculated using TERC/III for 1x1x6 mm ^{7}LiF TLDs encased in various materials.

Nuclide	Gamma-ray Energy, T_γ (MeV)	Mass Energy Absorption Coefficient $(\mu_{en}(T_\gamma)/\rho)_M$ (cm^2/g)	Calculated Dose Ratio $f(T_\gamma)$
	Encasement Material (M) of Lead, Z = 82		
Co-57	0.122	1.7480	0.04597
	0.136	1.4373	0.05479
Ce-141	0.145	1.2483	0.06002
Hg-203	0.279	0.3359	0.1902
Sn-113	0.393	0.1518	0.3425
Cs-137	0.662	0.06444	0.6929
Co-60	1.173	0.03423	1.0931
	1.333	0.03099	1.1589
	Encasement Material (M) of Tantalum, Z = 73		
Co-57	0.122	1.6679	0.04552
	0.136	1.3077	0.05504
Ce-141	0.145	1.0892	0.06069
Hg-203	0.279	0.2634	0.2071
Sn-113	0.393	0.1176	0.3810
Cs-137	0.662	0.05263	0.7508
Co-60	1.173	0.03040	1.1179
	1.333	0.02803	1.1712
	Encasement Material (M) of Tin, Z = 50		
Co-57	0.122	0.8543	0.06036
	0.136	0.6313	0.07563
Ce-141	0.145	0.4955	0.08485
Hg-203	0.279	0.1079	0.3450
Sn-113	0.393	0.05413	0.6111
Cs-137	0.662	0.03295	0.9619
Co-60	1.173	0.02485	1.1705
	1.333	0.02376	1.1938
	Encasement Material (M) of Zirconium, Z = 40		
Co-57	0.122	0.4985	0.08318
	0.136	0.3655	0.1061
Ce-141	0.145	0.2846	0.1200
Hg-203	0.279	0.06761	0.4790
Sn-113	0.393	0.04010	0.7565
Cs-137	0.662	0.02950	1.0135
Co-60	1.173	0.02456	1.1365
	1.333	0.02372	1.1501

Table B.13. - continued

Nuclide	Gamma-ray Energy, T_γ (MeV)	Mass Energy Absorption Coefficient $(\mu_{en}(T_\gamma)/\rho)_M$ (cm^2/g)	Calculated Dose Ratio $f(T_\gamma)$
	Encasement Material (M) of Copper, Z = 29		
Co-57	0.122	0.2092	0.1604
	0.136	0.1547	0.2065
Ce-141	0.145	0.1214	0.2346
Hg-203	0.279	0.04061	0.0707
Sn-113	0.393	0.03159	0.9063
Cs-137	0.662	0.02793	1.0281
Co-60	1.173	0.02481	1.0885
	1.333	0.02407	1.0964
	Encasement Material (M) of Iron, Z = 26		
Co-57	0.122	0.1557	0.2031
	0.136	0.1164	0.2604
Ce-141	0.145	0.09245	0.2953
Hg-203	0.279	0.03655	0.7653
Sn-113	0.393	0.03055	0.9254
Cs-137	0.662	0.02808	1.0115
Co-60	1.173	0.02523	1.0570
	1.333	0.02452	1.0626
	Encasement Material (M) of Stainless Steel		
Co-57	0.122	0.1526	0.2068
	0.136	0.1142	0.2651
Ce-141	0.145	0.09075	0.3005
Hg-203	0.279	0.03628	0.7710
Sn-113	0.393	0.03055	0.9270
Cs-137	0.662	0.02805	1.0158
Co-60	1.173	0.02529	1.0614
	1.333	0.02457	1.0679
	Encasement Material (M) of Aluminum, Z = 13		
Co-57	0.122	0.03305	0.7011
	0.136	0.03036	0.7704
Ce-141	0.145	0.02873	0.8125
Hg-203	0.279	0.02785	0.9506
Sn-113	0.393	0.02855	0.9655
Cs-137	0.662	0.02821	0.9791
Co-60	1.173	0.02597	0.9924
	1.333	0.02520	0.9958
	Encasement Material (M) of LiF		
Co-57	0.122	0.02241	1.0000
	0.136	0.02274	1.0000
Ce-141	0.145	0.02295	1.0000
Hg-203	0.279	0.02621	1.0000
Sn-113	0.393	0.02729	1.0000
Cs-137	0.662	0.02708	1.0000
Co-60	1.173	0.02494	1.0000
	1.333	0.02424	1.0000

Table B.14. Mass energy absorption coefficients and resulting dose ratios calculated using TERC/III for 1x1x6 mm CaF_2 TLDs encased in various materials.

Nuclide	Gamma-ray Energy, T_γ (MeV)	Mass Energy Absorption Coefficient $(\mu_{en}(T_\gamma)/\rho)_M$ (cm^2/g)	Calculated Dose Ratio $f(T_\gamma)$
	Encasement material (M) of lead, Z = 82		
Co-57	0.122	1.7480	0.05622
	0.136	1.4373	0.06160
Ce-141	0.145	1.2483	0.06489
Hg-203	0.279	0.3359	0.1824
Sn-113	0.393	0.1518	0.3278
Cs-137	0.662	0.06444	0.6694
Co-60	1.173	0.03423	1.080
	1.333	0.03099	1.145
	Encasement Material (M) of Tantalum, Z = 73		
Co-57	0.122	1.6679	0.05709
	0.136	1.3077	0.0638
Ce-141	0.145	1.0892	0.06792
Hg-203	0.279	0.2634	0.2033
Sn-113	0.393	0.1176	0.3721
Cs-137	0.662	0.05263	0.7372
Co-60	1.173	0.03040	1.108
	1.333	0.02803	1.163
	Encasement Material (M) of Tin, Z = 50		
Co-57	0.122	0.8543	0.08955
	0.136	0.6313	0.1024
Ce-141	0.145	0.4955	0.1102
Hg-203	0.279	0.1079	0.3624
Sn-113	0.393	0.05413	0.6267
Cs-137	0.662	0.03295	0.9739
Co-60	1.173	0.02485	1.179
	1.333	0.02376	1.202
	Encasement Material (M) of Zirconium, Z = 40		
Co-57	0.122	0.4985	0.1373
	0.136	0.3655	0.1572
Ce-141	0.145	0.2846	0.1693
Hg-203	0.279	0.06761	0.5163
Sn-113	0.393	0.04010	0.7881
Cs-137	0.662	0.02950	1.035
Co-60	1.173	0.02456	1.149
	1.333	0.02372	1.162

Table B.14. - continued

Nuclide	Gamma-ray Energy, T_γ (MeV)	Mass Energy Absorption Coefficient $(\mu_{en}(T_\gamma)/\rho)_M$ (cm^2/g)	Calculated Dose Ratio $f(T_\gamma)$
	Encasement Material (M) of Copper, Z = 29		
Co-57	0.122	0.2093	0.2949
	0.136	0.1547	0.3339
Ce-141	0.145	0.1215	0.3577
Hg-203	0.279	0.0406	0.7770
Sn-113	0.393	0.0316	0.9545
Cs-137	0.662	0.0280	1.0568
Co-60	1.173	0.0248	1.1060
	1.333	0.0241	1.1123
	Encasement Material (M) of Iron, Z = 26		
CO-57	0.122	0.1557	0.3840
	0.136	0.1164	0.4300
Ce-141	0.145	0.09245	0.4581
Hg-203	0.279	0.03655	0.8457
Sn-113	0.393	0.03055	0.9771
Cs-137	0.662	0.02808	1.042
Co-60	1.173	0.02523	1.075
	1.333	0.02452	1.079
	Encasement Material (M) of Stainless Steel		
Co-57	0.122	0.1526	0.3914
	0.136	0.1142	0.4379
Ce-141	0.145	0.09075	0.4663
Hg-203	0.279	0.03628	0.8520
Sn-113	0.393	0.03055	0.9784
Cs-137	0.662	0.02805	1.046
Co-60	1.173	0.02529	1.080
	1.333	0.02457	1.084
	Encasement Material (M) of Aluminum, Z = 13		
Co-57	0.122	0.03305	1.557
	0.136	0.03036	1.424
Ce-141	0.145	0.02873	1.343
Hg-203	0.279	0.02785	1.061
Sn-113	0.393	0.02856	1.025
Cs-137	0.662	0.02821	1.014
Co-60	1.173	0.02597	1.015
	1.333	0.02520	1.017

Table B.14. - continued

Nuclide	Gamma-ray Energy, T_γ (MeV)	Mass Energy Absorption Coefficient $(\mu_{en}(T_\gamma)/\rho)_M$ (cm^2/g)	Calculated Dose Ratio $f(T_\gamma)$
		Encasement Material (M) of LiF	
Co-57	0.122	0.02241	2.3554
	0.136	0.02274	1.9471
Ce-141	0.145	0.02295	1.6986
Hg-203	0.279	0.02621	1.1182
Sn-113	0.393	0.02729	1.0619
Cs-137	0.662	0.02708	1.0383
Co-60	1.173	0.02494	1.0266
	1.333	0.02424	1.0248

APPENDIX C: Raw TLD Data.

Contained within this appendix are tabulations of the raw TLD energy response and sleeve thickness data. Also included are tabulations of the corresponding TLD sort results.

Table C.1. Raw energy response data obtained using encased ^{7}LiF TLDs exposed to the nominal 5.06 mCi Co-57 source[a].

Encasement Material	Radial Wall Mass Thickness (g/cm^2)	Exposure Radius (cm)	Net TLD Response[b] (nC)	Sensitivity Corrected Net TLD Response[b] (nC)
Pb	0.734	20.4	1.106 ± 0.020	1.099 ± 0.016
Ta	0.696	20.4	1.183 ± 0.034	1.184 ± 0.012
Sn	0.608	20.4	2.368 ± 0.024	2.365 ± 0.028
Zr	0.541	20.4	2.656 ± 0.026	2.659 ± 0.016
Cu	0.694	20.4	2.172 ± 0.042	2.221 ± 0.020
Fe	0.656	20.4	2.275 ± 0.017	2.271 ± 0.023
S.S.	0.693	20.4	2.256 ± 0.027	2.247 ± 0.023
Al	0.514	20.4	2.097 ± 0.023	2.0981 ± 0.016
LiF	0.483	15.5	3.618 ± 0.052	3.623 ± 0.027

[a]Exposure time was 90.75 h.

[b]Average of ten TLD responses.

Table C.2. Raw energy response data obtained using encased ^{7}LiF TLDs exposed to the nominal 3.52 mCi Ce-141 source[a].

Encasement Material	Radial Wall Mass Thickness (g/cm^2)	Exposure Radius (cm)	Net TLD Response[b] (nC)	Sensitivity Corrected Net TLD Response[b] (nC)
Pb	0.734	20.4	0.812 ± 0.010	0.812 ± 0.012
Ta	0.696	20.4	0.977 ± 0.032	0.977 ± 0.025
Sn	0.608	20.4	1.846 ± 0.025	1.861 ± 0.019
Zr	0.541	20.4	1.887 ± 0.011	1.911 ± 0.016
Cu	0.694	20.4	1.599 ± 0.016	1.609 ± 0.015
Fe	0.656	20.4	1.597 ± 0.017	1.611 ± 0.012
S.S.	0.693	20.4	1.551 ± 0.019	1.559 ± 0.014
Al	0.514	20.4	1.575 ± 0.016	1.587 ± 0.012
LiF	0.483	15.5	2.824 ± 0.028	2.855 ± 0.020

[a]Exposure time was 186 h.

[b]Average of ten TLD responses.

Table C.3. Raw energy response data obtained using encased ^{7}LiF TLDs exposed to the nominal 4.25 mCi Hg-203 source[a].

Encasement Material	Radial Wall Mass Thickness (g/cm^2)	Exposure Radius (cm)	Net TLD Response[b] (nC)	Sensitivity Corrected Net TLD Response[b] (nC)
Pb	0.734	20.4	2.794 ± 0.023	2.781 ± 0.021
Ta	0.696	20.4	2.663 ± 0.036	2.653 ± 0.023
Sn	0.608	20.4	2.257 ± 0.021	2.254 ± 0.016
Zr	0.541	20.4	2.003 ± 0.020	2.022 ± 0.026
Cu	0.694	20.4	1.860 ± 0.021	1.860 ± 0.014
Fe	0.656	20.4	1.793 ± 0.015	1.803 ± 0.028
S.S.	0.693	20.4	1.799 ± 0.026	1.805 ± 0.015
Al	0.514	20.4	1.739 ± 0.031	1.742 ± 0.018
LiF	0.483	15.5	3.057 ± 0.044	3.073 ± 0.022

[a]Exposure time was 41.5 h.

[b]Average of ten TLD responses.

Table C.4. Raw energy response data obtained using encased ^{7}LiF TLDs exposed to the nominal 5.65 mCi Sn-113 source[a].

Encasement Material	Radial Wall Mass Thickness (g/cm^2)	Exposure Radius (cm)	Net TLD Response[b] (nC)	Sensitivity Corrected Net TLD Response[b] (nC)
Pb	0.734	20.4	2.858 ± 0.040	2.813 ± 0.024
Ta	0.696	20.4	2.564 ± 0.040	2.539 ± 0.032
Sn	0.608	20.4	2.044 ± 0.017	2.028 ± 0.012
Zr	0.541	20.4	1.882 ± 0.027	1.882 ± 0.016
Cu	0.694	20.4	1.700 ± 0.018	1.709 ± 0.009
Fe	0.656	20.4	1.725 ± 0.011	1.722 ± 0.015
S.S.	0.693	20.4	1.730 ± 0.017	1.724 ± 0.025
Al	0.514	20.4	1.719 ± 0.018	1.710 ± 0.016
LiF	0.483	15.5	3.051 ± 0.021	3.050 ± 0.024

[a]Exposure time was 42.7 h.

[b]Average of ten TLD responses.

Table C.5. Raw energy response data obtained using encased ^{7}LiF TLDs exposed to the nominal 5.27 mCi Cs-137 source[a].

Encasement Material	Radial Wall Mass Thickness (g/cm^2)	Exposure Radius (cm)	Net TLD Response[b] (nC)	Sensitivity Corrected Net TLD Response[b] (nC)
Pb	0.734	20.4	3.629 ± 0.056	3.583 ± 0.033
Ta	0.696	20.4	3.141 ± 0.043	3.107 ± 0.025
Sn	0.608	20.4	2.423 ± 0.025	2.402 ± 0.025
Zr	0.541	20.4	2.380 ± 0.019	2.374 ± 0.018
Cu	0.694	20.4	2.196 ± 0.008	2.180 ± 0.023
Fe	0.656	20.4	2.250 ± 0.021	2.234 ± 0.018
S.S.	0.693	20.4	2.261 ± 0.028	2.251 ± 0.017
Al	0.514	20.4	2.206 ± 0.022	2.193 ± 0.016
LiF	0.483	15.5	3.857 ± 0.051	3.858 ± 0.035

[a]Exposure time was 19.3 h..

[b]Average of ten TLD responses.

Table C.6. Raw energy response data obtained[a] using encased ^{7}LiF TLDs exposed to the nominal 5.06 mCi Co-60 source[a].

Encasement Material	Radial Wall Mass Thickness (g/cm^2)	Exposure Radius (cm)	Net TLD Response[b] (nC)	Sensitivity Corrected Net TLD Response[b] (nC)
Pb	0.734	20.4	12.140 ± 0.142	12.046 ± 0.119
Ta	0.696	20.4	11.163 ± 0.178	11.090 ± 0.086
Sn	0.608	20.4	9.735 ± 0.151	9.707 ± 0.111
Zr	0.541	20.4	9.423 ± 0.067	9.434 ± 0.096
Cu	0.694	20.4	8.936 ± 0.074	8.925 ± 0.085
Fe	0.656	20.4	8.966 ± 0.079	9.007 ± 0.084
S.S.	0.693	20.4	8.910 ± 0.103	8.934 ± 0.086
Al	0.514	20.4	8.734 ± 0.107	8.732 ± 0.090
LiF	0.483	15.5	14.930 ± 0.216	14.999 ± 0.107

[a]Exposure time was 18.2 h.

[b]Average of ten TLD responses.

Table C.7. Raw energy response data obtained[a] using encased CaF_2:Mn TLDs exposed to the nominal 4.96 mCi Co-57 source[a].

Encasement Material	Radial Wall Mass Thickness (g/cm^2)	Exposure Radius (cm)	Net TLD Response[b] (nC)	Sensitivity Corrected Net TLD Response[b] (nC)
Pb	0.734	20.4	1.546 ± 0.023	1.587 ± 0.017
Ta	0.696	20.4	1.897 ± 0.069	1.895 ± 0.020
Sn	0.608	20.4	3.854 ± 0.033	3.867 ± 0.026
Zr	0.541	20.4	3.863 ± 0.052	3.911 ± 0.020
Cu	0.694	20.4	3.768 ± 0.041	3.787 ± 0.014
Fe	0.656	20.4	3.856 ± 0.049	3.887 ± 0.021
S.S.	0.693	20.4	3.864 ± 0.034	3.892 ± 0.032
Al	0.514	20.4	3.940 ± 0.030	3.964 ± 0.022
LiF	0.483	15.5	6.731 ± 0.049	6.794 ± 0.050

[a]Exposure time was 41 h.

[b]Average of ten TLD responses.

Table C.8. Raw energy response data obtained using encased CaF_2:Mn TLDs exposed to the nominal 2.97 mCi Ce-141 source[a].

Encasement Material	Radial Wall Mass Thickness (g/cm^2)	Exposure Radius (cm)	Net TLD Response[b] (nC)	Sensitivity Corrected Net TLD Response[b] (nC)
Pb	0.734	20.4	1.031 ± 0.015	1.031 ± 0.015
Ta	0.696	20.4	1.302 ± 0.022	1.301 ± 0.020
Sn	0.608	20.4	2.147 ± 0.022	2.148 ± 0.034
Zr	0.541	20.4	1.952 ± 0.041	2.037 ± 0.011
Cu	0.694	20.4	1.879 ± 0.006	1.877 ± 0.012
Fe	0.656	20.4	1.974 ± 0.014	1.978 ± 0.007
S.S.	0.693	20.4	1.963 ± 0.020	1.966 ± 0.014
Al	0.514	20.4	-- --	-- --
LiF	0.483	20.4	-- --	-- --

[a]Exposure time was 55.5 h.

[b]Average of ten TLD responses.

Table C.9. Raw energy response data obtained using encased CaF_2:Mn TLDs exposed to the nominal 4.51 mCi Hg-203 source[a].

Encasement Material	Radial Wall Mass Thickness (g/cm^2)	Exposure Radius (cm)	Net TLD Response[b] (nC)	Sensitivity Corrected Net TLD Response[b] (nC)
Pb	0.734	20.4	3.243 ± 0.033	3.244 ± 0.023
Ta	0.696	20.4	3.095 ± 0.044	3.084 ± 0.025
Sn	0.608	20.4	2.835 ± 0.018	2.832 ± 0.013
Zr	0.541	20.4	2.612 ± 0.030	2.623 ± 0.017
Cu	0.694	20.4	2.537 ± 0.027	2.535 ± 0.016
Fe	0.656	20.4	2.570 ± 0.027	2.585 ± 0.011
S.S.	0.693	20.4	2.524 ± 0.023	2.527 ± 0.014
Al	0.514	20.4	2.535 ± 0.017	2.609 ± 0.032
LiF	0.483	15.5	4.564 ± 0.055	4.522 ± 0.037

[a]Exposure time was 40 h.

[b]Average of ten TLD responses.

Table C.10. Raw energy response data obtained using encased CaF_2:Mn TLDs exposed to the nominal 5.45 mCi Sn-113 source[a].

Encasement Material	Radial Wall Mass Thickness (g/cm^2)	Exposure Radius (cm)	Net TLD Response[b] (nC)	Sensitivity Corrected Net TLD Response[b] (nC)
Pb	0.734	20.4	2.054 ± 0.021	20.47 ± 0.011
Ta	0.696	20.4	1.901 ± 0.027	1.899 ± 0.017
Sn	0.608	20.4	1.547 ± 0.021	1.550 ± 0.020
Zr	0.541	20.4	1.457 ± 0.018	1.471 ± 0.010
Cu	0.694	20.4	1.349 ± 0.013	1.354 ± 0.011
Fe	0.656	20.4	1.347 ± 0.016	1.357 ± 0.007
S.S.	0.693	20.4	1.355 ± 0.012	1.365 ± 0.011
Al	0.514	20.4	-- --	-- --
LiF	0.483	15.5	-- --	-- --

[a]Exposure time was 16 h.

[b]Average of ten TLD responses.

Table C.11. Raw energy response data obtained using encased CaF_2:Mn TLDs exposed to the nominal 5.27 mCi Cs-137 source[a].

Encasement Material	Radial Wall Mass Thickness (g/cm^2)	Exposure Radius (cm)	Net TLD Response[b] (nC)	Sensitivity Corrected Net TLD Response[b] (nC)
Pb	0.734	20.4	5.792 ± 0.073	5.795 ± 0.024
Ta	0.696	20.4	5.219 ± 0.049	5.230 ± 0.035
Sn	0.608	20.4	4.248 ± 0.058	4.256 ± 0.038
Zr	0.541	20.4	4.201 ± 0.050	4.254 ± 0.034
Cu	0.694	20.4	3.900 ± 0.033	3.927 ± 0.050
Fe	0.656	20.4	3.956 ± 0.043	3.996 ± 0.025
S.S.	0.693	20.4	3.991 ± 0.042	4.028 ± 0.031
Al	0.514	20.4	3.962 ± 0.036	3.993 ± 0.046
LiF	0.483	15.5	6.904 ± 0.070	7.002 ± 0.057

[a]Exposure time was 18 h.

[b]Average of ten TLD responses.

Table C.12. Raw energy response data obtained using encased CaF_2:Mn TLDs exposed to the nominal 5.06 mCi Co-60 source[a].

Encasement Material	Radial Wall Mass Thickness (g/cm^2)	Exposure Radius (cm)	Net TLD Response[b] (nC)	Sensitivity Corrected Net TLD Response[b] (nC)
Pb	0.734	20.4	21.909 ± 0.174	21.943 ± 0.120
Ta	0.696	20.4	20.743 ± 0.320	20.673 ± 0.186
Sn	0.608	20.4	17.983 ± 0.157	17.963 ± 0.145
Zr	0.541	20.4	16.638 ± 0.204	16.759 ± 0.082
Cu	0.694	20.4	17.025 ± 0.181	17.030 ± 0.107
Fe	0.656	20.4	15.879 ± 0.177	15.945 ± 0.133
S.S.	0.693	20.4	15.917 ± 0.142	15.971 ± 0.113
Al	0.514	20.4	15.929 ± 0.181	15.956 ± 0.080
LiF	0.483	15.5	27.273 ± 0.262	27.817 ± 0.168

[a]Exposure time was 15 h.

[b]Average of ten TLD responses.

Table C.13. Raw sleeve thickness data obtained using encased ^{7}LiF TLDs exposed to the nominal 3.01 mCi Co-57 source[a,b].

Radial Wall Mass Thickness (g/cm^2)	TLD I.D. Number	Net TLD Response (nC)	Radial Wall Mass Thickness (g/cm^2)	TLD I.D. Number	Net TLD Response (nC)
Lead Encasements Exposure Radius = 10.8 cm			Zirconium Encasements Exposure Radius = 10.8 cm		
0.734	18	3.160	0.187	64	11.568
0.864	79	2.424	0.269	88	11.567
1.109	49	1.633	0.352	7	11.664
1.440	81	1.117	0.434	44	10.563
1.728	99	0.879	0.517	59	10.268
2.160	95	0.770	0.541	27	10.168
2.592	101	0.748	0.682	2	9.511
3.456	62	0.707	1.549	39	6.670
4.321	68	0.673	2.415	34	4.168
8.641	51	0.533			
Tantalum Encasements Exposure Radius = 10.8 cm			Copper Encasements Exposure Radius = 15.5 cm		
0.338	23	7.904	0.257	11	4.642
0.632	84	4.066	0.371	65	4.548
0.696	35	3.926	0.485	71	4.257
0.845	38	3.203	0.599	42	4.502
1.265	52	1.405	0.694	37	4.175
1.623	56	0.919	0.712	85	3.965
2.108	63	0.735	0.940	75	3.823
3.162	45	0.617	1.623	86	3.528
			2.135	55	3.185
Tin Encasements Exposure Radius = 10.8 cm			Stainless Steel Encasements Exposure Radius = 15.5 cm		
0.210	57	12.763	0.244	30	4.214
0.302	82	12.063	0.323	47	4.371
0.395	73	10.868	0.422	93	4.313
0.488	94	10.164	0.521	78	4.245
0.580	28	9.862	0.620	66	4.268
0.608	25	9.205	0.693	80	4.157
0.766	50	7.584	0.818	29	4.078
1.322	40	5.244	1.413	5	3.828
1.739	36	3.774	1.858	8	3.396
2.712	77	1.837	2.899	22	3.030

Table C.13.- Continued

Radial Wall Mass Thickness (g/cm^2)	TLD I.D. Number	Net TLD Response (nC)	Radial Wall Mass Thickness (g/cm^2)	TLD I.D. Number	Net TLD Response (nC)
Iron Encasements Exposure Radius = 15.5 cm			Aluminum Encasements Exposure Radius = 15.5 cm		
0.226	33	4.560	0.069	97	3.800
0.362	3	4.327	0.103	24	3.868
0.426	16	4.306	0.137	60	3.591
0.526	14	4.327	0.171	76	3.846
0.626	6	4.228	0.206	83	3.697
0.656	89	4.186	0.274	20	3.706
0.824	98	4.110	0.343	19	3.957
1.425	87	3.713	0.514	74	3.825
1.875	92	3.624	0.686	100	3.780
2.925	1	2.897	1.028	41	3.592
			1.371	69	3.777
			LiF Encasements Exposure Radius = 15.5 cm		
			0.483	31	3.599
			0.483	26	3.612
			0.483	90	3.585
			0.870	4	3.597
			0.870	61	3.394
			0.870	15	3.671

[a]TLD sort set 3-A was used.

[b]Exposure time was 180 h.

Table C.14. Raw sleeve thickness data obtained using encased ^{7}LiF TLDs exposed to the nominal 0.27 mCi Ce-141 source[a,b].

Radial Wall Mass Thickness (g/cm^2)	TLD I.D. Number	Net TLD Response (nC)	Radial Wall Mass Thickness (g/cm^2)	TLD I.D. Number	Net TLD Response (nC)
Lead Encasements Exposure Radius = 10.8 cm			Zirconium Encasements Exposure Radius = 10.8 cm		
0.734	10	0.825	0.187	68	1.795
0.864	36	0.677	0.269	11	1.823
1.109	62	0.491	0.352	13	1.802
1.440	73	0.284	0.434	69	1.734
1.728	1	0.197	0.517	42	1.663
2.160	63	0.143	0.541	98	1.671
2.592	55	0.115	0.682	3	1.609
3.456	83	0.100	1.177	29	1.406
4.321	34	0.089	1.549	51	1.300
8.641	58	0.062	2.415	91	0.960
Tantalum Encasements Exposure Radius = 10.8 cm			Copper Encasements Exposure Radius = 15.5 cm		
0.338	89	2.078	0.257	100	0.789
0.632	93	1.061	0.371	90	0.731
0.696	66	0.884	0.485	8	0.758
0.845	2	0.829	0.599	25	0.748
1.265	65	0.514	0.694	4	0.732
1.623	86	0.291	0.712	40	0.717
2.108	95	0.187	0.940	9	0.720
3.162	79	0.115	1.623	23	0.667
			2.135	33	0.622
Tin Encasements Exposure Radius = 10.8 cm			Stainless Steel Encasements Exposure Radius = 15.5 cm		
0.210	37	2.277	0.244	14	0.617
0.302	44	2.149	0.323	28	0.652
0.395	41	1.965	0.422	94	0.692
0.488	19	1.910	0.521	102	0.700
0.580	59	1.729	0.620	43	0.754
0.608	45	1.805	0.693	18	0.740
0.766	97	1.627	0.818	27	0.730
1.322	60	1.184	1.413	85	0.772
1.739	72	0.942	1.858	7	0.705
2.712	74	0.670	2.899	6	0.764

Table C.14 - Continued

Radial Wall Mass Thickness (g/cm^2)	TLD I.D. Number	Net TLD Response (nC)	Radial Wall Mass Thickness (g/cm^2)	TLD I.D. Number	Net TLD Response (nC)
Iron Encasements Exposure Radius = 15.5 cm			Aluminum Encasements Exposure Radius = 15.5 cm		
0.226	35	0.739	0.069	46	0.763
0.362	96	0.751	0.103	87	0.744
0.426	5	0.692	0.137	71	0.772
0.526	15	0.695	0.171	81	0.748
0.626	47	0.690	0.206	17	0.760
0.656	80	0.719	0.274	49	0.782
0.824	76	0.662	0.343	57	0.743
1.425	67	0.631	0.514	24	0.760
1.875	50	0.641	0.686	22	0.751
2.925	84	0.586	1.028	70	0.757
			1.371	77	0.723
			LiF Encasements		
			0.483	54	0.718
			0.483	82	0.681
			0.483	38	0.692
			0.870	88	0.680
			0.870	30	0.719
			0.870	101	0.720

[a]TLD sort set 2-A was used.

[b]Exposure time was 976 h.

Table C.15. Raw sleeve thickness data obtained using encased ^{7}LiF TLDs exposed to the nominal 0.32 mCi Hg-203 source[a,b].

Radial Wall Mass Thickness (g/cm^2)	TLD I.D. Number	Net TLD Response (nC)	Radial Wall Mass Thickness (g/cm^2)	TLD I.D. Number	Net TLD Response (nC)
Lead Encasements Exposure Radius = 10.8 cm			Zirconium Encasements Exposure Radius = 10.8 cm		
0.734	146	6.107	0.187	176	4.995
0.864	129	6.228	0.269	177	5.151
1.109	106	5.701	0.352	181	5.125
1.440	117	5.057	0.434	160	4.707
1.728	142	4.718	0.517	139	5.053
2.160	115	3.823	0.541	203	4.967
2.592	153	3.012	0.682	204	4.849
3.456	165	2.314	1.177	144	4.823
4.321	167	1.569	1.549	127	4.519
8.641	192	0.304	2.415	194	4.321
Tantalum Encasements Exposure Radius = 10.8 cm			Copper Encasements Exposure Radius = 15.5 cm		
0.338	124	6.926	0.257	108	2.151
0.632	173	6.724	0.371	182	2.060
0.696	197	6.027	0.485	113	2.137
0.845	187	5.943	0.599	162	2.030
1.265	175	5.095	0.694	116	2.107
1.623	193	4.378	0.712	171	2.169
2.108	112	4.040	0.940	141	1.987
3.162	132	2.912	1.623	164	1.988
			2.135	185	1.992
Tin Encasements Exposure Radius = 10.8 cm			Stainless Steel Encasements Exposure Radius = 15.5 cm		
0.210	161	5.926	0.244	103	2.015
0.302	156	5.911	0.323	130	1.953
0.395	126	5.681	0.422	135	2.068
0.488	179	5.590	0.521	155	2.136
0.580	105	5.481	0.620	170	1.978
0.608	118	5.317	0.693	152	2.037
0.766	134	5.253	0.818	196	2.043
1.322	122	4.833	1.413	150	1.969
1.739	111	4.897	1.858	147	1.999
2.712	202	4.133	2.899	191	1.891

Table C.15 --Continued

Radial Wall Mass Thickness (g/cm^2)	TLD I.D. Number	Net TLD Response (nC)	Radial Wall Mass Thickness (g/cm^2)	TLD I.D. Number	Net TLD Response (nC)
Iron Encasements Exposure Radius = 15.5 cm			Aluminum Encasements Exposure Radius = 15.5 cm		
0.226	140	2.130	0.069	133	1.880
0.362	184	2.096	0.103	138	1.992
0.426	149	2.052	0.137	199	1.892
0.526	166	2.009	0.171	172	1.968
0.626	121	2.135	0.206	169	2.017
0.656	154	2.157	0.274	201	1.993
0.824	174	1.958	0.343	158	1.924
1.425	189	2.024	0.514	163	1.877
1.875	104	1.955	0.686	190	1.824
2.925	200	1.900	1.028	137	1.859
			1.371	148	1.834
			LiF Encasements Exposure Radius = 15.5 cm		
			0.483	157	1.839
			0.483	159	1.963
			0.483	151	1.828
			0.870	136	1.813
			0.870	168	1.871
			0.870	195	1.850

[a]TLD sort set 2-B was used.

[b]Exposure time was 448 h.

Table C.16. Raw sleeve thickness data obtained using encased ^{7}LiF TLDs exposed to the nominal 1.80 mCi Sn-113 source[a,b].

Radial Wall Mass Thickness (g/cm^2)	TLD I.D. Number	Net TLD Response (nC)	Radial Wall Mass Thickness (g/cm^2)	TLD I.D. Number	Net TLD Response (nC)
Lead Encasements Exposure Radius = 10.8 cm			Zirconium Encasements Exposure Radius = 10.8 cm		
0.734	118	14.264	0.187	125	9.362
0.864	181	13.056	0.269	152	8.582
1.109	119	12.367	0.352	120	9.079
1.440	132	12.068	0.434	137	9.020
1.728	156	11.362	0.517	143	9.220
2.160	199	10.239	0.541	139	9.032
2.592	121	9.670	1.177	107	9.060
3.456	127	8.335	1.549	136	8.962
4.321	201	7.078	2.415	146	7.992
8.641	189	2.894	0.682	144	8.876
Tantalum Encasements Exposure Radius = 10.8 cm			Copper Encasements Exposure Radius = 15.5 cm		
0.338	148	12.654	0.257	134	4.122
0.632	147	12.761	0.371	164	4.011
0.696	123	12.668	0.485	183	4.014
0.845	197	12.358	0.599	188	3.990
1.265	117	11.252	0.694	126	3.908
1.623	185	10.926	0.712	190	3.694
2.108	124	10.056	0.940	150	3.806
3.162	163	8.739	1.623	105	3.664
				2.135	122
Tin Encasements Exposure Radius = 10.8 cm			Stainless Steel Encasements Exposure Radius = 15.5 cm		
0.210	104	10.556	0.244	151	3.975
0.302	109	9.952	0.323	175	3.852
0.395	169	10.355	0.422	202	3.605
0.488	149	9.966	0.521	106	3.979
0.580	195	10.064	0.620	160	3.845
0.608	194	10.159	0.693	191	3.839
0.766	116	9.853	0.818	135	3.767
1.322	155	9.519	1.413	140	3.931
1.739	114	9.329	1.858	179	3.801
2.712	168	8.921	2.899	172	3.649

Table C.16 - Continued

Radial Wall Mass Thickness (g/cm^2)	TLD I.D. Number	Net TLD Response (nC)	Radial Wall Mass Thickness (g/cm^2)	TLD I.D. Number	Net TLD Response (nC)
Iron Encasements Exposure Radius = 15.5 cm			Aluminum Encasements Exposure Radius = 15.5 cm		
0.226	138	3.769	0.069	157	3.722
0.362	154	4.102	0.103	162	3.855
0.426	174	3.868	0.137	177	3.854
0.526	108	3.897	0.171	153	3.741
0.626	130	3.868	0.206	187	3.772
0.656	145	3.814	0.274	193	3.636
0.824	141	3.897	0.343	165	3.680
1.425	102	3.716	0.514	166	3.632
1875	133	3.992	0.686	159	3.534
2.925	200	3.631	1.028	103	3.641
			1.371	142	3.736
			LiF Encasements Exposure Radius = 15.5 cm		
			0.483	129	3.743
			0.483	176	3.566
			0.483	198	3.543
			0.879	110	3.804
			0.870	115	3.530
			0.870	128	3.715

[a]TLD sort set 3-B was used.

[b]Exposure time was 180 h.

Table C.17. Raw sleeve thickness data obtained using encased ^{7}LiF TLDs exposed to the nominal 5.27 mCi Cs-137 source[a,b].

Radial Wall Mass Thickness (g/cm^2)	TLD I.D. Number	Net TLD Response (nC)	Radial Wall Mass Thickness (g/cm^2)	TLD I.D. Number	Net TLD Response (nC)
Lead Encasements Exposure Radius = 25.3 cm			Zirconium Encasements Exposure Radius = 25.3 cm		
0.734	170	11.172	0.187	150	7.007
0.864	168	10.869	0.269	105	6.844
1.109	120	10.753	0.352	179	7.065
1.440	195	10.051	0.434	141	7.039
1.728	128	10.564	0.517	191	6.680
2.160	183	9.853	0.541	142	6.985
2.592	124	9.313	0.682	196	6.958
3.456	129	9.086	1.177	189	7.010
4.321	158	8.280	1.549	148	6.989
8.641	184	6.026	2.415	186	6.708
Tantalum Encasements Exposure Radius = 25.3 cm			Copper Encasements Exposure Radius = 25.3 cm		
0.338	175	10.174	0.257	176	6.841
0.632	180	10.064	0.371	173	6.764
0.696	152	9.441	0.485	200	6.600
0.845	202	9.685	0.599	106	6.747
1.265	119	9.339	0.694	143	6.386
1.623	169	9.502	0.712	122	6.642
2.108	181	9.029	0.940	155	6.497
3.162	113	8.406	1.623	112	6.181
			2.135	193	6.423
Tin Encasements Exposure Radius = 25.3 cm			Stainless Steel Encasements Exposure Radius = 25.3 cm		
0.210	151	7.887	0.244	182	6.599
0.302	161	7.564	0.323	163	6.897
0.395	118	7.563	0.422	--	--
0.488	103	7.569	0.521	107	6.780
0.580	130	7.647	0.620	109	6.544
0.608	117	7.655	0.693	188	6.682
0.766	126	7.557	0.818	185	6.761
1.322	136	7.315	1.413	135	6.295
1.739	116	7.662	1.858	159	6.442
2.712	187	6.770	2.899	156	6.251

Table C.17 - Continued

Radial Wall Mass Thickness (g/cm^2)	TLD I.D. Number	Net TLD Response (nC)	Radial Wall Mass Thickness (g/cm^2)	TLD I.D. Number	Net TLD Response (nC)
Iron Encasements Exposure Radius = 25.3 cm			Aluminum Encasements Exposure Radius = 25.3 cm		
0.226	177	6.611	0.069	125	6.498
0.362	198	6.614	0.103	174	6.570
0.426	147	6.870	0.137	140	6.542
0.526	114	6.583	0.171	167	6.464
0.626	172	6.295	0.206	164	6.375
0.656	199	6.779	0.274	108	6.228
0.824	139	6.682	0.343	165	6.266
1.425	102	6.705	0.514	166	6.088
1.875	111	6.798	0.686	133	6.090
2.925	171	6.420	1.028	153	5.864
			1.371	146	5.893
			LiF Encasements Exposure Radius = 25.3 cm		
			0.483	149	6.065
			0.483	137	6.221
			0.483	144	6.274
			0.870	178	6.704
			0.870	110	6.155
			0.870	201	6.193

[a]TLD sort set 4-B was used.

[b]Exposure time was 96 h.

Table C.18. Raw sleeve thickness data obtained using encased ^{7}LiF TLDs exposed to the nominal 4.68 mCi Co-60 source[a,b].

Radial Wall Mass Thickness (g/cm^2)	TLD I.D. Number	Net TLD Response (nC)	Radial Wall Mass Thickness (g/cm^2)	TLD I.D. Number	Net TLD Response (nC)
Lead Encasement Exposure Radius = 20.4 cm			Zirconium Encasements Exposue Radius = 20.4 cm		
0.734	96	6.198	0.187	1	4.659
0.864	23	6.126	0.269	27	4.402
1.109	38	6.204	0.352	43	4.568
1.440	88	6.354	0.434	44	4.614
1.728	45	6.219	0.517	60	4.583
2.160	14	6.002	0.541	64	4.689
2.592	63	6.132	0.682	56	4.673
3.456	41	6.051	1.177	10	4.692
4.321	90	5.690	1.549	61	4.523
8.641	37	4.833	2.415	--	--
Tantalum Encasements Exposure Radius = 20.4 cm			Copper Encasements Exposure Radius = 20.4 cm		
0.338	54	5.728	0.257	6	4.612
0.632	93	5.536	0.371	48	4.758
0.696	75	5.766	0.485	4	4.282
0.845	86	5.592	0.599	89	4.331
1.265	33	5.758	0.694	32	4.435
1.623	62	5.858	0.712	--	--
2.108	69	5.746	0.940	99	4.513
3.162	13	5.731	1.623	83	4.536
			2.135	22	4.480
Tin Encasements Exposure Radius = 20.4 cm			Stainless Steel Encasements Exposure Radius = 20.4 cm		
0.210	55	4.664	0.244	71	4.413
0.302	94	4.613	0.323	65	4.551
0.395	70	4.970	0.422	36	4.425
0.488	12	4.785	0.521	9	4.579
0.580	39	4.793	0.620	72	4.690
0.608	19	4.837	0.693	98	4.587
0.766	47	4.769	0.818	100	4.472
1.322	25	4.898	1.413	51	4.241
1.739	11	4.839	1.858	7	4.264
2.712	21	4.602	2.899	101	4.254

Table C.18 - continued

Radial Wall Mass Thickness (g/cm^2)	TLD I.D. Number	Net TLD Response (nC)	Radial Wall Mass Thickness (g/cm^2)	TLD I.D. Number	Net TLD Response (nC)
Iron Encasements Exposure Radius = 20.4			Aluminum Encasements Exposure Radius = 20.4 cm		
0.226	50	4.704	0.069	46	5.049
0.362	78	4.521	0.103	58	4.870
0.426	85	4.750	0.137	73	4.612
0.526	15	4.287	0.171	80	4.674
0.626	81	4.305	0.206	17	4.478
0.656	84	4.456	0.274	20	4.486
0.824	87	4.367	0.343	74	4.419
1.425	4	4.439	0.514	95	4.302
1.875	91	4.142	0.686	34	4.319
2.925	53	4.271	1.028	79	4.405
			1.371	26	4.201
			LiF Encasements Exposure Radius = 20.4 cm		
			0.483	97	4.484
			0.483	68	4.329
			0.483	24	4.242
			0.870	92	4.159
			0.870	2	4.145
			0.870	28	4.241

[a]TLD sort set 4-A was used.

[b]Exposure time was 16.5 h.

Table C.19. Raw sleeve thickness data obtained using encased CaF_2:Mn TLDs exposed to the nominal 3.88 mCi Co-57 source[a,b].

Radial Wall Mass Thickness (g/cm^2)	TLD I.D. Number	Net TLD Response Counts	Radial Wall Mass Thickness (g/cm^2)	TLD I.D. Number	Net TLD Response Counts
Lead Encasements Exposure Radius = 25.3 cm			Zirconium Encasements Exposure Radius = 25.3 cm		
0.734	192	3.566 (5)	0.187	158	1.189 (6)
0.864	139	2.736 (5)	0.269	186	1.008 (6)
1.109	159	1.755 (5)	0.352	164	1.000 (6)
1.440	182	1.051 (5)	0.434	105	9.711 (5)
1.728	122	8.667 (4)	0.517	196	9.113 (5)
2.160	155	7.164 (4)	0.541	127	9.159 (5)
2.592	144	6.681 (4)	0.682	130	8.818 (5)
3.456	180	6.058 (4)	1.177	195	6.665 (5)
4.321	163	5.730 (4)	1.549	117	5.548 (5)
8.641	149	5.133 (4)	2.415	202	3.824 (5)
Tantalum Encasements Exposure Radius = 25.3 cm			Copper Encasements Exposure Radius = 25.3 cm		
0.338	191	9.127 (5)	0.257	188	9.271 (5)
0.632	203	4.761 (5)	0.371	194	9.303 (5)
0.696	193	4.624 (5)	0.485	156	8.617 (5)
0.845	110	4.476 (5)	0.599	184	8.846 (5)
1.265	118	1.780 (5)	0.694	104	9.120 (5)
1.623	176	1.086 (5)	0.712	157	8.615 (5)
2.108	183	7.544 (4)	0.940	137	8.147 (5)
3.162	178	5.752 (4)	1.623	172	7.487 (5)
			2.135	190	6.837 (5)
Tin Encasements Exposure Radius = 25.3 cm			Stainless Steel Encasements Exposure Radius = 25.3 cm		
0.210	107	1.330 (6)	0.244	181	9.196 (5)
0.302	140	1.120 (6)	0.323	146	9.211 (5)
0.395	141	1.097 (6)	0.422	166	9.116 (5)
0.488	167	1.065 (6)	0.521	171	9.022 (5)
0.580	--	--	0.620	153	8.861 (5)
0.608	129	9.510 (5)	0.693	154	8.664 (5)
0.766	168	7.963 (5)	0.818	120	8.523 (5)
1.322	109	5.170 (5)	1.413	148	8.321 (5)
1.739	150	3.625 (5)	1.858	201	7.238 (5)
2.712	174	1.859 (5)	2.899	152	6.411 (5)

Table C.19 - Continued

Radial Wall Mass Thickness (g/cm^2)	TLD I.D. Number	Net TLD Response Counts	Radial Wall Mass Thickness (g/cm^2)	TLD I.D. Number	Net TLD Response Counts
Iron Encasements Exposure Radius = 25.3 cm			Aluminum Encasements Exposure Radius = 25.3 cm		
0.226	199	9.212 (5)	0.069	--	--
0.362	114	9.191 (5)	0.103	165	9.111 (5)
0.426	170	8.811 (5)	0.137	124	8.962 (5)
0.526	115	8.856 (5)	0.171	119	9.179 (5)
0.626	134	8.799 (5)	0.206	133	9.070 (5)
0.656	197	8.677 (5)	0.274	111	9.029 (5)
0.824	147	8.748 (5)	0.343	160	8.974 (5)
1.425	173	8.112 (5)	0.514	175	9.136 (5)
1.875	145	7.871 (5)	0.686	125	9.070 (5)
2.925	179	6.575 (5)	1.028	187	9.195 (5)
			1.371	106	9.205 (5)
			LiF Encasements Exposure Radius = 25.3 cm		
			0.483	198	8.325 (5)
			0.483	121	8.519 (5)
			0.483	177	7.995 (5)
			0.870	135	8.838 (5)
			0.870	116	8.821 (5)
			0.870	161	8.401 (5)

[a]TLD sort set 2-B was used.

[b]Exposure time was 281 h.

Table C.20. Raw sleeve thickness data obtained using encased CaF_2:Mn TLDs exposed to the nominal 1.86 mCi Ce-141 source[a,b].

Radial Wall Mass Thickness (g/cm^2)	TLD I.D. Number	Net TLD Response Counts	Radial Wall Mass Thickness (g/cm^2)	TLD I.D. Number	Net TLD Response Counts
Lead Encasements Exposure Radius = 15.5 cm			Zirconium Encasements Exposure Radius = 15.5 cm		
0.734	146	6.715 (5)	0.187	173	1.381 (6)
0.864	204	4.998 (5)	0.269	111	1.348 (6)
1.109	178	3.306 (5)	0.352	159	1.337 (6)
1.440	109	1.693 (5)	0.434	192	1.277 (6)
1.728	193	1.103 (5)	0.517	198	1.282 (6)
2.160	110	5.172 (4)	0.541	156	1.228 (6)
2.592	205	2.800 (4)	0.682	179	1.160 (6)
3.456	132	1.894 (4)	1.177	145	9.791 (5)
4.321	151	1.204 (4)	1.549	--	--
8.641	171	1.296 (4)	2.415	189	6.751 (5)
Tantalum Encasements Exposure Radius = 15.5 cm			Copper Encasements Exposure Radius = 20.4 cm		
0.338	131	1.284 (6)	0.257	155	7.849 (5)
0.632	116	8.416 (5)	0.371	136	6.879 (5)
0.696	123	8.278 (5)	0.485	149	6.842 (5)
0.845	108	6.537 (5)	0.599	143	6.715 (5)
1.265	--	--	0.694	113	6.363 (5)
1.623	140	1.933 (5)	0.712	107	6.353 (5)
2.108	147	1.027 (5)	0.940	202	6.161 (5)
3.162	174	2.690 (4)	1.623	167	5.910 (5)
			2.135	203	5.447 (5)
Tin Encasements Exposure Radius = 15.5 cm			Stainless Steel Encasements Exposure Radius = 20.4 cm		
0.210	122	1.791 (6)	0.244	197	9.122 (5)
0.302	144	1.575 (6)	0.323	118	8.790 (5)
0.395	130	1.566 (6)	0.422	--	--
0.488	157	1.478 (6)	0.521	165	7.367 (5)
0.580	166	1.347 (6)	0.620	164	7.032 (5)
0.608	183	1.374 (6)	0.693	112	7.126 (5)
0.766	152	1.237 (6)	0.818	177	6.924 (5)
1.322	168	8.899 (5)	1.413	129	6.677 (5)
1.739	142	6.705 (5)	1.858	134	6.453 (5)
2.712	114	4.055 (5)	2.899	196	5.523 (5)

Table C.20 - Continued

Radial Wall Mass Thickness (g/cm^2)	TLD I.D. Number	Net TLD Response Counts	Radial Wall Mass Thickness (g/cm^2)	TLD I.D. Number	Net TLD Response Counts
Iron Encasements Exposure Radius = 20.4 cm					
0.266	195	8.768 (5)			
0.362	--	--			
0.426	124	7.709 (5)			
0.526	105	7.183 (5)			
0.626	161	7.347 (5)			
0.656	191	6.962 (5)			
0.824	190	6.731 (5)			
1.425	200	5.993 (5)			
1.875	104	6.013 (5)			
2.925	199	5.395 (5)			

[a]TLD sort set 1-B was used.

[b]Exposure time was 931 h.

Table C.21. Raw sleeve thickness data obtained using encased CaF_2:Mn TLDs exposed to the nominal 1.21 mCi Hg-203 source[a,b].

Radial Wall Mass Thickness (g/cm^2)	TLD I.D. Number	Net TLD Response Counts	Radial Wall Mass Thickness (g/cm^2)	TLD I.D. Number	Net TLD Response Counts
Lead Encasements Exposure Radius = 15.5 cm			Zirconium Encasements Exposure Radius = 15.5 cm		
0.734	--	--	0.187	83	1.340 (6)
0.864	62	1.467 (6)	0.269	80	1.285 (6)
1.109	86	1.334 (6)	0.352	38	1.339 (6)
1.440	1	1.124 (6)	0.434	72	1.303 (6)
1.728	26	1.016 (6)	0.517	22	1.186 (6)
2.160	87	7.883 (5)	0.541	29	1.187 (6)
2.592	25	6.527 (5)	0.682	51	1.252 (6)
3.456	52	5.023 (5)	1.177	13	1.141 (6)
4.321	76	3.642 (5)	1.549	65	1.088 (6)
8.641	32	5.955 (4)	2.415	101	1.058 (6)
Tantalum Encasements Exposure Radius = 15.5 cm			Copper Encasements Exposure Radius = 20.4 cm		
0.338	8	1.591 (6)	0.257	54	7.265 (5)
0.632	34	1.420 (6)	0.371	4	7.180 (5)
0.696	94	1.337 (6)	0.485	66	6.891 (5)
0.845	58	1.373 (6)	0.599	5	6.850 (5)
1.265	9	1.211 (6)	0.694	19	6.932 (5)
1.623	23	9.991 (5)	0.712	33	6.493 (5)
2.108	--	--	0.940	47	6.614 (5)
3.162	37	6.723 (5)	1.623	88	6.256 (5)
			2.135	35	6.186 (5)
Tin Encasements Exposure Radius = 15.5 cm			Stainless Steel Encasements Exposure Radius = 20.4 cm		
0.210	73	1.612 (6)	0.244	70	7.156 (5)
0.302	11	1.475 (6)	0.323	85	7.167 (5)
0.395	48	1.421 (6)	0.422	55	7.277 (5)
0.488	89	1.324 (6)	0.521	43	7.273 (5)
0.580	102	1.329 (6)	0.620	64	6.998 (5)
0.608	60	1.369 (6)	0.693	90	7.128 (5)
0.766	93	1.311 (6)	0.818	78	6.967 (5)
1.322	96	1.241 (6)	1.413	74	6.610 (5)
1.739	20	1.070 (6)	1.858	12	5.983 (5)
2.712	77	1.025 (6)	2.899	46	6.216 (5)

Table C.21 - Continued

Radial Wall Mass Thickness (g/cm^2)	TLD I.D. Number	Net TLD Response Counts	Radial Wall Mass Thickness (g/cm^2)	TLD I.D. Number	Net TLD Response Counts
Iron Encasements Exposure Radius = 20.4 cm			Aluminum Encasements Exposure Radius = 20.4 cm		
0.226	75	7.122 (5)	0.069	68	6.907 (5)
0.362	41	7.244 (5)	0.103	91	6.942 (5)
0.426	59	7.039 (5)	0.137	30	6.761 (5)
0.526	21	6.941 (5)	0.171	61	6.591 (5)
0.626	69	7.220 (5)	0.206	50	6.894 (5)
0.656	71	7.216 (5)	0.274	3	6.762 (5)
0.824	82	6.504 (5)	0.343	97	6.874 (5)
1.425	44	6.571 (5)	0.514	7	6.941 (5)
1.875	56	6.420 (5)	0.686	49	6.952 (5)
2.925	98	5.477 (5)	1.028	99	6.851 (5)
			1.371	16	6.434 (5)
			LiF Encasements Exposure Radius = 20.4 cm		
			0.483	81	6.223 (5)
			0.483	79	6.710 (5)
			0.483	27	6.382 (5)
			0.870	92	6.156 (5)
			0.870	57	6.748 (5)
			0.870	40	6.910 (5)

[a]TLD sort set 2-A was used.

[b]Exposure time was 348 h.

Table C.22. Raw sleeve thickness data obtained using encased CaF_2:Mn TLDs exposed to the nominal 3.23 mCi Sn-113 source[a,b].

Radial Wall Mass Thickness (g/cm^2)	TLD I.D. Number	Net TLD Response Counts	Radial Wall Mass Thickness (g/cm^2)	TLD I.D. Number	Net TLD Response Counts
Lead Encasements Exposure Radius = 25.3 cm			Zirconium Encasements Exposure Radius = 25.3 cm		
0.734	78	5.310 (5)	0.187	79	3.849 (5)
0.864	70	5.445 (5)	0.269	23	3.836 (5)
1.109	10	5.170 (5)	0.352	37	3.783 (5)
1.440	29	4.829 (5)	0.434	24	3.885 (5)
1.728	87	4.485 (5)	0.517	61	3.853 (5)
2.160	93	4.189 (5)	0.541	5	3.730 (5)
2.592	50	3.811 (5)	0.682	94	3.812 (5)
3.456	95	3.173 (5)	1.177	55	3.888 (5)
4.321	73	2.667 (5)	1.549	84	3.554 (5)
8.641	9	1.124 (5)	2.415	74	3.647 (5)
Tantalum Encasements Exposure Radius = 25.3 cm			Copper Encasements Exposure Radius = 25.3 cm		
0.338	52	5.410 (5)	0.257	38	3.659 (5)
0.632	49	5.180 (5)	0.371	22	3.726 (5)
0.696	81	4.868 (5)	0.485	32	3.514 (5)
0.845	13	5.016 (5)	0.599	39	3.679 (5)
1.265	15	4.831 (5)	0.694	67	3.704 (5)
1.623	80	4.328 (5)	0.712	47	3.662 (5)
2.108	99	4.415 (5)	0.940	102	3.615 (5)
3.162	33	3.579 (5)	1.623	17	3.610 (5)
			2.135	62	3.694 (5)
Tin Encasements Exposure Radius = 25.3 cm			Stainless Steel Encasements Exposure Radius = 25.3 cm		
0.210	31	4.634 (5)	0.244	44	3.941 (5)
0.302	34	4.350 (5)	0.323	83	3.754 (5)
0.395	2	4.326 (5)	0.422	88	3.594 (5)
0.488	91	4.134 (5)	0.521	58	3.540 (5)
0.580	71	4.259 (5)	0.620	25	3.658 (5)
0.608	75	4.325 (5)	0.693	43	3.633 (5)
0.766	59	4.211 (5)	0.818	76	3.567 (5)
1.322	82	4.047 (5)	1.413	20	3.625 (5)
1.739	41	4.055 (5)	1.858	98	3.712 (5)
2.712	3	3.692 (5)	2.899	30	3.603 (5)

Table C.22 - Continued

Radial Wall Mass Thickness (g/cm^2)	TLD I.D. Number	Net TLD Response Counts	Radial Wall Mass Thickness (g/cm^2)	TLD I.D. Number	Net TLD Response Counts
Iron Encasements Exposure Radius = 25.3 cm					
0.226	101	3.854 (5)			
0.362	14	3.579 (5)			
0.426	97	3.647 (5)			
0.526	36	3.569 (5)			
0.626	48	3.577 (5)			
0.656	42	3.401 (5)			
0.824	12	3.554 (5)			
1.425	4	3.395 (5)			
1.875	92	3.342 (5)			
2.925	103	3.446 (5)			

[a]TLD sort set 3-A was used.

[b]Exposure time was 156 h.

Table C.23. Raw sleeve thickness data obtained using encased CaF_2:Mn TLDs exposed to the nominal 5.27 mCi Cs-137 source[a,b].

Radial Wall Mass Thickness (g/cm^2)	TLD I.D. Number	Net TLD Response (nC)	Radial Wall Mass Thickness (g/cm^2)	TLD I.D. Number	Net TLD Response (nC)
Lead Encasements Exposure Radius = 25.3 cm			Zirconium Encasements Exposure Radius = 25.3 cm		
0.734	152	22.812	0.187	164	16.527
0.864	175	22.812	0.269	191	15.409
1.109	121	22.112	0.352	162	15.925
1.440	169	21.718	0.434	199	16.223
1.728	140	20.815	0.541	206	15.626
2.160	108	20.680	0.682	185	15.525
2.592	167	20.275	1.177	165	15.815
3.456	172	18.373	1.549	204	15.828
4.321	141	17.778	2.415	106	14.522
8.641	116	12.167			
Tantalum Encasements Exposure Radius = 25.3 cm			Copper Encasements Exposure Radius = 25.3 cm		
0.338	125	19.425	0.257	133	15.416
0.632	183	19.785	0.371	182	15.002
0.696	155	19.397	0.485	177	15.819
0.845	161	21.011	0.599	132	15.506
1.265	109	20.313	0.694	160	15.719
1.623	119	21.211	0.712	128	15.320
2.108	104	20.909	0.940	181	15.124
3.162	139	18.315	1.623	171	14.825
			2.135	142	15.022
Tin Encasements Exposure Radius = 25.3 cm			Stainless Steel Encasements Exposure Radius = 25.3 cm		
0.210	173	17.320	0.244	184	16.104
0.302	120	17.217	0.323	117	15.809
0.395	107	17.014	0.422	158	15.991
0.488	143	16.519	0.521	111	15.615
0.580	124	17.213	0.620	114	15.115
0.608	150	16.117	0.693	118	15.310
0.766	168	16.214	0.818	105	14.816
1.322	126	16.713	1.413	137	14.705
1.739	151	16.612	1.858	123	14.918
2.712	170	15.496	2.899	149	14.107

Table C.23 - Continued

Radial Wall Mass Thickness (g/cm^2)	TLD I.D. Number	Net TLD Response (nC)	Radial Wall Mass Thickness (g/cm^2)	TLD I.D. Number	Net TLD Response (nC)
Iron Encasements Exposure Radius = 25.3 cm			Aluminum Encasements Exposure Radius = 25.3 cm		
0.226	159	15.223	0.069	194	16.524
0.362	196	15.123	0.103	129	16.124
0.426	186	15.016	0.137	112	16.011
0.526	187	15.020	0.171	110	16.022
0.626	154	14.625	0.206	146	15.932
0.656	144	14.926	0.274	188	15.418
0.824	153	14.626	0.343	200	16.125
1.425	179	14.620	0.514	156	14.822
1.875	195	14.428	0.686	176	15.620
2.925	136	14.195	1.028	189	15.320
			1.371	135	15.392
			LiF Encasements Exposure Radius = 25.3 cm		
			0.483	147	13.826
			0.483	178	14.428
			0.483	193	13.896
			0.870	138	14.338
			0.870	157	14.819
			0.870	130	14.523

[a]TLD sort set 3-B was used.

[b]Exposure time was 111 h.

Table C.24. Raw sleeve thickness data obtained using encased CaF_2:Mn TLDs exposed to the nominal 4.84 mCi Co-60 source[a,b].

Radial Wall Mass Thickness (g/cm^2)	TLD I.D. Number	Net TLD Response (nC)	Radial Wall Mass Thickness (g/cm^2)	TLD I.D. Number	Net TLD Response (nC)
Lead Encasements Exposure Radius = 25.3 cm			Zirconium Encasements Exposure Radius = 25.3 cm		
0.734	146	33.221	0.187	173	23.923
0.864	204	32.414	0.269	111	24.025
1.109	178	33.124	0.352	159	24.726
1.440	109	31.624	0.434	192	24.201
1.728	193	31.919	0.517	198	24.625
2.160	110	31.620	0.541	156	24.224
2.592	205	31.525	0.682	179	24.127
3.456	132	29.521	1.177	145	23.426
4.321	151	28.917	1.549	185	24.127
8.641	171	25.168	2.415	189	22.820
Tantalum Encasements Exposure Radius = 25.3 cm			Copper Encasements Exposure Radius = 25.3 cm		
0.338	131	29.622	0.257	155	24.820
0.632	116	30.124	0.371	136	24.015
0.696	123	29.920	0.485	149	23.509
0.845	108	30.414	0.599	143	24.025
1.265	148	30.121	0.694	113	23.724
1.623	140	29.520	0.712	107	24.113
2.108	147	29.122	0.940	202	23.624
3.162	174	28.205	1.623	167	24.227
			2.135	203	23.003
Tin Encasements Exposure Radius = 25.3 cm			Stainless Steel Encasements Exposure Radius = 25.3 cm		
0.210	122	26.526	0.244	197	25.104
0.302	144	26.130	0.323	118	25.125
0.395	130	25.428	0.422	--	--
0.488	157	26.005	0.521	165	23.622
0.580	166	25.024	0.620	164	23.827
0.608	183	25.126	0.693	112	24.129
0.766	152	26.425	0.818	177	23.620
1.322	168	25.329	1.413	129	23.324
1.739	142	25.125	1.858	134	23.424
2.712	114	25.025	2.899	196	22.122

Table C.24 - Continued

Radial Wall Mass Thickness (g/cm^2)	TLD I.D. Number	Net TLD Response (nC)	Radial Wall Mass Thickness (g/cm^2)	TLD I.D. Number	Net TLD Response (nC)
Iron Encasements Exposure Radius = 25.3 cm			Aluminum Encasements Exposure Radius = 25.3 cm		
0.226	195	24.525	0.069	172	27.419
0.362	121	23.220	0.103	150	28.424
0.426	124	24.024	0.137	181	27.034
0.526	105	23.826	0.171	141	25.226
0.626	161	24.825	0.206	128	25.525
0.656	191	23.327	0.274	153	24.520
0.824	190	23.704	0.343	117	23.927
1.425	--	--	0.514	139	23.621
1.875	104	23.214	0.686	154	23.126
2.925	199	22.808	1.028	120	23.523
			1.371	176	22.907
			LiF Encasements Exposure Radius = 25.3 cm		
			0.483	186	21.925
			0.483	137	21.429
			0.483	194	21.629
			0.870	158	22.228
			0.870	175	21.330
			0.870	182	21.625

[a]TLD sort set 1-B was used.

[b]Exposure time was 44 h.

Table C.25. ^{7}LiF TLD Sort Number 2-A.

TLD I.D. NO.	RATIO	TLD I.D. NO.	RATIO
61	1.1109	71	0.9950
16	1.0885	87	0.9934
56	1.0849	46	0.9919
78	1.0829	33	0.9919
75	1.0677	23	0.9894
58	1.0646	9	0.9883
34	1.0600	40	0.9873
83	1.0443	4	0.9858
55	1.0377	25	0.9853
10	1.0377	8	0.9853
63	1.0366	90	0.9828
1	1.0366	100	0.9817
73	1.0361	84	0.9817
62	1.0341	50	0.9817
36	1.0341	67	0.9792
79	1.0326	76	0.9777
95	1.0316	80	0.9761
86	1.0316	47	0.9706
65	1.0316	15	0.9706
2	1.0275	5	0.9695
66	1.0260	96	0.9690
93	1.0229	35	0.9690
89	1.0219	91	0.9660
74	1.0219	51	0.9639
72	1.0219	29	0.9639
60	1.0209	3	0.9629
97	1.0204	98	0.9624
45	1.0204	42	0.9543
59	1.0189	69	0.9538
19	1.0189	13	0.9528
39	1.0133	11	0.9523
41	1.0128	68	0.9492
44	1.0107	101	0.9472
37	1.0107	30	0.9472
6	1.0102	88	0.9467
7	1.0097	38	0.9456
85	1.0092	82	0.9436
27	1.0087	54	0.9416
18	1.0077	32	0.9395
43	1.0072	21	0.9375
102	1.0036	12	0.9375
94	1.0026	92	0.9355
28	1.0026	48	0.9355
14	1.0026	53	0.9329
77	1.0011	20	0.9268
70	1.0000	52	0.9253
22	0.9995	64	0.9233
24	0.9980	31	0.9223
57	0.9975	99	0.9212
49	0.9975	26	0.9172
17	0.9975		
81	0.9960		

Table C.26. ^{7}LiF TLD Sort Number 2-B.

TLD I.D. NO.	RATIO	TLD I.D. NO.	RATIO
145	1.1227	169	1.0027
119	1.0982	172	1.0006
114	1.0939	199	1.0001
183	1.0913	138	0.9990
107	1.0811	133	0.9974
186	1.0673	185	0.9963
125	1.0651	164	0.9963
192	1.0630	141	0.9942
167	1.0577	171	0.9926
165	1.0571	116	0.9926
153	1.0555	162	0.9905
115	1.0550	113	0.9899
142	1.0518	182	0.9819
117	1.0438	108	0.9819
106	1.0406	200	0.9803
129	1.0390	104	0.9798
146	1.0347	189	0.9787
132	1.0347	174	0.9766
112	1.0342	154	0.9745
193	1.0326	121	0.9745
175	1.0321	166	0.9734
187	1.0294	149	0.9734
197	1.0289	184	0.9707
173	1.0289	140	0.9707
124	1.0283	194	0.9702
202	1.0278	127	0.9691
111	1.0262	144	0.9681
122	1.0235	204	0.9665
134	1.0230	203	0.9595
118	1.0225	139	0.9590
105	1.0225	160	0.9558
179	1.0209	181	0.9547
126	1.0209	177	0.9547
156	1.0193	176	0.9515
161	1.0182	195	0.9505
191	1.0150	168	0.9478
147	1.0134	136	0.9467
150	1.0129	151	0.9419
196	1.0113	159	0.9409
152	1.0097	157	0.9377
109	1.0091	120	0.9323
170	1.0086	128	0.9313
155	1.0086	198	0.9307
135	1.0081	143	0.9179
130	1.0075	123	0.9110
103	1.0070	110	0.9094
148	1.0059	180	0.9051
137	1.0059	131	0.8987
190	1.0054	188	0.8982
163	1.0054	178	0.8731
158	1.0033		
201	1.0027		

Table C.27. ^{7}LiF TLD Sort Number 3-A.

TLD I.D. NO.	RATIO	TLD I.D. NO.	RATIO
67	1.1342	100	1.0023
58	1.1174	74	1.0023
91	1.1096	19	1.0018
43	1.0892	20	1.0013
70	1.0861	83	1.0003
48	1.0840	76	0.9997
53	1.0834	60	0.9987
72	1.0808	24	0.9982
21	1.0803	97	0.9966
32	1.0745	55	0.9961
9	1.0735	86	0.9955
51	1.0641	75	0.9924
68	1.0620	85	0.9919
62	1.0615	37	0.9898
101	1.0609	42	0.9882
95	1.0599	71	0.9851
99	1.0562	65	0.9851
81	1.0531	11	0.9846
49	1.0526	1	0.9840
79	1.0489	92	0.9830
18	1.0484	87	0.9830
45	1.0479	98	0.9814
63	1.0468	89	0.9799
56	1.0432	6	0.9751
52	1.0432	14	0.9746
38	1.0411	16	0.9725
35	1.0384	3	0.9725
84	1.0369	33	0.9720
46	1.0353	34	0.9689
23	1.0343	39	0.9662
77	1.0316	54	0.9642
36	1.0306	2	0.9642
40	1.0285	27	0.9615
50	1.0280	59	0.9594
25	1.0254	44	0.9594
28	1.0207	7	0.9594
94	1.0191	88	0.9594
73	1.0186	64	0.9563
82	1.0175	15	0.9542
57	1.0139	61	0.9511
22	1.0128	4	0.9432
8	1.0123	90	0.9354
5	1.0112	26	0.9349
29	1.0102	31	0.9328
80	1.0097	13	0.9328
66	1.0091	12	0.9322
78	1.0055	10	0.9312
93	1.0044	17	0.9291
47	1.0044	96	0.8867
30	1.0044		
69	1.0039		
41	1.0029		

Table C.28. ^{7}LiF TLD Sort Number 3-B.

TLD I.D. NO.	RATIO	TLD I.D. NO.	RATIO
178	1.1335	175	1.0035
196	1.1226	151	1.0035
113	1.1143	142	1.0014
186	1.1122	103	1.0014
197	1.0956	159	1.0009
112	1.0940	166	0.9994
131	1.0930	165	0.9994
184	1.0815	193	0.9988
182	1.0711	187	0.9973
171	1.0711	153	0.9973
180	1.0701	177	0.9962
173	1.0685	162	0.9931
161	1.0685	157	0.9921
111	1.0649	122	0.9916
167	1.0612	105	0.9916
158	1.0602	150	0.9910
189	1.0555	190	0.9895
201	1.0550	126	0.9890
127	1.0514	188	0.9879
121	1.0508	188	0.9864
199	1.0482	164	0.9858
156	1.0425	134	0.9858
132	1.0420	200	0.9853
119	1.0389	133	0.9853
181	1.0373	102	0.9853
118	1.0368	170	0.9848
163	1.0352	141	0.9822
124	1.0352	145	0.9786
185	1.0342	130	0.9786
117	1.0332	108	0.9786
192	1.0306	174	0.9780
123	1.0306	154	0.9770
147	1.0300	138	0.9760
148	1.0290	146	0.9744
168	1.0264	136	0.9734
114	1.0259	107	0.9728
155	1.0248	144	0.9687
116	1.0248	139	0.9687
194	1.0228	143	0.9661
195	1.0207	137	0.9656
149	1.0186	120	0.9656
169	1.0150	152	0.9619
109	1.0150	125	0.9583
104	1.0129	128	0.9567
172	1.0124	115	0.9562
179	1.0113	110	0.9562
140	1.0092	198	0.9453
135	1.0092	176	0.9453
191	1.0087	129	0.9271
160	1.0087		
106	1.0087		
202	1.0040		

Table C.29. ^{7}LiF TLD Sort Number 4-A.

TLD I.D. NO.	RATIO	TLD I.D. NO.	RATIO
42	1.1496	95	1.0055
66	1.1373	74	1.0055
8	1.1357	20	1.0049
31	1.1019	17	1.0044
29	1.0918	80	1.0017
59	1.0821	73	0.9996
52	1.0773	58	0.9990
16	1.0773	46	0.9980
49	1.0719	22	0.9974
40	1.0666	83	0.9964
5	1.0660	99	0.9953
37	1.0601	57	0.9942
90	1.0585	32	0.9942
41	1.0585	89	0.9937
63	1.0575	4	0.9931
14	1.0575	48	0.9926
45	1.0564	6	0.9921
88	1.0516	53	0.9915
38	1.0478	91	0.9899
23	1.0478	3	0.9872
96	1.0462	87	0.9851
13	1.0408	84	0.9840
69	1.0349	81	0.9781
62	1.0349	15	0.9771
33	1.0328	85	0.9755
86	1.0323	78	0.9755
75	1.0317	50	0.9744
93	1.0307	30	0.9744
54	1.0296	61	0.9738
21	1.0290	10	0.9733
11	1.0285	56	0.9728
25	1.0248	64	0.9722
47	1.0226	60	0.9696
19	1.0221	44	0.9685
39	1.0210	43	0.9658
12	1.0210	27	0.9615
70	1.0194	1	0.9594
94	1.0183	28	0.9578
55	1.0178	2	0.9578
101	1.0167	92	0.9572
7	1.0162	24	0.9562
51	1.0146	68	0.9524
100	1.0135	97	0.9519
98	1.0135	35	0.9320
72	1.0130	18	0.9310
9	1.0124	67	0.9219
36	1.0119	82	0.9186
65	1.0108	76	0.9138
71	1.0098	77	0.8897
26	1.0098		
79	1.0071		
34	1.0065		

Table C.30. ^{7}LiF TLD Sort Number 4-B.

TLD I.D. NO.	RATIO	TLD I.D. NO.	RATIO
154	1.1104	165	0.9996
160	1.1033	108	0.9991
132	1.1017	164	0.9958
115	1.0979	167	0.9953
162	1.0968	140	0.9931
123	1.0935	174	0.9909
194	1.0805	125	0.9893
157	1.0805	193	0.9887
121	1.0789	112	0.9877
127	1.0762	155	0.9860
184	1.0675	122	0.9860
158	1.0675	143	0.9844
129	1.0593	106	0.9844
124	1.0533	200	0.9828
183	1.0512	173	0.9817
128	1.0495	176	0.9790
195	1.0490	171	0.9790
120	1.0485	111	0.9784
168	1.0463	102	0.9784
170	1.0436	139	0.9779
113	1.0430	199	0.9773
181	1.0414	172	0.9703
169	1.0414	114	0.9703
119	1.0371	147	0.9681
202	1.0360	198	0.9665
152	1.0360	177	0.9665
180	1.0354	186	0.9659
175	1.0354	148	0.9648
178	1.0343	189	0.9643
116	1.0343	196	0.9638
136	1.0322	142	0.9610
126	1.0322	191	0.9600
117	1.0322	141	0.9594
130	1.0311	179	0.9567
103	1.0305	105	0.9562
118	1.0295	150	0.9556
161	1.0229	201	0.9545
151	1.0219	110	0.9540
156	1.0202	187	0.9529
159	1.0186	144	0.9464
135	1.0170	137	0.9448
185	1.0159	149	0.9442
188	1.0153	104	0.9404
109	1.0121	192	0.9339
107	1.0099	190	0.9339
131	1.0088	197	0.9241
163	1.0050	145	0.9209
182	1.0034	134	0.9149
146	1.0023	138	0.8937
153	1.0018		
133	1.0007		
166	1.0001		

Table C.31. CaF_2:Mn Sort Number 1-B.

TLD I.D. NO.	RATIO	TLD I.D. NO.	RATIO
81	1.0637	47	1.0001
3	1.0634	77	0.9975
35	1.0563	69	0.9968
23	1.0454	100	0.9965
16	1.0415	64	0.9962
68	1.0377	99	0.9959
48	1.0377	4	0.9930
29	1.0335	10	0.9923
102	1.0332	40	0.9920
7	1.0329	46	0.9917
90	1.0309	33	0.9914
6	1.0296	52	0.9898
75	1.0280	96	0.9891
101	1.0264	1	0.9888
43	1.0258	97	0.9882
71	1.0248	87	0.9882
44	1.0248	88	0.9853
37	1.0242	58	0.9846
45	1.0235	2	0.9840
5	1.0235	21	0.9833
20	1.0226	18	0.9830
13	1.0222	92	0.9827
28	1.0206	86	0.9824
11	1.0181	82	0.9824
39	1.0165	42	0.9814
65	1.0161	76	0.9792
49	1.0161	53	0.9788
80	1.0155	95	0.9766
63	1.0139	89	0.9737
54	1.0132	56	0.9698
27	1.0129	8	0.9698
41	1.0110	70	0.9689
19	1.0107	79	0.9676
93	1.0104	72	0.9673
31	1.0094	55	0.9653
26	1.0094	91	0.9640
74	1.0084	34	0.9634
9	1.0081	83	0.9612
61	1.0078	24	0.9566
62	1.0075	32	0.9554
22	1.0071	84	0.9538
15	1.0068	67	0.9534
94	1.0065	57	0.9370
73	1.0049	12	0.9364
17	1.0049	66	0.9132
51	1.0042	98	0.9107
36	1.0036	60	0.9084
14	1.0030	59	0.9078
50	1.0023	85	0.8663
25	1.0017	30	0.8550
38	1.0004		
78	1.0001		

Table C.32. CaF_2:Mn Sort Number 2-A.

TLD I.D. NO.	RATIO	TLD I.D. NO.	RATIO
36	1.0706	68	0.9942
15	1.0571	35	0.9936
95	1.0524	88	0.9920
84	1.0487	47	0.9917
32	1.0472	33	0.9908
76	1.0466	19	0.9896
52	1.0466	5	0.9889
25	1.0447	66	0.9886
87	1.0429	4	0.9871
26	1.0413	54	0.9868
1	1.0413	98	0.9865
86	1.0398	56	0.9865
62	1.0395	44	0.9855
28	1.0395	82	0.9852
37	1.0361	71	0.9852
6	1.0361	69	0.9849
23	1.0321	21	0.9843
9	1.0290	59	0.9822
58	1.0281	41	0.9822
94	1.0256	75	0.9815
34	1.0253	101	0.9797
8	1.0247	65	0.9797
77	1.0244	13	0.9775
20	1.0238	51	0.9769
96	1.0201	29	0.9766
93	1.0182	22	0.9754
60	1.0179	72	0.9744
102	1.0173	38	0.9744
89	1.0167	80	0.9738
48	1.0161	83	0.9692
11	1.0142	40	0.9667
73	1.0133	57	0.9661
46	1.0133	92	0.9640
12	1.0130	27	0.9624
74	1.0127	79	0.9615
78	1.0121	81	0.9541
90	1.0117	100	0.9526
64	1.0111	18	0.9526
43	1.0080	2	0.9526
55	1.0050	17	0.9519
85	1.0010	24	0.9516
70	1.0010	39	0.9489
16	1.0010	14	0.9381
99	0.9994	10	0.9307
49	0.9994	67	0.9202
7	0.9988	31	0.9011
97	0.9982	42	0.9002
3	0.9973	45	0.8949
50	0.9960	53	0.8924
61	0.9948	63	0.8499
30	0.9945		
91	0.9942		

Table C.33.CaF_2:Mn Sort Number 2-B.

TLD I.D. NO.	RATIO	TLD I.D. NO.	RATIO
98	1.0693	41	0.9909
60	1.0640	88	0.9903
47	1.0567	70	0.9903
61	1.0564	35	0.9875
78	1.0474	55	0.9869
42	1.0456	2	0.9869
53	1.0450	82	0.9845
20	1.0419	54	0.9808
80	1.0410	92	0.9805
57	1.0398	86	0.9805
37	1.0382	77	0.9802
90	1.0370	43	0.9799
76	1.0345	71	0.9796
81	1.0342	45	0.9793
74	1.0327	95	0.9740
16	1.0315	32	0.9740
8	1.0305	13	0.9734
91	1.0290	68	0.9713
101	1.0259	12	0.9710
89	1.0241	97	0.9697
72	1.0241	100	0.9682
48	1.0201	15	0.9679
7	1.0201	93	0.9624
66	1.0195	28	0.9611
27	1.0192	25	0.9608
30	1.0176	94	0.9596
65	1.0167	3	0.9593
39	1.0164	62	0.9581
38	1.0164	84	0.9522
102	1.0158	56	0.9507
5	1.0146	59	0.9482
50	1.0127	14	0.9464
99	1.0078	33	0.9424
46	1.0078	75	0.9415
18	1.0060	19	0.9396
52	1.0051	96	0.9390
51	1.0051	11	0.9387
10	1.0035	21	0.9381
69	1.0032	1	0.9381
64	1.0029	36	0.9319
44	1.0023	49	0.9218
79	1.0020	34	0.9169
4	0.9998	24	0.9157
85	0.9977	29	0.9154
23	0.9974	40	0.9071
73	0.9971	6	0.8939
58	0.9949	26	0.8902
9	0.9946	83	0.8868
31	0.9943	87	0.8862
17	0.9928	67	0.8816
22	0.9915		
3	0.9909		

Table C.34. CaF_2:Mn Sort Number 3-A.

TLD I.D. NO.	RATIO	TLD I.D. NO.	RATIO
96	1.1310	17	0.9939
56	1.0653	102	0.9929
9	1.0590	47	0.9916
73	1.0463	67	0.9913
95	1.0380	39	0.9903
50	1.0340	32	0.9879
93	1.0333	22	0.9879
87	1.0333	38	0.9859
29	1.0326	103	0.9816
10	1.0320	92	0.9812
70	1.0316	4	0.9809
78	1.0300	12	0.9802
33	1.0296	42	0.9796
99	1.0290	48	0.9792
80	1.0286	36	0.9779
15	1.0283	97	0.9776
13	1.0283	14	0.9772
81	1.0253	101	0.9716
49	1.0253	74	0.9702
52	1.0223	84	0.9696
3	1.0219	55	0.9689
41	1.0213	94	0.9686
82	1.0206	5	0.9659
59	1.0203	61	0.9652
75	1.0199	24	0.9652
71	1.0186	37	0.9589
91	1.0169	23	0.9576
2	1.0163	79	0.9556
34	1.0159	77	0.9549
31	1.0133	89	0.9525
30	1.0116	11	0.9525
98	1.0109	68	0.9485
20	1.0109	60	0.9449
76	1.0099	85	0.9392
43	1.0099	27	0.9339
25	1.0086	90	0.9322
58	1.0076	7	0.9305
88	1.0059	53	0.9255
83	1.0049	40	0.9255
44	1.0046	21	0.9255
86	1.0043	26	0.9209
77	1.0036	45	0.9192
16	1.0036	100	0.9169
54	1.0016	6	0.9122
57	0.9996	35	0.9038
46	0.9989	51	0.9035
8	0.9979	63	0.8998
1	0.9973	28	0.8938
65	0.9969	19	0.8922
69	0.9959	64	0.8605
66	0.9943	18	0.8498
62	0.9943		

Table C.35. CaF_2:Mn Sort Number 3-B.

TLD I.D. NO.	RATIO	TLD I.D. NO.	RATIO
148	1.0728	181	0.9896
116	1.0553	128	0.9889
141	1.0508	160	0.9886
172	1.0594	132	0.9872
167	1.0488	177	0.9869
108	1.0460	182	0.9855
140	1.0419	133	0.9828
169	1.0412	136	0.9817
121	1.0381	195	0.9810
175	1.0336	179	0.9807
152	1.0326	153	0.9804
139	1.0326	144	0.9804
125	1.0326	154	0.9793
183	1.0299	187	0.9783
155	1.0288	186	0.9773
161	1.0264	196	0.9731
109	1.0264	159	0.9721
119	1.0250	106	0.9683
104	1.0247	204	0.9676
170	1.0223	165	0.9676
151	1.0223	185	0.9656
126	1.0199	206	0.9639
168	1.0168	127	0.9584
150	1.0164	199	0.9573
124	1.0147	162	0.9566
143	1.0144	191	0.9546
107	1.0140	164	0.9532
120	1.0137	130	0.9529
173	1.0130	157	0.9477
149	1.0130	193	0.9467
123	1.0130	138	0.9425
137	1.0085	178	0.9419
105	1.0075	147	0.9412
118	1.0072	113	0.9408
114	1.0065	122	0.9329
111	1.0058	201	0.9295
158	1.0054	192	0.9278
117	1.0030	115	0.9260
184	1.0027	203	0.9229
135	1.0027	134	0.9209
189	1.0020	202	0.9171
176	0.9999	145	0.9168
156	0.9996	180	0.9130
200	0.9958	131	0.9044
188	0.9958	174	0.8924
146	0.9948	163	0.8920
110	0.9944	197	0.8906
112	0.9941	190	0.8776
129	0.9924	205	0.8772
194	0.9903	198	0.8731
142	0.9903	166	0.6971
171	0.9900		

Table C.36. CaF_2:Mn Sort Number 4-A.

TLD I.D. NO.	RATIO	TLD I.D. NO.	RATIO
50	1.0968	70	0.9986
33	1.0934	10	0.9986
40	1.0917	46	0.9962
93	1.0904	72	0.9948
97	1.0785	75	0.9945
89	1.0751	64	0.9938
35	1.0686	25	0.9931
48	1.0638	78	0.9928
49	1.0608	38	0.9928
36	1.0601	102	0.9924
31	1.0594	47	0.9907
41	1.0587	5	0.9887
83	1.0553	77	0.9884
94	1.0550	68	0.9873
91	1.0547	79	0.9863
62	1.0465	45	0.9856
96	1.0431	27	0.9846
61	1.0414	101	0.9843
92	1.0397	11	0.9812
100	1.0394	12	0.9799
58	1.0377	26	0.9785
56	1.0377	55	0.9778
20	1.0353	99	0.9771
42	1.0349	54	0.9754
82	1.0339	28	0.9741
32	1.0332	23	0.9717
30	1.0329	9	0.9710
59	1.0292	21	0.9683
44	1.0254	76	0.9680
24	1.0210	22	0.9676
37	1.0207	17	0.9649
81	1.0200	16	0.9629
60	1.0200	19	0.9598
88	1.0173	84	0.9588
51	1.0173	80	0.9584
39	1.0173	18	0.9564
95	1.0169	67	0.9561
87	1.0149	7	0.9503
53	1.0145	15	0.9448
73	1.0139	1	0.9438
6	1.0122	90	0.9404
85	1.0118	2	0.9387
93	1.0115	74	0.9285
34	1.0111	14	0.9221
66	1.0091	63	0.9139
29	1.0088	57	0.9013
69	1.0081	4	0.8986
52	1.0077	8	0.8908
13	1.0057	65	0.8860
71	1.0054	3	0.8850
43	1.0023		
86	1.0006		

Table C.37. CaF_2:Mn Sort Number 4-B.

TLD I.D. NO.	RATIO	TLD I.D. NO.	RATIO
161	1.3558	190	0.9965
140	1.0558	189	0.9965
115	1.0517	116	0.9958
185	1.0479	113	0.9930
182	1.0459	196	0.9927
166	1.0411	112	0.9913
145	1.0411	146	0.9906
132	1.0393	179	0.9893
134	1.0387	157	0.9869
126	1.0373	199	0.9855
119	1.0373	176	0.9834
139	1.0352	121	0.9824
137	1.0318	164	0.9797
162	1.0315	173	0.9773
191	1.0304	163	0.9773
186	1.0297	122	0.9769
142	1.0297	202	0.9728
130	1.0294	125	0.9728
153	1.0287	148	0.9725
108	1.0280	143	0.9701
106	1.0256	114	0.9684
177	1.0246	180	0.9680
192	1.0229	167	0.9680
172	1.0194	124	0.9673
200	1.0188	203	0.9622
149	1.0167	204	0.9615
117	1.0160	156	0.9594
104	1.0160	194	0.9584
110	1.0143	111	0.9567
152	1.0133	144	0.9564
127	1.0126	193	0.9553
107	1.0119	170	0.9533
160	1.0116	141	0.9522
187	1.0109	123	0.9519
128	1.0105	147	0.9502
158	1.0098	129	0.9474
138	1.0092	174	0.9468
165	1.0071	195	0.9457
168	1.0064	120	0.9306
197	1.0061	118	0.9300
105	1.0037	135	0.9276
188	1.0030	131	0.9262
175	1.0020	159	0.9214
133	1.0020	183	0.9180
178	1.0013	184	0.9049
155	1.0009	154	0.8967
169	0.9996	150	0.8919
151	0.9985	201	0.8912
103	0.9982	181	0.8905
198	0.9975	109	0.8771
171	0.9972		

APPENDIX D: Ionization Theory

Theory appropriate to describe the relationship between the experimentally determinable quantity -- the absorbed dose in the TLD, and the desired quantity -- the absorbed dose in the material surrounding the TLD, must account for interactions which occur inside the TLD. This theory, referred to as solid-state ionization theory, makes allowances for the sum of contributions from electrons produced in the surrounding medium which excite the TLD and those electrons produced inside the TLD. These two gamma ray induced electron sources result in a total TLD absorbed dose which is determined indirectly through the measurement of the TL. The fraction of the total dose stemming from both media -- the surrounding material and the TLD, must be calculated since an experimental technique has not been developed for measuring the individual components.

Solid state ionization theory is based upon a gamma-ray energy T_γ dependent parameter, the theoretically derived dose ratio

$$f(T_\gamma) = \frac{E_D}{E_M} \qquad (D.1)$$

where E_D is the absorbed dose in the TLD and E_M is the absorbed dose in the surrounding medium. If $f(T_\gamma)$ is known and E_D evaluated from the TL emitted by the TLD following irradiation, the desired quantity -- the absorbed dose in the surrounding medium, is determined using the equation

$$E_M = \frac{E_D}{f(T_\gamma)} \; . \qquad (D.2)$$

The general expression developed for calculating $f(T_\gamma)$ is

$$f(T_\gamma) = F_M(T_\gamma) \int_o^T N_M(T_\gamma, T_o)\, dT_o \left[\frac{1}{T_o} \int_o^{T_o} \frac{S_{coll_D}(T)}{S_{coll_M}(T)}\, dT\right] +$$

$$+ F_D(T_\gamma) \frac{\left[\frac{\mu_{en}(T_\gamma)}{\rho}\right]_D}{\left[\frac{\mu_{en}(T_\gamma)}{\rho}\right]_M} \quad . \tag{D.3}$$

This equation is easily understood when rewritten as

$$f(T_\gamma) = F_M(T_\gamma)\ f_s(T_\gamma) + F_D(T_\gamma)\ f_\ell(T_\gamma) \tag{D.4}$$

where

$f_s(T_\gamma)$ = f ratio assuming small cavity theory

$f_\ell(T_\gamma)$ = f ratio assuming larve cavity theory

$F_M(T_\gamma)$ = primary electron attenuation factor in the TLD

$F_D(T_\gamma)$ = buildup factor for primary electrons generated in the TLD.

If $\beta(T_\gamma)$ is defined as the attenuation coefficient for electrons of energy T_γ, $F_M(T_\gamma)$ becomes

$$F_M(T_\gamma) = \int_o^g e^{-\beta(T_\gamma)\ x}\, dx \Big/ \int_o^g dx$$

$$= \frac{1 - \exp[-\beta(T_\gamma)g]}{\beta(T_\gamma)g} \tag{D.5}$$

and

$$F_D\ (T_\gamma) = 1 - F_M(T_\gamma) \tag{D.6}$$

g is defined as the mean chord length of the TLD

$$g = \frac{4V\rho}{S} \quad (g/cm^2) \tag{D.7}$$

where V is the volume, ρ the density and S is the surface area of the TLD. For all of the calculations reported, the Katz and Penfold expression

$$\beta(T_\gamma) = -\frac{\ln 0.01}{R(T_\gamma)} \tag{D.8}$$

was used to estimate $\beta(T_\gamma)$ where the range of the primary electron $R(T_\gamma)$ of maximum energy T_γ was calculated using

$$R(T_\gamma) = \begin{cases} 0.412\ T_\gamma^n & \text{for } 0.01 \leq T_\gamma \leq 3 \text{ MeV} \\ 0.530\ T_\gamma - 0.106 & \text{for } 3.0 < T_\gamma \leq 20 \text{ MeV} \end{cases} \quad (D.9)$$

and

$$n = 1.265 - 0.0954 \ln T_\gamma .$$

The large-cavity term $f_1(T_\gamma)$ in Eq. D.3 is derived by assuming that the TLD is much larger than the range of the primary electrons. Therefore, the energy absorbed in the TLD is only a function of the properties of the TLD material. Similarly, the energy absorbed in the surrounding material is a function of the properties of the material. For a gamma-ray source, the energy absorbed is a function of the mass-energy absorption coefficient in either case. Hence, the energy absorbed in the TLD per unit mass can be related to the energy absorbed per unit mass in the surrounding medium, by the ratio of the mass energy absorption coefficients,

$$\frac{E_D}{E_M} = f_1(T_\gamma) = \frac{(\mu_{en}/\rho)_D}{(\mu_{en}/\rho)_M} . \quad (D.10)$$

Evaluation of the small cavity term $f_s(T_\gamma)$ requires calculating the electron spectrum $N_M(T_\gamma, T_o)$ and the mass stopping powers $S_{coll}(T)$. Spectrum calculations included both Compton and pair production interactions. For Compton scattered gamma rays, number of electrons scattered into (T_o, dT_o) per unit of gamma-ray flux is given by the Klein-Nishina cross section

$$\frac{d\sigma}{dT_o}(T_\gamma) = \pi r_o^2 \frac{m_o c^2}{T_\gamma^2} \left\{ 2 + \left(\frac{T_o}{T_\gamma - T_o} \right)^2 \left[\left(\frac{m_o c^2}{T_\gamma} \right)^2 + (T_\gamma - T_o) \left(\frac{T_o - 2m_o c^2}{T_\gamma T_o} \right) \right] \right\} \quad (D.11)$$

The fraction of energy lost via the Compton scattering process and given to electrons in (T_o, dT_o) is

$$N_{CE}(T_\gamma, T_o)dT_o = \frac{dT_o \frac{d\sigma}{dT_o}(T_\gamma)T_o}{\int_o^{T_\gamma} dT_o \frac{d\sigma}{dT_o}(T_\gamma)T_o} \tag{D.12}$$

The positron energy distribution from the pair production process is given by

$$\frac{d\sigma}{dT_+} = \frac{\bar{\Phi}}{T} \frac{p_+ p_-}{3} \left\{ -\frac{4}{3} - 2E_+E_- \frac{p_+^2 + p_-^2}{p_+^2 p_-^2} + m_o^2c^4 \left(\frac{E_+ \varepsilon_-}{p_-^3} + \frac{E_- \varepsilon_+}{p_+^3} - \frac{\varepsilon_+ \varepsilon_-}{p_+ p_-} \right) \right.$$

$$+ L \left(\frac{T_\gamma^3}{3 p_+^3 p_-^3} (E_+^2 E_-^2 + p_+^2 p_-^2) - \frac{8}{3} \frac{E_+E_-}{p_+p_-} - T_\gamma \frac{m_o^2c^4}{2p_+p_-} \left(\frac{E_+E_- - p_-^2}{p_-^3} \varepsilon_- \right. \right. \tag{D.12}$$

$$\left. \left. \left. + \frac{E_+E_- - p_+^2}{p_+^3} \varepsilon_+ + \frac{2T_\gamma E_+ E_-}{p_+^2 p_-^2} \right) \right) \right\}$$

where E_+ = the total energy of the positive electron,

E_- = the total energy of the negative electron,

$p_\pm$ = the momentum of the positive/negative electron multiplied by c,

$$\varepsilon_\pm = 2\ell n \frac{E_\pm + p_\pm}{m_o c^2}$$

$$L = \frac{2\ell n E_+E_- + p_+p_- + m^2c^4}{T_\gamma m_o c^2}$$

$m_o c^2$ = rest mass of electron

and $\bar{\Phi} = \frac{Z^2}{137} r_o^2$. This equation is useful for both positive and negative electrons and produces a symmetric distribution. The asymmetry introduced by the coulombic attraction or repulsion of the nucleus was not accounted for, nor was the effect of screening.

When the quantity $\gamma = 100 \frac{T_\gamma\, mc^2}{E_+ E_- Z^{1/3}}$ is less than 15, the following equation, which does include screening, was used:

$$\frac{d\sigma}{dT_+} = 4\,\bar{\Phi}\,\frac{1}{T_\gamma^3}\,(E_+^2 + E_-^2 + \tfrac{2}{3}E_+E_-)\left(\ell n\,\frac{2E_+E_-}{T_\gamma m_o c^2} - \tfrac{1}{2} - C(\gamma)\right) \qquad (D.14)$$

The function $C(\gamma)$ was found by second order polynomial interpolation within a table of values.

Collision mass stopping powers were calculated using the equation

$$S_{coll} = \frac{2\pi N_a r_o^2 m_o c^2}{\beta^2}\,\frac{Z}{A}\left\{\ell n\left[\frac{\tau^t(\tau+2)}{2\,(I/m_o c^2)^2}\right] + F - \delta\right\} \qquad (D.15)$$

where N_a = Avogadros's number (6.022×10^{23} electrons/mole),

r_o^2 = radius of first Bohr orbit, (7.9403×10^{-26} cm^2),

$m_o c^2$ = rest mass energy of electron, (0.510976 MeV),

τ = kinetic energy of electron in units of $m_o c^2$,

$\beta = [\tau(\tau+2)]^{1/2}/(\tau+1)$,

Z = atomic number of medium,

A = atomic weight of medium,

$F = 1-\beta^2 + [\tau^2/8 - (2\tau+1)\,\ell n2]/(\tau+1)^2$,

δ = density effect correction,

I = ionization potential of medium (eV).

δ is given by

$$\delta = \begin{cases} 0 & , x < x_o \\ 4.606x + C + a(x_1 - x)^m, & , x_o \le x < x_1 \\ 4.606x + C & , x \ge x_1 \end{cases}$$

where

$$x = (\log_{10} e)\,\frac{1}{2}\,\ell n\,[\beta^2/(1-\beta^2)] = 0.21715\,\ell n[\beta^2/(1-\beta^2)].$$

The parameters C, a, x_1, x_2, m, Z, A, and I are input to the TERC/III code (see Appendix B) for each encasement material.

^{7}LiF AND CaF_2:Mn EXPERIMENTAL DATA FOR EVALUATING TLD ENERGY RESPONSE THEORY

by

Robert Mark Ostmeyer
B.S., Kansas State University, 1979

AN ABSTRACT OF A MASTER'S THESIS

submitted in partial fulfillment of the
requirements for the degree

MASTER OF SCIENCE

Department of Nuclear Engineering
KANSAS STATE UNIVERSITY
Manhattan, Kansas

1980

ABSTRACT

The gamma-ray energy responses of encapsulated ^{7}LiF and CaF_2:Mn thermoluminescent dosimeters (TLDs) were measured and compared to calculated values. These measurements were accomplished by exposing encased 1x1x6 mm TLDs to gamma rays with energies ranging from 0.122 to 1.333 MeV. The studied encasement materials included lead, tantalum, tin, zirconium, copper, stainless steel, iron, aluminum, and natural LiF. Calculations were based upon solid state ionization theory and were performed using the TERC/III computer code.

An encasement thickness investigation was also performed to compliment the energy response data. For this investigation, ^{7}LiF and CaF_2:Mn response data were obtained using a variety of encasement sizes. The gamma-ray energies and encasement materials investigated were the same as those used for the energy response measurements.

A prescription to correct the TERC/III calculations for encasement wall attenuation (a phenomenon inherent to the encased TLD measurement of gamma dose) is discussed. For this correction, effective attenuation coefficients were determined from the sleeve thickness data. Comparisons between corrected calculations and the energy response data are reported.